ABSTRACT

The Development of Novel Polyester-Based PolyHIPE Foams as Matrices for Tissue Engineering

Wendy Busby

Submitted for Ph.D. October 2001

Motivations for exploring the creation of man-made tissues (cell transplantation) and the growth of artificial organs (neoorgans) are varied. Early matrices, following on from the injection of cells into other tissues, were constructed from extracellular matrix proteins, e.g. collagen. Limitations in structure and strength led to current materials that are either a composite matrix, i.e. a fibre mesh supported by a second polymer; or a monolithic sponge-like structure – foam. PolyHIPE (High Internal Phase Emulsion) polymers are emulsion-derived foams. The product has an open-cellular macroporous morphology. Porosity can be varied between 74 and 99% and cell size from 5 – 200 μm.

In this thesis, polycaprolactone and polylactide diols have been end-capped with acrylate groups to yield macromonomers. A series of novel PolyHIPE scaffolds were prepared by free-radical homopolymerisation of the macromonomers or copolymerisation of macromonomers with styrene or methyl methacrylate. The PolyHIPEs produced were shown by SEM to be porous with cell sizes ranging from 5 – 100 μm and pores from 1 – 10 μm. The morphology of the materials was affected by diluent type, polyester content, surfactant concentration, NaCl content and the initiator used.

Biodegradability has been achieved because polycaprolactone and polylactide contain weak ester linkages that can be hydrolysed *in vivo*. An *in vitro* study has shown that the PolyHIPEs demonstrated some biodegradability during a 10 week period but a longer experiment is necessary.

PolyHIPEs prepared from 1 g of PCL or PL and 4 g styrene have been shown to support the growth and proliferation of human and rat skin fibroblasts and chicken embryo tissue containing various cell types. A 10 week *in vivo* study showed that the scaffolds did not invoke any immune or inflammatory responses and are, therefore, not toxic in the early stages after implantation.

THE DEVELOPMENT OF NOVEL POLYESTER-BASED POLYHIPE FOAMS AS MATRICES FOR TISSUE ENGINEERING

A thesis submitted to the University of Durham in accordance with the regulations governing the award of the degree of Doctor of Philosophy

WENDY BUSBY

Department of Chemistry
University of Durham
Durham

October 2001

Declaration

The material contained within this thesis has not previously been submitted for a degree at the University of Durham or any other University. The research reported within this thesis has been conducted by the author unless indicates otherwise

Wendy Busby
October 2001

ACKNOWLEDGEMENTS

I would like to acknowledge the financial support from the Engineering and Physical Sciences Research Council that allowed me to undertake this PhD.

Thank you to my supervisor Dr Neil Cameron, for the project, his supervision, guidance and introducing me to such an interesting and at sometime in the future, beneficial area of study.

I must acknowledge the following people all staff in the Biology department at the University of Durham Dr Colin Jahoda, for his time and input on all things biological in this thesis and Sue Davies for the initial cell studies, Judith Chambers for showing me the cell culturing techniques and Christine Richardson for showing me the fixing and staining techniques and operation of a temperamental critical point dryer.

At the University of Newcastle, Grant Staines, Pauline and especially Richard Baron, of the Materials Analysis Unit for SEM analysis above and beyond the call of duty.

A big thank you to Dr Audrey Cameron, for your friendship and for proof reading my thesis.

Thank you to my mum and dad for taking in half of the contents of a house when I returned to being a student.

Thanks to the ever expanding lab for endless days of entertainment, you know who you all are.

And finally.....

Thanks to Dave, for still being here, I love you.

"In those days there were heroes and villains, and darkness walked the earth. There were dragons to be slain, captured princesses to be saved, and mighty deeds were accomplished by knights in shining armour.

Many tales are told of that time, tales of steadfast bravery and derring-do.

This isn't one of them"

Abbreviations

ABBREVIATIONS

DCM	dichloromethane
DFDBA	demineralised freeze-dried bone allograft
DNA	deoxyribonucleic acid
DPPA	diphenylphosphorylazide
ECM	extracellular matrix
FDA	Food and drug administration
FRROP	free radical ring-opening polymerisation
HIPE	high internal phase emulsion
HLB	hydrophilic-lypophilic balance
IPA	*iso*-propanol
MALDI-tof	matrix assisted laser desorption of ionization – time of flight
MEMS	micro electo mechanical system
M_n	number average molar mass
MMA	methyl methacrylate
NMR	nuclear magnetic reasonance
PAA	poly (acid anhydride)
PBS	poly (butylene succinate)
PCA	poly (α-cyanoacrylate)
PCL	poly (ε-caprolactone) or polycaprolactone
PDGF	platelet-derived group factor
PDLL	poly (D,L-lactide) or PL or PDLLA
PEA	poly (ester amide)

PEC	poly (ester carbonate)
PEG	poly (ethylene glycol)
PEO	poly (ethylene oxide)
PES	poly (ethylene succinate)
PET	polyethylene terephthalate
PG	polyglycolide
PGA	polyglycolic acid
PGALA	poly (glycolide-*co*-lactide), poly (glycolic acid-*co*-lactic acid)
PHA	poly (hydroxyalkanoate)
PHB	poly (3-hydroxybutyrate)
PHBA	Poly (β-hydroxybutyric acid)
PHB-PHV	Polyhydroxybutyrate-hydroxyvalerate
PIT	phase inversion temperature
PL	polylactide
PLA	polylactic acid
PLG	poly (lactide-co-glycolide)
PLGA	poly (lactide-co-glycolic acid)
PLL	poly (L-lactide)
PLLA	poly (L-lactic acid)
PMMA	poly (methyl methacrylate)
P(NIPAAm)	poly (N-isopropylacrylamide)
POE	poly (orthoester)
PolyHIPE	HIPE in which continuous phase contains a polymer or monomer
PPO	poly (propylene oxide)

Abbreviations

PTFE	poly tetrafluoroethylene
PTMC	poly (trimethylene carbonate)
PVA	polyvinyl alcohol
PVBC	poly vinylbenzyl chloride
RGD	arginine, glycine and aspartic acid – single letter representation of each amino acid
ROP	ring opening polymerisation
SEM	scanning electron microscope / micrograph
Tg	glass transition temperature
VA	vinyl acetate

Table of Contents

Chapter 1		
1	**INTRODUCTION**	**1 – 4**
Chapter 2		
2	**LITERATURE REVIEW**	**5**
2.1	Tissue Engineering Using Biodegradable Networks	5 – 21
2.2	Biodegradable Networks	21 – 35
2.3	High Internal Phase Emulsions (HIPEs) and PolyHIPEs	35 – 42
2.3.1	Application of HIPEs and PolyHIPEs	42 – 46
2.4	Aims	46 – 47
Chapter 3		
3	**PREPARATION AND CHARACTERISATION OF PCL FOAMS**	**48**
3.1	Introduction	48
3.1.1	Ionic Ring Opening Polymerisation	48 – 49
3.1.2	Preparation of Biodegradable Polyesters for Biomedical Applications	49
3.1.3	Radical Ring-Opening Polymerisation of Cyclic Ketene Acetals	49 – 53
3.1.4	Copolymerisation of ε-Caprolactone	54
3.1.5	Production of Biodegradable Networks From PCL Macromonomers	55
3.2	Experimental	56
3.2.1	Materials and Instrumentation	56
3.2.1.1	Materials	56
3.2.1.2	Instrumentation	56 – 57
3.2.2	General Methodology	57
3.2.2.1	Macromonomer Synthesis	57 – 58
3.2.2.2	Network Formation	58
3.2.2.3	PolyHIPE Formation	58 – 59
3.2.2.4	Emulsion Tests	59
3.2.2.5	Swelling Studies	60
3.2.3	Experiments	60
3.2.3.1	PCL $\overline{M}_n$=2000 Macromonomer Synthesis (2)	60 – 61
3.2.3.2	PCL $\overline{M}_n$=530 Macromonomer Synthesis (1)	61 – 62
3.2.4	Network Formations	62
3.2.5	PolyHIPE Formation	64
3.2.6	Emulsion Tests	64
3.3	Results and Discussion	64
3.3.1	Macromonomer Synthesis and Network Formation	64 – 68
3.3.2	PolyHIPE Preparation	69 – 70
3.3.2.1	PCL and Styrene	70 – 75
3.3.2.2	PCL and MMA	75 – 78
3.3.2.3	PCL and Toulene	78 – 79
3.3.3	Swelling Studies	79 – 80

Table of Contents

3.3.3.1	Swelling Studies of Low Molecular Mass PCL Foams	80 – 81
3.3.3.2	Swelling Studies of High Molecular Mass PCL Foams	82 – 83
3.4	Conclusions	83 – 84
Chapter 4		
4	**PREPARATION AND CHARACTERISATION OF PL FOAMS**	**85**
4.1	Introduction	85
4.1.1	Basic Polymer Science and Stereochemistry	85 – 86
4.1.1.1	Molecular Weight	86
4.1.1.2	Amorphous and Crystalline Polymers	86
4.1.1.3	Glass Transition Temperature (T_g)	86 – 87
4.1.1.4	Stereochemistry	87 – 89
4.1.2	Lactic Acid, Glycolic Acid and Their Polymers	89
4.1.2.1	Lactic Acid / Lactide and Glycolyic Acid / Glycolide	89
4.1.2.2	Synthesis of PL, PG and PLG	90 – 91
4.1.2.3	Differences in Polylactides and Comparison to PCL	92 – 94
4.2	Experimental	94
4.2.1	Materials and Instrumentation	94
4.2.1.1	Materials	94
4.2.1.2	Instrumentation	94 – 95
4.2.2	General Methodology	95
4.2.2.1	Polymer Synthesis	95
4.2.2.2	Macromonomer Synthesis	96 – 97
4.2.2.3	PolyHIPE Formation	97 – 98
4.2.2.4	Swelling Studies	98 – 99
4.2.3	Experiments	99
4.2.3.1	PL $\overline{M}_n$=2000, Polymer Synthesis	99
4.2.3.2	PL diacrylate, Macromonomer Synthesis	100
4.2.3.3	PolyHIPE Formation	100 – 102
4.3	Results and Discussion	102
4.3.1	Polymer Synthesis	102 – 103
4.3.2	Macromonomer Synthesis	103 – 105
4.3.3	PolyHIPE Preparation	106
4.3.3.1	PL and Styrene	106 – 108
4.3.3.2	PL and MMA	108 – 110
4.3.3.3	PL and Toluene	110 – 112
4.3.4	Swelling Studies	112
4.3.4.1	Swelling Studies of PL Foams	112 – 114
4.3.4.2	Comparison of PL and PCL Swelling Studies	114 – 117
4.4	Conclusions	117
Chapter 5		
5	**BIODEGRADATION STUDY**	**118**
5.1	Introduction	118
5.1.1	Introduction to Degradation in General	118 – 122
5.1.2	Degradation of PCL	122 – 124
5.1.3	Degradation of PL	124 – 127

Table of Contents

5.2	Experimental	127
5.2.1	Apparatus and Reagents	127
5.2.1.1	Soaking Solution	127
5.2.1.2	Container	128
5.2.1.3	Temperature Control	128
5.2.1.4	Control of Buffer Solution	128
5.2.1.4.1	Changes in pH	128
5.2.1.4.2	Clouding of Buffer Solution	128
5.2.2	Real-time degradation	128 – 129
5.2.3	Physicochemical tests	129
5.2.3.1	Balance	129
5.2.3.2	Vacuum Oven	129
5.2.3.3	Preparation of test samples	129 – 130
5.2.3.4	Test Procedure	130 – 131
5.3	Results and Discussion	131 – 132
5.3.1	Change in pH	132 – 133
5.3.2	Change in Weight	133 – 138
5.3.3	Changes in Sample Diameter and Thickness	138 – 140
5.3.4	Changes in Internal and External Morphology	140 – 146
5.3.5	Visual Assessment of Changes in Size and Appearance	147 – 149
5.4	Conclusions	149
Chapter 6		
6	**OPTIMISING MORPHOLOGY**	**150**
6.1	Introduction	150 – 151
6.2	Experimental	151
6.2.1	Materials and Instrumentation	151
6.2.1.1	Materials	151
6.2.1.2	Instrumentation	152
6.2.2	Methodology	152 – 153
6.3	Results and Discussion	153
6.3.1	Effect of salt Content	153 – 157
6.3.2	Effect of Surfactant and Salt Concentration	157 – 160
6.3.3	Miscellaneous	161 – 164
6.3.4	Mercury-Intrusion Porosimetry Results	164 – 166
6.3.4.1	Comparison of PCL and PL Foams	166 – 167
6.3.4.2	Salt Content	167 – 168
6.3.4.3	Potassium Persulphate Vesus AIBN	168 – 169
6.4	Conclusion	169
Chapter 7		
7	**CELL STUDIES**	**170**
7.1	Introduction	170
7.1.1	Cells	170 – 171
7.1.2	Tissue	171
7.1.3	Fibroblasts	171
7.1.4	Cells and Biomaterials	172

7.1.4.1	Cell Attachment to Biomaterials	172 – 173
7.1.4.2	Effect of Cell Concentration on Growth	173 – 174
7.1.4.3	Characterisation of Cell Growth	174 – 175
7.2	Experimental	176
7.2.1	Materials and Instruments	176
7.2.1.1	Materials	176
7.2.1.2	Instruments	176
7.2.2	Experiments	176
7.2.2.1	General Information	176 – 177
7.2.2.2	Foam Disc Preparation	177 – 178
7.2.3.1	Cell Seeding and Tissue Growth	178 – 179
7.2.3.2	Rat Explant	179
7.2.3.3	Chicken Explant	179
7.2.3.4	Chicken Egg CAM (Chorioallantioc Membrane)	179 – 180
7.2.3.5	Human Cells	180
7.2.3.6	6 Day Experiment	181
7.2.4	Preparation of Cells For SEM . Giemsa Stain	181
7.2.4.1	Preparation of Cells for SEM	181 – 182
7.2.4.2	Preparation of Cells for Giemsa Stain	183
7.2.5	*In Vivo* Implants	183 – 184
7.3	Results and Discussion	184 – 185
7.3.1	Cell and Explant Studies	186
7.3.1.1	Growth of Human Fibroblasts on 0.2-H-S	186 – 187
7.3.2	Chicken and Rat Explant Experiments	187
7.3.2.1	Chicken Explant	187 – 189
7.3.2.2	Rat Explant	189 – 190
7.3.3	Study of Cell Attachment and Growth Over 6 Days	191 – 194
7.3.4	*In Vivo* Chicken CAM and Rat Implants	194
7.3.4.1	Chicken CAM	194
7.3.4.2	PCL Rat Implants	195 – 198
7.3.4.3	PL Implants	198 – 200
7.3.4.4	*In Vivo* Degradation of the Implants	201
7.4	Conclusion	202
Chapter 8		
8	**CONCLUSIONS AND FUTURE WORK**	**203**
8.1	Conclusions	203
8.2	Future Work	204
8.2.1	Future Work on the PolyHIPEs	204
8.2.2	Biodegradation	204
8.2.3	Further Work on Cell Studies	205
References		206 – 217
Appendix		218 – 222

List of Figures

Chapter 1

1.1	SEM of a PolyHIPE material	4

Chapter 2

2.1	Biodegradable Polymer Mesh	10
2.2	Photographs of nose and ear cartilage grown on 3D polymer Scaffolds	16
2.3	Biodegradable heart valve	19
2.4	SEM pictures of polylactin mesh	35
2.5	Emulsions and HIPEs, packing of the droplet phase	36
2.6	Sorbitan monooleate (Span 80)	37
2.7	PEO-PPO-PEO triblock copolymer surfactant	38

Chapter 3

3.1	Equipment for macromonomer synthesis	57
3.2	Equipment for foam synthesis	59
3.3a	^{1}H NMR spectrum (macromonomer 2)	66
3.3b	Close up of acrylate endgroup region	67
3.4	MALDI spectrum (macromonomer 1)	67
3.5	MALDI spectrum (macromonomer 2)	68
3.6	SEMs of 0.2-H-S and 0.2-L-S	71
3.7	Chart of phase separation of 0.2-L-S HIPEs heated at 60°C	72
3.8	SEMs of 0.3-L-S and 0.3-H-S	74
3.9	SEMs of 0.2-L-M and 2-H-M	76
3.10	SEMs of 0.4-L-M and 0.4-H-M	77
3.11	SEMs of 0.2-L-T and 0.2-H-T	78
3.12	SEMS of 0.5-L-T and 0.5-H-T	79
3.13	Swelling study of low molecular mass PCL foams	80
3.14	Swelling study of high molecular mass PCL foams	82

Chapter 4

4.1	Typical polymer sample molar mass distribution	85
4.2	Chirality	87
4.3	Relationship between nomenclature systems for lactic acid	89
4.4	Equipment for macromonomer synthesis	96
4.5	Equipment for foam synthesis	98
4.6	Structure of polylactide	102
4.7	MALDI spectrum for PL	103
4.8	^{1}H NMR spectrum for PL	104
4.9	MALDI spectrum for PL diacrylate	105
4.10	SEMs of 0.2-S	106
4.11	SEMs of 0.4-S and 0.6-S	108
4.12	SEMs of 0.2-M	109
4.13	SEMs of 0.4-M	110
4.14	SEMs of 0.2-T	111

List of Figures

4.15	SEMs of 0.4-T	111
4.15	SEMs of 0.6-T	111
4.16	Swelling study of PL foams	113
4.17	Comparison in swelling 20 wt. % PCL and PL foams	115
4.18	Comparison in swelling 40 wt. % PCL and PL foams	116
Chapter 5		
5.1	Chart of change in average pH with time	133
5.2	Chart of average change in weight of 4 different foams over 70 Days	134
5.3	Charts of PL thin changes in thickness and diameter	139
5.4	Charts of PL thick changes in thickness and diameter	139
5.5	Charts of PCL thin changes in thickness and diameter	140
5.6	Charts of PCL thick changes in thickness and diameter	140
5.7	SEMs of PL thin biodegradation	143
5.8	SEMs of PL thick biodegradation	144
5.9	SEMs of PCL thin biodegradation	145
5.10	SEMs of PCL thick biodegradation	146
5.11	Photographs PL thin samples	147
5.12	Photographs of PL thick samples	148
5.13	Photographs of PCL thin samples	148
5.14	Photographs of PCL thick samples	149
Chapter 6		
6.1	SEMs of 0 g salt (NS)	154
6.2	SEMs of 1 g salt (DS)	155
6.3	SEMs of 1.5 g salt (HS)	155
6.4	SEMs of 2 g salt (2gs)	156
6.5	SEMs of 3 g salt (3gs)	156
6.6	SEMs of 0.5 g surfactant (LS)	158
6.7	SEMs of 0.5 g surfactant, 0 g salt (LSNS)	158
6.8	SEMs of 0.5 g surfactant, 1 g slat (LSDS)	159
6.9	SEMs of 0.75 g surfactant, 1.5 g salt (LSHS)	159
6.10	SEMs of 1.5 g surfactant, 1 g salt (HSDS)	160
6.11	SEMs of AIBN, 0 g salt (AIBNns)	161 – 162
6.12	SEMs of 27 ml water (HW)	163
6.13	0.5 g surfactant, 1.5 g PCL (LS1.5g)	163 – 164
6.14	SEMs of PMS	164
6.15	Chart comparing PCL and PL porosimetry results	167
6.16	Chart comparing pore size with increasing salt content	168
6.17	Chart comparing potassium persulphate (PCL/PL-styrene) with AIBN	169
Chapter 7		
7.1	Electron micrograph of a rat liver cell	170
7.2	*In vitro* interaction of cells with scaffolds	172
7.3	Diagram of moulds used to make polyHIPE discs	177

List of Figures

7.4	Diagram of egg before and after incubation	180
7.5	SEMs of cells on 0.2-H-S and 0.2-M-S	185
7.6	Photograph of stained human fibroblasts on 0.2-H-S and SEM	186
7.7	SEMs of human fibroblasts	187
7.8	Chicken explant photographs	188
7.9	Rat explant photographs	190
7.10	PCL photographs from time experiment	192
7.11	PL photographs from time experiment	193
7.12	In vivo PCL rat implant photographs	196
7.13	In vivo PCL rat implant optical pictures	197
7.14	In vivo PL rat implant photographs	199
7.15	In vivo PL rat implant optical pictures	200
7.16	PCL implant and PL implant x0.6 optical picture	201

List of Tables

Chapter 2

2.1	Progression to date of tissue engineering studies	20 – 21
2.2	Advantages and disadvantages of natural versus synthetic Polymers	26

Chapter 3

3.1	HLB values of surfactants used	72
3.2	PolyHIPE foams prepared with PCL	73
3.3	Formation and stability of HIPEs containing MMA at different Surfactant HLB values	75

Chapter 4

4.1	Stereostructures upon polymerisation of lactic acid and stereoisomers	92
4.2	Comparison of T_g and T_m of 4 polyesters	93
4.3	PolyHIPEs foams prepered with PL	107

Chapter 5

5.1	F-test results for PL thin	136
5.2	F-test results for PL thick	136
5.3	F-test results for PCL thin	137
5.4	F-test results for PCL thick	137

Chapter 6

6.1	Compositions used for optimisation of morphology	153
6.2	Average Pore Size as measured by mercury-intrusion Porosimetry	165 – 166

Chapter 7

7.1	Effect of cell seeding concentrations on average weights of resorbable polymer implants after 12 weeks	174

List of Schemes

Chapter 1

1.1	Breakdown mechanism for ester group	3
1.2	Applying ester hydrolysis to a long chain polymer	3

Chapter 2

2.1	Lactides to polylactides	9

Chapter 3

3.1	untitled	50
3.2	untitled	51
3.3	Pathway a	51
3.4	Pathway b	52
3.5	5,6 and 7 membered cyclic ketene acetals	52
3.6	untitled	53
3.7	Macromonomer synthesis	65
3.8	Assignment of H's in acrylate groups	66

Chapter 4

4.1	The coordination-insertion mechanism of functionalised aluminium alkoxides	92
4.2	Macromonomer synthesis	104

Chapter 5

5.1	Division of biodegradable polymers by application	118

Introduction

Chapter 1

1. INTRODUCTION

Motivations for exploring the creation of man-made tissues (cell transplantation) and the growth of artificial organs (neoorgans) are varied. They start from increasing a patient's comfort, providing a solution where therapy is not available, to being able to supply whole organs to the thousands of people admitted to hospital everyday with a malfunctioning organ. In America in 1989, 30, 000 deaths resulted from liver disease, only 7% of patients requiring transplants received new organs [1]. In 1997, the American Heart Association reported that of 40, 000 Americans requiring heart transplants, only 2 300 received new hearts [2]. Kidneys and skin for burn victims are also scarce. Unlike cars, humans do not yet have a supply of spare parts available off the shelf. Meanwhile, prosthetic or artificial replacements can lead to infection and they have limited tolerance to external forces. Their use in children is unsatisfactory because they need continuous replacement as the child matures.

Liver tissue regenerates rapidly. It is conceivable that a living donor could donate a small amount of liver tissue, which in the space of a few weeks would regenerate to its original size allowing the transplant to keep its original mass.

In the case of the liver, cell transplantation offers the advantages of :

1 Early intervention for diseases of the liver;

2 Avoiding emergency operations;

3 Determination of successful functioning of the transplant before the native liver has to be removed;

4 Removal of the need for immune suppressive drugs because of reduced immunogenicity of the transplant.

Early attempts at cell transplantation looked at the injection of suspended, dissociated cells into other tissues e.g. fat, liver and spleen [1]. However, this resulted in damage to the structure and function of existing cells. The next developments involved an extrogenous (external) matrix; early matrices were constructed from natural extracellular matrix (ECM) proteins e.g. collagen. Poor mechanical properties were addressed by the development of a hybrid matrix composed of inert microcarrier bead supports coated with ECM proteins. From this further development led to fibre-based matrices providing high porosity and high surface area. Limitations in the structure and strength have led to current materials that are either a composite matrix, i.e. a fibre mesh supported by a second polymer, or a monolithic sponge-like structure – foam.

The matrix, a three-dimensional scaffold constructed from biodegradable polymers, is implanted with cells from either the patient or a suitable donor. The matrix is then transplanted into the wound site where the cells replicate to form new tissue. Consecutively, the polymer scaffold degrades to leave only biocompatible and preferably natural products in the body. A biodegradable polymer is a polymer containing a weak link or unit e.g. an ester unit in the main chain. The mechanism for degradation is shown in Scheme 1.1 and its application to a long chain polymer in Scheme 1.2.

Artificially grown tissue is already available for medical use e.g. skin, cartilage, bone, ligament and tendon [2]. In 1998, as this current study began, an article reported work by Mooney et al that spanned the gulf between tissue engineering and gene therapy [3]. A team of biomedical engineers from the University of Michigan impregnated a poly (lactide-co-glycolide) porous matrix with PDGF (platelet-derived growth factor) and therapeutic DNA. Implants placed under the skin of rats promoted blood vessel and

Scheme 1.1 Breakdown mechanism for ester group

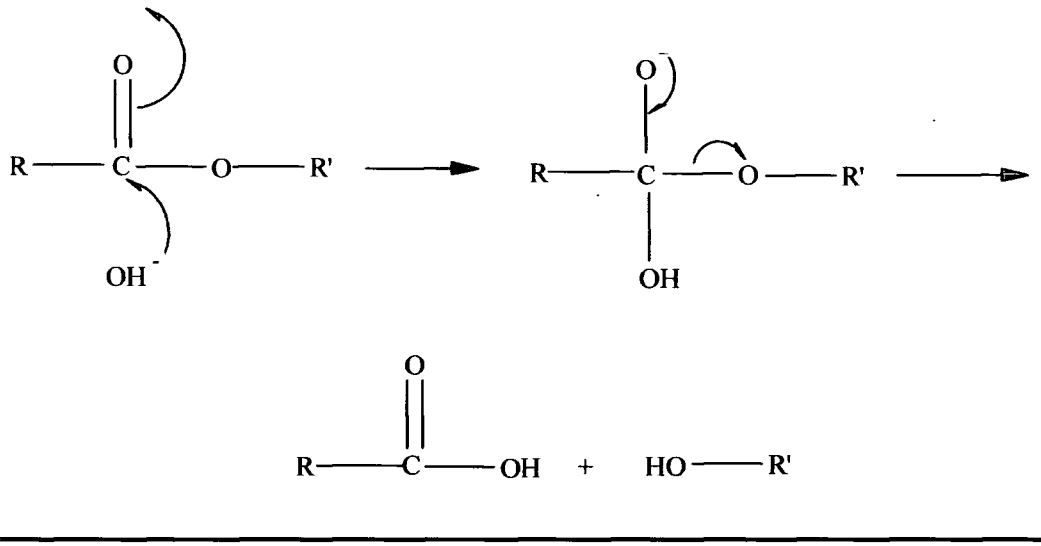

Scheme 1.2 Applying ester hydrolysis to a long chain polymer

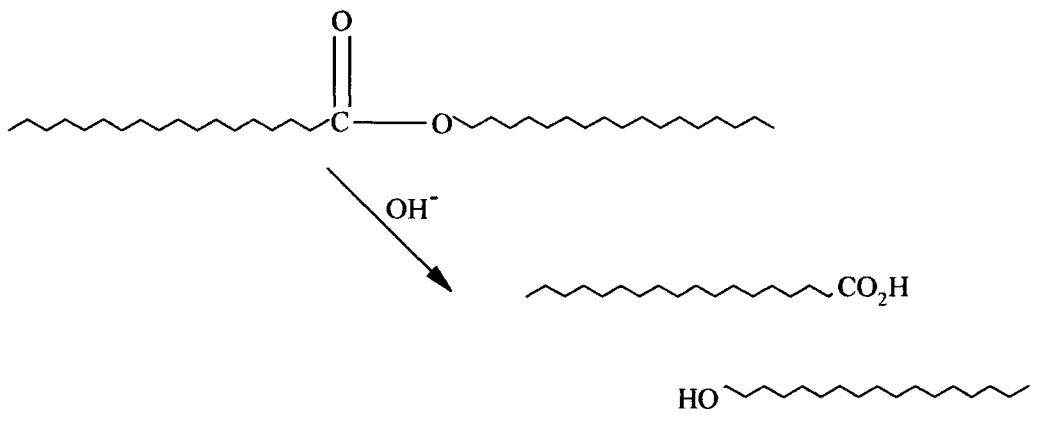

tissue growth. Cells migrating into the scaffold therefore incorporated and expressed the chosen gene.

There are several approaches that can be taken to form porous foams suitable for supporting the growth of cells, for example salt leaching or phase separation, both will be discussed in more detail later. There are a number of physical properties of importance

in an application such as cell growth: porosity; cell size; surface area. The material needs to have an open structure with high porosity to provide support and allow diffusion of nutrients and waste material, the pore size can be variable depending on the tissue type to be cultivated, e.g the liver requires pores of a minimum diameter of 60μm, avascualar tissue such as cartilage has no such constraints [1]. In the case of salt leaching the pore size is dependent on the salt crystals and varies greatly. Phase separation provides specific but very limited pore sizes.

In this work we have chosen to make foams from PolyHIPEs. PolyHIPE polymers are foams derived from high internal phase emulsions. The product has an open-cellular macroporous morphology. Porosity varies between 74% and 99% and cell size from 10 to 200μm. Conditions can be set to control the former attributes, as well as surface area and cellular interconnectedness. A scanning electron micrograph (SEM) of a typical poly(styrene/divinylbenzene) PolyHIPE is shown in Fig. 1.1

Figure 1.1 SEM of a PolyHIPE material

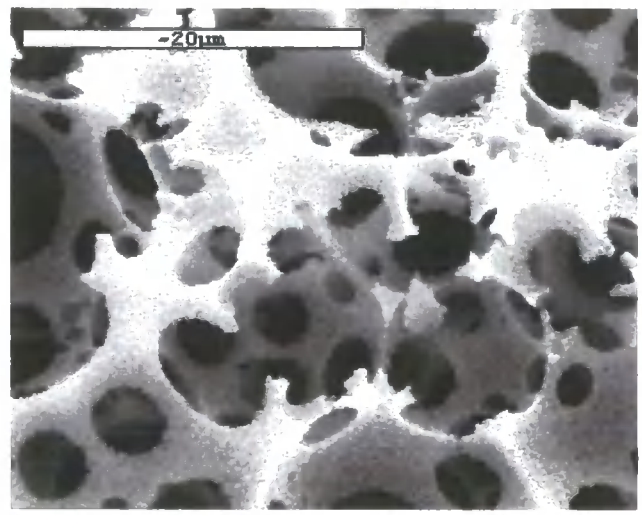

Literature Review

Chapter 2

2 LITERATURE REVIEW

2.1 Tissue Engineering Using Biodegradable Networks

Tissue engineering is the process by which natural tissue is formed within an artificial support matrix to re-establish the missing organ function. The two ways to achieve cell transplantation are either to seed cells into a porous material or to induce / rely on ingrowth of cells and tissue into the support material (tissue induction). Transplanted cells can be obtained from one of 3 sources: autogeneic (same genotype); allogeneic (same species, different genotype); xenogeneic (a different species). If the cells in need of replacing are capable of proliferation, a small number can be harvested and their number increased in vitro. In the case of organ failure from genetic disease, in the future, gene therapy may allow correction of the abnormality, expansion and re-implanting. Both allogeneic or xenogeneic cell types involve suppression of rejection of non-genotype cells. For proliferation, cells need a temporary substrate until they secrete their own ECM. A great deal of research has been focused on developing degradable scaffolds and cell culture on these scaffolds.

The first example of tissue engineering can be dated back to 1933 when Bisceglie produced evidence for the survival of mouse tumour cells surrounded by a polymer membrane and implanted into the abdominal cavity of chick embryos [4]. The concept of replacing one tissue by another can be traced back further to the 16th century; Tagliacozzi reported construction of a nose replacement from a forearm flap [5]. Joseph and Charles Vacanti feel that the ultimate goal for tissue engineering would be 'to create large cell banks composed of universal cells that would be immunologically transparent to any

individual.... accepted by any individual or...stem cell reservoirs...differentiate into differing lineages for specific structural applications [5].

In 1954, Joseph Murray MD performed the first successful organ transplant, a kidney [6]. The achievement marked a new era for medicine and surgery. Renal and bone marrow transplantation evolved rapidly over the following 25 years, but transplantation of other organs remained experimental until the late 1970s when it underwent an explosive growth upon improvement of things such as monitoring and control of organ rejection and anaesthetic techniques. Whilst organ transplantation is responsible for saving many lives every year, it is increasingly unlikely that demand can ever match the need. In 1985, Paul Russell wrote an article on cell transplantation [7]. The paper visualised that if a way could be found to transplant only the necessary cellular elements needed for functioning it would hold a conceptual advantage. Earlier, in the 1970s, John Burke MD had been searching for a solution to the problem of massive burn wounds, due to the lack of availability of donor skin. He began to formulate an idea to tackle this problem and went on to produce the first method of manufacturing a matrix of neodermis from natural elements, collagen and glycosaminoglycans. Burke and his colleagues managed to use natural substances to create a new organ in two dimensions. By 1983, a number of commercially produced synthetic skins / wound dressings were available. The best known at the time were IP-758, Epigard®, Biobrane®, Hydron® and Op-site. Gogolewski and Pennings [8] produced an artificial skin based on a polylactide / polyurethane mix cast as a film with pores from 40 to 200 μm to facilitate tissue ingrowth. Because the degradable polymer layer would undergo partial swelling it had to be strongly attached to the non-degradable, medical grade silicone that was present to protect the wound from bacterial invasion but allow water vapour transport.

In 1986 surgeon Joseph Vacanti made an inspirational connection that allowed the first step towards a long-term goal he and a colleague Robert Langer, a biomedical engineer, had been working on for more than a year. They had been attempting to grow thick layers of tissue in the laboratory using biodegradable polymers as a support matrix. As the thickness of tissue developed the interior cells were unable to uptake nutrients or oxygen or rid themselves of carbon dioxide. They were therefore not able to produce a thickness of tissue viable towards their future goal of growing replacements for damaged tissue and ultimately organs. Whilst on holiday in Cape Cod, Vacanti spotted floating seaweed branches soaking up nutrients from the sea - nature utilises branching as a way of supplying nutrients to thick tissues [6].

From the above early work Vacanti and colleagues began to wonder whether they could transfer the principle of the two-dimension organ growth to three dimensions. Russell's paper in 1985 [7] reported harvesting cells, dispersing them in a suspension and inoculating them into various tissues. In order to avoid damaging or usurping the tissue, Demetriou and coworkers in 1986 reported using inert micro carrier bead supports coated with extracellular matrix proteins to support hepatocytes (liver cells)[9]. Whilst partially successful, the method left unresolved questions concerning long-term cell survival and definitive cellular functioning.

Vacanti in 1988 reported the first successful attachment of liver, intestine and pancreatic cells into bio-erodable (biodegradable) polymer scaffolds that were then implanted into animals [10]. They termed this method of cell transplantation, 'chimeric neomorphogenesis'. Three synthetic absorbable polymers were used to fabricate the branching fibre scaffolds, PLGA, polyorthoesters and polyanhydride.

In 1990, a group of scientists from the Netherlands were looking into the use of porous biodegradable polymers as implants in meniscus reconstruction [11]. Menisci play an important role in the function of the knee joint. They constructed porous foams using a freeze drying / salt-leaching technique from PLL. They noted that the size, interconnectivity and total volume of pores were very important for meniscus reconstruction and also, sensibly, that the products produced during degradation of the polymer should be non-toxic.

A review paper in 1991 from Vacanti, Langer et al covered the work up to that time in developing novel matrices for cell transplantation and associated problems [12]. The work focused on developing matrices for liver and cartilage cells. Even though cartilage is composed of only one cell type and is avascular and liver is comprised of several cell types that are highly vascularised (parenchymal cells are no more than one cell away from the blood supply), the approach for developing a suitable matrix was the same. The material should

I be biocompatible, i.e. does not provoke a connective tissue response,

II be resorbable to leave a completely natural tissue replacement,

III be processable into a variety of 3D structures capable of retaining its structure once implanted and

IV have a surface that should interact with the cells to allow retention of differentiated function and promote growth where necessary.

Attempts to use non-reabsorbable materials had proved unsuccessful for reasons such as promotion of undesired connective tissue response and a permanent risk of infection [1].

Scheme 2.1 Latides to Polylactides

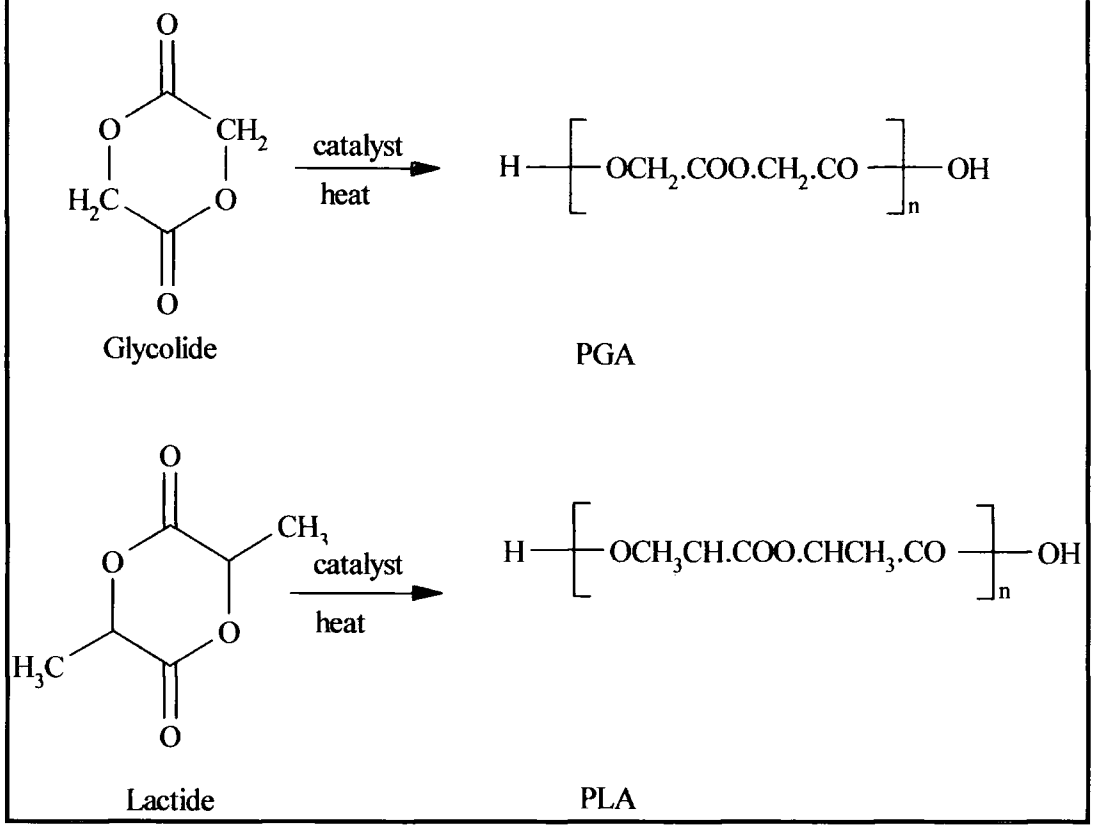

Synthetic polymers proved to have a number of advantages over natural polymers such as collagen, including processability, biocompatibility and degradability. The FDA had already approved the use of PLA and PGA (Scheme 2.3) and their copolymers, PLGA for use in suture materials, support fabrics and controlled release devices. They also met with the above 4 criteria. Using melt and solvent techniques they could be processed into a number of configurations. Degradation by hydrolysis yielded natural metabolic intermediates. By varying the relative ratio of the monomers the rate of reabsorption could be varied from months to years. From a morphological point of view, an open structure of high porosity was deemed necessary for nutrient transport. For

significant cell / polymer interactions, a high surface area to volume ratio was significant. Optimal average pore size / interstitial space varied for different cell types. Avascular tissue like cartilage could tolerate a wide pore size range whilst liver tissue required pores with a minimum diameter of 60μm. Early work had to use two-dimensional fibre meshes since the three-dimensional structures made from the chosen polyesters were not commercially available. At the time of the paper (1988) a number of limitations had been identified using the fibre-based matrices, for example they compressed together under pressure. The environment dictated the shape of the mesh because the fibres had little structural strength. In the case of the liver cells it was also believed that the curvature of the fibres was hindering the cell-substrate interactions. Two novel approaches were therefore employed to produce

I a composite matrix based on the fibre mesh, using a second polymer to provide a mechanically stable structure,

II a monolithic sponge like structure produced by a particulate / leaching technique.

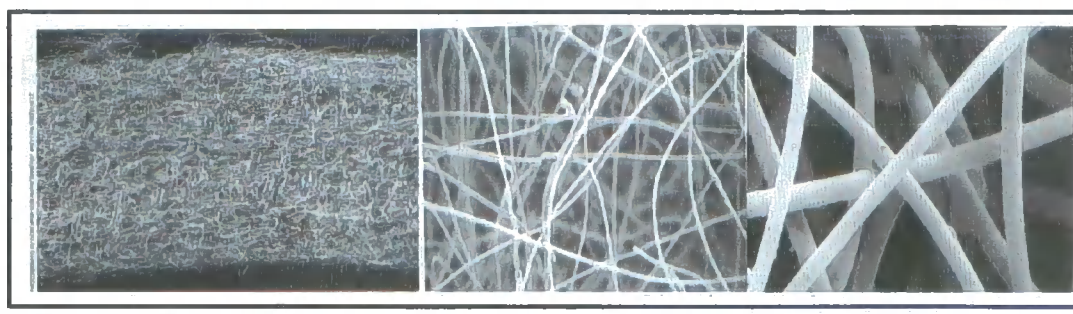

Figure 2.1 Biodegradable Polymer Mesh Shown at Increasing Magnification [13]

Vacanti et al [14] reported the first case in which a stable mature cartilage was created in soft tissue not adjacent to native bone or cartilage using a synthetic polymer

matrix. They showed that chondrocytes (cartilage cells) did adhere to the synthetic biodegradable matrix and performed differentiated functions in vitro. Following successful surgical implementation into nude mice, the new cartilage matured with time, maintaining the approximate configuration and dimension of the matrix. They concluded the technology would be useful for plastic and reconstructive surgery as well as for replacing cartilage.

A second summary paper [15] in 1993 from J. Vacanti and Langer reported the following updates on tissue engineering. *Nervous* - the use of natural and synthetic polymers to enhance nerve regeneration. Where nerve injury resulted in a gap that was too wide for natural healing the polymer would act as a nerve guide either protecting the regenerating nerve from scar tissue or directing it toward the target [16]. *Cornea* - the successful growth of cornea using corneal epithelial cells on polyvinyl alcohol hydrogels and transplantation onto rabbit corneas has sparked long term studies [17]. *Skin* – there have been many advances in providing suitable skin graft material. One approach used a degradable PGA mesh and human neonatal dermal fibroblasts. Clinical trials showed good graft acceptance and no evidence of immune rejection [18]. *Liver* – researchers were looking at procedures for liver replacement that used isolated hepatocytes attached to polymer networks [19]. *Pancreas* – the approach reported was to take a tubular membrane coiled in a housing that contained islets. The membrane was connected to a polymer graft that was connected to blood vessels [20]. *Tubular Structures* – e.g. ureter, bladder and urethra. Cell polymer implants had been explored as replacement therapy e.g. urothelial cells had been seeded onto degradable PGA tubes and implanted into rats and rabbits [21]. In a further example, copolymer tubes made of lactic and glycolic acids were used to replace a 5cm portion of esophageal tubing in dogs. In time the polymer was

shown to degrade and was replaced by new tissue growth, the dogs were capable of drinking and eating semisolid food [22]. *Cartilage, bone and muscle* – collagen-glycosaminoglycan templates were being used to create new cartilage tissue [23]. In mice, chondrocytes were grown on highly porous scaffolds of PGA or PLA and retained their three dimensional structure over a period of 6 months [24]. Attempts to replace bone pieces with synthetic and natural polymers for the purpose of repair had met with problems due to optimal strength and degradation properties. Attempts to use synthetic polymers to induce bone growth have met with greater success [25]. *Blood vessels and cells* – this is an active area of research and development must take into account the prevention of scarring and clotting. One idea was to line polymers (no type given) *in vitro* with endothelial cells. Polymers (again none specified) were also being considered because their surfaces could be modified by chemical means e.g. protein adsorption that would be useful for interaction with cells [26].

Continuing research by Vacanti et al [27,28] looked at chondrocyte growth *in vitro* on PGA and PLLA foam scaffolds. They established that, *in vivo* for a period of up to 6 months, the chondrocytes maintained the shape of the original scaffold and resulted in cartilage formation. They also produced laminated three-dimensional foams using a novel contour mapping process.

PLLA and poly (DL-lactic-co-glycolic acid) polymers were known to be hydrophobic [29]. This was leading to an insufficient cell mass as a majority of the pores were remaining empty. For the creation of tissue, it is important to obtain an even distribution of cells throughout the volume of the foam. In an earlier study [14],

prewetting of the foam with ethanol had produced a uniform cell distribution. A two-step immersion process of water and ethanol caused no swelling or shrinkage of the polymer foams and subsequently led to improved tissue growth.

Two studies by Ishaug-Riley et al [30, 31] used three dimensional porous PLGA foams to form a calcified bone-like tissue *in vitro* from rat stromal osteoblasts. A range of pore sizes within the foam from 150 – 710 μm did not hinder cell growth. In the second study growth of fibrovascular tissue improved the depth of cell growth into the foam, probably by providing metabolic requirements.

In 1994, Whang et al [32] developed an emulsion freeze-drying technique to develop PLGA foam scaffolds. Their technique removed the need for monomers, crosslinkers (such as divinylbenzene) and surfactants that would not be acceptable for medical uses.

Work published by Thomson, Wake et al in 1995 [33] summed up the aims and problems experienced by researchers looking at regenerating a number of organs - cartilage, bone, urothelium, intestine, nerve and liver. Initial studies for cartilage used a degradable PGA scaffold of fibres or fibre-based felt. *In vitro* and *in vivo* studies demonstrated the adherence of chondrocyte cells to the matrix, proliferation and maintenance of differentiated function. The polymer showed degradation in a 7 week period and longer studies showed the cells mimicked a structure similar to that of the scaffold. Further studies that used PLLA scaffolds, while successful, produced less proliferation and differentiated function. Bone is capable of self-regeneration, consequently many researchers have followed the pathway of tissue induction. Scaffolds have been formed from PPLA, PLGA and PGA and have been shown to be useful as substrates for osteoblasts, but experiments have only been performed in non-load bearing

situations. Vicryl (a knitted mesh of polylactin) fibres seeded with foetal rat intestinal cells formed the first study for the intestine. Still in its early stages, the authors felt that PGA fibres could provide an alternative to existing techniques, although no indication of these were given. In the quest to replace damaged brain tissue, porous non-degradable hydrogels were cross-linked around astrocytes and undifferentiated neurones. The entrapped cells in an *in vitro* environment achieved normal differentiation and maturation.

The above mentioned article also introduces the concept of prevascularisation of scaffolds. Natural metabolic organs have their own supply of capillary networks. These capillaries are responsible for the transport of essential nutrients and removal of waste. Their absence in scaffolds can lead to cell death in the centre of the matrix. Studies using PLLA and PLGA foams found that high porosity and / or a large pore size supported increased vascular tissue ingrowth. It was also found that growth was faster in the crystalline than amorphous parts of the polymer scaffold. The main drawback of this work was that space filled by a vascularisation system had reduced the availability for cell seeding.

Finally, the paper summarises the use of tissue induction for skin, nerve, oesophagus, ligaments and bone. Nerve, repairing gaps in sciatic nerves using PGA fibres formed into a u-shape with a flat cover; oesophagus, using a stent, a silicone tube coated with a porous collagen sponge, tissue growth was induced and completed within 4 – 5 weeks. Stenosis was a major drawback that needs to be solved before functional replacement can occur.

Work by Han and Hubbell [34] adopted a different approach to synthesising scaffolds. When using polymers to form scaffolds, there is no biospecific interaction

with cells, so many scaffolds can support the growth of a number of cell types. PEG has been shown to reduce protein absorption and this paper looks at incorporating PEG into a biodegradable network to reduce protein formation leading to cell adherence. PEG has: low interfacial free energy with water; a lack of binding sites for proteins; high chain mobility and steric stabilisation effects, all of which contribute to its ability to reduce protein formation. In the future, these scaffolds could be coated with or have incorporated specific peptide ligands, RGD, tyrosine-isoleucine-glycine-serine-argenine in laminin*.

Continued research in 1997 into ways to achieve bone replacements showed that PLGA foams were capable of supporting both cell proliferation and differentiation functions. This was demonstrated by an increase in acitivity of both DNA and alkaline phosphatase [35].

Work by Li et al. [36] looked at using PVA foams as encapsulation devices for dopamine-secreting cells as a possible treatment for Parkinson's disease. An internal matrix provided support for cell growth with an outer permselective membrane that allowed transport of metabolites and other small molecules while preventing immune cell contact. In the absence of an internal matrix, the cells adhere to one another forming large clusters and necrotic regions. Previous studies used no matrix, sodium alginate or precipitated chitosan. Li's study compared a chitosan and PVA foam matrix. *In vitro* studies showed a 10-fold increase in catecholamines for the foam over the chitosan matrix. *In vivo* studies showed no difference however the foam scaffold did appear to control cell proliferation and maintain higher cell viability, reducing areas of necrotic cells.

* a large fibrous protein, major component of the basal lamina, a thin sheet of ECM underlying the epithelia

A comprehensive review in Scientific American highlighted the research up to 1999. The first article in the review [37] looked at the use of injectable biodegradable polymers for orthopedic applications. The polymers used could be moulded to fill even irregular shaped defects; they provided a skeletal structure with similar mechanical properties to the bone they were replacing, allowing new bone to fill the space as the polymer degraded. Another research group seeded three dimensional polymer scaffolds with plasmids. When inserted into animals the DNA from the plasmids found their way into the cells as they migrated into the scaffold, expressing chosen proteins. This paves the way for precisely controlling tissue formation. The work pioneered by Langer and Vacanti in the 1980's of growing neoorgans on three dimensional scaffolds in the body

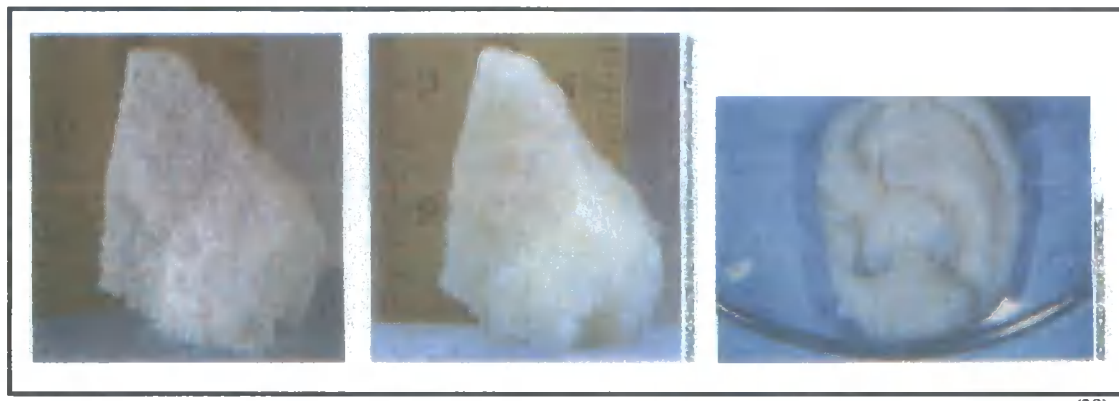

Figure 2.2 Photographs of nose and ear cartilage grown on 3D polymer scaffolds [38]

rather than an artificial, external environment is currently in clinical use in patients with skin wounds (Transcyte which received FDA approval for use in the U.S. in 1997) [39]. Also, in the treatment of cartilage damage, regulatory approval has been won by a Massachusetts company for Carticel, a replacement for damaged knee cartilage [37]. A group of researchers from Carolinas Medical Centre are looking at applying tissue engineering to a major women's health issue. They are attempting to grow replacement breast tissue. Whilst the breast would not contain the complex numerous cell types, it

would contain soft tissue mass possibly suitable for providing an alternative to breast prosthesis and implants. For the next few years, it is likely that less complex tissues such as cartilage, bone and skin will dominate the success stories. However, work by Vacanti et al [6] has developed sufficiently to allow growth of liver-like tissue and to allow drug delivery in order to promote growth of transplanted cells. For now only single chemical functions of the liver can be replaced. A group at the university of Toronto [6] are working towards the goal of growing a heart. It is likely that heart valves and blood vessels will become available in the near future but whole organs such as the liver and heart could take up to 20 years.

A second article in the Scientific American special report [40] looked at creating new materials. Tissue engineering is concerning itself with trying to create biodegradable materials that reduce / do not induce scar tissue formation. To date synthetic materials provide advantages because their strength, degradation rate, microstructure and permeability can be controlled however cells still adhere more easily to natural materials. By taking artificial materials and providing regions of biological activity, researchers are attempting to combine the best of both worlds. Fibronectin is an extracellular matrix protein, one of its components is a polymer composed of 3 amino acids (RGD – arginine, glycine and asparagine respectively) which many cell types can bind to. By introducing RGD into a polymer it is hoped to provide a more natural environment for cell growth. Tissue engineered nerves are the target of a group of researchers. They are attempting to produce polymers capable of conducting electricity in an attempt to produce tissue engineered nerves.

In February 1999, a group of researchers headed by A. Atala realised a nine-year goal and reported the successful growth, implantation and acceptance of an artificially

grown urinary bladder that appeared to function normally [41]. A bladder-shaped mould was composed and on the outside, smooth muscle cells were seeded following urothelial cells applied to the inside. Following 7 days nurturing the synthetic organ, they replaced 6 beagle bladders with the neoorgans. Within 3 months the polymer had degraded, and blood vessels were supplied to the bladder tissue. The shape of the bladder was normal; the neo-organs held a normal quantity of urine and the dogs were capable of 'emptying themselves'. A second set of researchers headed by Niklason in Durham, North Carolina also reported the growing of functioning pig arteries [6]. The article finished with the quote "...anyone in tissue engineering....., believes that any tissue or organ can be grown outside the body".

The new millennium heralds tissue engineering in the 21st century. A paper by JP Vacanti et al [42] summarises his group's demonstration of how polymer scaffolds have been utilised for the reconstruction of the following tissues: liver; intestines; heart valve leaflets; bone; cartilage; over the previous decade. *Liver* – treatment of end-stage liver disease. Hepatocytes require a steady oxygen and nutrient supply to meet their high metabolic requirements and the scaffold needs to ensure survival of an adequate mass of transplanted cells in order to restore liver function. *In vivo* the scaffold should also be structured to allow reorganisation of the hepatocytes and neovascularisation from surrounding tissue, to ensure long-term survival of the cells and therefore, function of the tissue. The group, therefore, fabricated a tube scaffold from non-woven PGA fibre mesh sheets, spraying the outer surface with 5% PLGA chloroform solution [43]. A technique – three-dimensional printing can be used to form any required shape or size by selectively directing a solvent onto polymer powder packed with sodium chloride particles

(45 to150 μm) it utilises very thin two-dimensional slices to build complex 3D structures [44]. In order to provide an adequate blood supply to the cells they are exploiting MEMS, using semiconductor wafer process technology developed for the computer industry [45]. A proposed second solution to increase the blood supply to the matrix and, therefore growing tissue, would be to provide direct access from the portal vein to the polymer scaffold [46]. *Small Intestine Regeneration* – treatment of short bowel syndrome. They first developed an intestinal epithelial organoid unit comprising of 'a villus structure with an overlining epithelium and a core of stromal cells', a villus being a hair or finger like structure. This unit was then seeded onto a nonwoven PGA fibre, tubular scaffold. The tissue engineered intestine, *in vivo*, was shown to increase in size for up to 36 weeks and contained villus with increased number, height and surface length compared to controls [47]. Current work is now focusing on the functions of the neoorgan, e.g. absorption and neural innervation.

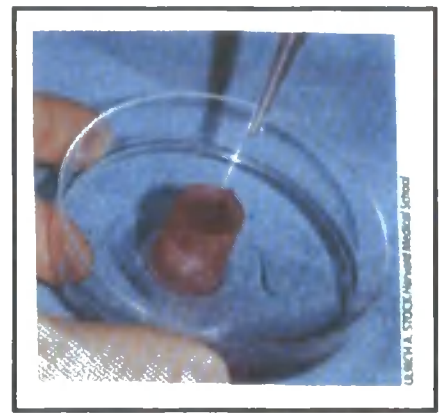

Figure 2.3 Biodegradable Heart Valve being seeded with cells From the lining of a sheep blood vessel [13]

Heart Valve Leaflets – treatment for valvular heart disorder. Leaflets were constructed from a composite, laminated structure, the outer layers of which was a non-woven mesh of PGA and the inner a woven mesh of PLGA. The outer layers sandwiched the inner

and were thermally fused at multiple points. Experiments used low-density lipoprotein negative cells seeded over 12 days. Examination of the implanted leaflets showed they were thicker and constrained in movement compared to native leaflets but showed no signs of stenosis* [48]. *Bone and Capillary* – the reconstruction of a human digit. The study used osteoblastic cells, chondrocytes and tenocytes to create a whole joint. Firstly the periosteum (a covering of areolar connective tissue) was placed on the PGA in the scaffold. From the periosteum, periosteal cells migrated, attached and spread generating bone. Chondrocytes and tenocytes were then seeded into the scaffold and shown to produce cartilage and tendon tissue respectively, growing in both the PGA and PLA parts of the fibrous mesh. The polymers were cross-linked to help the scaffold retain specific shapes. After 5 months, dissection of the implants showed formation of new tissue with the shape of human phalanges and joints [49].

Stock and Vacanti have recorded the current research studies and progress to date[50]. The tissue types and stages are shown in Table 2.1:

Table 2.1 Progression to date of tissue engineering studies

Tissue	In vitro studies	Preclinical – in vivo studies	Clinical Studies
Bladder		☆	
Blood vessels		☆	
Bone		☆	
Cartilage – joints + urethral sphincter			☆
Ear		☆	
Eye	☆		
Genitals		☆	

* narrowing or constriction of any duct, orifice or tubular passage often as a result of disease

Tissue	In vitro studies	Preclinical – in vivo studies	Clinical Studies
Heart muscle		☆	
Heart valves		☆	
Intestine		☆	
Joints		☆	
Kidney		☆	
Liver		☆	
Meniscus		☆	
Oral mucosa		☆	
Ureter		☆	
Urethra		☆	
Nerves (peripheral)		☆	
Pancreas		☆	
Salivary gland		☆	
Skin			☆
Spinal cord		☆	
Trachea		☆	

2.2 Biodegradable Networks

The potential of PGA as a low cost tough fibre-forming polymer was established in 1954 [51]. Attempts had been made to copolymerise it to increase its hydrolytic instability but always resulted in a comparably inferior product. The addition of small amounts of PGA to PET introduced weak links that were capable of changing the surface finish of fibres. In 1962, a company, American Cyanamid Co., developed the first synthetic absorbable suture using PGA, Dexon®, which became commercially available in 1970. Du Pont also considered PLA for the same application. PGA, PLA and their copolymers PGLA as a result of Dexon®, were used in the development of biodegradable

materials for dental and orthopaedic surgery applications and also drug delivery. Until 1979 no basic information concerning molecular, compositional and morphological information for this class of polymers was available from open literature. Gilding and Reed proved that homo and copolymers of glycolic and lactic acids were achievable. The crystallinity of PGA was approximately 50% compared to 37% for PLLA. For copolymers of PGLA where GA comprised 25 – 70 mol%, the structure was amorphous.

In 1983, Gogolewski and Pennings, as previously introduced, used the biodegradable copolymer PLA / polyurethane as a biodegradable artificial skin [8]. The membrane was composed of 2 layers. The under layer to be exposed to the wound composed of biodegradable PLA / polyurethane and the upper-layer of a medical-grade silicon rubber to protect against bacteria. The artificial skin worked by allowing tissue in-growth through the PLA / polyurethane's pores (40 - 200μm), the layer would degrade by hydrolysis to be replaced by the new connective tissue. Once the wound healed the protective silicone layer could be stripped off.

By 1993 other aliphatic polyesters had also found their way into the biodegradable materials field, polydioxane, PCL, PTMC and their co- and terpolymers [52]. The semi-crystalline morphology of the above polymers is well suited for applications as fibres. For tissue scaffolds and fixation devices, a more rigid construct was necessary, this required composite structures. The composite structure contained directionally reinforced fibres embedded in a matrix or a cross-linked network of liquid polyester pre-polymers. Difficulty arose in finding suitable cross-linking chemistry. It was decided a totally polyester network would be ideal. Storey and Hickey proposed using epoxy-terminated polyester oligomers with amine or anhydride cross-linkers [52]. However, care was needed to avoid toxic amine linkages.

Storey et al were looking at developing bio-absorbable polymer networks by endcapping 3-arm polyesters (PCL) using methacryloyl chloride [53]. The aim was to cross-link the methacrylate-endcapped polyesters. Whilst ester and anhydride linkages hydrolyse to easily absorbed free acids and alcohols, the remaining hydrocarbon chains may have been proved difficult, even impossible to absorb. Work by Bailey et al (see chapter 3) on ring opening of cyclic ketene acetals paved the way to the possibility of producing completely bio-absorbable networks. Storey et al were, therefore also attempting as a secondary objective, to copolymerise the methacrylate-endcapped polyesters with one such cyclic ketene acetal, to produce a completely bio-absorbable network. A pre-polymer, i.e. the endcapped polyester, PCL, was successfully homo- and copolymerised with methyl methacrylate and styrene. Co-polymerisation with the cyclic ketene acetal was unsuccessful; it was believed that a higher curing temperature was needed. Using PDLL, successful homo- and copolymerisation were achieved with both methyl methacrylate and styrene. Therefore methacrylate-terminated polyesters were established as viable intermediates for forming biodegradable networks.

Published in 1995 [32], Whang et al introduced a novel method of fabricating bio-absorbable scaffolds. Scaffolds were fabricated using PLGA with porosities in excess of 90% and average pore sizes in 2 ranges, 15 -35μm's and greater than 200μm's. Increases in the volume fraction of the dispersed phase and inherent viscosity increased the average pore size. Previous methods for formation of biodegradable scaffolds included solvent casting / salt leaching, dating back to 1982. A solid such as sodium chloride salt or saccharose crystals are sieved into polymer particles or a polymer solvent solution. After freeze-drying, water is used to leach out the solid particles, leaving a porous material. Porosity can vary from 87% to 91% and pore size is very varied and dependent on the

size of particles used. For saccharose the pore size would be between 150 - 300μm [54]. Another preparation technique is phase separation, which was developed in the 1980s. The polymer is dissolved in a suitable solvent, placed in a mould and rapidly frozen. The solvent is removed by freeze-drying and sublimation preserves the morphology, leaving again a porous material. The size of the pores is very well defined and determined by the separation process. A liquid-liquid phase separated system before freezing gives small pores between 1 - 20μm's, where as a liquid-solid system gives larger pores of 100μm's [55]. The new method Whang et al developed uses an "emulsion freeze-drying technique".

In the same year, a review article describes tissue engineering, the types of materials and methods of forming degradable scaffolds [33]. It reiterates many statements made in previous papers as well as introducing a few new ideas. The purpose of the scaffold is to organise and direct the growth of cells and promote the formation of their own ECM. Porous structures with good interconnected pore morphology achieve such a role. High porosity and surface area are necessary to provide a large void volume to seed cells and upon which they can attach themselves. A high surface area is indicative of a small pore diameter, however, a constraint is placed by the minimum pore size a cell in suspension can penetrate $\approx$ 10μm.

As a result of their biocompatibility, i.e. they do not cause an adverse reaction from patients' immune systems [33], metals, ceramics and polymers have all been employed in biomedical applications ranging from hip prostheses to artificial hearts. The following are given as essential criteria for a successful scaffold:

1. A surface property capable of promoting cell adhesion, proliferation and differentiation.
2. To be biodegradable with a controllable degradation rate.
3. To be biocompatible with the products of degradation being able to be excreted via physiologic metabolic pathways.
4. Possessing a high surface area / volume ratio.
5. The material should be easily processable into 3-dimensional shapes often of irregular geometry.
6. Have mechanical properties sufficient to withstand any in vivo stresses.

Point (2) rules out the use of all metals and most ceramics, while some ceramics do degrade, their rate is not currently controllable and they are difficult to process. Many natural and synthetic polymers meet the criteria, with the latter possessing the greater adaptability because they can be tailored towards specific applications. The main favourable and unfavourable points of both types of polymer have been tabulated in Table 2.2.

The work by Mikos et al. [33] is concerned with 3 main synthetic polymers. PGA is highly crystalline and hydrophilic and its degradation rate is dependent on the crystallinity of the polymer; PLLA is less crystalline, more hydrophobic and very strong. The degradation rate is affected by hydrophobicity and steric hindrance from its backbone methyl groups; PLGA is amorphous for glycolic acid contents between 25 and 75%. Varying the ratio of lactic to glycolic acid can control the degradation rate. All of these are approved by the FDA for use in biomedical applications.

Table 2.2 Advantages and disadvantages of natural versus synthetic polymers

Natural Polymers	Synthetic polymers
POSITIVE ATTRIBUTES:	
1. Highly organised structure (both at molecular and microscopic levels)	1. Varying control of Mw and its distribution affects e.g. strength and degradation rate
2. Strength	2. Degradation generally by hydrolysis – constant for all individuals and animals
3. Ability to induce tissue in-growth	3. Copolymers – monomer ratio controls degradation
4. Polypeptides – important to cell adhesion and function through amino acid sequences	4. More easily processable
NEGATIVE ATTRIBUTES:	
1. Immunogenecity – stimulation of immune response, possibly rejection	1. Release of toxic levels of acid from for e.g. PLLA & PGA. By varying high and low Mw's in scaffold can attempt to release acid over time
2. Degrade enzymatically – rates vary for individuals	

Following on from Whang and coworkers, further methods for forming scaffolds have been described. One such method is fibre bonding. PGA has been commercially available for many years as long fibres for use as biodegradable suture material [32]. Whilst providing a large surface area to volume ratio, the fibres had little structural stability. Initially PLLA was dissolved in methylene chloride* and applied to the PGA. Following removal of the solvent, the PLLA – PGA was heated above PGA's melting point to fuse where the fibres were crossed. After quenching the PLLA was removed leaving bonded PGA fibres. The technique however does not lend itself to all polymers and the control of porosity and pore size were not possible. Since then a second method,

* Methylene chloride is a non-solvent for PGA

that involved spray coating with an atomised PLLA or PLGA solution, has solved the first problem. Tubing can be formed in this way and has been proposed for use in intestine regeneration. For the solvent casting / particle leaching methods the main disadvantage in the production of three-dimensional scaffolds is that it can only be used to produce scaffolds (membranes) of a maximum 2mm thickness. A way around this problem would be to use membrane lamination. This can be achieved by forming a contour plot of the desired three-dimensional structure. Chloroform can be used to bond subsequent layers cut to the shape of the contours from the membranes. A structure with properties identical to each membrane with no observable boundaries was synthesised. The final method described was melt moulding. Scaffolds were formed by mixing PLGA powder and sieved gelatine microspheres. Placed in a mould, the polymer was melted and then the gelatine was removed by leaching in distilled-deionised water. Porosity would be controlled by the amount of gelatine and the pore size by the size of gelatine particles.

Langer and co-workers reported a method to synthesise polymers to interact bio-specifically with cells [56, 57]. They copolymerised lactide and a 6-membered cyclic co-monomer containing lysine via anionic ring opening polymerisation. The presence of an amine group on the side chain of the lysyl residue could be used to attach, for example, RGD to induce cell adhesion.

In 1996, poly (α-hydroxy esters) e.g. PLA and PLGA / PGLA were being investigated for the regeneration of several tissue types, e.g. cartilage, bone, liver and intestine [58]. Any biodegradable matrix to be used as a scaffold, in addition to the features mentioned previously must also aid cell proliferation and differentiation. Each tissue type also requires individual physical properties, pore morphology, porosity,

degradation rate and also varying mechanical properties. The rate of fibrovascular in growth is determined by pore morphology. Tissue grows faster on large interconnecting pores, important for skin and intestine tissue. The mechanical strength is significant for bone regeneration. Intestine and blood vessels require a pliable tubular scaffold while non-tubular soft tissue e.g. skin requires a flexible matrix that can be contoured. Conley et al. were investigating PLGA and PEG blends because of their enhanced hydrophilicity and flexibility. Foams were made using a solvent-casting and particulate leaching technique. These foams produced a large interconnecting network of large pore configurations (median diameters 71 - 154μm). The foams they produced would be best suited to soft tissue requiring rapid and complete vascularisation e.g. skin or intestine.

Synthetic PVA foam is available under the tradename Ivalon®; its past use has been as an implant in plastic, reconstructive and cardiovascular surgery but has been replaced by biodegradable polymers [36]. Li and co-workers looked at using it in an encapsulation device. The device works by capturing xenogeneic or allogeneic cells* within a semi-permeable polymer membrane. Previous matrices had used collagen, natural polysaccharides e.g. agarose and alginate and water-insoluble polyacrylates as hydrocolloids or hydrogels. However, while highly permeable in their natural state, once filled with cells, transport of metabolites was prevented, work by Li et al showed that using a foam could circumvent the problem.

As the success rate of seeding and growing cells on polymer scaffolds has become more apparent, it has been clear that the lack of an internal vascular system prevents a mass of cells growing, sufficient for transplantation. J.P. Vacanti and co-workers utilised a 3D printing system to insert channels into a porous scaffold. The process works by

* see beginning of section 2.1 for meaning of xenogeneic and allogenic

'selectively directing a solvent onto polymer powder packed with sodium chloride particles (45 to 150 μm) to build complex 3D structures as a series of very thin two-dimensional slices' [44].

A comparison of 2 non-woven scaffolds Ethisorb made from PGA / PLLA (90/10) and V 7-2 synthesised from pure PLLA, showed the importance of degradation time on the growth of chondrocytes [59]. The degradation times in vitro were 3 weeks and 6 weeks respectively. Experiments were also carried out on a fleece made from Agarose, however a decrease in the size of the scaffold made the material unsuitable for cartilage reconstruction in head and neck surgery. The paper by Rotter et al. states that previous studies had shown chondrocytes to have a tolerance for high levels of glycolic and lactic acid, the latter being more tolerated of the two. The materials were also favoured because of the ratio of high internal surface area to low quantities of biomaterial. The paper concludes that the PGLA material was more supportive of the chondrocyte phenotype, and induced comparable cartilage formation to native systems, while the PLLA – V 7-2 supported fibrocartilage growth rather than the chondrocyte phenotype. Therefore, the shorter degradation time of the PGLA material was suited to cartilage matrix products that were restrained by the more stable Ethisorb.

Biodegradable polymers were reviewed comprehensively in the literature recently [60]. In place of metal implants, approximately 40 different biodegradable polymers and copolymers were being used. The most widely used material for sutures were Dexon (made from PGA), Vicryl (from PGLA, 8% PLLA: 92%PGA) and PDS (poly (p-dioxanone)). The paper dates the use of PGA, PLA and PGLA back to the late 1960s. It was felt that the most significant and resourceful use for biodegradable polymers was as controlled drug delivery devices and that blends of 2 or 3 component materials denoted

an area of significant interest for the future. Other areas, which the paper noted would become of interest, were the use of low-molecular weight plasticisers and photoactive materials and blending of natural and synthetic materials.

The main group of synthetic polymers used to synthesise scaffolds have been covered already, besides collagen other natural polymers that have been utilised include alginate and hyaluronic acid [61]. The types of scaffolds so far covered have all been rigid in structure and require implanting surgically e.g. calcium alginate [62] and Pluronics, copolymers of PEO and PPO [63]. A suitably pliable scaffold could be injected removing the need for surgery. One way of accomplishing this would be to exploit the principle of lower critical solution phase separation. At or above a given lower critical solution temperature, any polymer exhibiting this property will phase separate. The accepted theory concerns the balance between the hydrophilic and hydrophobic components within a polymer chain and contributions from hydrogen bonding. A change in favour of conditions to polymer-polymer and water-water interactions from hydrogen bonding between polymer and water, results in a dehydrated hydrophobic structure from a hydrated hydrophilic one [61]. One such polymer exhibiting this characteristic, P(NIPAAm) has a lower critical solution temperature of approximately 32°C [64]. Above 32°C, the polymer chains form insoluble aggregates turning the solution turbid. The effect is reversible but at a considerably reduced rate. P(NIPAAm) can be cross-linked to form a hydrogel that above 32°C expels most of its pore water to become stiff and opaque. Copolymerisation with a hydrophilic monomer causes the phase separation to occur at a higher temperature and reduces the extent of aggregation, with a hydrophobic monomer having the opposite effect. Work by Stile and co-workers produced hydrogels

that phase-separated at 37°C and were injectable through a 2mm syringe; a hydrogel formed from copolymerisation of P(NIPAAm) with acrylic acid produced positive results when characterised using bovine articular chondrocytes [61]. The P(NIPAAm-co-AAc) hydrogel demonstrated a higher water content and less extensive volume change at 37°C.

The inorganic element of bone has been closely mimicked chemically in the ceramics hydroxyapatite and tricalcium phosphate [65]. Porous forms tend to be brittle and non-pliable. Alternatives have included the poly(α-hydroxy esters) described previously as well as poly(phosphazenes), poly(anhydrides) and poly(propylene fumarate). The most extensively studied of the four groups, PLGA was found to be limited in its uses due to the formation of acidic pockets upon degradation [66] and collapse when in culture conditions if not used with a sufficient binding agent [67]. They have also been seen to collapse when being sterilised using steam or ethylene oxide [65]. Goldsrein et al. report using PLGA foams of 6mm thickness, compared to the limit of 2mm previously quoted, prepared by solvent casting / particulate leaching. Characterisation showed that, with increasing weight percent of salt, although porosity increased, there was a decrease in the internal surface area and an observable increasing shrinkage of seeded foams to un-seeded foams. They suggested that foams used for growing osteoblasts had a maximum porosity of 80% as foams with higher porosity made using smaller NaCl particles (average 150 - 300μm) exhibited the above mentioned problems.

While work by many has been directed towards polyesters, other researchers have utilised saccharides, polysaccharides, fatty acids, α-amino acids and glycols. Huang and Ho have been looking at polymers derived from α-amino acids because of their variety of

structural features. They also offer an alternative to the high acid degradation products of polyesters, producing both acids and amines. They produced a variety of poly(amide-ester)s from dicarboxylic acids, glycols and α-amino acids with differing properties and degradability [68].

Most of the work covered so far, whether natural or synthetic, has concerned organic molecules. An article by Allcock et al. concerns polymers made from a mix of organic and inorganic molecules [69]. The structure was based on polyphosphazene, $[N=PR_2]_n$ (where R = for e.g. amino acid esters, glucosyl, glyceryl, glycolate or lactate, the polymer could be hydrolysed to phosphate, ammonia and the free side unit. The presence of groups such as aryloxy, fluoroalkoxy and alkyl ether could be used to inhibit or impede hydrolysis. By protecting and de-protecting the functional side groups the polymer can be cross-linked. If R is $-OC_6H_4COOH$, a hydrogel can be formed that can be water-soluble as a sodium or potassium salt or water-insoluble with a calcium counter ion [69], a phenomenon that can be utilised for microencapsulation devices.

The design of scaffolds relies mostly on trial and error; researchers Kohn et al. have constructed two-dimensional and three-dimensional grids that tabulate a range of chemical and physical characteristics of polymers that can be applied to potential musculoskeletal applications [70].

As researchers started looking at scaffolds for use in bone and cartilage repair, they adopted the mistaken belief that a suitable material to restore function would be one that possessed the mechanical strength and structure resembling that of the missing bone. Today with new knowledge of cell development and factors that regulate proliferation and differentiation, along with the technology to deliver these factors, bone and cartilage repair have become a fast changing discipline. Much research, some already covered, has

looked at seeding polymer scaffolds and while materials capable of supporting chondrocytes and oesteoblast formation exist [59, 55], none are capable of supporting the load bearing in an orthopaedic application. Many of the current scaffolds have the basic characteristic median pore size 250 – 300 μm with a range from 150 – 500 μm and porosity between 60 and 70%. Studies by Whang and co-workers [71] used PLGA scaffolds with a median pore size less than 50 μm and porosities in excess of 90%. They found that blood clot formation supported bone growth and that the growth occurred throughout the material rather than by a creeping healing process, this was found only to be viable where a scaffold was able to stabilise the clot (haematoma).

Scaffolds can be enhanced for bone growth in one of 2 ways: 1) addition of proteins e.g. FGF-2 which enhance vascularisation; 2) incorporation of demineralised bone known to activate osteoinductive factors. The commercially available product for the second method is, DFDBA, properties of which include promotion of bone formation and osteogenesis. Besides the scaffold structure, studies have also revealed that chondrocytes are sensitive to the surface of the material, [72, 73, 74] e.g. surface chemistry and roughness along with the mechanical environment imposed by the scaffold. Also the maturation state of the cells, when exposed to that surface has an effect on proliferation, differentiation and ECM production. Current research is effective enough to produce scaffolds for the purpose of cartilage growth for ears and noses, however there is still much to be done where load-bearing is a factor [75].

Collagen-based materials have been used as a means of arresting bleeding (haemostasis) for clinical applications and membranes for drug delivery systems [76]. Chevally and co-workers prepared collagen sponges using collagen extracted from dermis, which were washed with pH 7.8 phosphate buffer and distilled water before

swelling in dilute acetic acid. The collagen gel was then freeze-dried and thoroughly dehydrated. The growth of mouse fibroblasts was investigated on these and on similar foams that had been cross-linked with DPPA. 'Normal' sponges were seen to contract even before seeding due to the denaturing of collagen's triple helix an effect that had also been noted for reconstituted collagen sponges [77]. A second study by Chevally et al. showed that human fibroblasts demonstrated growth and biosynthetic activity on the afore mentioned materials, were on a par with 'normal' collagen sponges [78]. Attempts to expand the thermal stability have included the following [55], incorporation of glycosaminoglycans or chitosan [76]. Glutaraldehyde, hexamethyl-enediisocyanate and aluminium alginate/acetate were found to have negative effects on cell behaviour and were therefore unsuitable for crosslinking; however carbodiimide, polyepoxy compounds and an acylazide method, the latter developed by the authors, have all proven suitable.

Below is listed the minimum requirements needed of a biomaterial for government approval [79]

1. **Non-toxic (biosafe)**: - non-pyrogenic, non-haemolytic, chronically non-inflammative, non-allergenic, non-carcinogenic, non-teratogenic, etc.
2. **Effective**: - functionality, performance, durability etc.
3. **Sterilisable**: - ethylene oxide, γ-irradiation, electron beams, autoclave, dry heating, etc.
4. **Biocompatible**: - interfacially, mechanically and biologically.

The use of biodegradable polymers has reduced the importance of biocompatibility. Toxicity from unpolymerised monomer, surfactants, initiators, etc. could be a major concern, e.g. polyethylene and silicone can invoke thrombosis and engulfment by collagenous fibrous tissues [80].

Polymer meshes synthesised from poly (α-hydroxy acids) have been found to be hindered in smooth cell seeding by large spaces formed by intersecting strands and the hydrophobic nature of the polymer group. Collagen produces the opposite effect, but as has been previously stated, has no mechanical strength. A number of groups have, therefore, attempted to produce a hybrid [81]. From the work published in 2000, the result was an interconnected microporous collagen foam which could sandwich or overlap the polymer mesh (Vicryl in the case given). The hybrid was used successfully to grow human skin fibroblasts. As knowledge grows and techniques are developed, scaffolds are being designed, slowly but surely, to be more effective.

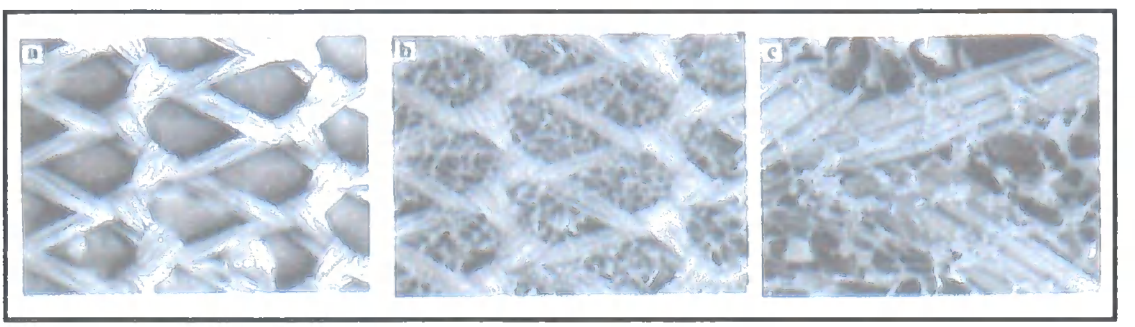

Figure 2.4 SEM pictures of Polylactin Mesh and its Hybrid Mesh with Collagen at (b) x 60 and (c) x 200 [81]

2.3 High Internal Phase Emulsions (HIPEs) and PolyHIPEs

An emulsion is defined as a mixture of two immiscible liquids, where one phase is dispersed as droplets within the other. Surfactant molecules adsorbed at the interface of the two phases provide stability and prevent the two phases separating [82]. The stability of an emulsion is represented by its resistance to form two separate phases [83, 84]. Aronson and Petko date initial investigations into concentrated emulsions back to the early part of last century [85]. Depending on the nature of the dispersed phase, emulsions can be oil-in-water (o/w) or water-in-oil (w/o). For conventional emulsions, the volume

fraction of the dispersed phase is lower than 74%. 74% represents the most efficient packing arrangement viable for identical spheres. In 1974, Lissant coined the phrase, high internal phase emulsions (HIPEs), for emulsions where the volume fraction of the dispersed phase was greater than 70% and more specifically 74.05% [86]. These emulsions also have a number of other names, high internal phase ratio emulsions (HIPRE), aphrons, biliquid foams, hydrocarbon gels and gel emulsions [85]. In HIPEs, the spheroidal droplets of the dispersed phase are deformed into polyhedra. The continuous phase forms a network of thin liquid films separating the dispersed phase, as seen in Fig. 2.5. Lissant and Mayhan showed using scanning electron microscopy that the droplets were polyhedral and relatively monodisperse in size [87].

Figure 2.5 Emulsions and HIPEs, packing of the Droplet Phase

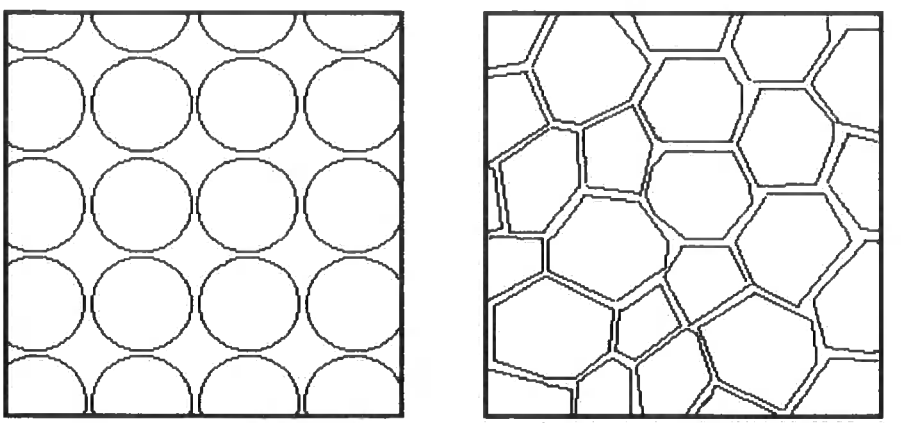

HIPEs are generally formed by the controlled addition of the internal phase to the external phase also containing the surfactant, under constant stirring. In HIPEs if either the oil phase is replaced by a hydrophobic monomer, or the water phase by a hydrophilic monomer, the resulting emulsion can be used as a precursor for preparing polymers [82].

Surfactants are molecules possessing both hydrophilic (water-loving) and hydrophobic (water-hating/ oil-loving) groups. They are classified in accordance with the charge on the part of the molecule that adsorbs to the interface, anionic, cationic, non-ionic or ampholytic. Surfactant molecules diffuse from the phase they are dissolved in, to the interface between two phases. The process of diffusion is affected by concentration of the solution and viscosity. The principal attraction between two or more droplets is van der Waals, long-range forces, which ionic surfactant molecules provide an electrostatic barrier against. By selecting a surfactant that is soluble only in the continuous phase, emulsion inversion is prevented thus allowing the formation of HIPEs. Non-ionic surfactants contain a hydrophilic polar head and in most cases the hydrophobic constituent is a long-chain hydrocarbon; an example of a nonionic surfactant is sorbitan monooleate, Figure. 2.6. The lengths of both surfactant components is variable leading to a variation in surfactant nature. It is also possible to use some polymeric materials as

Figure 2.6 Sorbitan monooleate (Span 80)

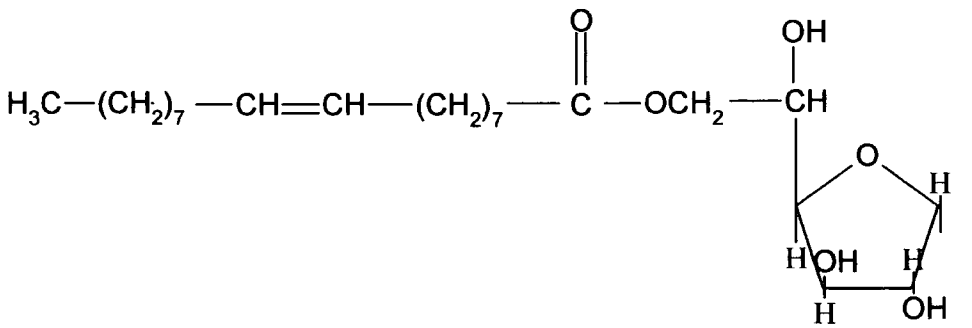

surfactants. Certain block copolymers consist of water-soluble hydrophilic blocks and organic compatible hydrophobic blocks. Such a range is available from ICI, Synperonic®. These consist of tri-block copolymers of poly (ethylene oxide) and poly (propylene oxide), Figure. 2.7.

Figure 2.7 PEO-PPO-PEO triblock copolymer surfactant

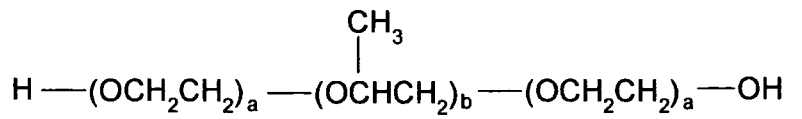

Surfactants, particularly non-ionics, can be classified by a HLB (hydrophile-lipophile balance) system introduced by Griffin in 1949 [58]. The HLB value assigned to a non-ionic surfactant can be related to the weight percentage of its hydrophilic element [88]. Surfactants are assigned a HLB value ranging from 0 – 30, hydrophobic surfactants are in the lower range, while hydrophilic surfactants have high numbers. Where a surfactant of intermediate value is required, 2 surfactants of a higher and lower value than the one

$$HLB_{mix} = \sum X_i (HLB_i)$$

that is required can be combined. The weight ratio of surfactants in the mixture can be calculated from the following formula [89]:

By substituting X_b=1 - X_a for surfactants HLB_a and HLB_b into the above formula:

$$X_a = \frac{HLB_{mix} - HLB_b}{HLB_a - HLB_b}$$

For all emulsions there will be an optimum HLB value. The HLB range over, which **w/o** emulsions can be formed, is very narrow and it has been shown that variation of surfactant HLB value within this range has little influence on emulsion stability [90]. In

contrast, there is a large range of HLB values that will form an **o/w** emulsion and pin pointing the optimum value is more important for maximum emulsion stability. The interactions generally associated with emulsions are van der Waals' forces, between the hydrocarbon chains of the surfactant and ion-dipole / dipole-dipole interactions between head groups. For Span 80 (Figure 2.6) the hydrocarbon chain would orientate on the oil side of the interface and the ring on the aqueous side. Repulsive forces between the surfactant head groups stabilise the emulsion. The ring also maintains a distance between one Span 80 molecule and the next at the interface. Shinoda and Freiberg noted that, as well as HLB number, the nature of the head and tail groups and the length of tail were important factors for stabilising emulsions [91]. These factors can help create a strong surfactant barrier stabilising the emulsion, for example, an increased number of head groups or a more polar group will produce a strong barrier.

There are 3 main processes that cause emulsion instability: coagulation (flocculation); coalescence; creaming [92]. By forming a thin film around the dispersed phase the surfactant provides a barrier against instability, lowering the interfacial energy. The tendency for inversion, i.e. the change from an **o/w** to a **w/o** emulsion, can be reduced by using a low volume of the dispersed phase. A monodisperse distribution of droplet sizes helps with emulsion stability by decreasing the chances of inversion. A high viscosity of the continuous phase can reduce creaming and coagulation by impeding Brownian motion, which allows emulsion droplets to come in to contact with one another. However, if the viscosity is too high then mixing of the two phases is prevented.

PolyHIPEs are formed by the polymerisation of the continuous (non-droplet) phase of a HIPE. Polymerisation around the dispersed phase droplets leaves each cell connected to all of its neighbours, although this is dependent on surfactant concentration

and ϕ. The removal of the dispersed phase from a polymerised HIPE leaves an open-cellular macroporous morphology of very low dry density. It is possible to control a number of the physical characteristics of PolyHIPEs. Cell size is defined by the stability of the emulsion. A smaller average droplet size results the longer the emulsion is agitated because of more efficient mixing. With **w/o** PolyHIPEs, salting out (the presence of salt in the aqueous phase which reduces its miscibility with the organic phase) prevents Ostwald ripening. Ostwald ripening is a process where the larger droplets grow at the expense of the smaller droplets [93]. This is because smaller droplets have a high surface to volume ratio and a tendency to dissolve. The choice of surfactant used also plays a part in droplet size (emulsion stability is dependent on emulsifier type). The specific surface area for a typical PolyHIPE is ~$5m^2g^{-1}$, but can be increased up to approximately $600m^2g^{-1}$. This can be achieved by use of a porogenic solvent in the organic phase, which generates a secondary pore structure within the cell walls [94]. Porosity, which can be as high as 99%, is defined by the internal phase volume ratio of the emulsion precursor. PolyHIPEs have 2 forms of internal structure, the cells formed by the water droplets and the interconnecting pore structure. It is known that the surfactant forms a thin film at the oil/water interface; and during polymerisation thinning of the film between adjacent droplets causes the pore formation. However, the film must be intact up to the point of gel formation or coalescence would occur. Thinning occurs from the result of contraction of the continuous phase as the monomer is converted to polymer, because the latter has a higher density and occupies a smaller volume of space [95].

Polymerisation inhibits the formation of HIPEs [86]. Since forming a HIPE is the first step in making PolyHIPEs, the polymerisation method needs to be controlled by an initiation step or catalyst. Radical addition polymerisation reactions have proved the

most effective. The most studied system comprises of styrene and DVB, which was patented by Barby and Haq (Unilever) in 1982 [96]; a typical SEM of the structure is shown in chapter 1, Figure 1.1. They produced styrene/DVB PolyHIPEs by using both oil-soluble (2, 2'-azo-bis-isobutyronitrile, AIBN) and water-soluble promoters (e.g. potassium persulphate). Polymerisation was initiated by placing the emulsion into a plastic bottle in an oven at 50°C for 24 hours. Researchers at Unilever confirmed that a low surfactant HLB value (2-6) was required because they were creating **w/o** emulsions. Other workers discovered that the concentration of surfactant, more than the internal phase volume, was vital to stable foam formation [97, 98]. Below 5 wt.% and above 80 wt.% surfactant with respect to the organic phase resulted in an unconnected or closed-cell material. Optimum surfactant levels were between 20 wt.% and 50 wt.%. Other PolyHIPEs include such systems as styrene and methyl methacrylate, stabilised with sodium hydroxide or triethanolamine, urea/formaldehdye, phenol/formaldehyde and melamine/formaldehyde [86].

From investigations on the effect of electrolytes e.g. sodium chloride on emulsion stability and properties, Aronson and Petko concluded that their presence improved **w/o** emulsion stability [99]. This was due to an increased resistance to coalescence by water droplets. Electrolytes are also known to affect viscosity, yield stress and droplet size. Aronson and Petko from their work on electrolytes concluded that while Otswald ripening contributed to emulsion destabilisation and was prevented by the presence of electrolytes, the dominating effect was coalescence [99]. They proposed that the presence of electrolytes in the dispersed phase reduced the oil/water interfacial tension by affecting density, packing or cohesion of the emulsion film. This reduces the average droplet size, stabilising the emulsion. They also speculate that the salts might react with unreacted

fatty acids present in some of the commercial non-ionic surfactants. Too much electrolyte however is detrimental to emulsion stability. Na^+ and Cl^- ions are hydrated preferentially over surfactant molecules, reducing the interaction between the surfactant polar head groups and water molecules, therefore [100]. This effect reduces the interfacial elasticity, therefore, emulsion stability and the interactions between the water and oil molecules and the polar head group of the surfactant molecules become equally as favourable.

Concentrated emulsions (HIPEs) can be used to generate porous foams, latexes and composites. Latexes can be formed when either the oil phase of an **o/w** emulsion is replaced by a hydrophobic monomer or the water phase of a **w/o** emulsion is replaced by a hydrophilic monomer [101]. If both phases were replaced at the same time the emulsion could be used to generate a composite.

2.3.1 Applications of HIPEs and PolyHIPEs

The most common use of HIPEs is the formation of PolyHIPEs. They are considered effective for a number of reasons [101]:

i) Conversion rate could be accelerated by the ordering of monomers at the interface between ordered surfactant molecules.

ii) Delay of bimolecular termination due to limited mobility within the cells.

iii) Emulsion precursor is a mould for the polymerised system.

Other applicationss of HIPEs include:

- The preparation of petroleum gels, a safety fuel for military purposes. Fire risk is reduced because spillage does not occur, the flash point is higher and the presence of a small amount of water improves the fuel's performance [86].

- **O/W** HIPEs formed from kerosene can be used to dissolve the oil from tar and oil sands. The aqueous phase prevents the oil from re-adhering. Similarly grease could be removed from other surfaces [86].
- The viscous nature of HIPEs has also led to investigation of their use for agricultural sprays, more viscous and large droplets leading to accurate coverage of crops with less drifting [86].

There are numerous ways in which groups have exploited the potential of PolyHIPEs. A paper by Cameron and Sherrington [86] mentions among others:

- Supports for solid phase peptide synthesis.
- As a catalytic support in foam form for flavin, or in granular form supporting a biocatalyst system.
- Supports for conducting polymers.

A second review paper on concentrated emulsion polymerisation [101] gives a selection of further applications:

- "Encapsulation", to either isolate or control the release of an active ingredient e.g. isolation of a reactive core from chemical attack and controlled drug release respectively.
- "Hydrophobic / hydrophilic microsponge molecular reservoirs". Two examples of uses for these would be i) ion exchange chromatography [102], by forming a porous material which contains a gel or gel-like substance within its pores; ii) porous nutshell particles, crosslinking of a fine PVBC matrix surrounded by a hydrophobic porous polystyrene highly cross-linked shell or, hydrophilic polyacrylamide encapsulating lightly cross-linked PEO. The author has used

these types of particles to trap carbonyl complexes and for immobilisation of lipase.

- "Selective composite membranes". The continuous phase produced a material that controlled the integrity of the membrane, while the dispersed phase led to a polymer that swelled to become permeable to the swelling solvent. Such composites consisting of polystyrene, within a polyacrylamide matrix could separate toluene from cyclohexane.
- Immobilisation of *Phanerochaete chrysosporium* (white rot fungus) using poly (styrene-divinylbenzene) carriers [103]. *Phanerochaete chrysosporium* excretes ligninase, an enzyme that degrades lignin and a variety of other compounds such as chlorinated alkanes, DDT and other chlorocarbons and polycyclic aromatics. The resulting carriers were shown to have high lignin peroxidase productivity. Spores were found to be more effective for immobilisation than pellets. The carriers were successfully used to degrade 2-chlorophenol, producing degradation activity of $355mgL^{-1}$ compared to $68mgL^{-1}$ for suspended cultures.

Porous foams possessing the property of heat resistance have potential in applications for acoustic or thermal insulation within engine compartments and enclosures [104]. Duke Jr et al. reported the synthesis of a wide range of N-substituted maleimides that were co-polymerised with styrene producing materials with improved thermal stability. The greatest glass transition increase was made using precursors with bulky or short chain N-substituents and maleimide solubility in both water and styrene was important in processing performance.

Formation of PolyHIPE into a monolith structure allows the passage of liquids and solvents at a low pressure. Attempts to functionalise an insoluble cross-linked

polymer for use as solid phase reagents and catalysts have been many [105]. In the case of functionalising polymer beads, stirring in reactors has led to grinding of the particles. A practical alternative would be to functionalise a porous structure by solvents and reactants flowing through it. Frèchet et al produced a porous monolith by phase separation, but the material contained too small pores requiring very high pressures [106]. Mercier et al.[105] used a (vinyl) polystyrene PolyHIPE as a precursor for a variety of functional groups, $PsCH{=}CH_2 \rightarrow PsCH_2\text{-}CH_2\text{-}X$. They reported addition using hydrogen bromide, thiols, hydroborane and disulfides.

Following on from the work by Unilever [96] a second patent in 1991 [107] looked at using PolyHIPE supports for entrapping cells, e.g. immobilisation of *Saccharomyces Cerevisiae* yeast cells on a (styrene-divinylbenzene) PolyHIPE. The immobilised supports were placed in reactors for 22 days during which time 98% conversion of sugar to alcohol was achieved. A second experiment replaced the sugar with a home-brewing kit and produced palatable wine. The patent stemmed from previous work using polymeric porous material sold under the trademark Accurel that had been used to immobilise lipase [108] and proteins [109].

A patent filed by Biopore Corporation [110], describes the synthesis of PolyHIPE materials as small beads, from hydrophilic monomers. These microbeads are capable of swelling in water to at least 100 times their original volume. Proposed applications include carriers to provide prolonged release of cosmetics and insecticides. A second international patent [111] describes the use of microcellular polymers as media for growing cells. They describe the synthesis of a PolyHIPE material made from styrene and divinylbenzene, variations in pore size were achieved using a range of temperatures of water, which was added from a number of feed points to a vessel containing the organic

phase. Polymerisation was initiated using potassium persulphate dissolved in the aqueous phase for 8 hours at 60°C. All variations tried centred around a basic styrene and divinylbenzene mix. One of the compositions produced was then used for growing chondrocytes, from human and bovine sources and rat fibroblasts. The patent does mention that polyesters could be used to produce biodegradable materials and that besides divinylbenzene it cites suitable hydrolysable cross-linkers, these being, ethylene glycol diacrylate, N,N'-diallytartardiamide, N,N'-(1,2-dihydroxyethane)-bis-acrylamide and N,N',N''-triallyl citrictriamide. The uses claimed for the material were the manufacture of contact lenses, dental fillings, cochlear implants, vascular supports including heart valves, cardiac pacemakers and drug delivery skin patches.

2.4 Aims

A series of aims were set out at the beginning of the project for this work and were as follows:

I To produce PolyHIPE biodegradable foams of controlled pore size, surface area and pore (or void) volume using materials such as polycaprolactone (PCL) and polylactic acid (PLA).

II To use various co-monomers including styrene or methyl methacrylate to produce a range of physical properties. Using the above for cross-linking will also vary composition and properties.

III To look at the biodegradation characteristics, especially the rates and products of degradation.

IV To use the biodegradable PolyHIPEs to grow cell tissues and implement them.

Preparation and Characterisation of PCL Foams

Chapter 3

3. PREPARATION AND CHARACTERISATION OF PCL FOAMS

3.1 Introduction

This section of the project details the formation of PolyHIPE material, with poly (ε-caprolactone) as the polymer. The preparation of PolyHIPE foams using the macromonomer, PCL diacrylate, was synthesised by free radical homo- or copolymerisation. Polymerisation was initiated in the continuous phase of HIPEs, followed by washing and drying of the PolyHIPEs to produce foams with low density and large cell diameters, between 5 – 100 μm. A series of PolyHIPEs was produced with increasing polymer content. At each stage of the process, the materials were fully characterised by IR and NMR and investigations into some of their properties were undertaken: phase separation on heating; swelling in solvents; water uptake.

3.1.1 Ionic Ring Opening Polymerisation

Cyclic monomers such as lactones, lactams, and cyclic amines and esters are traditionally polymerised via a ring-opening reaction using either cationic or anionic initiators. Anionic initiators are more favourable for lactone and lactam reactions [112].

The ring-opening reaction is dependent on the ring size e.g. ring-opening is unfavourable for γ-butyrolactone but favourable for δ-valerolactone. The main influence for ring-opening is the relief of strain on the ring, which is caused by non-bonded interactions, bond angle distortion and conformation strain. Rings with greater than 6 members tend not to have significant ring strain and if they do polymerise, the reaction is unfavourable because of low ceiling temperatures [112].

To form the PolyHIPEs used in this project requires an aqueous-based system. The ionic ring-opening polymerisation would compete with water acting as a H-donor, and in the case of cationic ring-opening, would terminate the polymerisation.

3.1.2 Preparation of Biodegradable Polyesters for Biomedical Applications

Bailey [113] recorded that free radicals can be used to ring-open unsaturated heterocyclic monomers and, for the first time, as a way of introducing functional groups, e.g. esters, amides, thioesters, carbonates and ketones into the backbone of an addition polymer. It also provided another route to synthesising oligomers capped with 2 reactive end-groups e.g. mercapto, amino, hydroxyl and carboxyl. These can be used in the synthesis of biodegradable and photodegradable polymers and to stabilise copolymers against decomposition. The higher the number of ester groups in a polymer, the faster it will degrade [114]. The introduction of a pyruvate ester group into the backbone of an addition polymer renders it more biodegradable than a simple ester. Pyruvates for example, pyruvic acid, $CH_3COCOOH$, are common intermediates in many biological systems [115]. The advantage in this project of using the free radical method is that the polymerisation can be carried out in an aqueous-based system.

3.1.3 Radical Ring-Opening Polymerisation of Cyclic Ketene Acetals

While there were many examples of ionic ring-opening polymerisation reactions, until the 1980's for cyclic monomers e.g. caprolactam and caprolactone, examples of free-radical ring-opening polymerisation reactions were limited [116]. Work by Bailey et al. showed that free radical ring-opening polymerisation (FRROP) was a viable and effective way to put a functional group into the backbone of an addition polymer. Whilst

researching various monomers they found that 5-membered cyclic ketene acetals underwent 50% ring-opening at 60°C by a free radical mechanism. The 7-membered cyclic ketene acetal, 2-methylene-1,3-dioxepane underwent almost complete ring-opening to give PCL [117] (Scheme 3.1).

Scheme 3.1

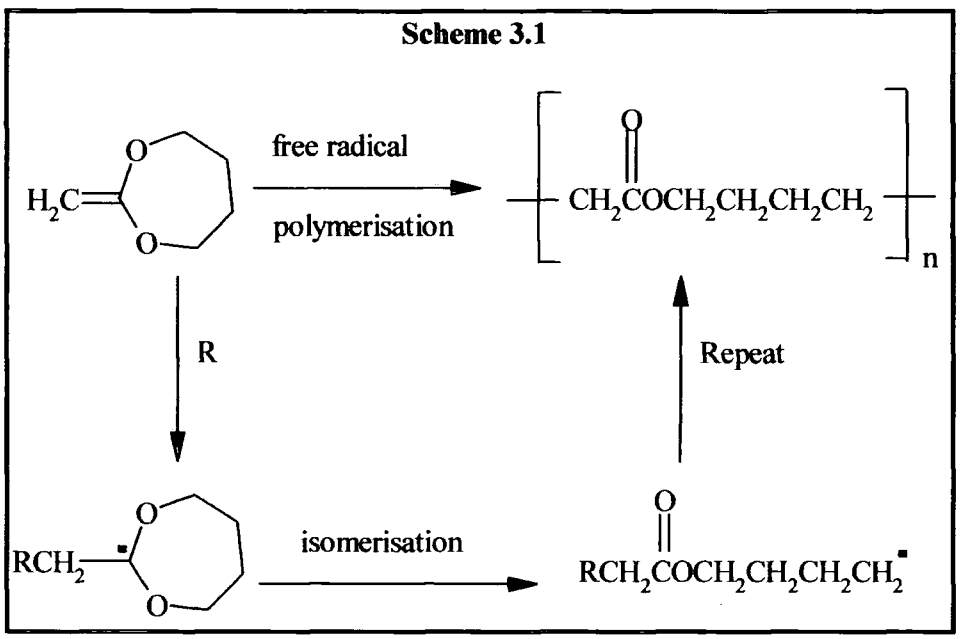

Copolymerisation of the 7-membered ring with several vinyl monomers resulted in ester linkages being incorporated in the backbone. It was expected that the incorporation of the ester linkages would have an effect on both the physical and chemical properties of the copolymers. The presence of the ester group was shown to:

i) increase the thermal stability of polymers that tended to depolymerise,

ii) render some copolymers biodegradable and

iii) permit the synthesis by hydrolysis of oligomers containing functional end-groups.

A further study [118] used 2-methylene-1,3-dioxolane which was polymerised at 125°C to yield a polymer with 83% ring-opened units. Its relatively low molecular weight caused

the monomer to be hydrophilic giving it a high reactivity toward moisture and acid. To overcome this, they used a cyclic ketene acetal - containing a hydrophobic, phenyl substituent, 2-methylene-4-phenyl-1,3-dioxolane - with success. The phenyl group was expected to increase the hydrophobic character of the monomer and also to enhance free-radical ring-opening by reducing the reactivity towards moisture and acid. Results showed that ring-opening was a function of temperature i.e. a lower temperature yielded a lower extent of ring-opening and that the phenyl group would be expected to determine the direction of ring-opening, see scheme 3.2. Free-radical ring-opening of the

Scheme 3.2

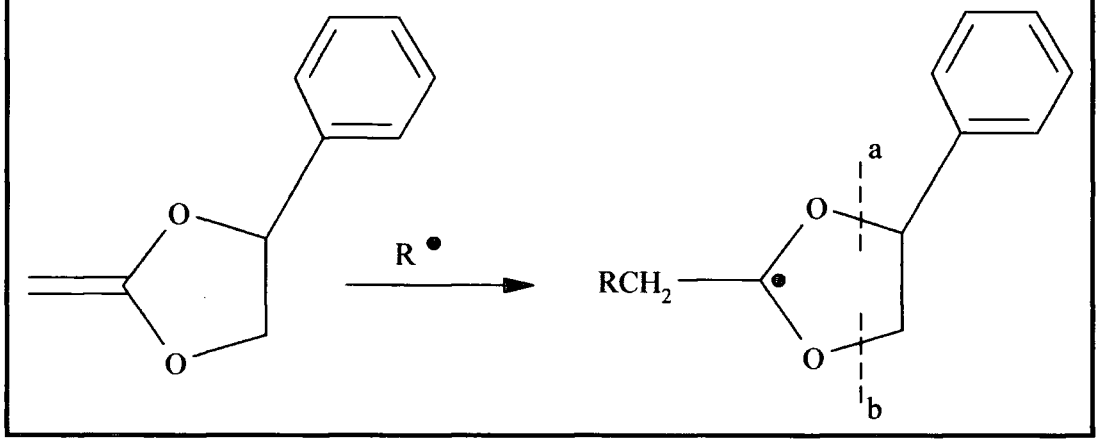

unsymmetrically substituted 1,3-dioxolane ring would have 2 possible pathways. These are shown in Scheme 3.3 and 3.4.

Scheme 3.3 pathway a

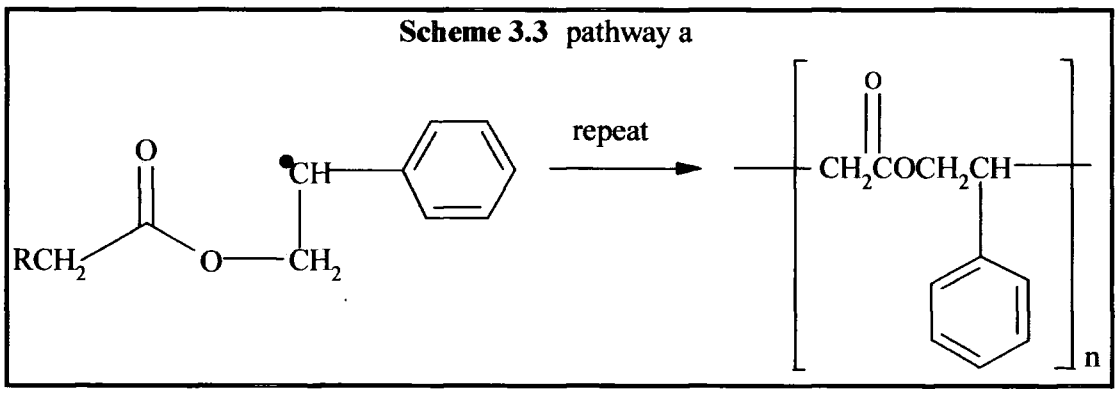

Scheme 3.3, following pathway (a) would yield a comparatively stable secondary benzyl radical similar to the radical intermediate in the polymerisation of styrene.

Scheme 3.4 pathway b

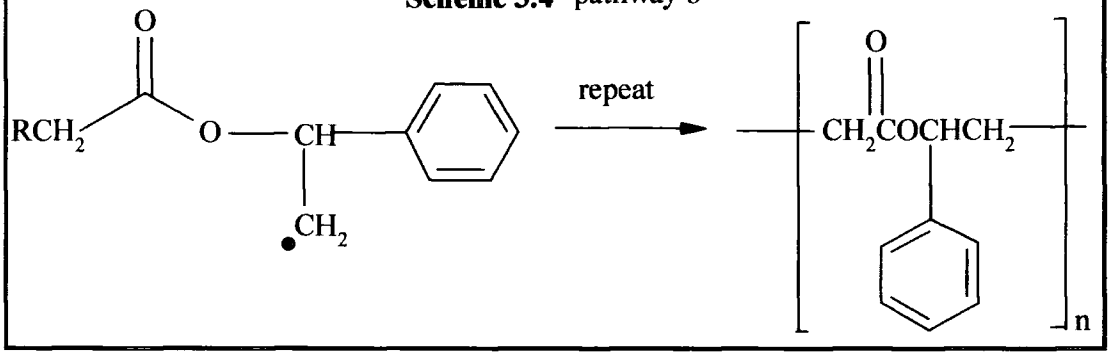

Scheme 3.4, pathway (b) gives a primary radical of relatively higher energy. 2-Methylene-1,3-dioxolane and 2-methylene-1,3-dioxane, under identical conditions, generated mixed ring-opened (85% at 130°C, 50% at 60°C) and non-ring-opened structures [117]. Copolymerisation of 2-methylene-1,3-dioxepane with styrene, MMA, or vinyl alcohol allowed once again the introduction of ester groups into the backbone of the addition polymer [117].

Scheme 3.5 5, 6 and 7-membered cyclic ketene acetals respectively

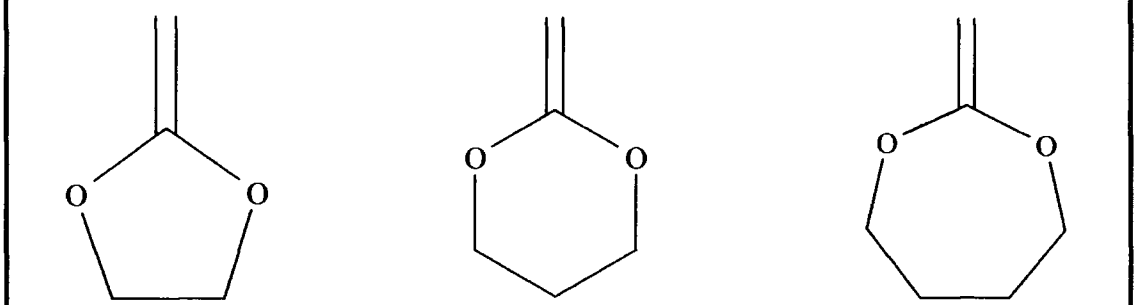

2-methylene-1,3-dioxolane 2-methylene-1,3-dioxane 2-methylene-1,3-dioxepane

In the FRROP of 4-n-hexyl and 4-n-decyl-2-methylene-1,3-dioxolane, it was again reasoned by Bailey et al. that the presence of a hydrocarbon side chain, this time

alkyl substituents, would make the monomer easier to handle [119]. Besides ester groups, other functional groups, e.g. carbonates, thioesters and amides were also successfully introduced into the backbone of an addition polymer, these groups could also lead to biodegradable materials. Following on from this, Bailey et al. reasoned that by hydrolysing these copolymers it would be possible to yield oligomers terminated with various combinations of hydroxyl, amino, thiol and carboxyl groups [117]; this was performed successfully. Copolymerisation of 2-methylene-1,3-dioxepane and styrene, followed by hydrolysis of the product gave polystyrene endcapped at one end with a hydroxyl group and at the other a carboxyl group [114]. Also the copolymerisation of ethylene with the cyclic ketene acetal yielded a series of biodegradable copolymers that hydrolysed to give oligomers of polyethylene with a hydroxyl and a carboxyl end group. In Bailey's laboratory, it was shown that copolymers of ethylene and 2-methylene-1,3-dioxepane with 10% ester-containing units were highly biodegradable, while those containing 6% degraded more slowly.

By introducing oxygen into the ring of 5- or 6-membered carbocyclic systems with exocyclic methylene groups they will undergo FRROP [113]. The driving force for ring-opening is the formation of the new carbon-oxygen double bond, which is more stable than the carbon-carbon bond, plus a fairly stable free radical [114] (Scheme 3.6).

Scheme 3.6

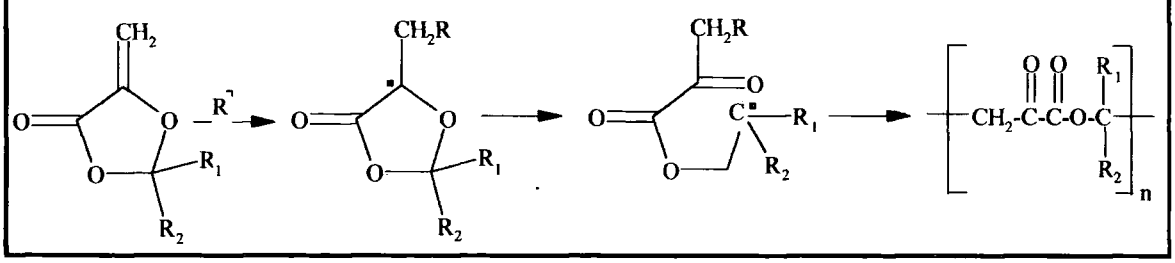

3.1.4 Copolymerisation of ε-Caprolactone

Copolyesters, such as those of glycolide and L-lactide, and homopolymers of glycolide have been useful in biomedical applications not only due to their mechanical properties but also because of their low immunogenicity and extremely low toxicity [120]. Further investigation to find other suitable materials included ε-caprolactone - its polymer degradation product, hydroxycaproic acid, has a relatively low toxicity. Copolyesters of ε-caprolactone and glycolide allowed for a broad range of physical and chemical properties. The flexible structure of PCL is contrasted to the rigid and highly crystalline PG.

Processability and tensile modulus (stiffness) of polymers can be controlled using plasticizers, however, for biomedical applications this was not appropriate [121]. PCL has emerged as a unique polymer capable of blending with a variety of amorphous and crystalline polymers over wide composition ranges to give materials with enhanced properties [122]. Blends were shown to occur in one of 3 ways: crystalline interaction products; truly compatible blends; and mechanically compatible blends. PHB-PHV was blended with biodegradable PCL in an attempt to produce a copolymer suitable for medical applications [121]. Results revealed that PHB-PHV/ PCL blends would be appropriate for applications where matrix porosity was important e.g. drug delivery systems. Applications reliant on physical or degradative properties were eliminated, because of an initial lower tensile modulus.

3.1.5 Production of Biodegradable Networks From PCL Macromonomers

Since the 1960s, there have been a number of studies made on the commercially available PG, PL and PCL for use as sutures, artifical skin and other surgical applications [51, 123]. However, their use as biodegradable composites had been limited by their high molecular weights, thermoplastic nature and semi-crystallinity. Early work that looked at using polymers with a double bond group to produce crosslinked networks by free-radical addition polymerisation was the basis for biodegradable networks produced by Storey et al [124]. Using PLGA fumarate [125] or poly (ε-caprolactone-co-D,L-lactide) fumarate [126] and Dexon (a PG surgical mesh), composites were made. However, the 1,2-disubstituted olefinic group used to form the network, required the addition of reactive diluents to ensure a high level of crosslinking. Storey et al. hoped to create a more reactive prepolymer by endcapping a polyester, 3-armed PCL triol, with methacryloyl chloride. They were also hoping to address the problem of non-biodegradable hydrocarbon polymer chains that were a product of the free-radical crosslinking reaction, by forming completely biodegradable networks. They hoped to apply work by Bailey at al., who had managed to copolymerise 2-methylene-1,3-dioxepane with methyl methacrylate [127]. They were able to copolymerise their methacrylate-terminated polyester with styrene and MMA but not with the cyclic acetal.

3.3 Experimental

3.3.1 Materials and Instrumentation

3.3.1.1 Materials

The monomers, styrene and methyl methacrylate, were freed of inhibitor by passing through a pad of basic Al_2O_3; all other products were used as supplied. Poly (ε-caprolactone) diol samples of M_n=530 and 2000 were obtained from Aldrich. Surfactants - Span 60 (sorbitan monostearate), Span 80 (sorbitan monooleate), Span 85 (sorbitan trioleate) and Tween 80 (polyoxyethylene sorbitan monoleate) - were obtained from Sigma. The surfactant Synperonic PE L121 was received from ICI Surfactants.

3.3.1.2 Instrumentation

FTIR spectra (KBr disks) were recorded on a Perkin Elmer 1600 Series FTIR spectrometer. NMR spectra were recorded on a Varian ASM-100 Unity-300 spectrometer at 300 MHz (^{1}H) and Bruker AM-250 spectrometer at 63 MHz (^{13}C) both using $CDCl_3$ as solvent. Solid state ^{13}C spectra were obtained with cross polarisation, high-power proton decoupling and magic angle spinning using a Varian unity-plus 300 spectrometer at 75.43MHz and ambient probe temperature (296K). A sapphire 7mm outer diameter rotor with Kel-F caps were used in a Doty probe. Elemental analysis (C, H and N) was performed using a Exeter Analytical E-440 elemental analyser. MALDI-tof spectra of samples immobilised in a mixture of 2,5-dihydroxybenzoic acid (gentisic acid) or dithranol and were recorded using a Kratos Kompact MALDI 4. Scanning electron microscopy was carried out at the University of Newcastle using a Hitachi S2400 electron microscope operating at 25kV. Fractured samples were prepared

for SEM by mounting on aluminium stubs using adhesive carbon disks to increase the conductivity. All samples were sputter coated with a thin layer of gold prior to viewing to enhance conductivity.

3.2.2 General Methodology

3.2.2.1 Synthesis of Macromonomers 1 and 2

Figure 3.1 Equipment for Macromonomer Synthesis

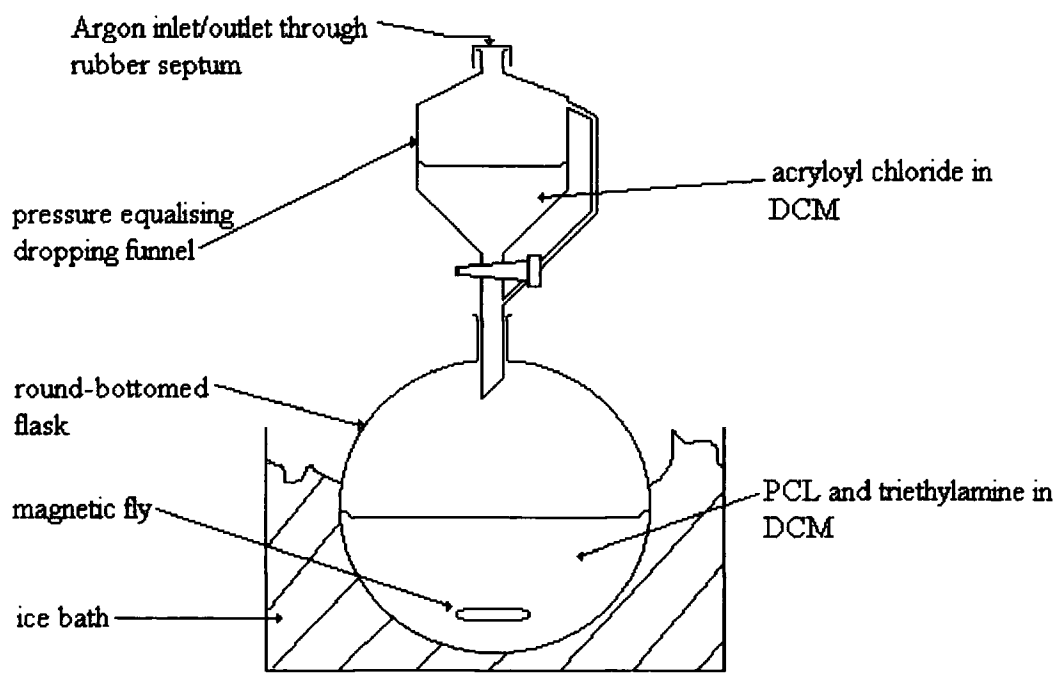

The equipment was set up as shown in Figure 3.1. The whole unit was purged with argon as the flask was cooled to ice temperature. The solution in the dropping funnel was added dropwise, over ca. one hour, to the contents of the round-bottomed flask, as it was stirred and kept at ice temperature. The system was then left stirring for a

further 20 hours during which time it returned to room temperature. The resulting solution was extracted with ca. 30ml portions of 3 wt. % KOH aqueous solution, followed by the same of 1% HCl solution until in both cases a colourless aqueous layer was obtained. The extracted organic layer was dried over $MgSO_4$ and placed on a rotary evaporator to remove most of the DCM, then concentrated *in vacuo* to a constant mass.

3.2.2.2 Network Formation

A 25ml round-bottomed flask was charged with 2.1g macromonomer 2, 0.94g of MMA or styrene, ca. 1mg AIBN and 10ml toluene. The system was purged through a rubber septum for 10 min. with argon then heated at 60°C for 20 hours. Network formation was confirmed by continued existence of a gel following immersion first in methanol for 10 min. then in toluene.

3.2.2.3 PolyHIPE Formation

The equipment was set up as shown in Figure 3.2. Firstly the contents of the 3-necked flask and then the pressure equalising dropping funnel, were purged by argon bubbling for 10 min. each. Then the content of the latter was added dropwise over ca. one hour whilst the content of the flask was mixed at ca. 300 r.p.m. using a D-shaped PTFE paddle powered by an overhead stirrer motor. The resultant emulsion, having a consistency similar to that of mayonnaise, was transferred to a polyethylene bottle that was heated at 60°C for 48 hours. After this, the PolyHIPE that had formed was removed from its container and extracted in a Soxhlet for 24 hours each with water then

isopropanol as the solvents. The PolyHIPE was finally dried to a constant mass *in vacuo*. This was according to a standard procedure [128].

Figure 3.2 Equipment for Foam Synthesis

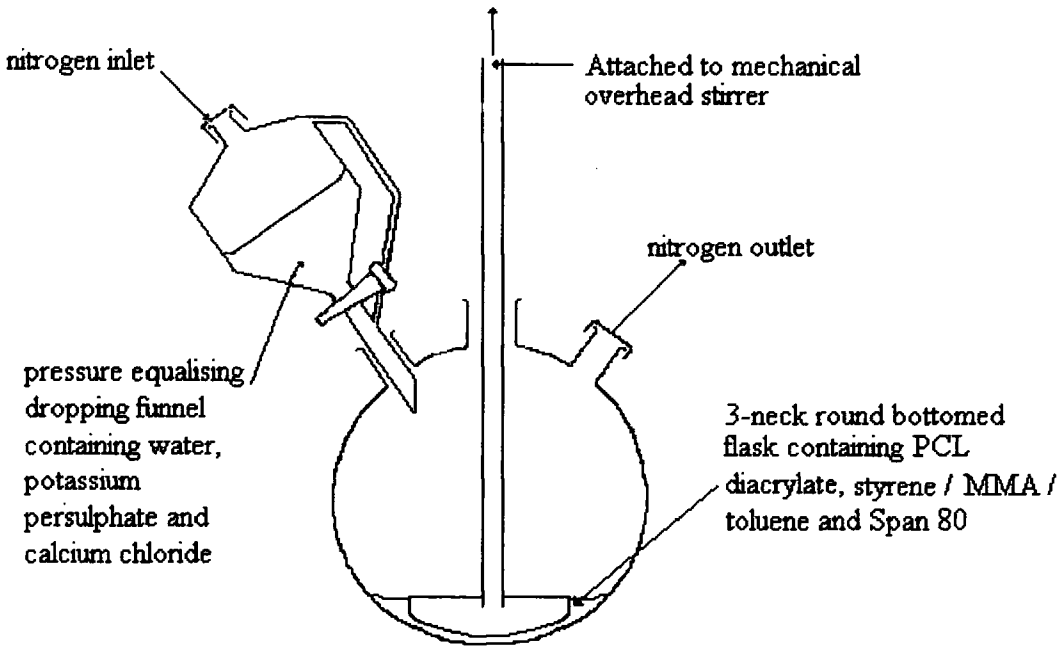

3.2.2.4 Emulsion Tests

A 25ml conical flask was charged with 0.2g PCL diacrylate, 0.8g monomer and 0.2g surfactant. A 9ml aqueous solution containing 0.1g of $CaCl_2.2H_2O$, was added dropwise while the contents of the flask was manually agitated. The stability of any HIPEs formed were evaluated by heating at 60°C and monitoring the percentage of separated liquid phase with time.

3.2.2.5 Swelling Studies

A series of pre-weighed sinter sticks 1 – 6 were immersed in each of the chosen solvents - toluene, water and *iso*-propanol - until a constant value was obtained. When subtracted from the dry weight, the quantity of each solvent taken up by the porous glass frit was determined. The following procedure was carried out in duplicate for each foam sample: ca. 0.1g of each PolyHIPE was accurately weighed and placed in a sinter stick. The sticks were immersed in solvent for 24 hours, removed and weighed, this process was repeated until a constant mass was obtained. The extent of solvent absorbed by each foam was determined by mass of (wet sample + stick) minus mass of (dry sample + dry stick + solvent absorbed by empty stick). A normalised value was then calculated from the previous value divided by the mass of dry sample and expressed as g solvent / g polymer. This experiment was based on a previous procedure [129].

3.2.3 Experiments

3.2.3.1 PCL $\overline{M}_n$=2000, Synthesis of Macromonomer **2**

Experiments were carried out as outlined in 3.2.2.1. Quantities used were as follows: poly (ε-caprolactone) diol (20 g, ≈ 10 mmol OH groups) dissolved in 200 ml DCM containing triethylamine (6.3 ml, 45 mmol); acryloyl chloride (6.0 ml, 74 mmol) in 30ml DCM.

Yield ~ 18.9g (95%)

IR (film): υ cm^{-1} = 2944, 2865 (C – H str.), 1724. (C = O)

^{1}H NMR: (300 MHz, $CDCl_3$), δ ppm = 6.40 (dd, 2H, $J_{Ha\text{-}Hc}$* = 17 Hz, $J_{Ha\text{-}Hb}$* = 2 Hz, H_a*), 6.10 (dd, 2H, $J_{Ha\text{-}Hc}$*= 15 Hz, $J_{Hb\text{-}Hc}$* = 9 Hz, H_c*), 5.80 (dd, 2H, $J_{Hb\text{-}Hc}$*= 9 Hz, $J_{Ha\text{-}Hb}$* =2 Hz, H_b*), 4.20 (t, 4H, J = 5 Hz), 4.15 (t, 4H, J = 7 Hz (-$CO_2C\underline{H}_2$-)), 4.05 (t, 29.2H, J = 8 Hz (-$C\underline{H}_2OC\underline{H}_2$-)), 3.70 (t, 4H, J = 5 Hz (-$OCC\underline{H}_2$-)), 2.30 (t, 33.2H, J = 8Hz (-$C\underline{H}_2CO_2$)), 1.65 (m, 66.4Hz (-$OCCH_2C\underline{H}_2CH_2C\underline{H}_2$-)), 1.40 (m, 33.2H (-$OCCH_2CH_2C\underline{H}_2CH_2$-)).

^{13}C NMR: (75 MHz, $CDCl_3$): δ ppm = 173.5, 166.0 (-$\underline{C}O_2CH_2$-), 130.0, 128.4 (C = C), 72.3, 69.0 (-$CO_2\underline{C}H_2$-), 64.1, 63.2, 62.4, 61.6, (-$\underline{C}H_2O\underline{C}H_2$-)34.0, 32.2, 28.2, 25.4, 25.2, 24.6, 24.5 (-$OC\underline{C}H_2\underline{C}H_2\underline{C}H_2\underline{C}H_2\underline{C}H_2CO_2$-).

Elemental Analysis: calcd. for $C_{109.6}H_{180}O_{38.2}$ C, 62.5%; H, 8.5%. Found C, 62.2%, H 8.8%.

MALDI-tof MS: *m/z* 2398, 2283, 2169, 2054, 1942, 1829, 1718, 1602, 1487, 1374, 1260, 1147 [$(\overline{M})_n + Na^+$]

3.2.3.2 PCL $\overline{M}_n$=530, Synthesis of Macromonomer 1

Experiments were carried out as outlined in 3.2.2.1. Quantities used were as follows, poly (ε-caprolactone) diol (20 g, ≈ 37.7 mmol) dissolved in 200 ml DCM containing triethylamine (2.1 ml, 15 mmol), acryoyl chloride (1.2 ml, 15 mmol) in 30 ml DCM.

Yield ~ 18.9g (95%)

IR (film): as for 2.3.1.

^{1}H and ^{13}C NMR: as for 2.3.1.

* see results and discussion for explanation

Elemental Analysis: calcd. For $C_{109.6}$ H_{180} $O_{38.2}$ C, 60.4, H, 7.9. Found C, 60.32, H, 8.07.

MALDI-tof MS: m/z 2062.8, 1948.5, 1835.2, 1720.1, 1606.0, 1492.6, 1378.4, 1263.8, 1149.8, 1035.6, 921.9, 807.9, 693.7 $[(\overline{M})_n + H^+]$

3.2.4 Network Formations

Experiments were carried out as outlined in 3.2.2.2. Quantities used were as follows, macromonomer **2** (2.1 g ≈ 1.0 mmol OH groups) or macromonomer **1** (2.1 g ≈ 4.0 mmol OH groups); methyl methacrylate (0.94 g, 9.4 mmol) or styrene (0.94 g, 9.0 mmol); AIBN (ca. 1 mg); and toluene (5 ml).

3.2.5 PolyHIPE Formation

Experiments were carried out as outlined in 3.2.2.3. Quantities used were as follows: macromonomer **2** (1 g ≈ 0.5 mmol)) or macromonomer **1** (1 g ≈ 1.9 mmol); styrene (4 g, 38 mmol) or MMA (4 g, 40 mmol) or toluene (4 g, 43 mmol); surfactant (1 g); water (45 ml); $K_2S_2O_8$ (0.1 g, 0.37 mmol); and $CaCl_2.2H_2O$ (0.5 g, 3.4 mmol).

Any reference to a PolyHIPE sample will be referred to using the following code X-Y-Z. For example in the case of a PolyHIPE made using 1.5 g of PCL macromonomer **1** and 3.5 g styrene, X = fraction (by weight of total oil phase*) of PCL macromonomer in the HIPE formulation, the total organic phase is 5 g therefore the PCL fraction = 1.5 /5 = 0.3 Y = macromonomer molar mass (L = macromonomer **1**, H = macromonomer **2**) therefore Y = L and Z = organic phase diluent (S = styrene, M = MMA, T = toluene),

* The surfactant mass was not included in the oil phase for the purpose of the calculation of percentage composition because it was likely to concentrate at the interface

therefore Z = S. For all the formulations the X-Y-Z code and full descriptions are as follows:

X-Y-Z	X PCL/g	fraction	Macromonomer Y	Diluent Z
0.2-L-S	1.0	1/5	1	styrene
0.3-L-S	1.5	1.5/5	1	styrene
0.4-L-S	2.0	2/5	1	styrene
0.2-L-M	1.0	1/5	1	MMA
0.4-L-M	2.0	2/5	1	MMA
0.2-L-T	1.0	1/5	1	toluene
0.5-L-T	2.5	2.5/5	1	toluene
0.2-H-S	1.0	1/5	2	styrene
0.3-H-S	1.5	1.5/5	2	styrene
0.4-H-S	2.0	2/5	2	styrene
0.2-H-M	1.0	1/5	2	MMA
0.4-H-M	2.0	2/5	2	MMA
0.2-H-T	1.0	1/5	2	toluene
0.5-H-T	2.5	2.5/5	2	toluene

PCL and styrene

IR (KBr disc): υ cm^{-1} = 3081, 3059, 3024, 2922 and 2850 (C-H str.), 1732 (C = O str.), 1600, 1503 (C = C str.), 1493, 1452 and 1360 (C-H deformation), 757and 697 (ipso- substituted benzene ring).

^{13}C NMR: (75.43MHz, solid state), δ ppm = 25, 29 and 34 ($-OC\underline{C}H_2\underline{C}H_2\underline{C}H_2\underline{C}H_2\underline{C}H_2CO_2-$), 40 (-CH-), 47ppm ($-CH_2-$), 64 ($\underline{C}H_2\underline{C}H_2O\underline{C}H_2\underline{C}H_2$), 126 (benzene ring) and 146 (C in ipso-position on benzene ring), 174 (-C = O)

PCL and MMA

IR (KBr disc): υ cm^{-1} = 3445 (O-H stretch), 2925 (C-H stretch), 1684, 1653, and 1636 (C = O str.) and 1559, 1541, 1507 (C=C str.).

^{13}C NMR: (75.43MHz, solid state), δ ppm = 16 ($-\underline{C}H_3$), 25, 29, 34 ($-OC\underline{C}H_2\underline{C}H_2\underline{C}H_2\underline{C}H_2\underline{C}H_2CO_2-$), 45 (quaternary C), 52 ($-O\underline{C}H_3-$), 56 ($-\underline{C}H_2-$), 178 (C = O).

PCL and toluene

IR (KBr disc): υ cm^{-1} = 2900 ($-CH_2-$), 1734 (C=O str.), 1458 (C – H Str.), 1167 (C - O str.), 753 (C = C).

^{13}C NMR: (75.43MHz, solid state), δ ppm = 26, 29 and 34 ($-OC\underline{C}H_2\underline{C}H_2\underline{C}H_2\underline{C}H_2\underline{C}H_2CO_2-$), 65 ($\underline{C}H_2\underline{C}H_2O\underline{C}H_2\underline{C}H_2$), 174 (C = O).

3.2.6 Emulsion Tests

Experiments were carried out as outlined in 3.2.2.4. Quantities used were as follows, macromonomer **2** (0.4 g ≈ 0.2 mmol)) or macromonomer **1**(0.4 g ≈ 0.75 mmol), surfactant (0.4 g), styrene (1.6 ml, 13.9 mmol) and $CaCl_2.2H_2O$ (0.1 g, 0.7 mmol).

3.3 Results and Discussion

3.3.1 Macromonomer Synthesis and Network Formation

The diacrylate macromonomers **1** and **2** were prepared from commercially available diols. The chemistry used is shown in Scheme 3.7.

Scheme 3.7 Macromonomer synthesis

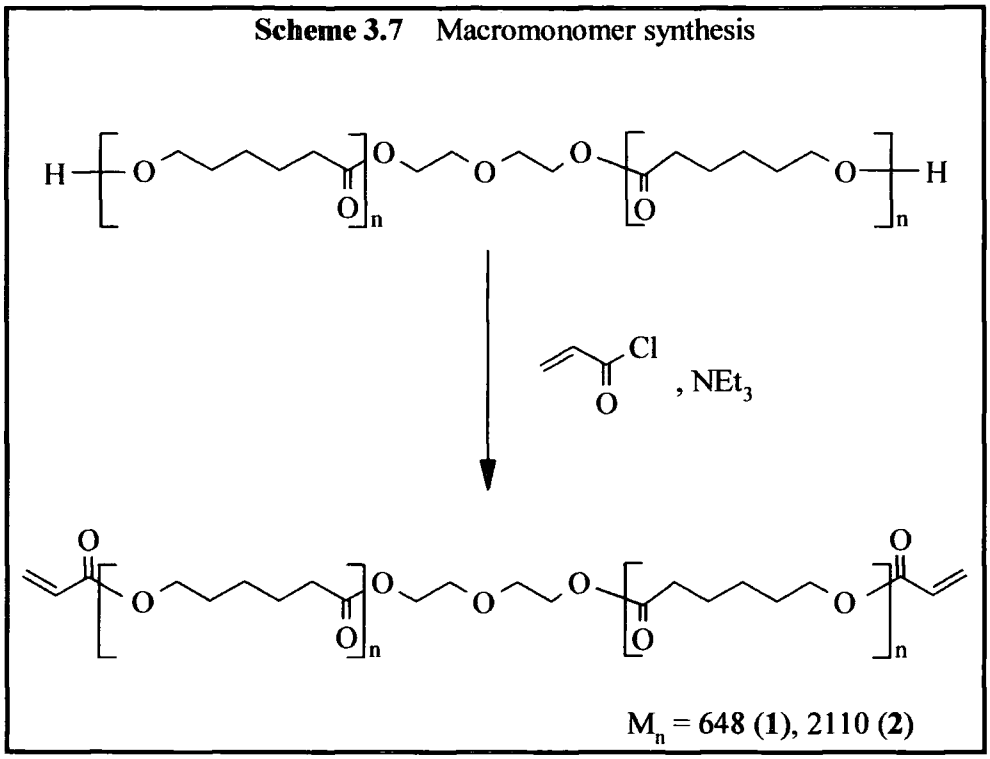

Initial characterisation to determine the conversion of diol to acrylates was achieved by NMR spectroscopy. Acrylate end groups have characteristic resonances in the ^{1}H NMR spectrum at δ5.8, δ6.1 and δ6.4 ppm and these can be clearly seen in Figure 3.3 (a) and (b) on the next page. From Scheme 3.8: H_c occurs at δ6.1ppm because the coupling constants are characteristic of trans (15Hz) and cis (9Hz) and H_c is the only one without geminal coupling. The doublet of doublets at δ5.8 ppm shows geminal coupling (2Hz) and a J_2 coupling constant of 9Hz, as the value is less than 12Hz, this coupling constant is characteristic of cis and was therefore assigned to H_a. The doublet of doublets at δ6.4 ppm again shows the geminal coupling (2Hz) but has a J_2 coupling constant of 17Hz, which being greater than 15Hz is characteristic of trans and was therefore assigned to H_b.

Scheme 3.8 Assignment of H's in Acrylate Groups

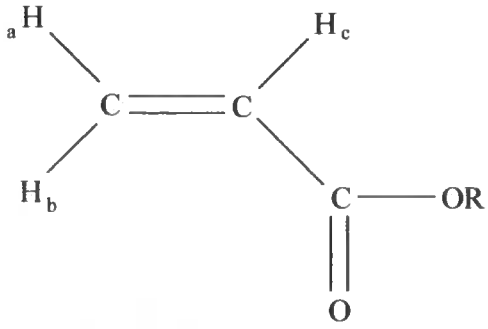

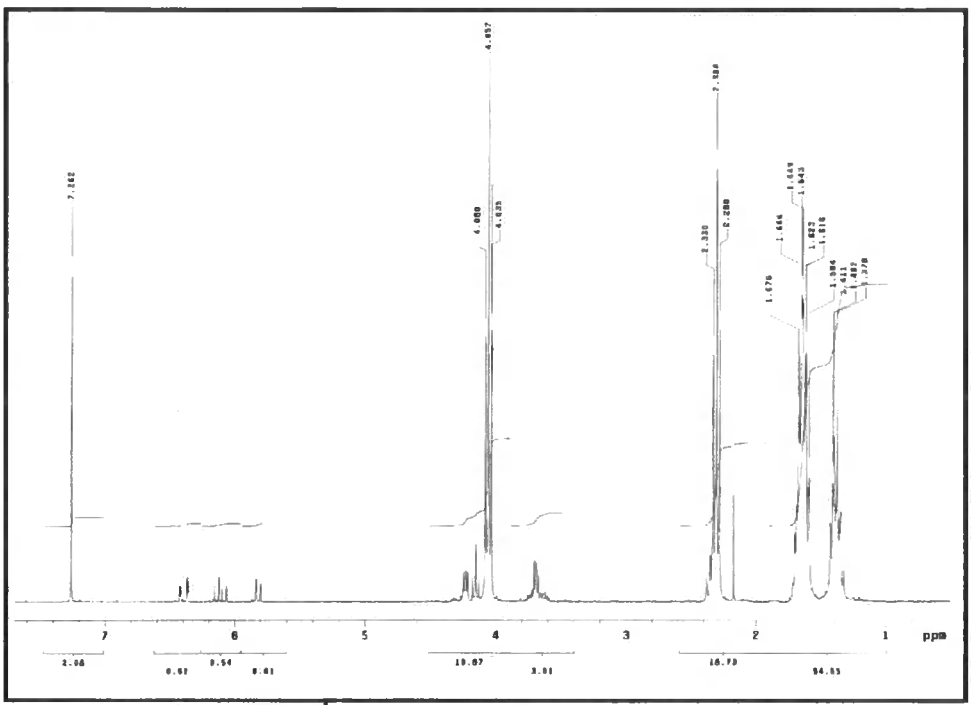

Figure 3.3a ^{1}H NMR spectrum (macromonomer **2**)

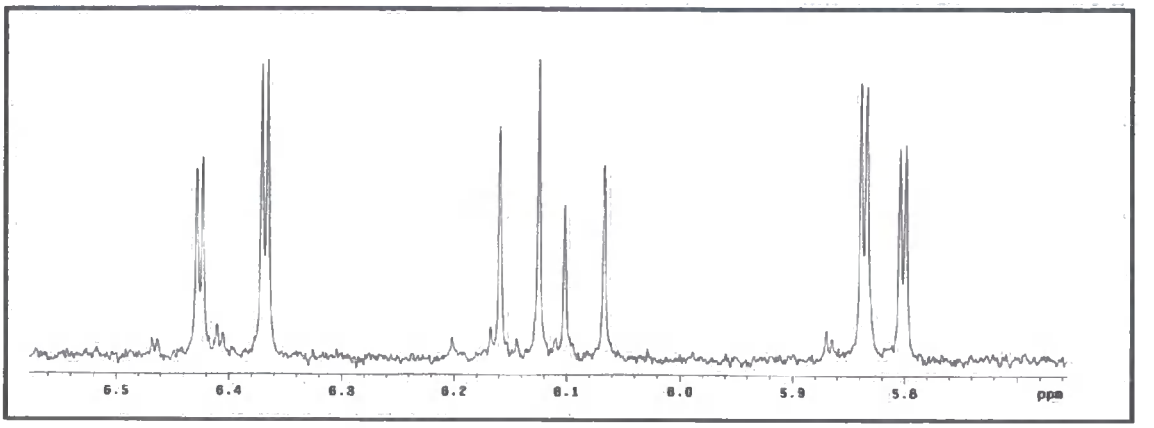

Figure 3.3b Close up of Acrylate End Group Region

The extent of conversion from alcohol to acrylate was established using MALDI-tof mass spectroscopy. The addition of 2 acrylate units causes an increase in molecular weight of 108 units, 2 x (H_2C=CH-CO-) minus 2 protons. This is clearly illustrated in Figure 3.4, where each peak of the diol starting material (red trace) is shifted to a higher molecular weight by 108 units in the diacrylate product (blue trace). In the case of the

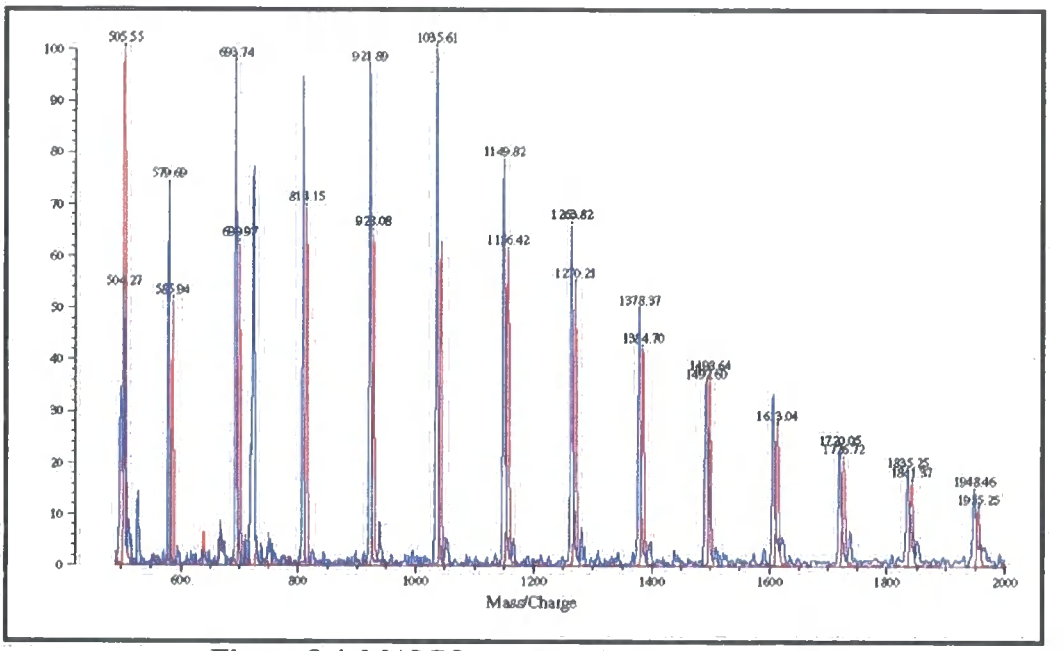

Figure 3.4 MALDI spectrum (macromonomer **1**)

higher molecular weight PCL starting material, first attempts at synthesis used insufficient acryloyl chloride; these were characterised by the additional peaks appearing at $[(\overline{M})_n + 54]$, as well as the expected $[(\overline{M})_n + 108]$, (red trace) and diol (blue trace) Figure 3.5. The green trace is the spectrum following addition of 7 equivalents of acryloyl chloride showing only peaks at $[(\overline{M})_n + 108]$ and no peaks at $[(\overline{M})_n + 54]$.

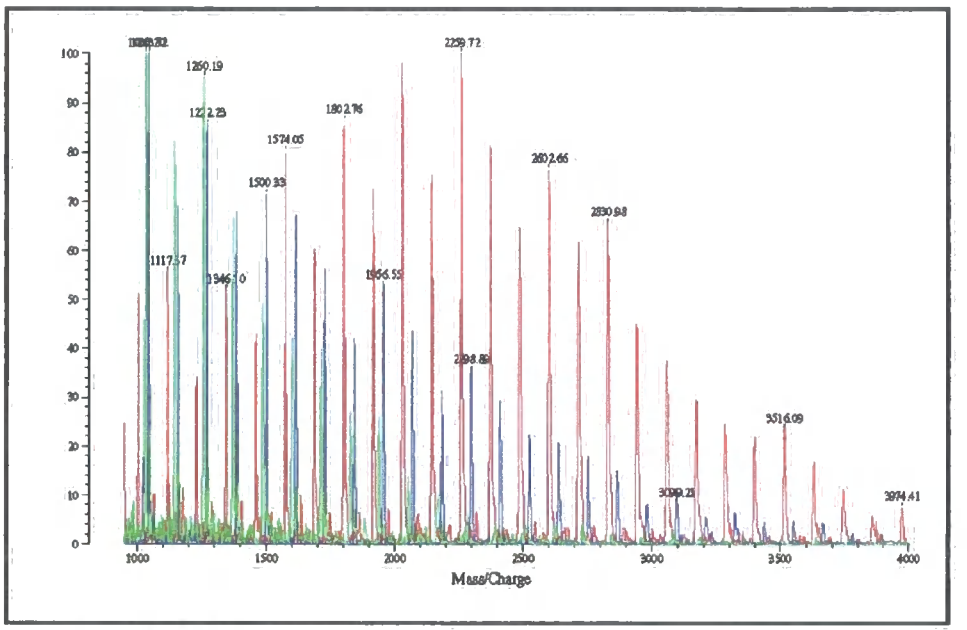

Figure 3.5 MALDI spectrum of macromonomer (**2**)

Once the structure had been established the next step was to determine that the macromonomers were capable of network formation with themselves and with the common vinyl monomers, styrene or MMA, in a ratio of 2:1 (by weight). Following several hours of heating at 60°C a series of clear, soft gels were obtained. The formation of homo- or copolymerised networks was confirmed by immersion of the gels into methanol, upon which they became white and opaque and did not dissolve on re-immersion in toluene.

3.3.2 PolyHIPE Preparation

Within the PolyHIPE morphology, there are 2 distinct structures, the *cells* formed by polymerisation about the water droplet and the *windows* or *pores* caused by thinning in the surfactant interface. A number of PolyHIPE preparation parameters can affect the overall structure of the foam. The choice of surfactant plays a part by affecting the interfacial tension γ and therefore, d, the diameter of HIPE droplets (a direct relationship between γ and d). A more stable emulsion has smaller droplets and a narrower droplet size distribution, which produces smaller foam cells. Decreasing γ also causes a thinning of the interfacial films separating the emulsion droplets [98] affecting the size of the windows interconnecting adjacent cells. Polymerisation causes shrinkage and therefore, larger windows to appear lowering γ. When a HIPE is formed below its optimal stability, phase separation can occur. Phase separation can be detected by a layer of liquid, above or below, the foam and in extreme cases, by absence of the foam structure.

Addition of a polymer to form a PolyHIPE can cause an increase in the continuous-phase viscosity. Smaller cells provide a kinetic barrier against the coalescence of droplets and this helps to increase the emulsion stability. Increase in the viscosity of the continuous-phase can also lead to creation of HIPEs from monomers e.g. methyl methacrylate. If the continuous phase viscosity becomes too high, it impedes the addition of the aqueous phase. The HIPE simply becomes too viscous to mix properly, with aqueous droplets sitting on and around the viscous opaque HIPE.

PolyHIPE morphology can also be affected by foam mechanical strength. Collapse on drying of a foam, produced by drying well above its T_g, then determination of the structure by SEM will not reflect the true structure after polymerisation. Work

done on polyHIPE materials assumes that the structure of the foam is a true reflection of the HIPE material at the gel point.

Despite all of these influences, the origin of the morphology of a PolyHIPE can be simply determined. The presence of a clear liquid and reduced quantity of PolyHIPE when compared to the emulsion show that phase separation has occurred to a degree. The detection by SEM of large cells, with a broad size distribution, and/ or micro cavities is also indicative of phase separation. An extreme case will produce areas of structure resembling that of a macroporous resin, a non-cellular morphology. In some cases, an unexpected cellular structure may be observed; rather than stability, other factors such as monomer density, viscosity or emulsion interfacial tension will have affected the structure. Mechanically weak foams can collapse during the drying process. All these factors are easy to observe and when combined with pictures of morphology provided by SEM, the source of the morphology can be straightforwardly determined.

3.3.2.1 PCL and Styrene

Preparations of PolyHIPE materials from styrene and divinylbenzene have been detailed [128] and were used as a basis for the PolyHIPEs prepared in this work. The initial experiments used a total of 5 g monomer with 20 wt.% of the styrene replaced with either macromonomer **1** or **2** while the quantity and concentration of surfactant, remained the same. HIPEs are intrinsically unstable and can be affected by moderate changes of emulsion composition. The presence of PCL and absence of DVB, as a change to the basic composition, had no significant effect on HIPE stability. Straightforward preparation and polymerisation of emulsions of $\phi = 0.9$ yielded corresponding PolyHIPE foams. SEM images of the resulting structures are shown on the next page (Fig. 3.6).

Both foams demonstrate the classic open-cellular PolyHIPE morphology as seen for styrene/ DVB systems. However, the larger cell size, 20μm, (Figures 3.6 (a) or (c), compared to foams prepared using high levels of divinylbenzene, average cell size 5μm,

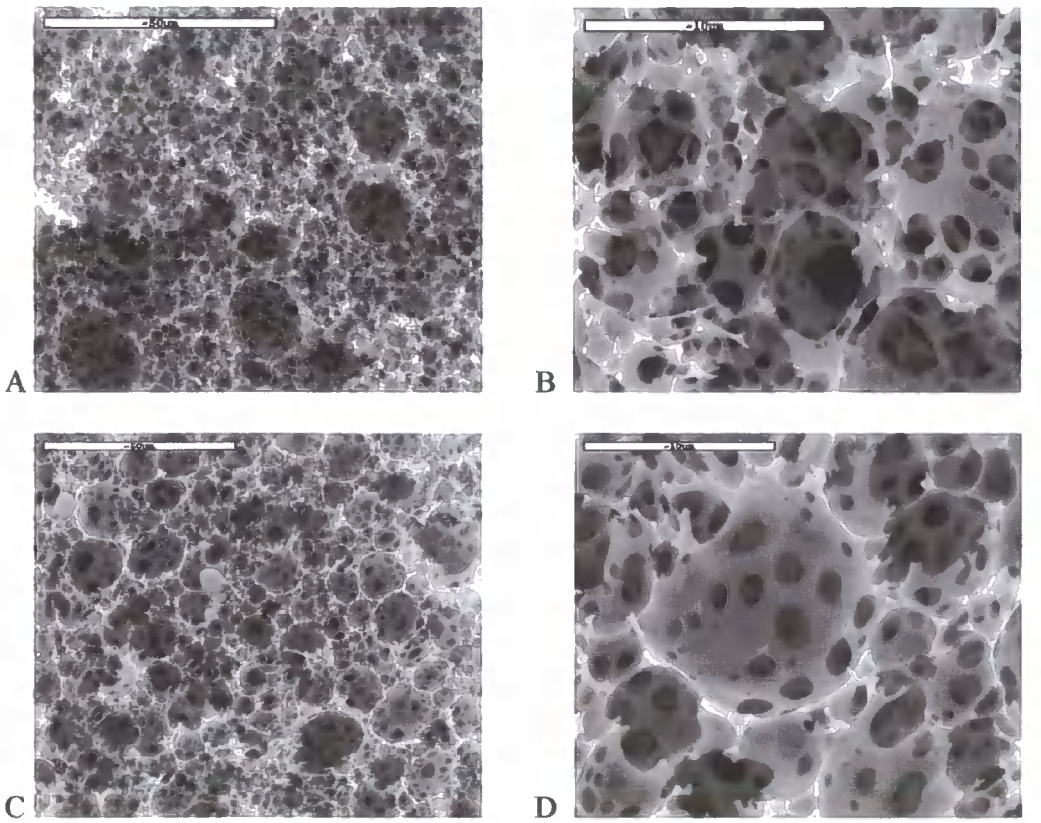

Figure 3.6 SEM Photographs (a) 0.2-H-S (50 μm scale bar); (b) 0.2-H-S (10 μm scale bar), (c) 0.2-L-S (50 μm scale bar); (d) 0.2-L-S (10 μm scale bar) *

indicate the precursor emulsions are not as stable†. In order to confirm that the HIPEs were being prepared using the optimum surfactant, an experiment was conducted looking at varying the HLB value (see section 2.4). The surfactants used for the experiment along with their HLB values are given in Table 3.1. Emulsion preparation was attempted using surfactant systems of 3 different HLB values 3.6 (HLB_{mix} , Span 80 and Span 85,

* See Experimental for key, page 63
† emulsion droplet and therefore cell diameter are inversely related to emulsion stability

Table 3.1 HLB Values of Surfactants Used

SURFACTANT	HLB value[a]
Span 80	4.3
Span 85	1.5
Tween 80	15
Synperonic PE L121	0.5

[a] value quoted by manufacturer

4.3 and 5.0 (HLB_{mix}, Tween 80and Span 80). Along with the HLB = 4.3, only the HLB = 3.6 formed a stable emulsion. These 2 emulsions were then heated at 60°C (polymerisation temperature) and their stability determined by monitoring the amount of separated liquid phase produced with time. The results are shown in Figure 3.7.

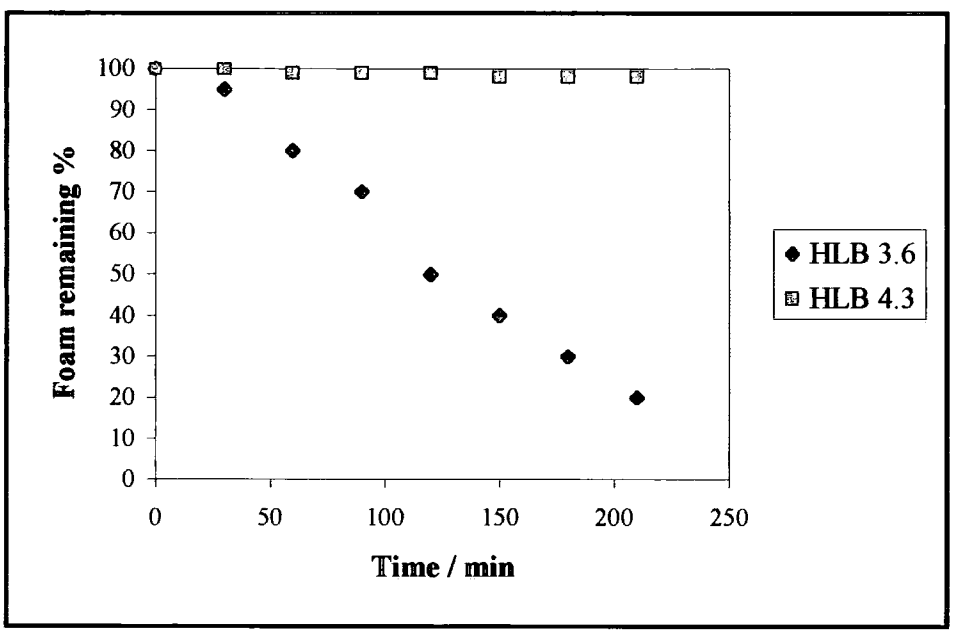

Figure 3.7 Phase Separation of 0.2-L-S HIPEs Heated at 60°C

The conclusion drawn was that Span 80 alone produced the most stable HIPE and was therefore near the optimum for this composition of emulsion. It is important to note that the HLB of a surfactant does not alone determine emulsion stability. Other factors include the length and nature of the hydrophobic and hydrophilic moieties and the phase

inversion temperature (PIT), as shown by Williams [130] who established it was not possible to form stable o/w HIPEs using sorbitan monosterate (Span 60) despite an HLB value of 4.7. However HLB is still useful as an indication for initial surfactant choice. Once the general composition has been determined, in subsequent experiments the quantity of PCL was gradually increased (reducing the styrene) in the foams, or replaced the styrene with MMA or used toluene as a diluent to allow self-crosslinking. Maximising the quantity of PCL is desirable because complete biodegradability and preferably re-absorbability are prerequisites for *in vivo* use. Substituting MMA for styrene is also beneficial as PMMA is an accepted biocompatiable biomaterial, already in use as bone cement in hip replacement surgery. Table 3.2 lists the compositions for all successfully produced HIPEs.

Table 3.2 PolyHIPE Foams Prepared with PCL

	Foam[a]	PCL / g	Diluent / g	HLB	Water / ml	ϕ
1	0.2-L-S	1.0	4.0	4.3[b]	45	0.90
2	0.3-L-S	1.5	3.5	4.3[b]	45	0.90
3	0.4-L-S	2.0	3.0	4.3[b]	35	0.88
4	0.2-L-M	1.0	4.0	1.0[c]	45	0.90
5	0.4-L-M	2.0	3.0	1.0[c]	30	0.84
6	0.2-L-T	1.0	4.0	4.3[b]	45	0.90
7	0.5-L-T	2.5	2.5	4.3[b]	15	0.75
8	0.2-H-S	1.0	4.0	4.3[b]	45	0.90
9	0.3-H-S	1.5	3.5	4.3[b]	45	0.90
10	0.4-H-S	2.0	3.0	4.3[b]	35	0.88
11	0.2-H-M	1.0	4.0	1.0[c]	45	0.90
12	0.4-H-M	2.0	3.0	1.0[c]	30	0.84
13	0.2-H-T	1.0	4.0	4.3[b]	45	0.90
14	0.5-H-T	2.5	2.5	4.3[b]	15	0.75

[a]see page 63 for key [b]Span 80 [c]0.4 PE L121 / 0.6 Span 85

The first stage of experiments, entries 2, 3, 9 and 10 show the incorporation of up to 40 wt.% of PCL into the PolyHIPE materials. Above 40 wt. % PCL, the high viscosity of the organic phase prevented efficient mixing with the aqueous phase. This also limited

the volume of aqueous phase that could be added as the PCL content of the PolyHIPEs was increased. Figure 3.8 shows the structure of polyHIPE materials produced with 30 wt. % and 40 wt. % PCL. Both the foams made using macromonomer **1** possessed the open cellular, pore morphology, although in Figure 3.8 (b), the cell structure is less easy

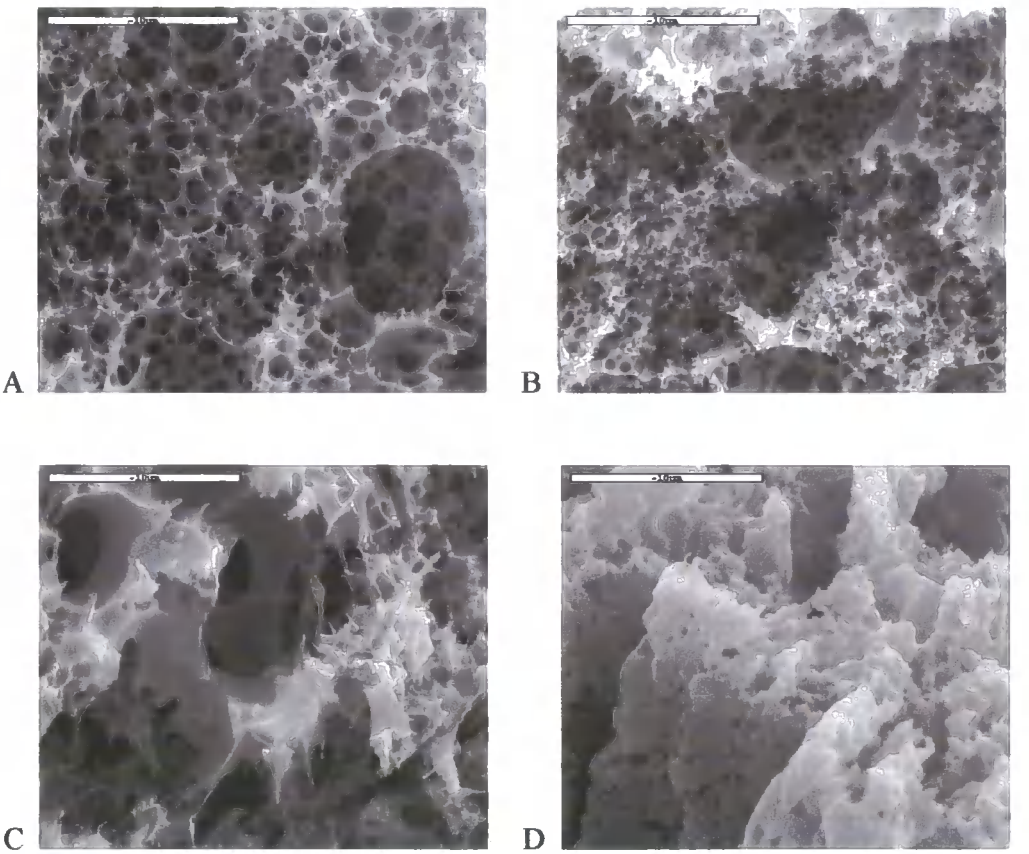

Figure 3.8 SEM Photographs (a) 0.3-L-S; (b) 0.4-L-S (c) 0.3-H-S; (d) 0.4-H-S (all 10 μm scale bars)

to discern. For foams made using the high molar mass PCL macromonomer **2**, at low PCL content, Figure 3.8 (c) shows that they also had a cellular structure. In Figure 3.8 (d), however, this is much less evident; while the foam is still porous it has a very different morphology. The morphology most likely results from inefficient mixing due to viscosity rather than phase separation up on heating. A non-porous structure would be

* See Experimental for key, page 63

more likely evidence for the latter. Another explanation could be an extreme increase in the diameter of interconnects between adjacent cells producing a morphology resembling a traditional macroporous resin. This transition has been found when using certain chlorinated organic phase diluents [94]. However, this form of structure is not evident in Figure 3.8 (d).

3.3.2.2 PCL and MMA

Retaining the conditions used to make the PCL and styrene foams, merely replacing the styrene with MMA, failed to produce a stable HIPE. The notably increased polarity of MMA compared to styrene makes HIPE formation more difficult, because the organic and aqueous phases are too 'similar'[101]. To form stable HIPEs, Ruckenstein et al. [131] found it necessary to prepolymerise the MMA to around 5% conversion and therefore, increase the viscosity of the organic phase. We decided to approach this problem by increasing the overall hydrophobicity of the organic phase, this was achieved by using a more hydrophobic surfactant. Table 3.3 presents the results obtained for

Table 3.3 Formation and Stability of HIPEs Containing MMA at Different Surfactant HLB Values

PCL used[a]	HLB_{mix}	Observation
L	2.6[b]	No HIPE formed
L	1.8[c]	HIPE stable for ca. 15 min. at room temp.
L	1.0[d]	HIPE stable at 60°C for several hours
H	2.6[b]	[e]
H	1.8[c]	[e]
H	1.0[d]	HIPE stable at 60°C for several hours

[a]L = low molar mass; H = high molar mass [b]0.3 Span 80 / 0.7 Span 85 [c]Span 85
[d]0.4 PE L121 / 0.6 Span85 [e]system not investigated

various HLB_{mix} values and shows that stable HIPEs were produced using a blend of Span 85 and PE L121 (HLB = 1). This composition was used to prepare PolyHIPEs from

macromonomers **1** and **2** containing 20 wt.% PCL and 80 wt.% MMA, their SEM pictures are presented in Figure 3.9.

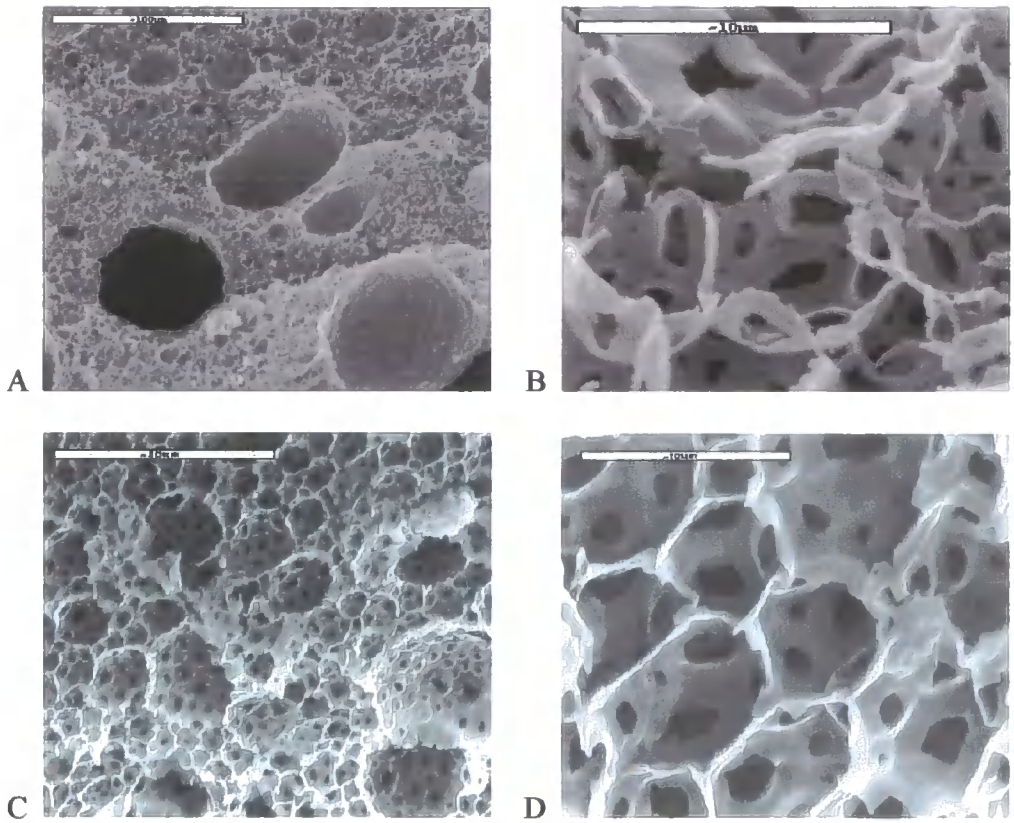

Figure 3.9 SEM Photographs (a) 0.2-L-M (100 μm scale bar); (b) 0.2-L-M (10 μm scale bar), (c) 0.2-H-M (50 μm scale bar); (d) 0.2-H-M (10 μm scale bar)

As with the PCL and styrene foams, an open-cellular morphology was produced upon polymerising the HIPE. However, at lower magnification the structure of the PolyHIPE appears to resemble frog spawn and at higher magnifications, the cells seem to be composed of fused rings. A possible explanation for the appearance of the 'fused cells' could arise from the higher density of MMA above styrene. The accepted explanation for formation of the interconnects is due to thinning at the monomer/ surfactant interface during polymerisation [132]. This phenomenon would be expected to

* See Experimental for key, page 63

occur less for a lower density change in polymerisation and this in turn would affect the overall morphology. Interfacial effects could also be affecting the morphology. A more stable emulsion will have thinner monomer/ surfactant films that would lead to a more open cellular morphology. In contrast, thicker interfacial films leading to fewer interconnects of smaller diameter would arise in a less stable HIPE. The former effect was observed for HIPEs containing chlorinated aromatic solvents that were inferred to cause a lowering of interfacial tension [94]. Shown more clearly in Figure 3.9 (a), to a lesser degree in Figure 3.9 (b), there is evidence of very large cells, implicating some coalescence of emulsion droplets. Therefore, MMA PolyHIPEs could be less stable than their equivalent styrene composition. As with styrene, we were able to increase the PCL content up to a maximum of 40 wt.% before high viscosity of the organic phase prevented further mixing. The upper limit for ϕ was 0.84 (Table 3.2, entry 12). SEMs of the PolyHIPEs prepared at 40 wt.% PCL with MMA are shown in Figure. 3.10.

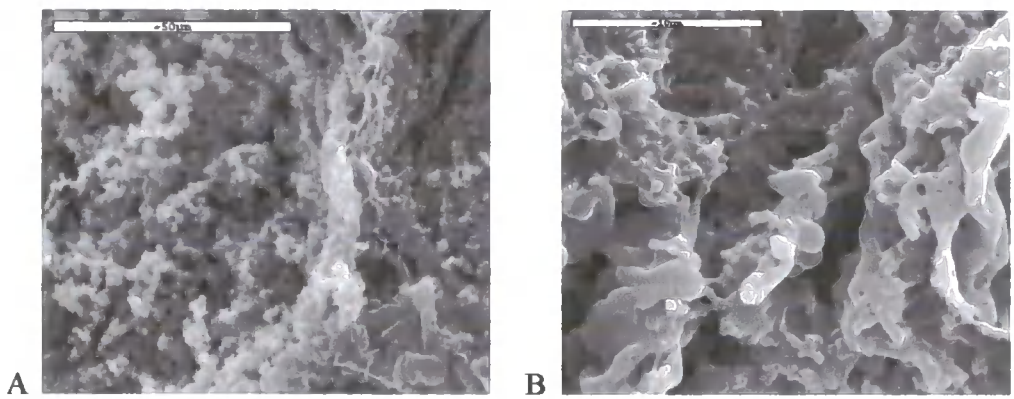

Figure 3.10 SEM Photographs (a) 0.4-L-M (50 μm scale bar); (b) 0.4-H-M (10 μm scale bar)*

The material prepared with macromonomer **1** (Fig. 3.10(a)) shows some evidence of cellular structure. Foams prepared from macromonomer **2** however produce a material

* See experimental for key, page 63

composed largely of aggregates of polymer microgel particles. This would indicate that before polymerisation the emulsion has undergone collapse to a certain extent.

3.3.2.3 PCL and Toluene

The final group of materials produced were composed almost entirely of polyester. This was achieved by replacing the vinyl monomer additive with a non-polymerisable organic phase diluent, toluene. Since toluene would be expected to have similar interfacial properties to styrene, a HLB value of 4.3, Span 80, was again used for the surfactant and as expected, stable emulsions were formed with 20 wt.% PCL. However, the mechanical properties of the foam were not good and they shrank by over 50% upon drying. The morphology of the foams can be seen in Figure 3.11. The shrinkage of the foams on drying was not unexpected as 2 vol.% in its expanded dry state

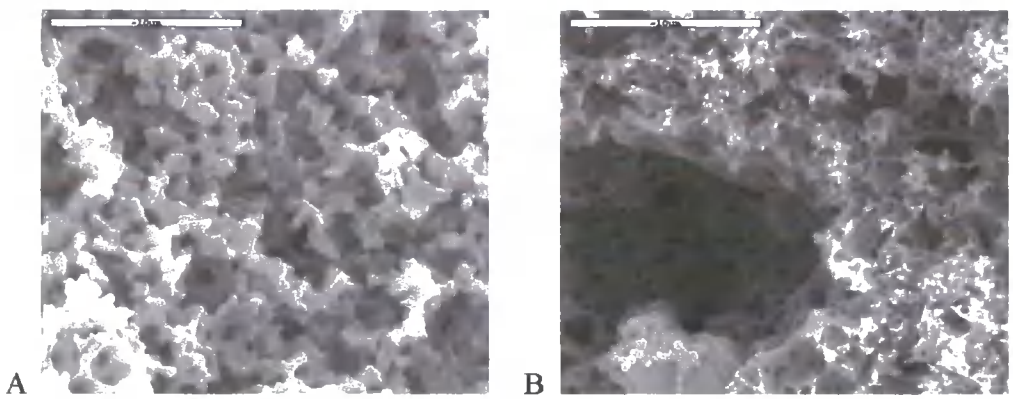

Figure 3.11 SEM Photographs(a) 0.2-L-T; (b) 0.2-H-T* (both 10 μm scale bars)

is solid polymer. Also the T_g of PCL can have an important role in the drying process, heating above the T_g can cause the foam to collapse. To try and solve the problem the PCL content was increased further to 50 wt.%, to create a more crosslinked network that would hopefully retain some structure. As before, a stable HIPE was obtained, but the

* See Experimental for key, page 63

high viscosity of the organic phase limited the values of ϕ (Table 3.2, entries 7 and 14). The increased PCL content did, however, improve the mechanical strength.

C 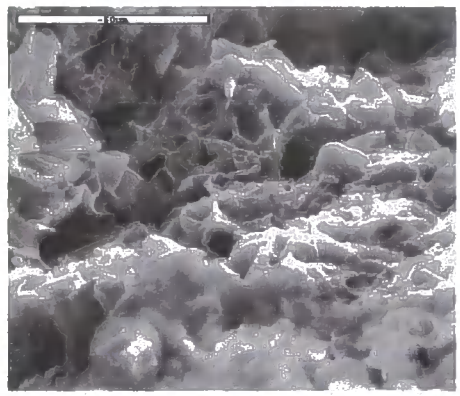 D 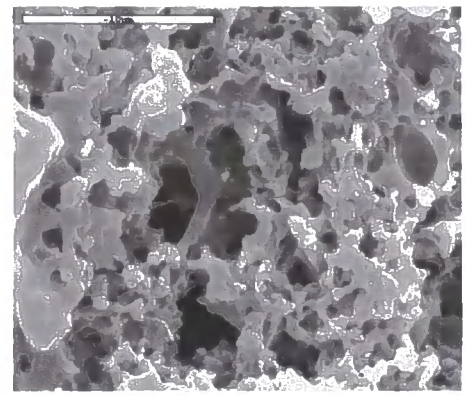

Figure 3.12 SEM Photographs (c) 0.5-L-T (50 μm scale bar); (d) 0.5-H-T* (10 μm scale bar)

Unlike the MMA foams, all the SEMs in Figure 3.11 and Figure 3.12 show a porous structure, with the foams made from macromonomer **2** retaining more of a cellular morphology. The lack of any agglomerated particulate structures infers that foams remained stable up to the point of gelation and there was no emulsion collapse. If the 'collapsed' structure has resulted from drying the foam *in vacuo* a possible solution would be to try an alternative method such as freeze-drying.

3.3.3 Swelling Studies

The swelling of all the foams listed in Table 3.2 were investigated. Accurately weighed quantities of each foam were immersed in excess solvent, toluene, IPA or water. The equilibrium mass of all solvents taken up by each foam was determined. The information gained provides data on the polarity of the materials and their response in an aqueous environment; important for their use in tissue engineering. For example, some

* See Experimental for key, page 63

of the foams were seen to absorb up to 20 times their dry mass of solvent, this would be as a result of their high porosity and interconnected structure. One of the problems facing tissue engineers is the uptake of fluids and nutrients to the developing tissue and removal of waste products, a material seen to swell in an aqueous environment would probably aid fluid intake and removal.

3.3.3.1 Swelling studies of Low Molecular Mass PCL Foams

Figure 3.13 below presents the swelling results for all foams prepared with macromonomer **1**. The following trends were identified:

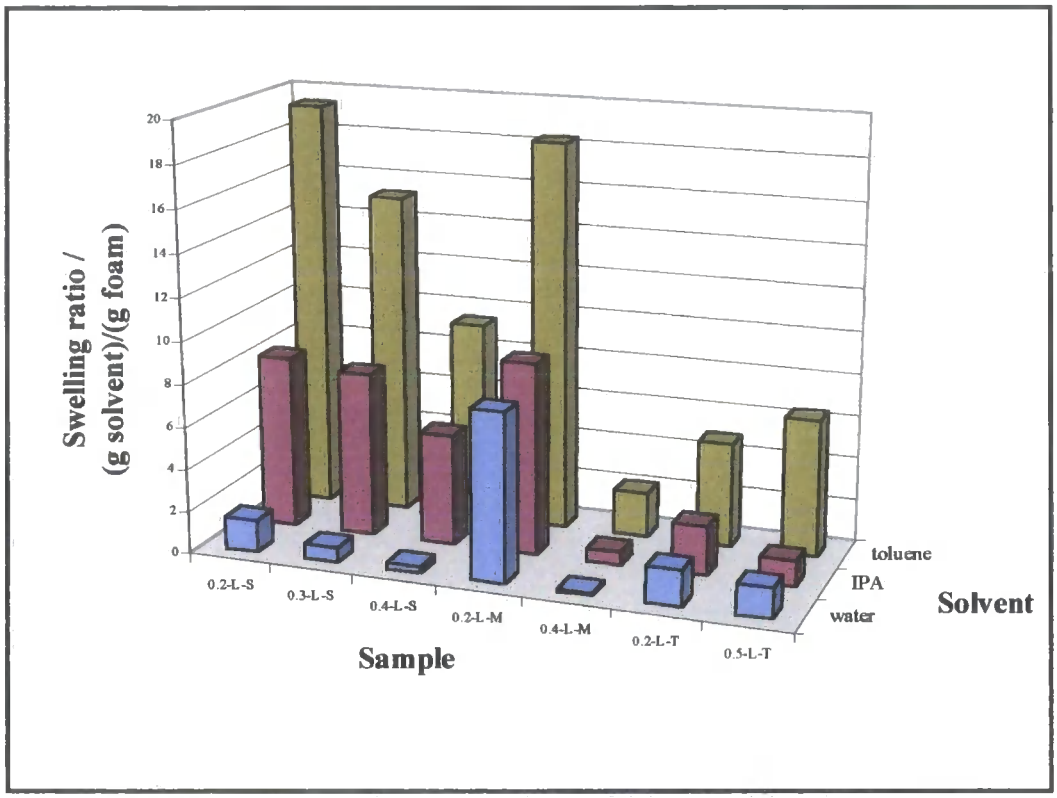

Figure 3.13 Swelling Study of Low Molecular Mass PCL Foams

i. The most hydrophobic foams, i.e. those with comonomer styrene, swelled the most in toluene.

ii. Swelling decreased as PCL content increased, due to higher levels of crosslinking of the difunctional macromonomer and lower hydrophobicity of PCL relative to styrene.

iii While the corresponding foams 0.2-L-S and 0.2-L-M showed similar swelling in toluene, their counterparts 0.4-L-S and 0.4-L-M did not. This can be attributed to a lower foam porosity (ϕ = 0.88 and 84 respectively), in the latter case, increased crosslinking and to some degree the lower affinity of MMA for toluene.

iv Foams prepared with toluene as a diluent showed increased swelling with increased PCL content, this inspite of a lower porosity, which is probably a reflection of the collapse experienced by the foam during the drying process. The foam prepared from the higher PCL content (0.5-L-T), despite a lower internal phase volume, retained more of its original void space upon drying.

v Trends observed in IPA were similar to those seen for toluene but on a reduced scale, reflecting the lower overall affinity of the foams for IPA compared with toluene.

vi In water, all, but the 20 wt.% PCL and MMA foam, exhibited very low swelling. Factors that will have allowed the foam to swell, will be a relatively low level of crosslinking together with the higher polarity of MMA.

3.3.3.2 Swelling Study of High Molecular Mass Foams

Figure 3.14 below presents the swelling results for all foams prepared with macromonomer **2**. The trends identified were generally similar to those prepared from macromonomer **1**, with some evident differences as follows:

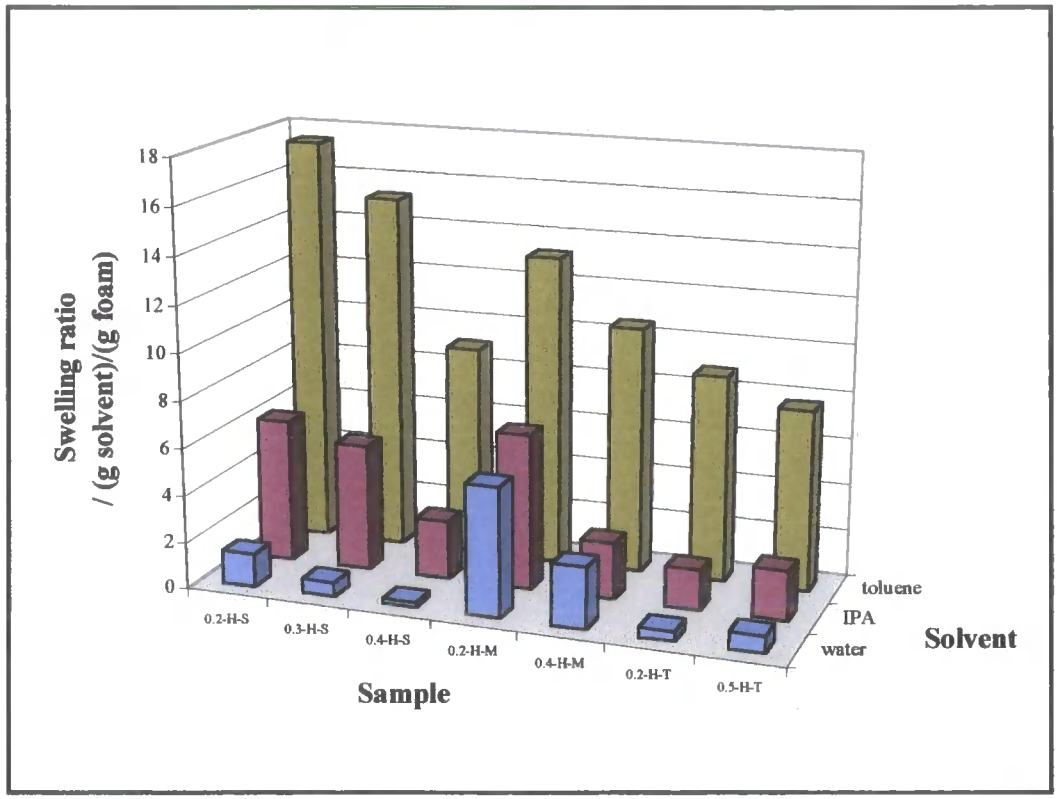

Figure 3.14 Swelling Study of High Molar Mass PCL Foams

i The swelling of the 0.4-H-M foam in toluene is approximately 5 times greater than its equivalent 0.4-L-M foam. As the porosity of both foams is equal, the difference cannot be attributed to a greater void volume in 0.4-H-M. The likely cause for this would be variations in network formation from the different molar masses of PCL starting material. Foams made using the higher molecular weight material would be less tightly crosslinked, permitting greater conformational freedom and hence, increased swelling capacity.

ii The 0.4-H-M displayed larger swelling values in IPA and water compared to 0.4-L-M and the 0.2-H-T had swollen around twice that of 0.2-L-T; both effects credited to the same reasons as (i).

iii For the styrene foams, the extent of swelling was independent of the molar mass of PCL macromonomer used. It would appear that the differences in network structure from using the high or low molecular weight material were overridden by the greater void volume from the higher porosity at high PCL levels (ϕ = 0.88 for 0.4-L/H-S). It would, therefore, be logical that the lower porosity of the high PCL content MMA foams reverts back to the influence of the networks chemical structure on the ability of the foam to swell.

iv Although the nominal porosity of the 0.2-L/H-T foams would be 0.9, determined from the HIPE internal phase volume, collapse of the network during drying means this figure is likely to be inaccurate. Again the network structure of the materials would appear to have a greater influence on the extent of swelling than porosity.

3.4 Conclusions

Using PCL macromonomers **1** or **2** either alone or with a comonomer (styrene or methyl methacrylate) a series of highly porous and permeable PolyHIPEs were prepared by free-radical polymerisation of precursor HIPEs. Foam morphologies were determined by scanning electron microscopy and their swelling properties investigated in solvents of differing polarities.

The concentration of PCL macromonomers **1** and **2** and the nature of the diluent added to the organic phase determined the foam structure. A maximum of 40 wt. % of

PCL, 60 wt. % comonomer was the optimum composition beyond which high solution viscosity inhibited HIPE formation. For PCL only, this optimum value was increased to 50 wt. %.

The swelling studies investigation discovered that the solvent type influenced the swelling of the foams in the order, water < *iso*-propanol < toluene, due to the strongly hydrophobic nature of most foams. Increasing the PCL content increased the level of crosslinking in the foams - the macromonomers **1** and **2** being difunctional – which led to a decrease in swelling. As the molar mass of PCL macromonomer increased, greater chain lengths produced a less tightly linked network with generally increasing swelling.

Preparation and Characterisation of PL Foams

Chapter 4

4 PREPARATION AND CHARACTERISATION OF PL FOAMS

4.1 Introduction

4.1.1 Basic Polymer Science and Stereochemistry

4.1.1.1 Molecular Weight

Polymers are molecules built up from repeating units, monomers. The synthesis of a polymer whether by step growth or addition results in a series of chains of varying length. This means that polymers cannot possess an exact molecular mass, but can be described by a number of molar mass averages. A typical polymer distribution is presented in Figure 4.1.

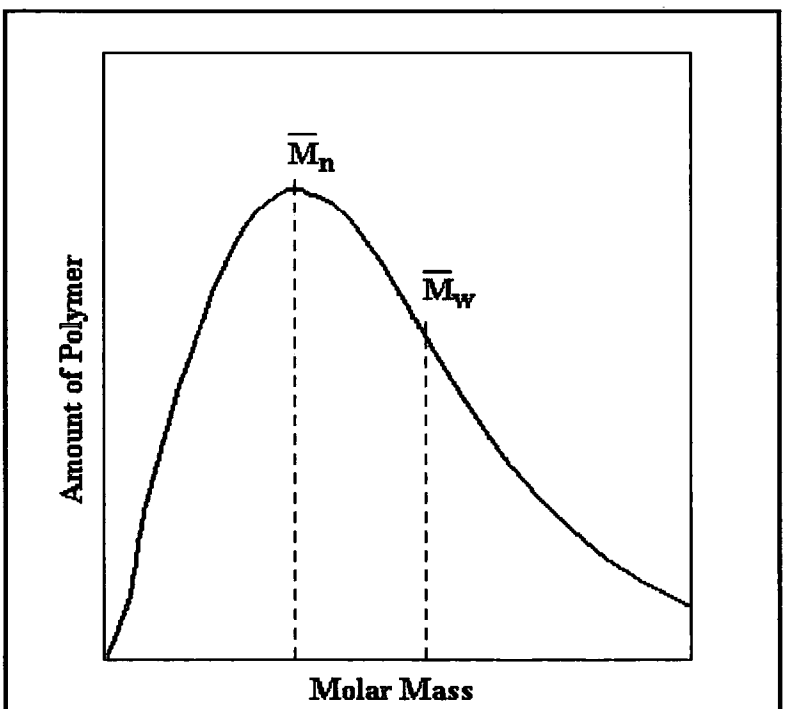

Figure 4.1 Typical Polymer Sample Molar Mass Distribution

In Figure 4.1, $\overline{M}_n$ is the number average molar mass and for a Gaussian distribution it is the value at the peak of the distribution curve, i.e the most common

molar mass. $\overline{M}_w$ is the weight average molar mass, calculation is based on the size rather than number of molecules. These values can be calculated using a number of techniques, e.g. GPC, MALDI-tof, light scattering ($\overline{M}_w$). The ratio of $\overline{M}_w$ to $\overline{M}_n$ also provides the spread of the molecular weigh distribution, the polydispersity, where a monodisperse polymer would give a ratio of 1.

4.1.1.2 Amorphous and Crystalline Polymers

Polymers adopt one of several conformations: amorphous, where the polymer chains possess no order; crystalline, where the polymer chains are all tightly packed and ordered – the degree of this order can vary; semi-crystalline, where both amorphous and crystalline regions exist.

There are two regular chain structures the crystalline regions typically adopt, eithyer a zig-zag or helical conformation, depending upon which conformation maximises the intermolecular van der Waals forces and / or hydrogen bonding.forces. The nature and degree of crystallinity, or its absence influences a number of the polymer characteristics such as mechanical response, tensile strength and viscoelasticity. This topic will be further discussed later in this chapter, as the properties of the polymers PL and PG and their copolymer PLGA are influenced by their crystalline or amorphous characteristics.

4.1.1.3 Glass Transition Temperature (T_g)

The temperature region over which a polymer changes from being a glassy solid to a rubber-like material and back again is known as the glass transition temperature (T_g). T_g rather than depending on polymer structure, is instead dependent on the chemical

nature, that influences the rotational freedom of the chains and can provide intermolecular attractions. Above the T_g the polymer chains move with a rapid motion, however, as the temperature is lowered, the thermal energy required for the chain segments to move is no longer available and the movement slows. At the T_g the chains become frozen in the position they adopted prior to the onset of T_g. A perfectly ordered crystal polymer would not show a T_g, because the material would contain no disordered chains, it would melt to give a viscous liquid. In practice even polymers described as crystalline contain some chains that are disordered and a transition range is observed before melting (T_m) occurs.

4.1.1.4 Stereochemistry

Compounds whose atoms are identically connected but can occupy different sites about a central point are known as stereoisomers. More commonly this is termed chirality, handedness, and the molecules if mirror images of one another, are described as enantiomers. Chirality exists when the four atoms attached to a central carbon are all different. Figure 4.2 shows a molecule and its 'mirror image', whilst each molecule contains 4 different atom groups (represented by 4 different coloured balls) and they

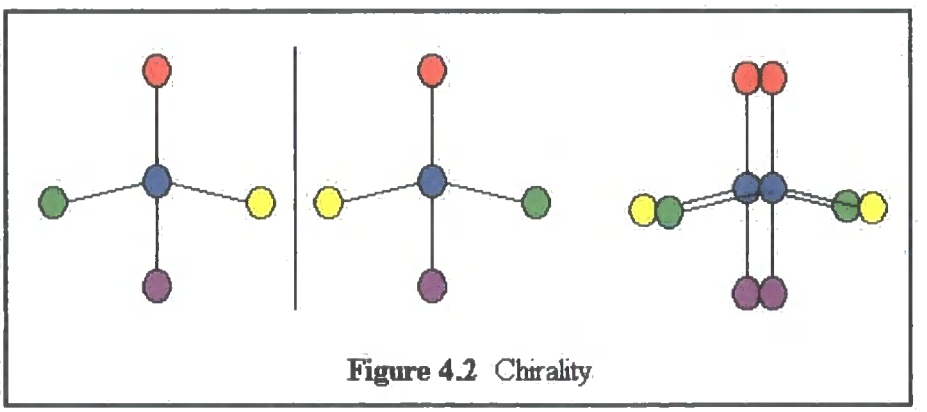

Figure 4.2 Chirality

appear to be identical, if the 2 molecules are overlapped it can be clearly seen that 2 pairs of the atoms occupy different areas of space. Two molecules showing chirality to one another will have the same physical properties, with the exception that they rotate the plane of plane-polarised light in opposing directions, shown as (+) or (-) in Figure 4.3. A racemic mixture contains equal quantities of both enantiomers and therefore will not show any optical activity. There are two different nomenclature systems used to distinguish the two enantiomers from each other. Chemists use an **R-** and **S-** system from the Cahn-Ingold-Prelog rules, this assigns priority to the different atoms around the stereocenter according to atomic number - the higher the atomic number, the higher the priority. If the order of prority is clockwise when the molecule is drawn with the lowest priority group facing to the back it is termed **R-** and if anticlockwise **S-**. Biologists however use an older, **D-**,**L**-system introduced by Rosanoff. These apply to lactic acid as shown in Figure 4.3. In the case of an amino acid a Fischer projection of the molecule is drawn with the acid group facing upwards and if the amino group is to the left, with the hydrogen to the right of the projection, the form is **L-** and vice versa is **D-**.

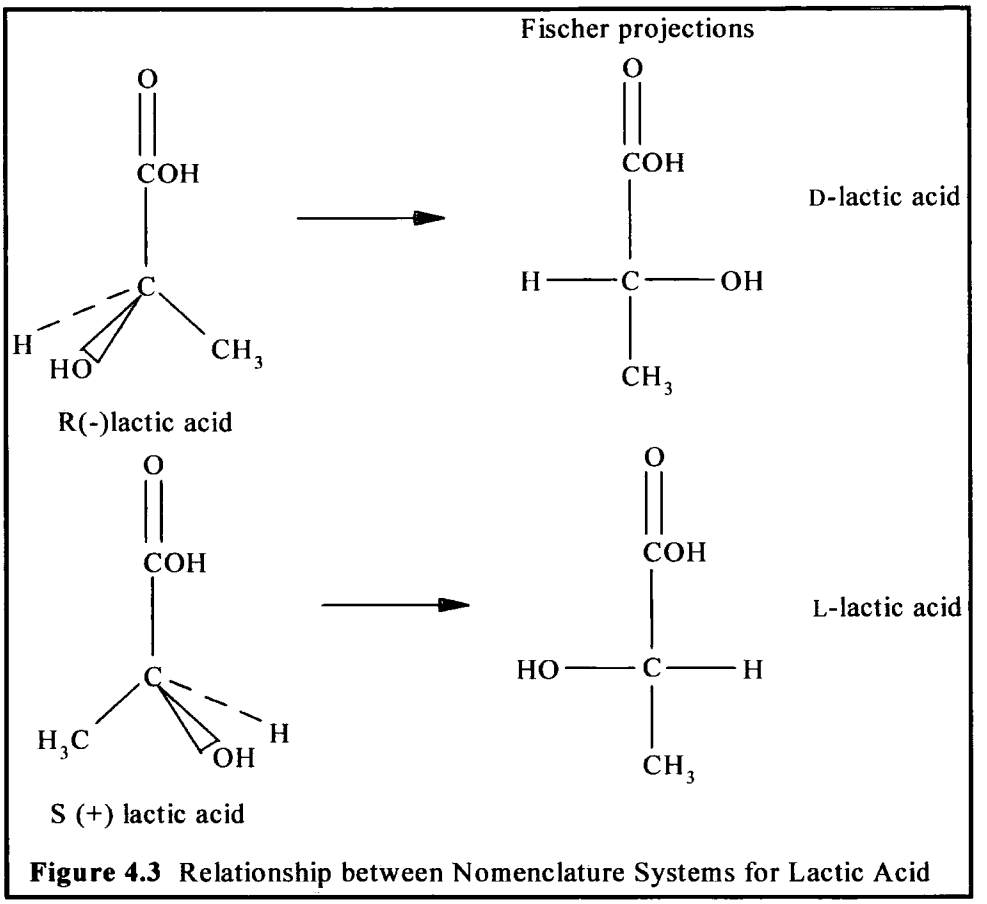

Figure 4.3 Relationship between Nomenclature Systems for Lactic Acid

4.1.2 Lactic Acid, Glycolic Acid and Their Polymers

4.1.2.1 Lactic Acid / Lactide and Glycolic Acid / Glycolide

Glycolic acid differs from lactic acid by the replacement of the CH_3 group by a hydrogen (see Figure 4.3, previous page). Using raw materials such as sugar cane / beat, potatoes or corn, *Latobacilli* produces the optically active L-lactic acid by fermentation [133]. Polymers can be synthesised from the acids or their corresponding lactones: glycolide; D,L-lactide; D,D-lactide; L,L-lactide which are produced from the acids. The structure of the lactones can be found in section 2.1, Scheme 2.3.

4.1.2.2 Synthesis of PL, PG and PLG

There are a number of possible methods for the preparation of polymeric foams from the lactones or their parent acid given in 4.2.1:- polycondensation; ROP; living ROP. Polycondensation of the acids has the advantages of being straightforward and cost-effective but produces oligomers of only a few thousand molecular weight [134]. Extreme conditions are required with long reaction times and high temperatures [135] in order to continuously remove the water produced and to yield a polymer with a high polydispersity [60].

ROP is the more typical method for generating PLA, using stannous octoate as the catalyst and lauryl alcohol to regulate the chain length [136, 137, 138]. Using temperatures in the range 120 – 140°C and varying the ratios of the components yield PLA with high molecular weights between thousands and several millions [139]. ROP of glycolide and lactide is also used to synthesise PLGA with high molecular weights [140, 141], using various catalysts, such as, tin tetrachloride [142] and tetraphenyltin [143] and the cyclic products of a self-condensation reaction, glycolide, 1,4-dioxane-2,5-dione (m.p. 87°C) [144] and lactide, 3,6-dimethly-1,4-dioxane-2,5-dione (L,L-lactide m.p. 95°C; D,L-lactide m.p. 127°C) [144]. Polymerisation is typically carried out at higher temperatures and in a molten state [145].

Teyssie, Dubois and coworkers have carried out extensive research into living ROP [146]. Dating back to the early 1980s, the controlled polymerisation of lactides has been achieved by using functionalised aluminium alkoxides such as: aluminium triisopropoxide ($Al(O^iPr)_3$) [147, 148, 149] and the basic structure Et_2AlOCH_2X, where X can be $-CH_2Br-$ or $CH_2OC(O)C(Me)=CH_2$ [150, 151]. Using $Al(O^iPr)_3$, bulk polymerisation of L,L-lactide, racemic D,L-lactide and a combination of equal molar quantities of each has

been carried out. The mechanism has been determined as a "living" coordination-insertion reaction at temperatures between 110°C and 150°C [152]. ROP is initiated by a alkoxide group, therefore, the initial molar ratio of aluminium isopropoxide to lactide and experimental monomer conversion can be used to accurately predict M_n [153]. The reaction has also been carried out at 70°C in toluene, with M_n accurate up to approximately 1800 and a polydispersity of 1.1 – 1.4 [154]. The reaction always yields a polymer in which one end group is an alkoxide that becomes hydrolysed to an alcohol whilst the other end will be an ester group and the derivative of the radical initiator, i.e, X [155, 149]. The coordination-insertion mechanism is shown in Scheme 4.1.

Although no further details were given, a number of anionic catalysts can also be used for the polymerisation, such as: potassium methoxide, potassium *tert*-butoxide and butyl lithium [60]. Stereoisomerism also has an important role to play in the formation of polylactide. Polymers containing the stereoisomers D- or L-lactic acid can adopt one of 3 conformations, isotatic: all the methyl groups will be *trans*- with respect to one another, i.e. on the same side of the chain therefore all D- or all L-; syndiotactic: where the methyl about the chiral centre alternate between the D- and L- form; atactic (heterotactic) where the arrangement of the methyl is random. The different stereo structures are given in table 4.1. The impact of the different structures is discussed in the next section.

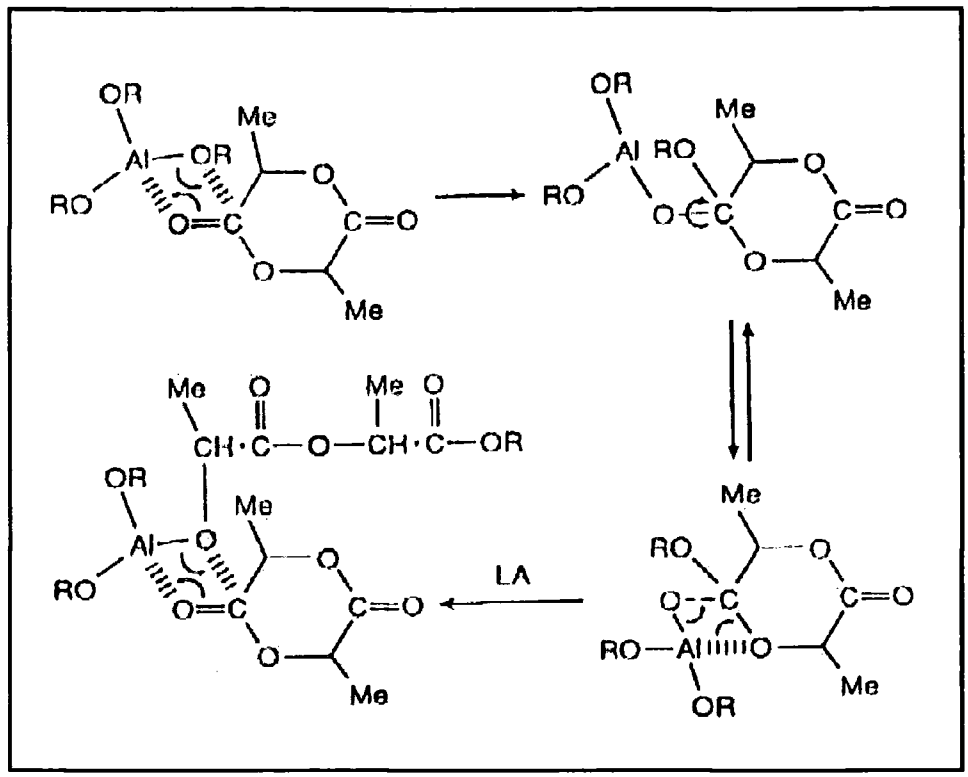

Scheme 4.1 The Coordination-Insertion Mechanism of Functionalised Aluminium Alkoxides [156]

Table 4.1 Stereo Structures upon Polymerisation of Lactic Acid and Stereoisomers

Monomer	Polymer
D-lactic acid	Isotactic P(DLA)*
L-lactic acid	Isotactic P(LLA)*
Racemic mix D/L-lactic acid	Atactic P((D,L)LA)†
D,D-dilactide or L,L-lactide	Isotactic P(DLA) or P(LLA)[157, 158]
Racemic mix D,D/L,L-lactide	Predominantly isotactic P(D,L)LA[159]
Diastereoisomer of D,L-lactide	Syndiotactic P(D,L)LA [157]

4.1.2.3 Differences in Polylactides and Comparison to PCL

Poly(L-lactic acid) is a slow degrading semi-crystalline polymer [160] - the isotatic nature of the polymer allowing tighter packing of the polymer chains, with weak

* unless occurrence of racemisation of the chiral centre (H. Kricheldorf et al., *Macromol. Chem.* **191**, 1057 (1990)) or tranesterification (H. Kricheldorf et al., *Macromol. Chem.* **194**, 1653 (1993), G. Schwach et al., *Polym. Bull.* **32**, 617 (1994))

† unless stereo-selective catalyst employed

interactions between molecules on different chains. Poly(D,L-lactic acid) is a faster degrading amorphous polymer [160] - the random and/or isotactic structure of the polymer mean the chains are going to be less tightly packed and therefore more flexible. The methyl group on the backbone of lactide polymers makes them hydrophobic and causes steric hinderance in the hydrolysis reaction that cleaves the ester linkage rendering the polymers biodegradable. In contrast, polymers synthesised from glycolide are highly crystalline and hydrophilic [33]. Polymers containing a mixture of lactic and glycolic acid, PLGA, where the latter comprises 25% - 75% of the composition are amorphous in nature, with the biodegradability of the polymer controllable by varying the quantity of lactide and glycolide in the polymer. The amorphous regions of the polymer besides allowing faster degradation allow it elastic functionality, while the crystalline regions give the polymer mechanical strength and acts to crosslink the polymer [161]. Table 4.2 lists the melting point and T_g, of the 3 lactide polymers and PCL for comparison. The range over which the amorphous regions of PGA changes from a glassy state to a

Table 4.2 Comparison of T_g and T_m of 4 Polyesters

Physical property	PGA	PLLA	PDLLA	PCL
T_m / °C	225 – 230	170 - 190	-	60
T_g / °C	40	50 - 60	50 - 60	-60

molten one is approximately half as much again as the 2 semi-crystalline polymers PLLA and PCL. PCL would be expected to be mechanically less strong but more pliable than its equivalent molecular weight PLLA counterpart at room temperature because it would be above its glass transition point, therefore, the polymer chains would be able to rotate and be more flexible than PLLA, which would still be in its glassy state. It should be noted, however, that the molecular weight also affects the nature of the polymer e.g. PCL

diol with an $\overline{M}_n$ = 530 is a viscous paste, however at $\overline{M}_n$ = 2000 the polymer has become solid with a waxy consistency.

4.2 Experimental

4.2.1 Materials and Instrumentation

4.2.1.1 Materials

Styrene and methyl methacrylate were freed of inhibitor by passing through a pad of basic Al_2O_3; the stannous 2-ethylhexanoate was dried *in vaccuo* for 24 h. and all other species were used as supplied. 3,6-dimethyl-1,4-dioxane-2,5-dione, stannous octanoate and 1,6-hexanediol were obtained from Aldrich. The surfactants, Span 80 (sorbitan monooleate) and Span 85 (sorbitan trioleate) were obtained from Sigma. The surfactant Synperonic PE L121 was received from ICI surfactants.

4.2.1.2 Instrumentation

FTIR spectra (KBr disks) were recorded on a Perkin Elmer 1600 Series FTIR spectrometer. NMR spectra were recorded on a Varian ASM-100 Unity-300 spectrometer at 300 MHz (^{1}H) and Bruker AM-250 spectrometer at 63 MHz (^{13}C) both using $CDCl_3$ as solvent. Solid state ^{13}C spectra were obtained with cross polarisation, high-power proton decoupling and magic angle spinning using a Varian unity-plus 300 spectrometer at 75.43MHz and ambient probe temperature (296K). A sapphire 7mm outer diameter rotor with Kel-F caps were used in a Doty probe. Elemental analysis (C, H and N) was performed using a Exeter Analytical E-440 elemental analyser. MALDI-tof spectra of samples immobilised in a mixture of 2,5-dihydroxybenzoic acid (gentisic acid) or dithranol were recorded using a Kratos Kompact MALDI 4. Scanning

electron microscopy was carried out at the University of Newcastle using a Hitachi S2400 electron microscope operating at 25kV. Fractured samples were prepared for SEM by mounting on aluminium stubs using adhesive carbon disks to increase the conductivity. All samples were sputter-coated with a thin layer of gold prior to viewing to enhance conductivity. Molecular weight was determined by GPC using a HPLC pump GBC LC 1120, a Knauer injection unit, a Viscotek differential refractometer, a differential viscometer and a right angle laser light scattering detector operating at 670 nm. Separation was carried out using 3 –10 μm gel columns and a 5 μm guard column.

4.2.2 General Methodology

4.2.2.1 Polymer Synthesis

A round-bottomed flask fitted with a rubber septum and magnetic fly was charged with 3, 6–dimethyl–1 ,4–dioxane–2 ,5-dione, stannous 2 ethylhexanoate (catalyst) and 1,6 hexanediol. The system was purged with Argon for 10 min. The flask and its contents were placed in a pre-heated oil bath (135°C) and fitted with a balloon filled with argon to provide a slow purge. The contents of the flask were left stirring at 135°C for 24 h. leaving a viscous liquid that cooled to give a glassy solid.

The polymer was then dissolved in a minimal quantity of DCM and re-precipitated over 24 h. by pouring into distilled petroleum ether (pet. ether) 40°C /60°C. The pet. ether was decanted and the precipitation process was then repeated. After decanting off the pet. ether again the polymer was re-dissolved in DCM and placed in a round-bottomed flask. The solvent was removed on a rotary vaporator and the contents

of the flask was heated to 60°C and dried *in vacuo* for 24 h. This was carried out according to a procedure described by Storey et al. [162].

4.2.2.2 Macromonomer Synthesis

The equipment was set up as shown in Figure 4.4. The whole unit was purged with Argon as the flask was cooled to ice-temperature. The solution, in the dropping funnel, was added dropwise over ca. one hour, to the contents of the round-bottomed flask, as it was stirred and kept at ice temperature. The system was then left stirring for a further 20 h. during which time it returned to room temperature. The resulting

Figure 4.4 Equipment for Macromonomer Synthesis

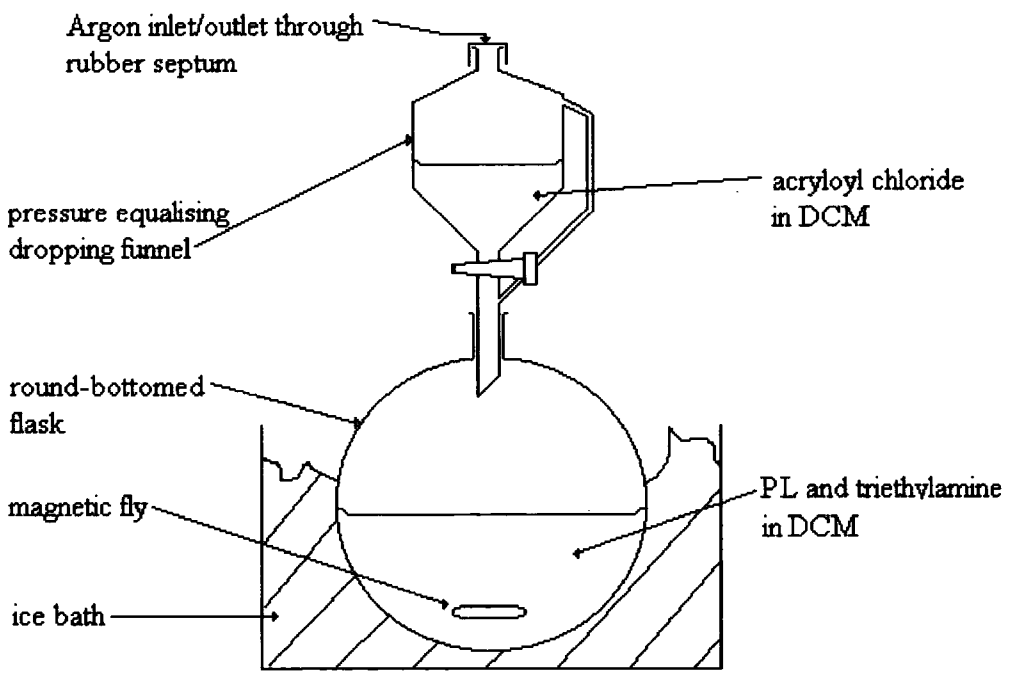

solution was extracted with ca. 30 ml portions of 3 wt. % KOH aqueous solution, followed by the same of 1 vol. % HCl solution until, in both cases a colourless aqueous

layer was obtained. The extracted organic layer was dried over $MgSO_4$, placed on a rotary vaporator to remove most of the DCM then concentrated *in vacuo* to a constant mass. The resultant polymer had the appearance of small yellow crystals.

4.2.2.3 PolyHIPE Formation

The equipment was set up as shown in Figure 4.5. Firstly the contents of the 3-necked flask and then the pressure equalising dropping funnel were purged by Argon bubbling for 10 min. each. Then the content of the latter was added dropwise over ca. 1 h. whilst the content of the flask was mixed at ca. 300 r.p.m. using a D-shaped PTFE paddle powered by an overhead stirrer motor. The resultant emulsion, having a consistency similar to that of mayonnaise, was transferred to a polyethylene bottle that was heated at 60°C for 48 hours. After this the PolyHIPE that had formed was removed from its container and washed by Soxhlet extraction for 24 hours with water then isopropanol as solvents successively. The PolyHIPE was finally dried to a constant mass *in vacuo*. This was according to a standard procedure [128].

Figure 4.5 Equipment for Foam Synthesis

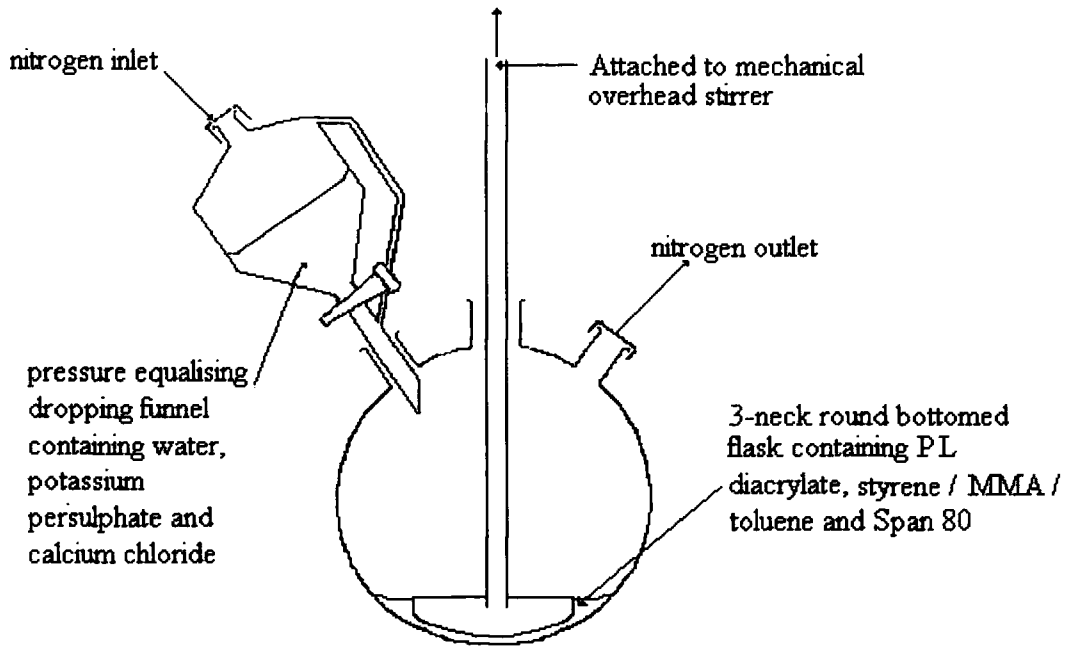

4.2.2.4 Swelling Studies

A series of pre-weighed sinter sticks 1 – 6 were immersed in each of the chosen solvents, toluene, water and *iso*-propanol, until a constant mass value was obtained. When subtracted from the dry weight, the quantity of each solvent taken up by the porous glass frit was determined. The following procedure was carried out in duplicate for each foam sample: ca. 0.1g of each PolyHIPE was accurately weighed and placed in a sinter stick. The sticks were immersed in solvent for 24 hours, removed and weighed, this process was repeated until a constant mass was obtained. The extent of solvent absorbed by each foam was determined by mass of (wet sample + stick) minus mass of (dry sample + dry stick + solvent absorbed by empty stick). A normalised value was then calculated

from the previous value divided by the mass of dry sample and expressed as g solvent / g polymer. This experiment was based on a previous procedure [129].

4.2.3 Experiments

4.2.3.1 PL $\overline{M}_n$=2000, Polymer Synthesis

Experiments were carried out as outlined in 4.2.2.1. Quantities were used as follows: 3, 6-dimethyl-1, 4-dioxane-2, 5-dione (20.26 g, 14.0 mmol); 1, 6-hexanediol (1.18 g, 10 mmol); stannous octanoate (0.05 g, 0.123 mmol); 100 ml DCM and 1000 ml pet. ether. Yield ~ 21.54g (100%).

IR (film): υ cm^{-1} = 3522 (OH stretch), 2993, 2943 (C – H str.), 1753 (C = O), 1188, 1092 (C-O str.);

^{1}H NMR (300 MHz, $CDCl_3$), δ ppm = 5.1 (-$CO_2C\underline{H}C\underline{H}_3CO_2$-), 4.3 (HO$C\underline{H}CH_3CO$-), 4.05 (-$CHC\underline{H}_3CO_2$-), 1.5 (-$OCH_2C\underline{H}_2C\underline{H}_2C\underline{H}_2CH_2CH_2O$-)

Elemental Anal. calcd. for $C_{96.8}H_{135.7}O_{62.7}$ C, 50.5%; H, 5.9%. Found C, 47.94%, H 5.75%. **MALDI-tof MS**, *m/z* 3601, 3531, 3459, 3384, 3312, 3244, 3167, 3097, 3025, 2952, 2882, 2811, 2735, 2667, 2592, 2519, 2448, 2376, 2305, 2231, 2162, 2087, 2019, 1943, 1876, 1799, 1728, 1655, 1585, 1510, 1441, 1370, 1295 $[(\overline{M})_n + Na^+]$,

GPC $\overline{M}_n$ = 2000 (calculated $\overline{M}_n$ 2300), $\overline{M}_w$ = 3,450, $\overline{M}_z$ = 4,640, Pd = 1.73 and $\overline{M}_p$ = 3, 550

4.2.3.2 PL diacrylate, Macromonomer Synthesis

Experiments were carried out as outlined in 4.2.2.2. Quantities used were as follows: PL (18.81 g, ≈ 9.4 mmol OH groups) dissolved in 200 ml DCM containing triethylamine (6.5 ml, 43 mmol); acryloyl chloride (3.5 ml, 43 mmol) in 30ml DCM. Yield ~ 16.36g (97%)

IR (film): υ cm^{-1} = 2992, 2943 (C – H str.), 1754 (C = O), 1186, 1091 (C-O str.),

^{1}H NMR (300 MHz, $CDCl_3$), δ ppm = 6.40 (dd, 2H, $J_{Ha\text{-}Hc}$* = 17 Hz, $J_{Ha\text{-}Hb}$* = 2 Hz, H_a*), 6.10 (dd, 2H, $J_{Ha\text{-}Hc}$* = 15 Hz, $J_{Hb\text{-}Hc}$* = 9 Hz, H_c*), 5.80 (dd, 2H, $J_{Hb\text{-}Hc}$* = 9 Hz, $J_{Ha\text{-}Hb}$* =2 Hz, H_b*), 4.05 (-CHC$\underline{H}_3CO_2$-).

^{13}C NMR (75 MHz, $CDCl_3$): δ ppm = 132 ($\underline{C}HCH_2$), 128 (-CH$\underline{C}H_2$), 76 (-$CO_2C\underline{C}H_3CO_2$-), 69 (-O$\underline{C}CH_3CO$-)$_n$, 68.5 (-$CO_2\underline{C}CH_3CO_2$-), 66 (O$\underline{C}H_2CH_2CH_2$-) 46 (-OCCH$_2\underline{C}H_2CH_2$-), 28 (-OCCH$_2CH_2\underline{C}H_2$-), 17 (-OC$\underline{C}H_3CO$-)$_n$.

Elemental Anal. calcd. for $C_{98.3}H_{133.4}O_{61.7}$ C, 51.3%; H, 5.8%. Found C, 48.4%, H 5.69%.

MALDI-tof MS, *m/z* 3253, 3179, 3106, 3043, 2967, 2891, 2817, 2752, 2672, 2605, 2533, 2457, 2386, 2314, 2240, 2171, 2099, 2023, 1880, 1809, 1734, 1665, 1594, 1519, 1451, 1379, 1302 [$(\overline{M})_n$ + H^+]

4.2.3.3 PolyHIPE Formation

Experiments were carried out as outlined in 4.3.2.3. Quantities used were as follows: PL diacrylate ($\overline{M}_n$ = 2000 (1.0 g ≈ 0.5 mmol)); styrene (4 g, 38 mmol) or MMA

* see results and discussion for explanation

(4 g, 40 mmol) or toluene (4 g, 43 mmol); surfactant (1 g); water (45 ml); $K_2S_2O_8$ (0.1 g, 0.37 mmol); and $CaCl_2.2H_2O$ (0.5 g, 3.4 mmol).

Any reference to a PolyHIPE sample will be referred to using the following code X-Y. For example in the case of a PolyHIPE made using 3 g of PL macromonomer and 2 g of styrene, X = fraction (by weight of total oil phase*) of PL macromonomer in the HIPE formulation, the total organic phase is 5 g therefore the PL fraction = 3/5 =0.6, Y = organic phase diluent (S = styrene, M = MMA, T = toluene) therefore Y = S. For all the formulations produced the X-Y code and full descriptions are as follows:

X-Y	X PCL/g	fraction	Macromonomer Y
0.2-S	1.0	1/5	styrene
0.4-S	2.0	2/5	styrene
0.6-S	3.0	3/5	styrene
0.2-M	1.0	1/5	MMA
0.4M	2.0	2/5	MMA
0.2-T	1.0	1/5	toluene
0.4-T	2.0	2/5	toluene
0.6-T	3.0	3/5	toluene

PL and styrene

IR (KBr disc): υ cm^{-1} = 3082, 3059, 3025, 3001, 2924 and 2852 (C-H str.), 1757cm^{-1} (C = O str.), 1629, 1600 (C = C str.), 1493, 1452 and 1365 (CH def.), 757 and 698 (ipso substituted benzene ring).

^{13}C NMR (75.43MHz, solid state): δ ppm = 170 ($CH_2OCO\underline{C}H\underline{C}H_3$-), 146 (C in ipso position on benzene ring), and 128 (benzene ring), 69 (-OCO-$\underline{C}H_2$-), 40 (-$\underline{C}$H-), 17 (-$\underline{C}H_2$-),

PL and MMA

IR (KBr disc): could not be prepared satisfactorily

* The surfactant mass was not included in the oil phase for the purpose of the calculation of percentage composition because it was likely to concentrate at the interface

^{13}C NMR (75.43MHz, solid state):, δ ppm = 178 (C = O), 45 (quaternary C), 16 (-$\underline{C}H_3$), 17 (-$\underline{C}H_2$-),

PCL and toluene

IR (KBr disc): υ cm^{-1} = 3548, 3405 (-O-H), 2995, 2945, 2858 (CHO), 1757 (C=O str.), 1052 – 1273 (C-O str.), 865, 751, 702 (olefinic C-H).

^{13}C NMR (75.43MHz, solid state): δ ppm = 170 ($\underline{C}H_2OCO\underline{C}H\underline{C}H_3$-), 69 (-OCO$\underline{C}$H-$_2$),, 55, 52, 45, 40, 29 and 26 (-O$\underline{C}H_2\underline{C}H_2\underline{C}H_2\underline{C}H_2\underline{C}H_2CO_2$-), 17 (-$\underline{C}H_2$-).

4.3 Results and Discussion

4.3.1 Polymer Synthesis

The polymer was synthesised via addition of cyclic monomer units, 3,6-dimethyl-1,4-dioxane-2,5-dione to a central unit, 1,6-hexandiol to give the structure shown in Figure 4.6.

Figure 4.6 Structure of Polylactide (PL)

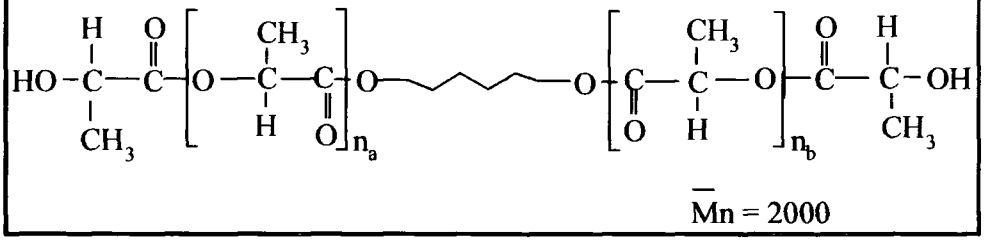

The resultant polymer was a glassy solid. Characterisation by GPC gave a $\overline{Mn}$ of 2000 and polydispersity index of 1.73. The spectra produced by MALDI-tof agreed with the structure shown in Figure 4.6. The central portion of the polymer, the 1, 6-hexanediol has a fixed mass totalling 116 and the 2 end units that are also constant

equalling 73 units each. The repeat units have a mass totalling 72. The minimum mass, therefore, for the structure given in Figure 4.6 would be 406, when both n_a and n_b equal 1. In Figure 4.7, the MALDI spectrum for PL, the starting total of $n_a + n_b$ is 14, working out at a mass of 1270, 1293 with the Na^+ ion, with an increase of one repeat unit for each peak. It is not possible to know whether the addition occurred symmetrically or asymmetrically.

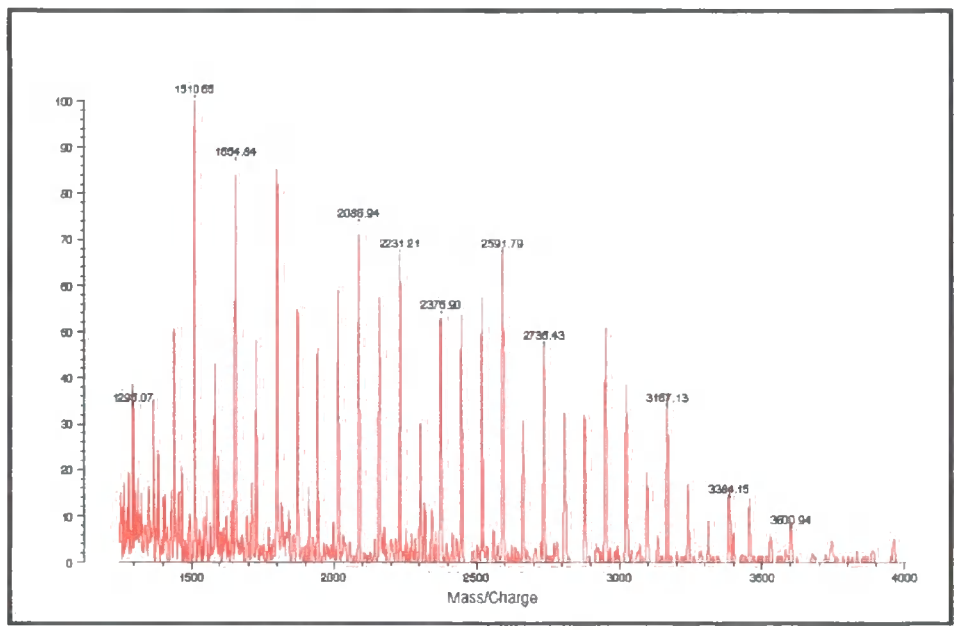

Figure 4.7 MALDI spectrum for PL

4.3.2 Macromonomer Synthesis

The diacrylate macromonomer was prepared using the chemistry shown in Scheme 4.2. As for the PCL (see chapter 3) NMR spectroscopy was used to determine that conversion of the diol endgroups to acrylate endgroups was achieved. As with the PCL, the acrylate end groups again showed the characteristic resonances in the ^1H NMR spectrum at δ 5.8, δ 6.1 and δ 6.4 ppm and these can be clearly seen in Figure 4.8.

Assignment of the acrylate peaks is the same as for the PCL and was covered in section 3.5.1.

Scheme 4.2 Macromonomer synthesis

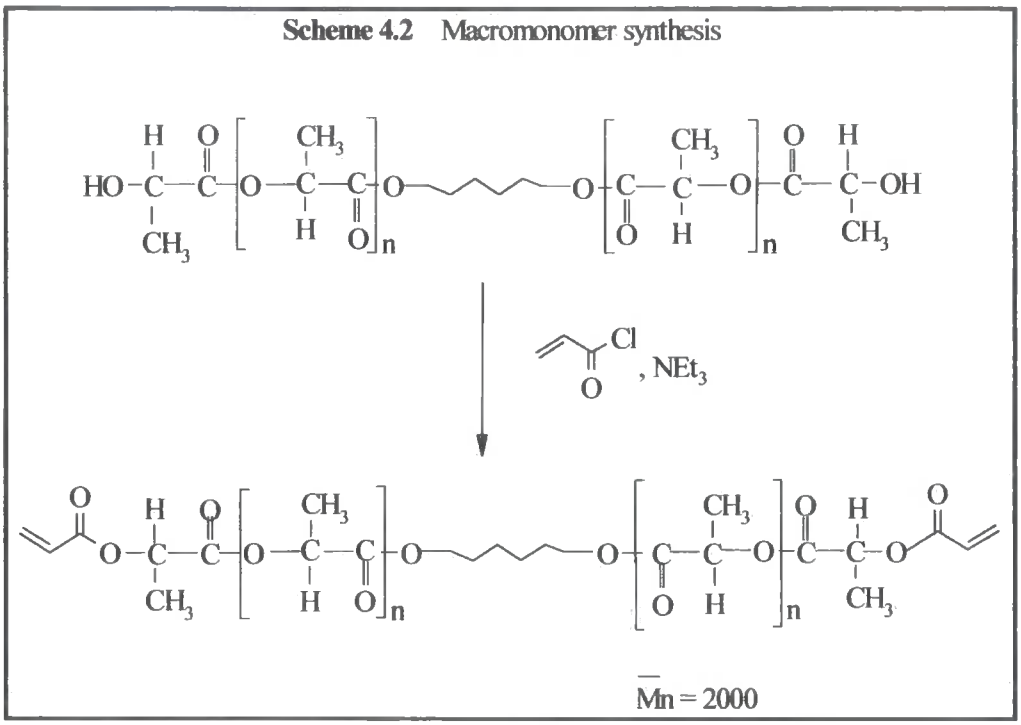

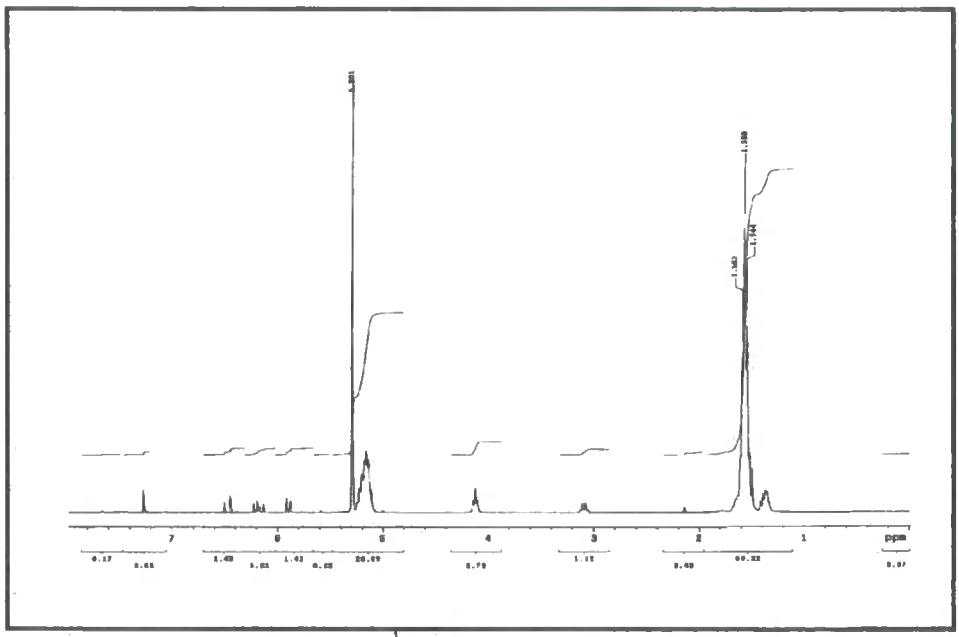

Figure 4.8 ^{1}H NMR spectrum for PL

The extent of conversion from alcohol to acrylate was again established using MALDI-tof mass spectroscopy. The addition of 2 acrylate units caused an increase in molecular weight of 108 units, 2 x (H_2C=CH-CO-) minus 2 protons. This is clearly illustrated in Figure 4.9 where each peak of the PL starting material (red trace) is shifted to a higher molecular weight by 108 units in the diacrylate product (blue trace). The presence of a blue trace for every red trace confirms that there has been no or little monodisfunctionalisation, each red trace corresponds to addition of a repeat unit and therefore each blue trace is 54 + 23 units from the previous red i.e. acrylate and Na^+. If monodisfunctionalisation had occurred then a blue peak would be absent.

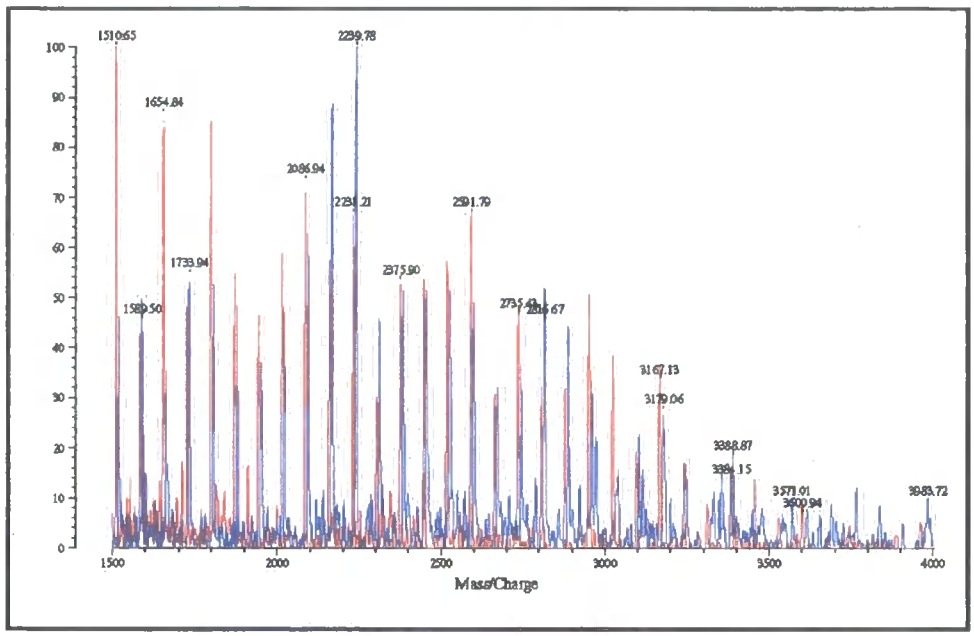

Figure 4.9 MALDI spectrum for PL diacrylate

Once the structure had been established we did not anticipate that the PL would behave differently to the PCL for PolyHIPE preparation and, therefore, proceeded straight onto the next stage without the need for confirming its crosslinking ability.

4.3.3 PolyHIPE Preparation

4.3.3.1 PL and Styrene

The same principle that was applied with the PCL work was also used for the PL PolyHIPEs. The initial experiments used a total of 5 g monomer with 20 wt.% of the styrene replaced with PL and remaining factors, quantity and concentration of surfactant, remained the same. HIPEs are intrinsically unstable and can be affected by moderate changes of emulsion composition. The presence of PL and absence of DVB as a change to the basic composition had no significant effect on HIPE stability. Straightforward preparation and polymerisation of emulsions of $\phi = 0.9$ yielded corresponding PolyHIPE foams. SEM images of the resulting structures are shown in Figure 4.10. The foam demonstrates the classic open-cellular PolyHIPE morphology as seen for styrene / DVB systems. However it is noticeable that, compared to the PCL foams (see Figure 3.6), the PL foams precursor emulsions are inherently more stable[†] having a cell size comparable to foams prepared using high levels of divinylbenzene, i.e. average cell size 5μm, rather than the 20μm seen with the PCL foams.

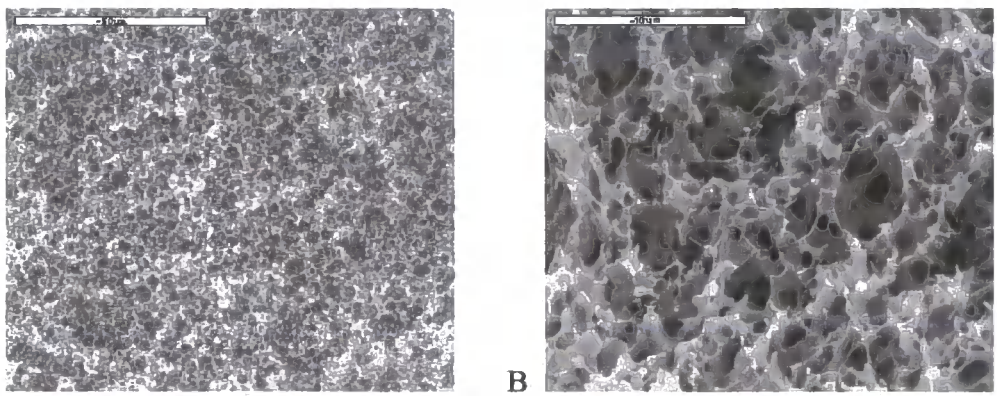

Figure 4.10 SEM Photographs (a) 0.2-S (50 μm scale bar); (b) 0.2-S (10 μm scale bar)[*]

[*] See Experimental for key, page 101
[†] emulsion droplet and therefore cell diameter are inversely related to emulsion stability

As for PCL, the subsequent experiments gradually increased the quantity of PCL (reducing the styrene) in the foams, or replaced the styrene with MMA or utilised toluene as a diluent to allow self crosslinking. The lower viscosity of the emulsion precursors made using PL also meant that PolyHIPEs were made with PL contents as high as 60 wt. %. Table 4.3 lists the compositions of all successfully produced HIPEs.

Table 4.3 PolyHIPE Foams Prepared with PL

Foam[a]	PCL / g	Diluent / g	HLB	Water / ml	ϕ
0.2-S	1.0	4.0	4.3[b]	45	0.90
0.4-S	2.0	3.0	4.3[b]	45	0.90
0.6-S	3.0	2.0	4.3[b]	15	0.75
0.2-M	1.0	4.0	1.0[c]	45	0.90
0.4-M	2.0	3.0	4.3[b]	30	0.84
0.2-T	1.0	4.0	4.3[b]	45	0.90
0.4-T	2.0	3.0	4.3[b]	35	0.88
0.6-T	3.0	2.0	4.3[b]	15	0.75

[a]see 4.2.3.3 for key [b]Span 80 [c]0.4 PE L121 / 0.6 Span 85

The first stage of experiments, entries 2 and 3 show the incorporation of up to 60 wt.% of PL into the PolyHIPE materials. Above 60% PL the high viscosity of the organic phase prevented efficient mixing with the aqueous phase. This also limited the volume of aqueous phase that could be added as the PL content of the PolyHIPEs was increased. Figure 4.11 shows the structure of PolyHIPE materials produced with 40 and 60% PL and styrene. Both the foams made using 40 and 60 wt. %. PL possess a porous morphology, although in cases the open-cell structure identified with PolyHIPEs is no

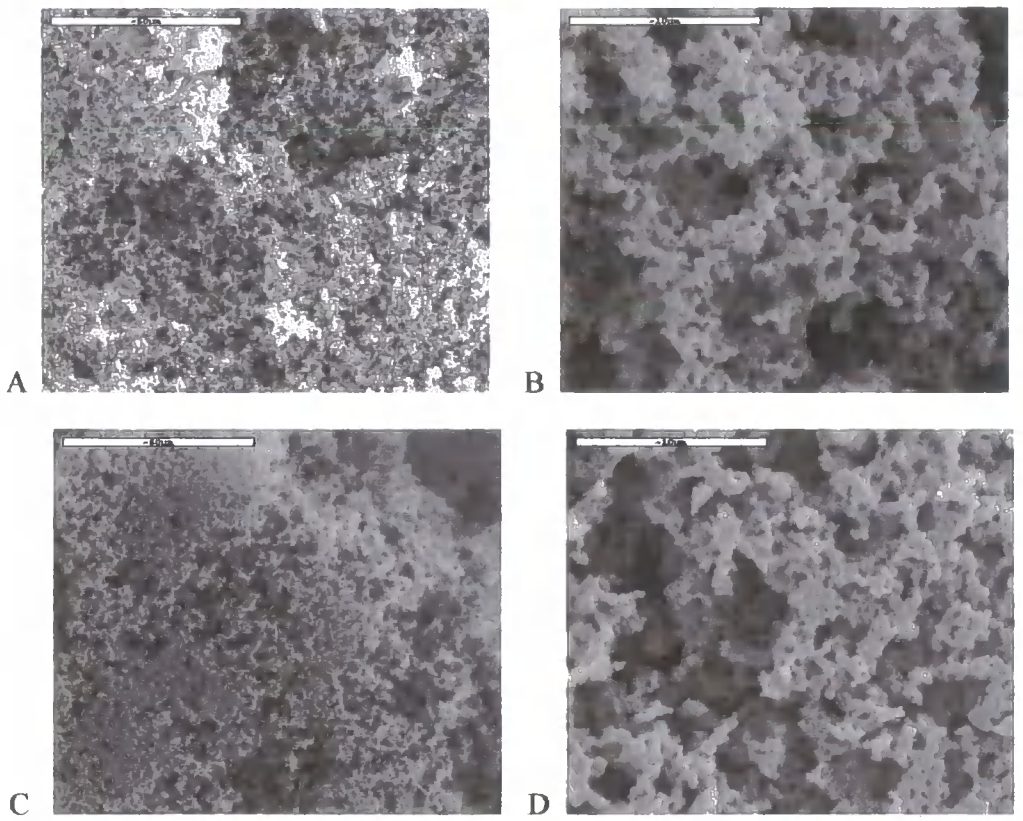

Figure 4.11 SEM Photographs (a) 0.4-S (50 μm scale bar); (b) 0.4-S (10 μm scale bar) (c) 0.6-S (50 μm scale bar); (d) 0.6-S (10 μm scale bar)

longer apparent. The morphology most likely results from inefficient mixing due to viscosity rather than phase separation upon heating. As with the PCL PolyHIPEs, a non-porous structure would be more likely evidence for the latter. In all cases there was no shrinkage of the foams during the drying process.

4.3.3.2 PCL and MMA

PL and MMA PolyHIPEs were made retaining the conditions used to make the PCL and MMA foams. This allowed the production of foams using 20 wt. % of PL and their SEM pictures are presented in Figure 4.12. The structures seen in the SEMs were identical to those seen for PCL and MMA foams and an explanation for the structure was

* See Experimental for key, page 101
* See Experimental for key, page 101

given in chapter 3, section 3.3.2.2. As with the PCL and styrene foams, an open-cellular morphology was produced. When the PL content was increased to 40 wt. %, however, the HLB_{mix} of 1 failed to stabilise the emulsion and a less hydrophobic surfactant was required, 4.3. PL is not as hydrophobic as PCL due to the lower number of carbons in the

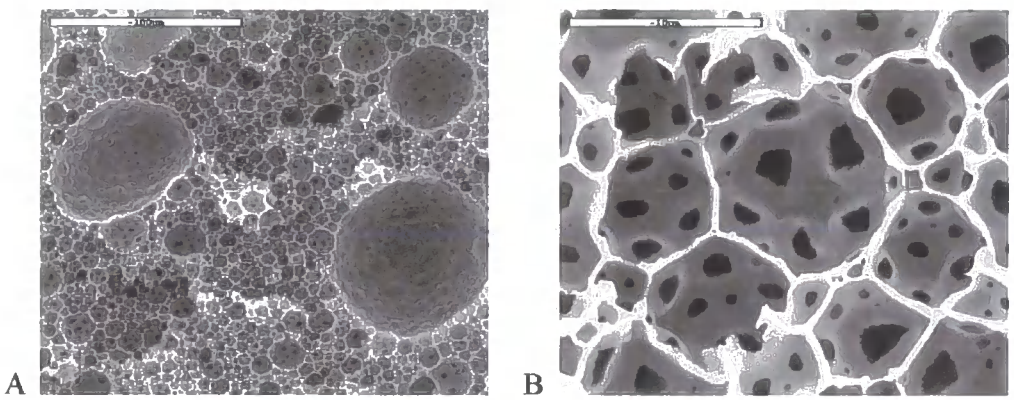

Figure 4.12 SEM Photographs (a) 0.2-M (50 μm scale bar); (b) 0.2-M (10 μm scale bar)*

corresponding monomer unit, this in turn would increase the 'similarity'[98] between the organic and aqueous phases and, therefore, the need for a hydrophobic surfactant. PL is less hydrophobic and, therefore, the monomer phase would be more hydrophilic and the resultant emulsion would be stabilised by a more hydrophobic surfactant. The production of foams in this case using a less hydrophobic surfactant would indicate that factors such as interfacial tension and viscosity were more important. By returning to a HLB of 4.3 (Span 80), PolyHIPEs were prepared using 40 wt.% PL with 60 wt.% MMA, again high viscosity of the organic phase prevented further mixing. The upper limit for ϕ was 0.84 (Table 4.3, entry 5). SEMs of the PolyHIPEs of both PL with MMA are shown in Figure. 4.13. In using a less hydrophobic surfactant, the thick wall structure seen for previous MMA foams has been lost and a 'normal' PolyHIPE morphology can be seen in Figure

* See Experimental for key, page 101

4.13 (a) and (b). The small cell and pore size would indicate that the precursor emulsion was very stable.

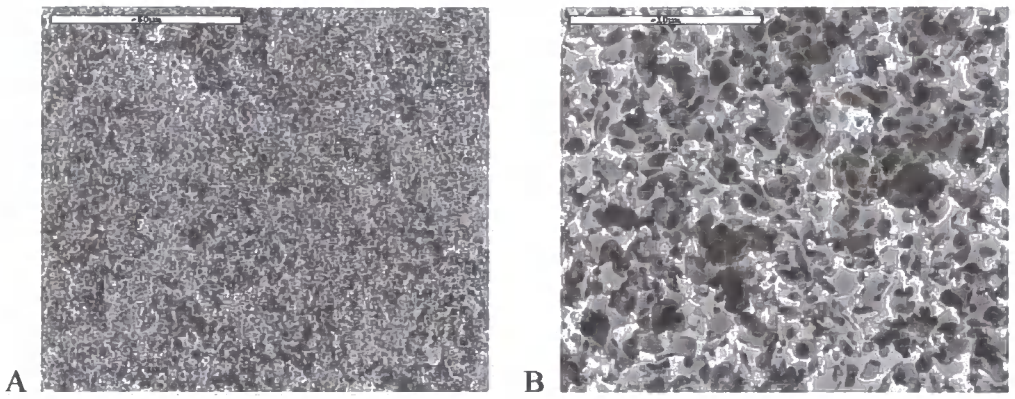

Figure 4.13 SEM Photographs (a) 0.4-M (50 μm scale bar); (b) 0.4-M (10 μm scale bar)*

4.3.3.3 PL and Toluene

The final set of materials consisted of foams that were composed almost entirely of polyester. As with the PCL-only materials, this was achieved by replacing the vinyl monomer additive with a non-polymerisable organic phase diluent again toluene. A surfactant with an HLB value of 4.3, Span 80, was again used and, as expected, stable emulsions were formed with 20 wt.% PCL. However, the mechanical properties of the foams were not good and they shrank by over 50% upon drying. The morphology of the foams can be seen in Figure 4.14. The shrinkage upon drying was not unexpected as only 2 vol.% of the foam in its expanded dry state is solid polymer. Again the T_g could have an important role in the drying process, heating above the T_g could cause the foam to collapse. Increasing the PL content created a more crosslinked network and improved mechanical strength but the foam still collapsed on drying. As before a stable HIPE was

* See experimental for key, page 101

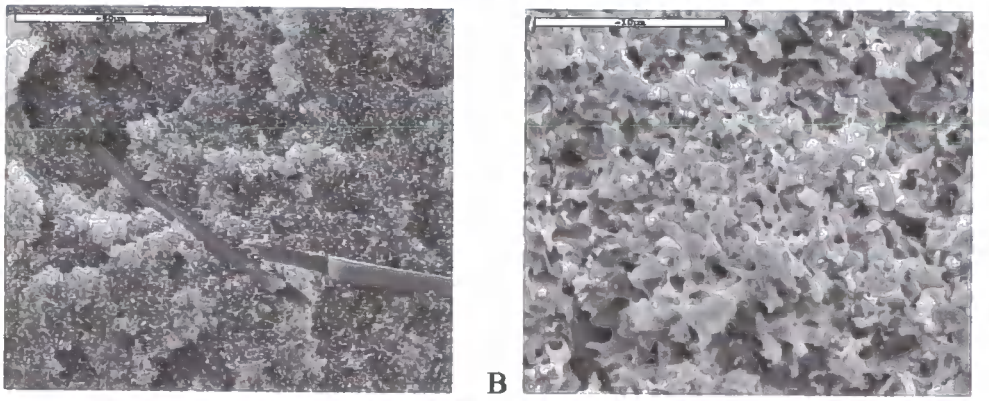

Figure 4.14 SEM Photographs (a) 0.2-T (50 μm scale bar); (b) 0.2-T (10 μm scale bar)

obtained, but the high viscosity of the organic phase limited the values of ϕ (Table 4.3, entries 7 and 8).

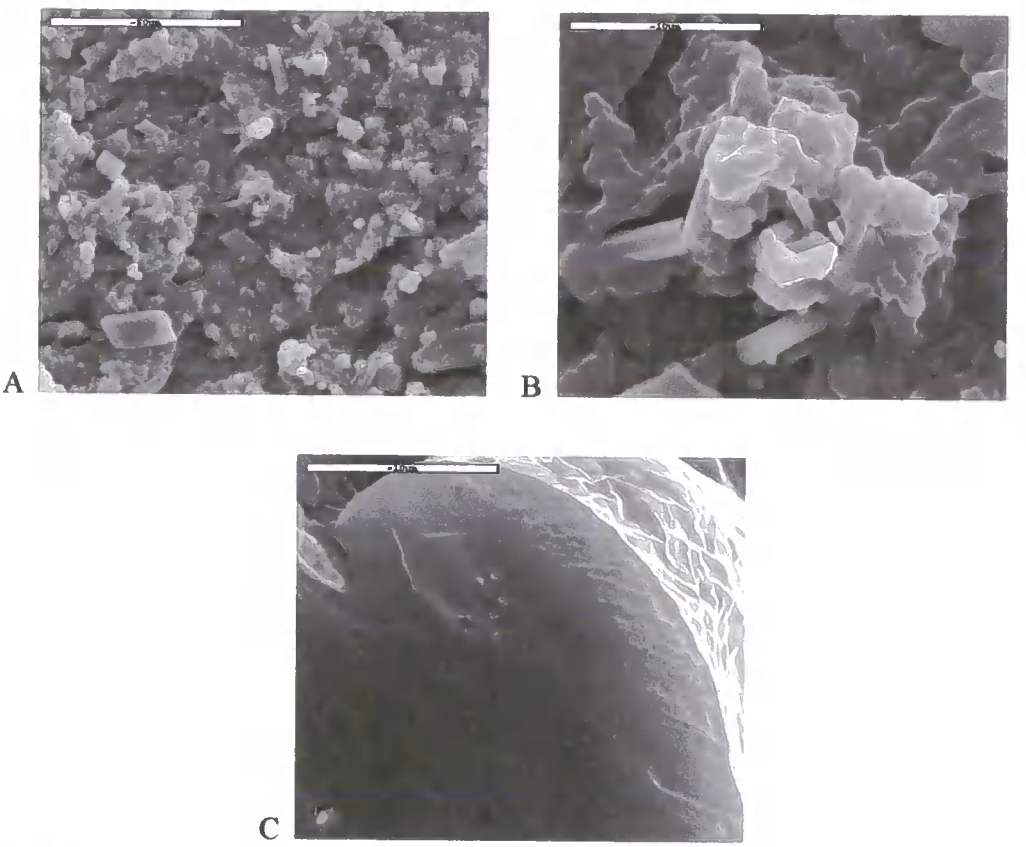

Figure 4.15 SEM Photograph (a) 0.4-T (50 μm scale bar); (b) 0.4-T (10 μm scale bar) (c) 0.6-T (10 μm scale bar)*

* See Experimental for key, page 101

There is little evidence of a porous structure for the 40 wt.% foams, however, the material did collapse during drying and the SEM pictures, Figure 4.15 (a) and (b) are, therefore, not accurate representations of the emulsion from which the PolyHIPE was polymerised. For the 60 wt.% foam, the porous structure is nonexistent, a stable precursor foam was produced so it is likely that collapse of the structure has occurred during polymerisation or during drying. The lack of any form of porous morphology would tend to indicate phase separation has occurred and that when the emulsion was polymerised there was no droplet phase present in the emulsion structure. For the MMA and toluene- based PL foams when using greater than 1g of polymer, it took up to 1½ hours for the polymer to dissolve. As with the PCL foams, if the 'collapsed' structure resulted from drying the foam *in vacuo*, a possible solution would be to try an alternative method such as freeze-drying.

4.3.4 Swelling Studies

The swelling of all the foams listed in Table 4.3 was investigated. Accurately weighed quantities of each foam were immersed in excess solvent, toluene, IPA or water. The equilibrium mass of all solvents taken up by each foam was determined. The information gained provides data on the polarity of the materials and their response in an aqueous environment; important for their use in tissue engineering.

4.3.3.1 Swelling studies of PL Foams

Figure 4.16 below presents the swelling results for foams prepared with PL. The following trends were identified:

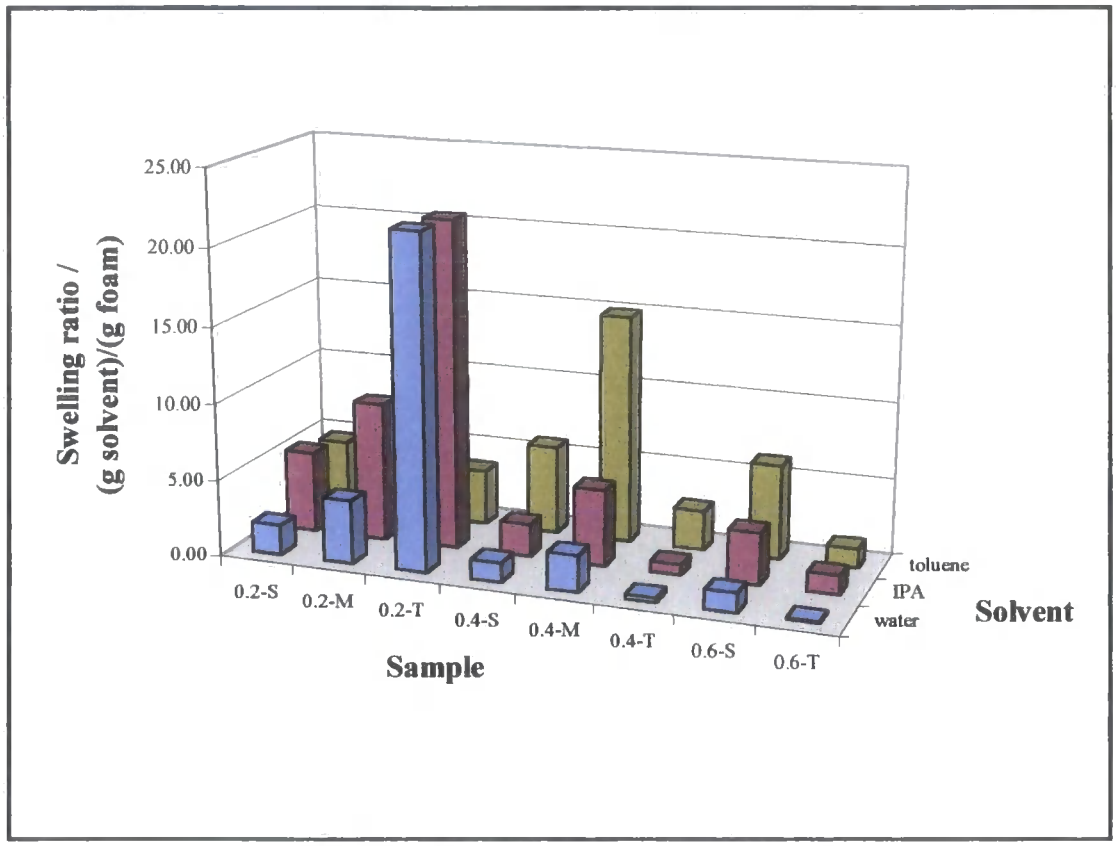

Figure 4.16 Swelling Study of PL Foams

i. With 3 noticeable exceptions, the foams did not show much swelling in any of the solvents, this would be a reflection of the overall smaller pore sizes seen in the SEM pictures, resulting in less void space for the solvent to enter and also the higher polarity of the PL foams in general due to the CH_3 and O groups in the backbone of the polymer.

ii. For all foams, with the exception of 0.4-M in toluene, swelling decreased as PL content increased, this would be due to higher levels of crosslinking of the difunctional macromonomer and lower foam porosity (ϕ = 0.90, 0.84 and 0.75) with increasing PL content.

iii The noticeable exception to the low swelling was the 0.2-T foams absorbing over 20 times their dry weight of IPA and water. This would indicate that

prior to collapse during drying, the foam was highly porous. This characteristic could be an advantageous composition for tissue engineering because, a material seen to swell in an aqueous environment would probably aid fluid intake and removal.

iv Both of the MMA foams can be seen to swell more than their styrene and toluene counterparts with the exception noted in (iii). This is likely to be due to an increase of porosity in the foams. This can be clearly seen for the styrene foams (Figures 4.10 and 4.11) where an increase in PL content lead to a loss of PolyHIPE structure.

v At low PL contents, swelling increased in polar solvents going from styrene to toluene, due to increased polarity of the materials.

vi As the PL content of the materials was increased, the extent of swelling was reduced - this would be due to an increased level of crosslinking, particularly in the toluene foams e.g. 0.4-T. The toluene in the foams is an inert diluent, therefore per gram of material, the toluene foams will be more highly crosslinked. This can be seen when comparing 0.4-M to 0.4T and 0.6-S to 0.6-T, where in both cases the toluene foams swell less.

4.3.4.2 Comparison of PL and PCL Swelling Studies

Figure 4.17 below presents a comparison of the swelling results for foams prepared using PCL macromonomer **2** (left side of each set of 2) and PL (right side of each set of 2) using 20 wt.% of polymer. The following observations can be made:

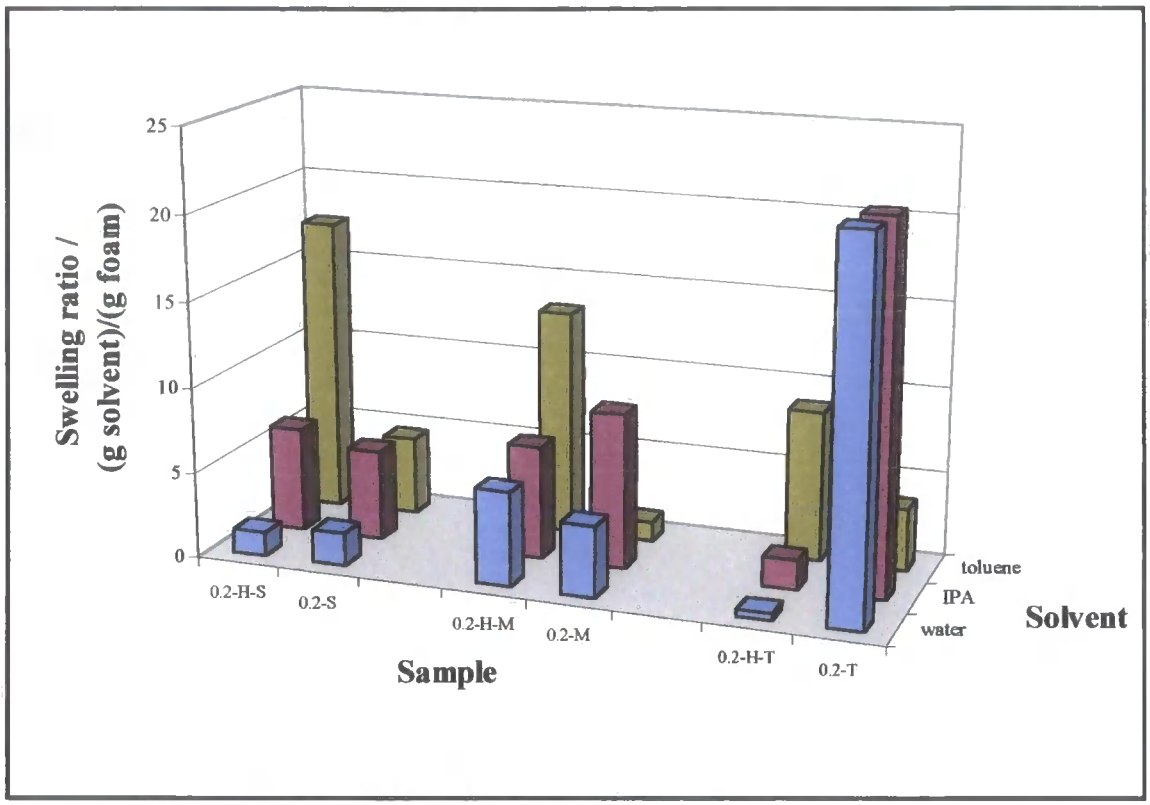

Figure 4.17 Comparison in Swelling 20 wt.% PCL and PL foams

i The PCL foams swelled more in the less polar solvents (toluene) because of their hydrophobic nature; caused by the large number of CH_2 groups. Conversely, the PL foams swelled more in water and IPA because of their more hydrophilic nature; fewer carbons.

ii In the non-polar solvent, toluene, the styrene foams swell more, but the PL-only foams exhibit a massive increase in swelling in the polar solvents . This cannot be accounted for by porosity with all the foams possessing $\phi = 0.90$. The effect is, therefore, likely to be as explained in (i). But the presence of the comonomers decreased the polar influence, they are less polar than PL, lowering polar solvent absorption. This is further backed up the 0.2-T-PL

foam which swells to over 20 times its dry weight in polar solvents. Polar solvents are, therefore, good solvents for polar molecules.

Figure 4.18 further compares PCL and PL foams made using 40 wt.% of polymer. The following points were identified:

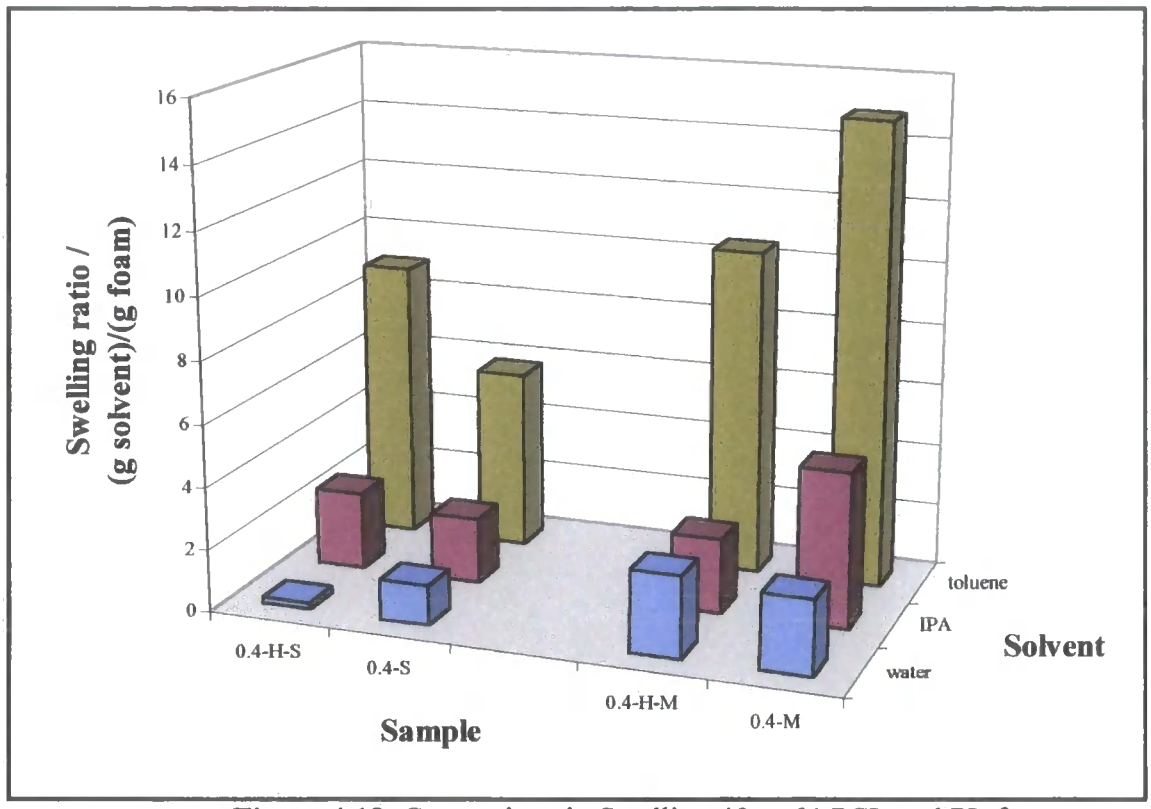

Figure 4.18 Comparison in Swelling 40 wt.% PCL and PL foams

i The swelling of these foams is most influenced by their structures, 0.4-H-S (Figure 3.8 (d)), 0.4-S (Figure 4.11 (b)) and 0.4-H-M (Figure 3.10 (b)) all possess porous structures to varying degrees, but not PolyHIPE morphology. 0.4-M (Figure 4.13 (b)) possess a typical PolyHIPE structure and this has been reflected in its overall increased swelling.

ii Generally, the PL foams swelled more or similarly to their PCL counterparts for a given solvent. As the porosities of these foams are similar, the likely

reason for this would be variation in network formation and steric hinderance caused by the CH_3 group in the PL, creating a more loosely crosslinked network and, therefore, greater void space for solvent molecules.

4.4 Conclusions

Using PL macromonomer either alone or with a comonomer (styrene or methyl methacrylate), a series of highly porous and permeable PolyHIPEs were prepared by free radical polymerisation of precursor HIPEs. Foam morphologies were determined by SEM and their swelling properties investigated in solvents of differing polarities.

The concentration of PL macromonomer and the nature of the diluent added to the organic phase determined the foam structure. The optimum composition was a maximum of 60 wt.% of PL added to the organic phase, 40 wt.% comonomer, beyond which high solution viscosity inhibited HIPE formation. At the higher poly (lactic acid) contents, processing of the organic phase was time consuming. The swelling studies found that solvent type influenced the swelling in the order, water < *iso*-propanol < toluene, due to the strongly hydrophobic nature of most foams with the exception of 0.2-T. However, the 20 wt.% only-PL foam swelled by over 20 times its dry weight in polar solvents. Increasing PL content increased the level of crosslinking in the foams (the macromonomers being difunctional) and hence decreasing swelling.

Biodegradation Study

Chapter 5

5 BIODEGRADATION STUDY

5.1 Introduction

5.1.1 Introduction to Degradation in General

There are two ways of defining biodegradability of materials. The most general definition would be any material that can degrade in a biological environment. This environment could have biological or biochemical processes occurring which may or may not have a role in the degradation, e.g. aqueous body fluids responsible for hydrolysis of polymers. More specifically, the term can be applied to those materials that only degrade due to a biochemical reaction. Enzymes typically catalyse these reactions. Biodegradation of synthetic polymers initially became of interest as an answer to the increasing problem of non-degradable plastics from waste disposal.

Scheme 5.1 Division of Biodegradable Polymers By Application

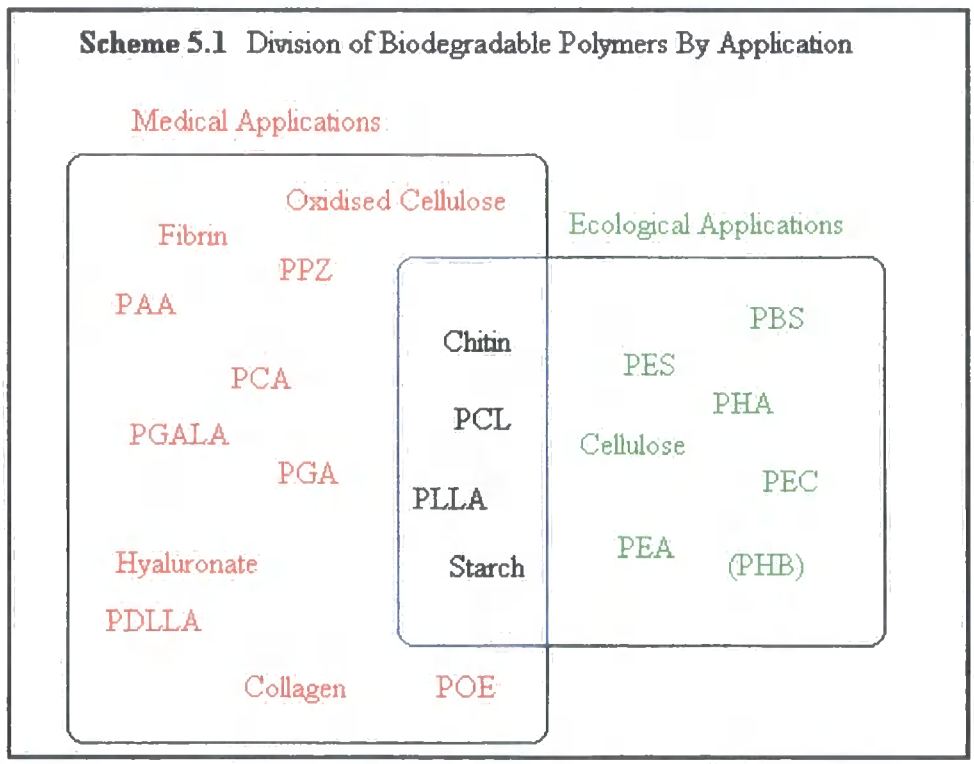

Biodegradation Study

Biodegradable polymers have found use in two major applications, medicine and environmental. Examples of such polymers are shown in Fig. 5.1 and it can also be noted that while most polymers have use in a specific field, a few have applications in both.

Cellulose is the most abundant biopolymer and consequently has been the most studied [163]. Degradation occurs by enzymes that are secreted from fungi and bacteria. Conditions can be aerobic or anaerobic with temperatures as high as 85°C or pH 9 [164, 165]. Relatively low molecular weight polyesters with low melting points are also biodegradable by enzyme-systems [90]. This has been attributed to the fact that PHBA - a polyester which many micro-organisms use as an energy store in the way that animals store fat - occurs widely in nature. In the case of bacterial polysaccharides degrading enzymes show a very high degree of substrate specificity not just for a specific polymer but also a bond or functional group located on the polymer [163].

While studying the PHB granules, it was noted that if the process of degradation by hydolysis was enzymatic, degradation was confined to the surface. Therefore, low molecular weight species were being continually formed and the overall mass continuously decreased, however, the molecular weight remained more or less constant. On the other hand with chemical hydrolysis, penetration of the film by an aqueous solution showed the molecular weight decreased constantly as random hydrolysis occurred, but weight loss did not occur until the polymer was severely degraded [166].

A basic requirement for any polymer being used in medical applications is that both the polymer and its degradation products must be biocompatible. Ideally, products after degradation should be water-soluble, small molecules and preferably naturally occurring metabolites.

Oligomers and polymers, especially polymers of high molecular weights, whose main chain consists only of carbon-carbon bonds - with the exception of those containing large polar groups e.g. PVA - tend not to be susceptible to degradation reactions. One way round this problem is to insert a "weak link" into or attached immediately to the polymer backbone. The purpose of the "weak link" is to control the degradation of a previously high molecular weight hydrophobic polymer into oligomers.

There are several classes of polymer that have been shown to be degradable and absorbable *in vivo*. Among them are the aliphatic polyesters e.g. polylactide and poly (caprolactone), where ester groups along the backbone provide the "weak link". Their biodegradable and re-absorbable properties have promoted their use in sutures and drug delivery systems [167].

The products of degradation for a number of these polymers e.g. lactic acid for polylactide, are resorbable, that is these products can be eliminated from the body by filtration via the kidneys or metabolisation. Therefore these polymers are more commonly classed as "bioresorbable".

When performing biodegradation tests, factors to consider that would affect the outcome of the results would be: i) particle size used; ii) the molecular weight (if either or both were small the degradation rate would be significantly higher); iii) chemical structure (nature of hydrolytically unstable bonds); iv) water permeability; v) morphology; vi) glass transition temperature (above which the polymer becomes less ordered - allowing water molecules to penetrate more easily).

The biodegradation rate of a polymer is principally governed by its intrinsic properties e.g. chemical structure (nature of hydrolytically unstable bonds), water permeability (hydropholicity / phobicity), morphology (crystalline / amorphous), Tg and

molecular weight. There are 2 ways of looking at polymer degradation, one in terms of the molecular structure of the polymer and the other its physical and mechanical properties. Molecular weight is the key component that governs all structural changes in the biodegradation process. For degradation to be considerable, fragmentation will occur due to main-chain cleavage in the polymer backbone. The molecular weight change can be detected through a number of less significant physical, chemical and mechanical effects. These include surface fragmentation, by-product formation, weight loss, degree of crystallinity, glass temperature, tensile and impact strength.

The degradation of these and related polyesters, e.g. polyglycolide, was established in the early 1980s by Chu [168] using *in vitro* studies and is known to occur in 2 stages. The carboxylic end groups of the polymers autocatalyse nonenzymatic bulk hydrolysis of the ester linkages. During this stage molecular weight ($\overline{M}_n$) will decrease but no weight loss will be observed. At the point where $\overline{M}_n$ approaches 3000 – 5000, chain scission slows, due to the production of oligomeric species small enough to diffuse away from the bulk and some weight loss becomes apparent. Fragmentation of the polymer, affecting the surface to volume ratio, plays a key factor and further erosion studies support intracellular degradation as the principal pathway [169]. Smaller fragments increase the surface to volume ratio and therefore, speed up the process of degradation. Degradation of this type is dependant initially on the uptake of water.

Within the amorphous and crystalline regions of the polymeric structure, the more loosely packed, less organised amorphous regions will be subject to hydrolysis first because water is able to penetrate more easily. The more highly ordered and densely packed crystalline part of the polymer will take longer for the water to hydrolyse. Degradation can also be affected by the hydrophobic / hydrophilic nature of the polymer.

A polymer that is neutral or hydrophobic will decrease the overall degradation rate by working against water uptake. Degradation of the amorphous regions and to a lesser extent, reordering of loose chain ends initially cause an increase in crystallinity of the polymer.

When being used as a scaffold, the degradation rate of the material is important. The polymer needs to be supportive until cell growth is well established (cells produce their own extra-cellular matrix) whereupon degradation is required to allow the cells / organ to heal into place.

5.1.2 Degradation of PCL

PCL has been employed as a biodegradable polymer predominantly for soil-degraded container material, its degradation product is ω-hydroxyhexanoic acid or caproic acid. Until 1981, little was known about the mechanism by which PCL degraded. Pitt et al. carried out a study [167] of the degradation of PCL in rabbits, rats and water. Degradation was measured by changes in intrinsic viscosity, weight, crystallinity, Young's modulus and molecular weight. Degradation was discovered to proceed by nonenzymatic random cleavage of ester linkages. Weight loss was dependent on the particle size.

By 1985, PCL had also found its utilisation as a biomaterial, e.g. in prosthetics and sutures. The biodegradation of PCL and related polyesters was known to occur in a minimum of 2 discrete stages [167]. Once the molecular weight of the polymer has decreased to 5000 or below, studies support intracellular degradation as the principal pathway [169]. Erosion is dependent on the surface to volume ratio, however, it is usually rapid - no longer than 3 months.

Biodegradation Study

The rate of degradation for a polymeric scaffold is important. The polymer needs to be supportive until cell growth is well established, whereupon degradation is required to allow the cells / organ to heal in place. Degradation can also be affected by adhesion between the implant and surrounding tissue. The tissue response to biodegradable polymers and its mechanism is an important factor [170]. Swelling due to degradation and expanding implants was noted in a number of patients 3 years after receiving PLLA bone plates and screws. When using 50/50 copoly (L-lactide/ε-caprolactone), degradation appeared to be affected by the biological surroundings. The cause was suggested to be enzymatic, mechanical or chemical in nature or a combination. No swelling was noted upto a year after implantation.

Degradation of polycaprolactone (PCL) was found to be slow due to its relatively high crystallinity [171]. By co-polymerising ε-caprolactone with other lactones e.g. glycolide and lactide, it was found the degradation rate could be further controlled. A high molecular weight copolymer of 50/50 L-lactide and ε-caprolactone has been used successfully in implants as a nerve guide. The degradation products, L-lactic acid and caproic acid, were found to be non-toxic and a minor foreign-body response occurred [170].

Synthetic polymers had previously been designed to resist degradation [172]. They are now needed to maintain their required properties in the short term and then degrade in a safe manner over a varied amount of time for use in e.g. the food and packaging industry and specific applications in medicine and agriculture. Synthetic polymers are not generally biodegradable because they have not been on the earth a sufficient time for micro-organisms to evolve the necessary enzymes. The enzymes capable of degrading

natural polymers e.g. starch and proteins, are the products of aeons of biological adaptations. Generally, addition polymers are not biodegradable because there is not yet an enzyme capable of cleaving only carbon-carbon bonds.

5.1.3 Degradation of PL

PLA, PGA and LA-GA polymers are of great interest because of their biocompatiability, bioresorbability and because by varying the chemical and configurational structure of the polyester chains, a range of physical, thermal, mechanical and biological properties can be produced. Poly (L,L-lactide) is a slow degrading, semicrystalline polymer and poly (D,D-lactide) is a faster degrading amorphous polymer. PLG, the copolymer, is amorphous and degrades faster than pure PLA (degradation time decreases with increasing glycolide content) [173]. They have already been utilised for bioabsorbable sutures, dating back to 1960s [174], and drug delivery systems. Their degradation products are L-lactic (PLA) acid and glycolyic acid (PGA) [170], resulting in the eventual formation of carbon dioxide and water [34]. Li et al[174, 175] conducted an experiment over 4 years looking into the degradation, *in vitro*, of poly (D,L-lactide) and PLGA. The experiments were carried out using a standardised investigation, e.g specimens all fabricated and processed in a similar manner. The interesting phenomenon presented was that for the thick samples of PLA, during studies, degradation occurred faster inside than at the surface of the material. This was attributed to 2 factors: (1) on the outer surface, diffusion of soluble oligomers into the buffer medium was easier than for inner surfaces and (2) the buffer medium would neutralise the carboxylic end groups on the outer surface. The effects of the above would reduce the acidity of the surface; whereas internally, the many carboxylic end groups would be autocatalysed

enhancing the degradation rate [176]. It should be noted that all the investigations discussed in this section and previously, unless otherwise stated, have been carried out on non-porous samples. A further study of LA/ GA copolymers by the same group [177] concluded that a neutral hydrophobic material would inhibit the uptake of water and increase the time taken for a sample to degrade, while a neutral hydrophilic material would have the opposite affect.

Hakkarainen et al. looked at degradation of PLA and PLGA copolymers in powder form in a phosphate buffer solution, pH 7.3, at both 37°C and 60°C [173]. They noted an immediate rapid decrease in molecular weight that tailed off to a slower rate. Mass loss was correlated to the formation of soluble low molecular weight oligomers, once these were removed from the polymer matrix the molecular weight distribution decreased. They also reported an increase in degradation rate with an increased content of glycolic acid units. This was attributed to glycolic acid having higher hydrophilicity in comparison to lactic acid and hence allowing an increased rate of water uptake. The hydrophilic nature was also believed to allow higher molecular weight oligomers to be removed, which was observed to decline with decreasing number of glycolide units.

Schmitt and coworkers looked at the affect of a water environment on PLGA by NMR [178]. They found a lower water uptake and an increase in rotational freedom of the bound water with an increase in lactide content. They concluded that the methyl group on the lactide molecule hindered hydrogen bonding of water molecules with the ester linkages and also provided steric hindrance to hydrolysis. Water absorption was also found to be dependent on pH [176]. At pH = 7.4, osmotic pressure causes water to be drawn into the polymer matrix, solvating the acidic endgroups; however, as the pH drops

and the medium becomes more acidic, the water absorption is no longer driven by the osmotic pressure.

A study comparing the degradation of PLGA microspheres *in vivo* and *in vitro* found that the rate was between 1.7 – 2.6 times faster in the former than the latter [179]. The same study also noted that the endgroup type had a greater effect on degradation than molecular weight. While lower molecular weight microspheres degraded more rapidly than those of a higher molecular weight, the hydrophobicity/hydrophilicity of the end groups had a greater effect. Mason et al. [180] attributed an increased rate of degradation of PLA in plasma, compared to buffer or water, to an increase in chain mobility from lipid components absorbed by the PLA from the plasma. Menei et al. [181] found faster degradation of PLG microspheres *in vivo* when compared to a saline *in vitro* experiment. They accredited the increased degradation rate to lipids or other biological compounds acting as plasticisers - influencing the uptake of water. Work by Grizzi and coworkers found that degradation of PLG devices was also affected by size, shape and porosity [182]. They found PLA devices such as large sized plates and millimeter-sized beads degraded faster than films of submillimeter thickness and particles. The authors believed the acidic PLG oligomers would escape less easily from larger or less porous materials.

PLGA scaffolds and sutures are known to elicit a small acute immune response but as the material is reabsorbed the response disappears and no chronic immune response replaces it [183, 34] due to the diffusion mechanism – the outer layer degrades less rapidly than bulk internal polymer.

An investigation into the *in vitro* degradation of porous PLA foams found that varying porosity, pore size and pore structure [184] had no affect on degradation rate.

However, pore wall thickness or pore surface/volume ratio did. $\overline{M}_w$ decreased significantly with an increase in the thickness of the pore walls.

5.2 Experimental

The procedure used for this biodegradation study was based on international standard ISO 13781 [185]. All test values have been predetermined as follows.

5.2.1 Apparatus and reagents

5.2.1.1 Soaking solution

The soaking solution used was a phosphate buffer solution, pH 7.2; Sőrensen buffer [186], consisting of sodium dihydrogen phosphate and disodium hydrogen phosphate in distilled water. The salts used were of analytical grade and dried to a constant mass *in vacuo* at 50°C.

Solution (a) 0.2M solution NaH_2PO_4, prepared by dissolving 27.60g (0.2 mol.) in 1 L. of water

Solution (b) 0.2M solution Na_2HPO_4, prepared by dissolving 35.61g (0.2 mol) in 1 L. of water

The buffer comprised a mixture of 95 ml. of solution (a) and 405 ml. of solution (b) made up with 500 ml. of distilled water to give a 1 L. of 0.1M buffer solution at pH 7.4 ± 0.2. To prevent any bacterial growth, the buffer also contained sodium azide (at a concentration of 0.03 wt. %) [187]. Therefore, assuming 0.03g of sodium azide in 100 ml. then 0.3 g in 1 L.

5.2.1.2 Container

Glass vials of the dimension (diameter x height) 2 cm by 7.2 cm, capable of holding 14 ml. of liquid with a screw cap lid, were utilised.

5.2.1.3 Temperature Control

A Constant-temperature Grant bath was used, (no model name or number given).

5.2.1.4 Control of Buffer Solution

5.2.1.4.1 Changes in pH

The pH of the buffer solution was measured in 2 different containers for each sample type used. Samples were tested at each test period and further tests taken where test points were 7 days apart. Any containers where the pH was outside the limit pH 7.4 ± 0.2 (with the exception of the samples being used to monitor pH change over the test period) necessitated the change of buffer for all containers containing that sample type.

5.2.1.4.2 Clouding of buffer solution

Addition of sodium azide to the buffer should prevent growth of microorganisms. Any clouding of the solution that could not attributed to sample degradation led to the sample being discarded.

5.2.2 Real-time degradation

The samples were placed in pre-weighed glass vials (1 per vial) and their initial weight (W_0) determined. A piece of folded filter paper was then immersed to ensure the samples (hydrophobic in nature) were submerged in the buffer

solution. Samples were covered with the soaking solution and the container was then sealed. The ratio of volume of the buffer solution in milliliters, to the test sample mass, in grams, was, as according to the standard procedure [185], greater than 30:1. The samples were maintained at a constant temperature of 37±1°C in the water bath. A minimum of 6 test points were recommended over the test time and these were pre-determined to be as follows: 0 days, 5 days, 8 days, 12 days, 15 days, 19 days, 22 days, 30 days, 56 days, 70 days

5.2.3 Physicochemical tests

5.2.3.1 Balance

All samples were weighed on a Philip Harris, HR-120-EC, analytical balance, accurate to ± 0.0001g.

5.2.3.2 Vacuum Oven

A Binder GmbH vacuum drying oven, VD23, was used.

5.2.3.3 Preparation of test samples

At each pre-determined time interval 6 samples of the same foam material were tested to allow for statistical analysis. The shape of the samples was determined by the size and shape that have been used for growing cells on, i.e. a 14 mm diameter disk of thickness 2 mm. In order to gain some judgment of the influence of sample size, samples of the same diameter were used and disks of 4 – 5 mm thickness were also tested. For

each thickness type, there were 2 PolyHIPE types utilised: PCL, 0.2-H-S* or PL, 0.2-S†. The samples were made from PolyHIPEs according to the methods described in the experimental sections of chapters 3 and 4. The PolyHIPE was transferred to PTFE moulds and then placed in an oven at 60°C for 48 h. The foams were removed from the moulds and washed thoroughly with water then isopropanol, disks were then stamped out using a cork borer before being dried to a constant mass *in vacuo*.

5.2.3.4 Test procedure

At each time interval, 6 samples for a given foam type and thickness were removed from the water-bath, the buffer solution was discarded from each vial and each sample rinsed in distilled water 3 times. The glass vial and sample were then dried at 50°C under vacuum to a constant mass. The samples were kept in their original vials to prevent loss and damage as they became more brittle.

Of the 6 samples the following charaterisation was determined: change in weight, dimension changes (photographs and measurements), colour changes.

From those 6 samples per foam type and thickness 2 were submitted for SEM, in each case to look at outer and inner surfaces.

Determination of the buffer's pH was also carried out throughout the test period. Six of the samples originally placed in the water bath did not have their buffer solution changed. The same sample was kept submerged in the same buffer solution for the duration of the testing period (10 weeks). At each time interval, the pH of the buffer was

* See Chapter 3 Experimental section for key
† See Chapter 4 Experimental section for key

decanted off and the pH determined before pouring back over the sample and placing back in the water bath. The above information produced a plot of change in pH with time.

The testing was terminated at a predetermined point i.e. after 10 weeks.

5.3 Results and Discussion

When setting up the biodegradation study, it was difficult to know where to start. There is little information in the literature and the experiments described were mostly on polyester samples that had been moulded to give a non-porous solid sample. In other cases where porous structures had been utilised the material was not crosslinked although some were copolymerised. The experiment was set up following guidelines set out by the International Organisation for Standardisation (ISO)[188, 184]. There was no prior knowledge of how long the samples would take to degrade. The only indication was from experiments looking at growing cells on similar foams, which indicated that degradation would start to occur within one month. The other major problem was that the crosslinked nature of the foams meant that measuring changes in molecular weight, one of the major components analysed when looking at the degradation of materials, was not possible.

The factors identified for analysis were changes in: pH; thickness and diameter of samples; visual size and appearance; external and internal morphology; weight. For pH, weight, thickness and diameter measurements, between 3 and 6 samples were used to allow for statistical or error analysis to be calculated. The remaining factors have been denoted by a representative sample. The experiment was performed over 70 days / 10 weeks - a factor determined by time constraints and number of samples needed.

Measurements were carried out on 4 different sets of samples, two PCL and two PL - all made using 1g of polyester and 4g of styrene using AIBN as the initiator. The diameters of all 4 sets were kept constant but for each polymer one set of foams was approximately 2.5 mm thick and the other 5mm.

5.3.1 Change in pH

6 samples for each foam type were left in the same buffer solution for the duration of the experiment and the change in pH was monitored. Both foams would produce acidic compounds from the degradation of the polymers - lactic acid for the PL and caproic acid from the PCL – therefore, a decrease in pH was expected. The polystyrene would not degrade in an *in vitro* or an *in vivo* situation, and under *in vivo* conditions it would probably be ejected from the patient. Figure 5.1 displays the average pH change for each sample at given time intervals. Error bars have not been added to the data in Figure 5.1 because they did not provide any significant value, i.e. when added to the data you could not see any error bars because they were obscured by the size of the data points. The average error values expressed as a percentage were: PCL thin, 0.16%; PCL thick, 0.22%; PL thin, 0.08%; PL thick 0.16%. On average over the 70 days time span, there was a decrease of 0.1 in pH. Comparison of these results to a number of experiments by Li and coworkers showed this was to be expected. In all cases, experiments by Li et al. looked at compression-moulded samples made from PLA and copolymers of LA and GA [11, 12, 13, 14]. Copolymers of poly (LGA) with an intrinsically amorphous morphology showed a pH change of 0.5 over 40 days. For copolymers of D and L-lactide, a ratio of 50:50 (PLA50) showed little pH change over 8 weeks and by

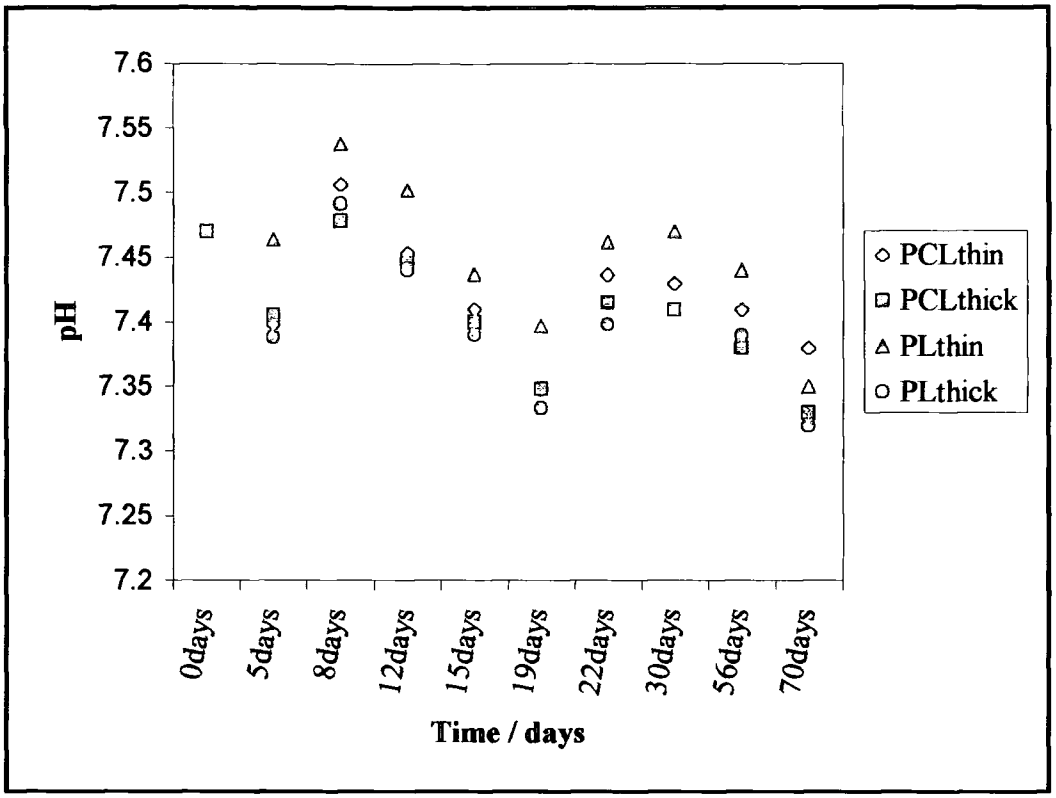

Figure 5.1 Change in Average pH with Time

10 weeks the pH had plummeted to 2. While a mixture of 96% L-lactide and 4% D-lactide (PLA96) changed only by 0.4 from pH 7.4 to 7.0 over 90 weeks and there was also a molecular weight difference with PLA96 being twice that of PLA50 at 130 000. While the PolyHIPEs are made from much lower $\overline{M}_w$ material, they are highly crosslinked and would, therefore, not be expected to degrade rapidly. The hydrophobic nature of the material would also make it difficult for water to penetrate; slowing down the acid production.

5.3.2 Change in Weight

In order to analyse any changes in weight at each given time interval, 6 samples for each PolyHIPE group were removed from the water bath and washed thoroughly with

distilled water to remove buffer, then dried under vacuum (50°C) for a minimum of 4 days. Subtraction of the re-weighed value from the original weight, then taking the mean of the 6 numbers gave the average change in weight. The original sets of numbers were also analysed by F-test - two samples for variances. This allowed the determination of any statistical significance between the weighed and re-weighed data at each time interval. Figure 5.2 shows that, with 2 exceptions, the weight of the foam samples on

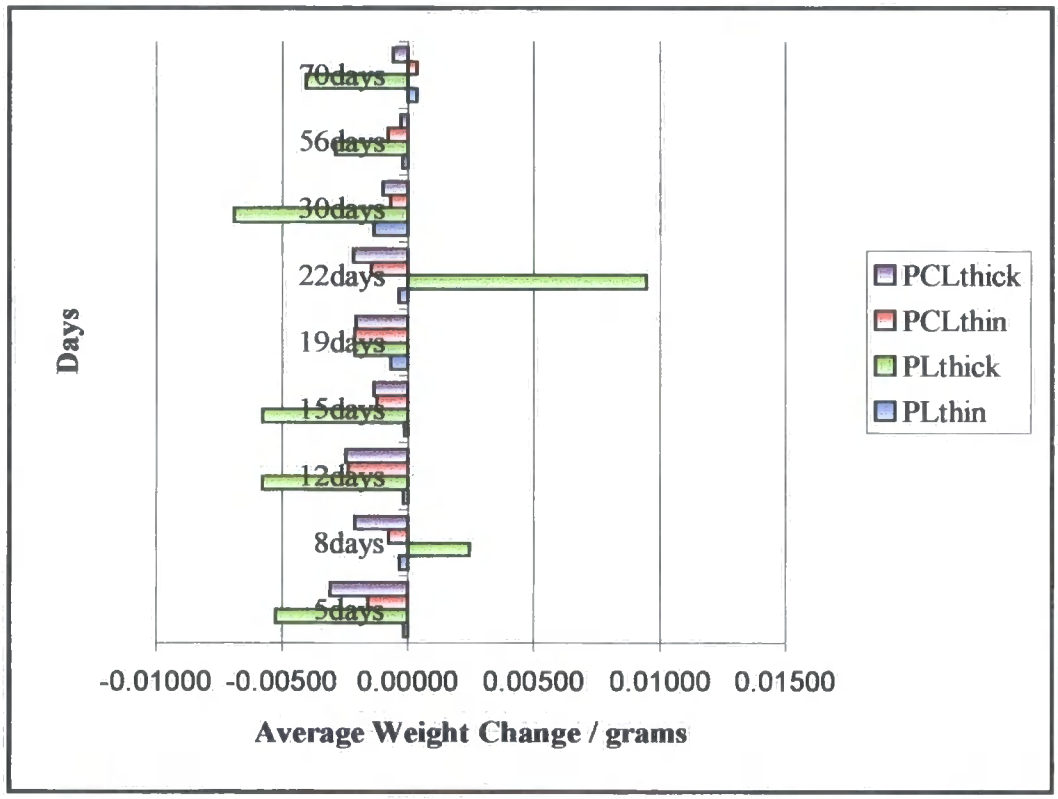

Figure 5.2 Average Change in Weight of 4 different foams over 70 Days

average increased rather then decreased. This is attributed to trapped water in the foams' pores. It is also likely that the initial period of biodegradation will involve breakdown of the cross-linking structure and of the polymer into lower molecular weight species, which would not show any change in actual weight. Towards the end of the 70 day period, pieces of the foams were starting to break away as they became more brittle - these were

included in the weights. Although the overall figure for most of the sample points reflect an increase rather than a decrease in weight, with the exception of the PLthick, there was evidence of weight decrease i.e. biodegradation for a majority of the time intervals for the 3 remaining foam types, but their change was not as significant as the weight increase and therefore, not reflected in the average change shown in Figure 5.2.

Using the weights of the afore mentioned samples, i.e. the sets of 6 foams from each time interval, statistical analysis to determine significant change was performed as follows. For each set of data, the mean average and the standard deviation for i) the initial weight, ii) weight after n days, where n = 5, 8, 13, 15, 19, 22, 30, 56 and 70 were calculated. For a change in weight due to degradation to be deemed significant, the weight of ii) needed to be greater than the standard deviation for the change in weight, while its equivalent initial weight must be within or below the standard deviation for the initial weights. Only results for which the n days weights were outside the mean average plus or minus the deviation have been tabulated. Bold type has been used to denote if the result was significant due to degradation. Tables 5.1 – 5.4, show that much of the weight change was not significant, variation in weight occurring within the random difference between samples as determined by standard deviation.

Table 5.1 F-Test Results for PLthin

Time / days	Initial wt.. mean / σ Range	n days wt. mean / σ Range	N days wt. equal to or outside σ	Was initial wt. Above(A)/ Below (B)/ Within σ (W)	Significant Y / N
5	0.0246 / 0.001 0.0256-0.0236	0.0247 / 0.001 0.0262-0.0232	0.0232, 0.0230, 0.268	B, B, A	N, N, N
8	0.0237 / 0.003 0.0271-0.0203	0.0241 / 0.003 0.0274-0.0207	0.0207, 0.0291	B, A	N, N
12	0.0217 / 0.003 0.0242-0.0191	0.0218 / 0.003 0.0245-0.0192	0.0252, 0.0180	W, B	Y, N
15	0.0239 / 0.002 0.0256-0.0222	0.024 / 0.002 0.0258-0.0222	0.0215, 0.0267	B, A	N, N
19	0.0232 / 0.002 0.0252-0.0211	0.023 / 0.002 0.0263-0.0215	0.0281, 0.0213	A, B	N, N
30	0.0228 / 0.003 0.0261-0.0194	0.0228 / 0.003 0.0273-0.0209	0.0188, 0.0284	A, A	N, N
56	0.0227 / 0.001 0.0236-0.0218	0.0229 /0.002 0.0241-0.0217	0.0212	W	**Y**
70	0.0237 / 0.002 0.0260-0.0213	0.0233 / 0.002 0.026-0.0207	0.0269, 0.0207	A, W	N, **Y**

Table 5.2 F-Test Results for PLthick

Time / days	Initial wt. mean / σ Range	n days wt. mean / σ Range	N days wt. equal to or outside σ	Was initial wt. Above(A)/ Below (B)/ Within σ (W)	Significant Y / N
5	0.1031 / 0.003 0.1055-0.1006	0.1084 / 0.002 0.1111-0.1057	0.1112, 0.1118, 0.1048	W, A, W	Y, N, Y
8	0.1017 / 0.008 0.1091-0.0942	0.0992 / 0.016 0.1150-0.0834	0.0697, 0.1152	A, W	**Y**, Y
12	0.0932 / 0.008 0.1015-0.0849	0.0990 / 0.010 0.1091-0.0889	0.0843, 0.1115	B, A	N, N
15	0.0947/ 0.006 0.1006-0.0888	0.1005 / 0.008 0.1084-0.0926	0.1121, 0.0917, 0.0918	A, W, B	N, Y, N
19	0.0984 / 0.006 0.1043-0.0925	0.1006 / 0.008 0.1094-0.0917	0.1127, 0.0896	A, B	N, N
22	0.1080 / 0.035 0.1435-0.0724	0.0985 / 0.010 0.1088-0.0882	0.1098, 0.0811	W, W	Y, **Y**
30	0.0994 / 0.007 0.1061-0.0926	0.1063 / 0.007 0.1130-0.0995	0.0978, 0.1169	B, A	N, N
56	0.1034/ 0.003 0.1056-0.1007	0.1060 /0.004 0.1101-0.1020	0.1115	A	N
70	0.0972 / 0.004 0.1013-0.0931	0.1013 / 0.003 0.1047-0.0979	0.1062	A	N

Table 5.3 F-Test Results for PCLthin

Time / days	Initial wt. mean / σ Range	n days wt. mean / σ Range	N days wt. equal to or outside σ	Was initial wt. Above(A)/ Below (B)/ Within σ (W)	Significant Y / N
5	0.0614 / 0.012 0.0738-0.0490	0.0630 / 0.012 0.0757-0.0503	0.0750, 0.0789	W, A	Y, N
8	0.0526 / 0.009 0.0617-0.0436	0.0534/ 0.011 0.0645-0.0423	0.0380	B	N
12	0.0608 / 0.012 0.0734-0.0481	0.0632 / 0.012 0.0753-0.0571	0.0816, 0.0453	A, B	N, N
15	0.0560 / 0.013 0.0690-0.0430	0.0569 / 0.012 0.0690-0.0449	0.0761	A	N
19	0.0550 / 0.010 0.0653-0.0447	0.0571 / 0.017 0.0608-0.0454	0.0481, 0.0751, 0.0611	W, A, W	Y, N, Y
22	0.0577 / 0.014 0.0715-0.0439	0.0591 / 0.013 0.0724-0.0459	0.0434, 0.0761	B, A	N, N
30	0.0640 / 0.018 0.0824-0.0456	0.0647 /0.015 0.0800-0.0494	0.0896, 0.0475	A, W	N, **Y**
70	0.0578 / 0.012 0.0700-0.0455	0.0574 / 0.010 0.0675-0.0473	0.0436, 0.0676	B, W	N, **Y**

Table 5.4 F-Test Results for PCLthick

Time / days	Initial wt. mean / σ Range	n days wt. mean / σ Range	N days wt. equal to or outside σ	Was initial wt. Above(A)/ Below (B)/ Within σ (W)	Significant Y / N
5	0.1022 / 0.005 0.1073-0.0971	0.1053 / 0.006 0.1116-0.0984	0.0944,	B	N
8	0.1005 / 0.004 0.1040-0.0970	0.1026 / 0.006 0.1082-0.0970	0.0966	W	**Y**
12	0.0938 / 0.007 0.1050-0.0917	0.1008 / 0.012 0.1130-0.0886	0.0785	B	N
15	0.0920/ 0.014 0.1070-0.0780	0.0938 / 0.041 0.1079-0.0796	0.0672	B	N
19	0.1013 / 0.009 0.1106-0.0919	0.1033 / 0.009 0.1124-0.0943	0.0871	B	N
22	0.1014 / 0.005 0.1065-0.0963	0.1036 /0.007 0.1107-0.0964	0.0963	B	N
30	0.1048 / 0.006 0.1111-0.0984	0.1058 / 0.005 0.1109-0.1006	0.1110, 0.985	W, W	Y, **Y**
56	0.1050/ 0.001 0.1059-0.1040	0.1053 /0.004 0.1066-0.1039	0.1072	A	N
70	0.0956 / 0.007 0.1027-0.0884	0.0962 / 0.006 0.1030-0.0893	0.1060	A	N

However, in all 4 cases, there is shown to be some significant weight loss due to degradation. In the cases of PL thick, Table 5.2 and PCL thin, Table 5.3 - more of the significant change in weight is due to gain rather than loss of weight. This would be most likely from water that has become trapped in the pores of the foam, therefore, giving an inaccurate final weight.

5.3.3 Changes in Sample Diameter and Thickness

Three representative samples at each time interval, from each of the 4 PolyHIPE types were measured accurately using calipers. From those measurements, the mean values for specimen thickness and diameter were calculated along with the mean percentage variation / error. The inner thickness refers to the thickness of the sample at its centre, while the outer thickness was taken at the edge of the sample. This was intended to show if the samples were showing different rates of change in different places. From these results, it was possible to observe if the samples were changing over a period of 7 weeks. The following graphs (Figures 5.3 – 5.6) show some samples decreasing in thickness and diameter and others showing very little change and the diameter over the 70 days, while the inner thickness of the sample remained about constant. For the PL thick samples (Figure 5.4) there was no general change over the duration of the experiment, although 3 of the data points stand out as being big changes: the outer thickness at 15 days; diameter at 15 and 22 days.

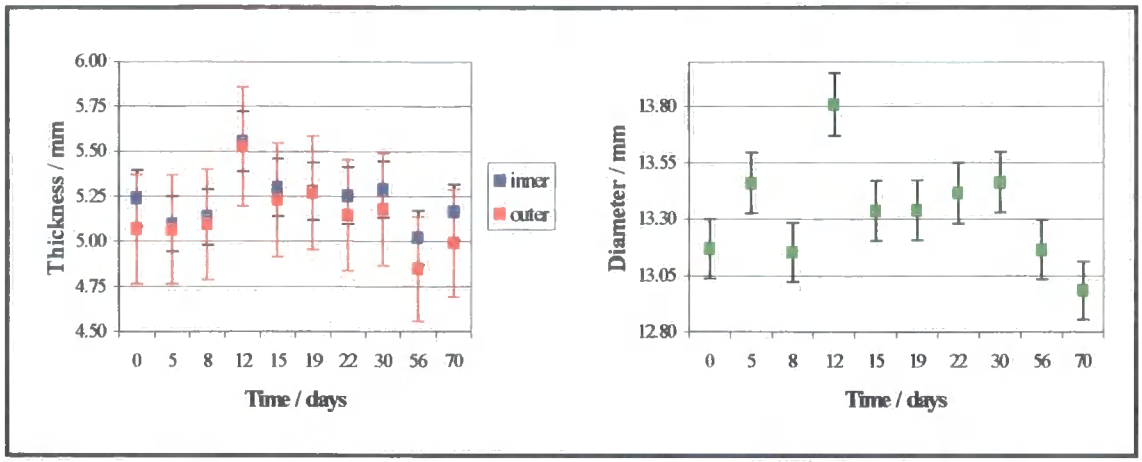

Figure 5.3 PL thin, Changes in Thickness and Diameter

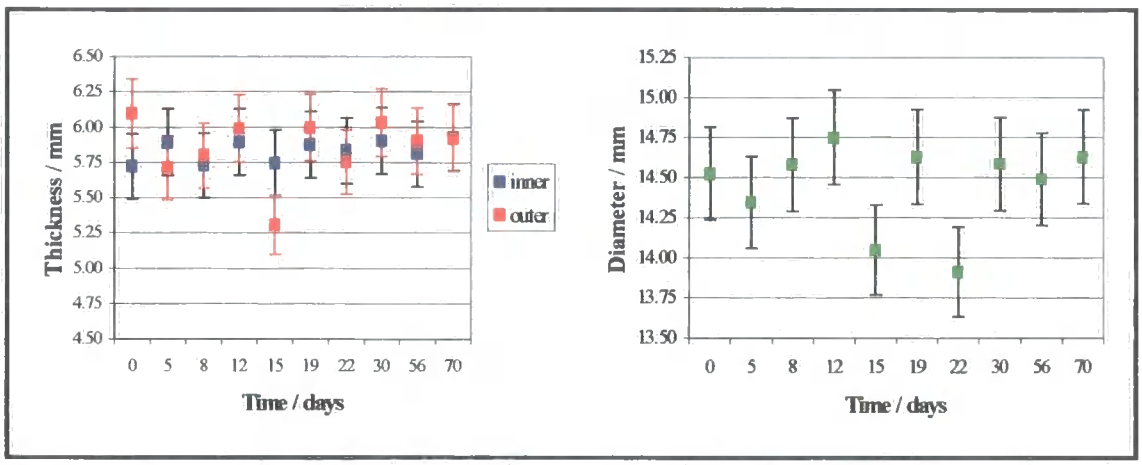

Figure 5.4 PL thick Changes in Thickness and Diameter

For the PCL thin samples there was a general decrease in all 4 areas (Figure 5.5) and for the PCL thick PolyHIPEs (Figure 5.6) the inner thickness remained relatively unchanged while the outer thickness and diameter was generally decreasing.

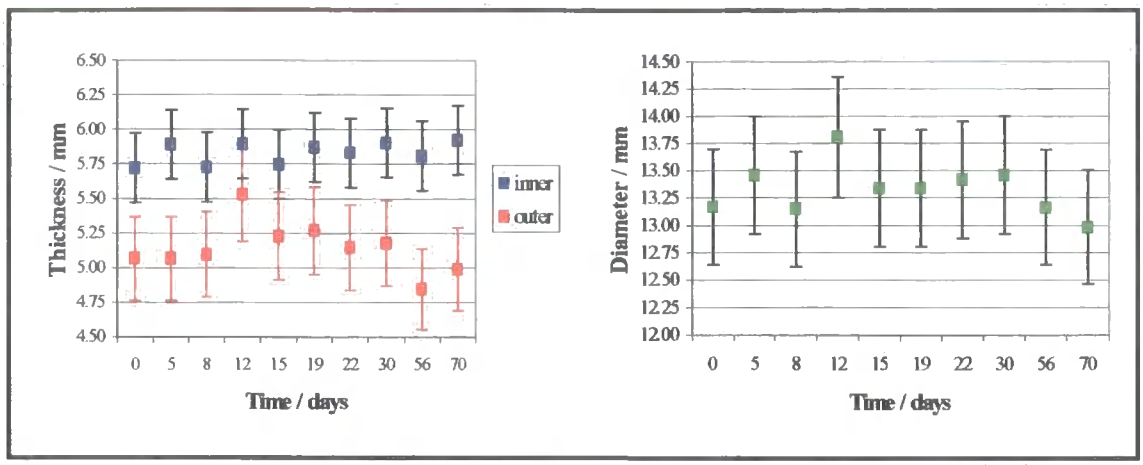

Figure 5.5 PCL thin Changes in Thickness and Diameter

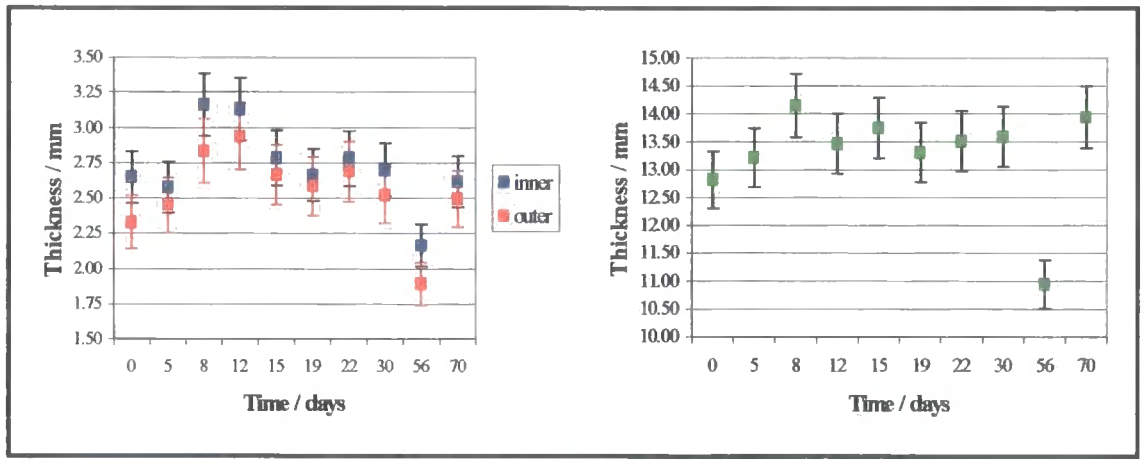

Figure 5.6 PCL thick Changes in Thickness and Diameter

5.3.4 Changes in Internal and External Morphology

Of the 6 samples weighed and used for statistical calculations, 2 representative samples were analysed by SEM. An inner and outer piece of each PolyHIPE sample was photographed. Pictures were then selected which best represented the change, or lack of, for each foam type, generally one from the beginning (5/8 days), one from the end (70 days) and a further from the middle section. The results are presented within the next few pages in Figures 5.7 – 5.10.

It is difficult to see from some of the micrographs of the outside face, whether the material was displaying an alteration of morphology from contact with the moulds surface or showing signs of degradation. However, in the case of the PL thin foams, shown in Figure 5.7, at the beginning of the experiment, the surface of the foam was smooth to look at with 2 or 3 small areas of a roughened appearance starting and in (Figure 5.7 (a)), while towards the upper center of the micrograph of the sample after 22 days (Figure 5.7 (b)) there is a visible area of surface roughness to the foam. On the inside faces, the material after 5 days was smooth (Figure 5.7 (d)), but again at 22 days, a rough appearance had started where degradation had occurred on the surface. It would appear there were some variations in the samples and neither the inner nor outer surfaces by 70 days show anything but a smooth face.

The PL thick foams are shown in Figure 5.8. Here the degradation was more pronounced and by 8 days (Figure 5.8 (a)), the surface of the foam was showing small patches of roughened appearance; by 22 days, the roughness was more widespread (Figure 5.8 (b)) and by 70 days a large patch of degraded surface has become visible to the left of the picture (Figure 5.8 (c)). On the inner face after 5 days the surface of the material was smooth (Figure 5.8 (d)), after 30 days a lot of the surface at the front of the picture were rough rather than smooth, Figure 5.8 (e). In Figure 5.8 (f) it is difficult to tell whether the roughened surface was the point at which the sample had been cleaved but closer examination of the picture shows that the textured surfaces were also present, albeit somewhat more sparsely, in the internal pores and were, therefore, probably produced by degradation.

The PCL foams would appear to have been less affected by the degradation process than the PL foams and this would be in keeping with previous findings discussed in the

introduction. PCL is a semi-crystalline material that takes months and more often several years to degrade (3 – 5 years [187]). The pictures of PCL thin foams are shown in Figure 5.9. Figures 5.9 (a) and (b) both suggest that a very small amount of degradation have started to begin at the surface but without a non-degraded sample for comparison, it is not possible to confirm this. In Figure 5.9 (c) it would appear that the surface of the foam has been altered, it has possibly been affected by contact with the moulds PTFE surface, but this does not explain why only some of the foam surfaces seem to be different. In all 3 pictures of the inner foam structure, there appear to have been no signs of degradation, all the visible surfaces were smooth.

For the thicker PCL foams, shown in Figure 5.10, there are a few small patches of foam that may be showing signs of a roughened surface, therefore, initial signs of degradation, Figure 5.10 (a), (b) and (c). Again with Figure 5.10 (c), it would appear the surface of the foam has been flattened and lost. As with the PCL thin samples, none of the pictures taken from an inner surface of the PCL thick foams, show anything but a smooth surface.

It is probable that the materials would degrade faster in an *in vivo* situation due to enzymatic hydrolysis in addition to hydrolysis by water. This was indeed observed with samples that were used for cell growth (Chapter 7), over a period of one month.

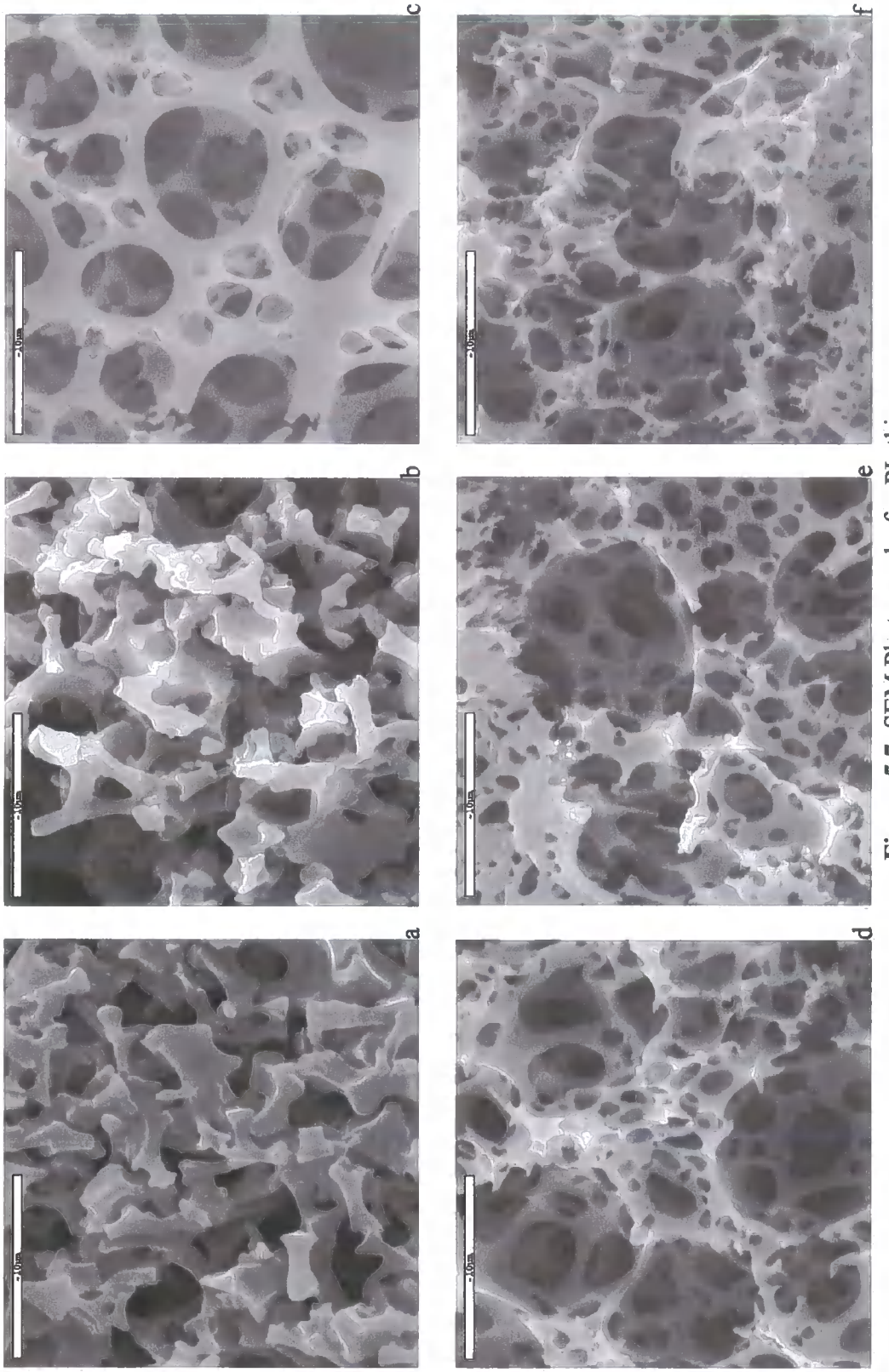

Figure 5.7 SEM Photographs for PL thin
Outer (a) 5 days, (b) 12 days, (c) 70 days Inner (d) 5 days, (e) 22 days, (f) 70 days (all 10 μm scale bars)

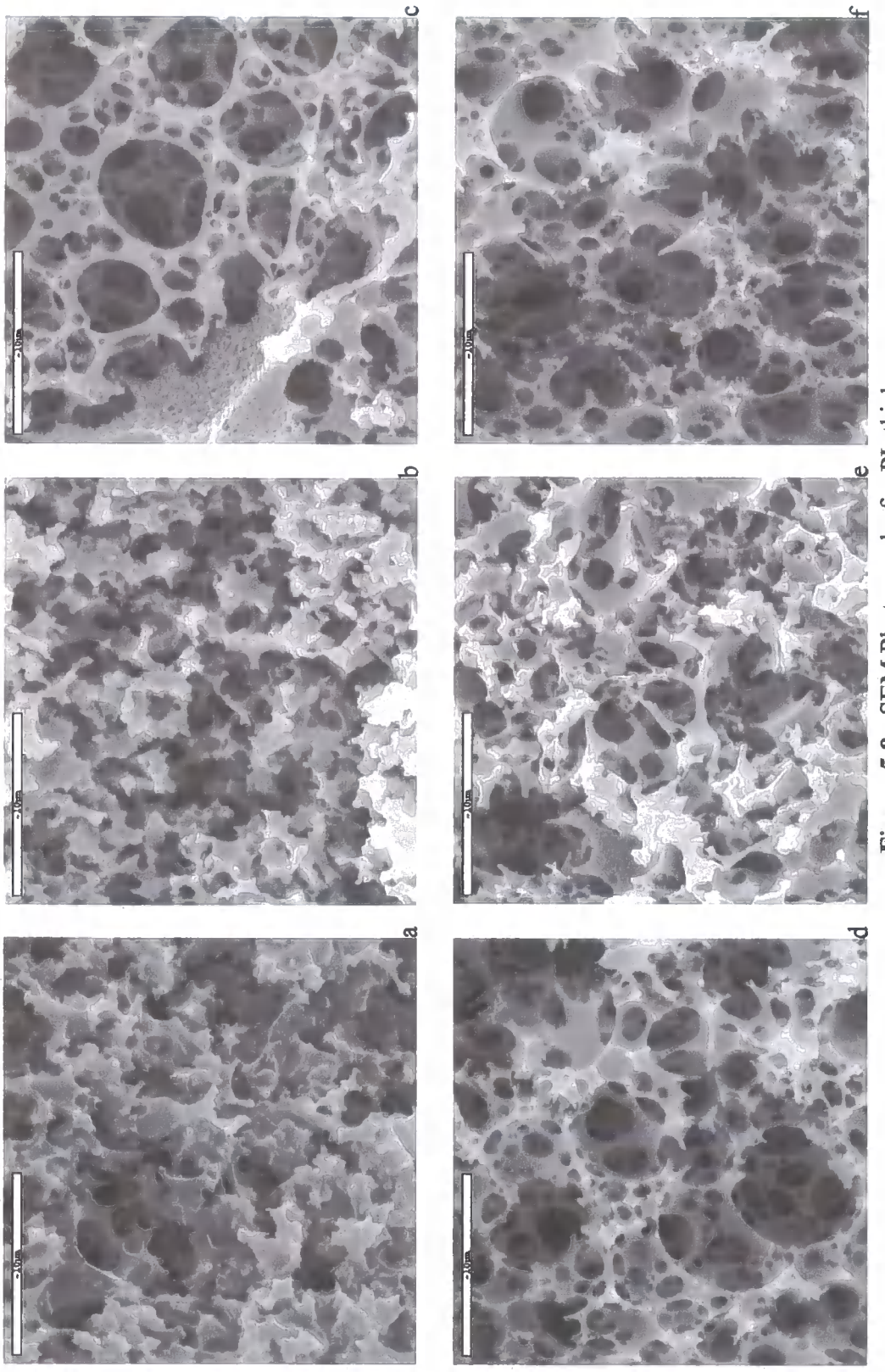

Figure 5.8 SEM Photographs for PL thick
Outer (a) 8 days, (b) 22 days, (c) 70 days Inner (d) 5 days, (e) 30 days, (f) 70 days (all 10 μm scale bars)

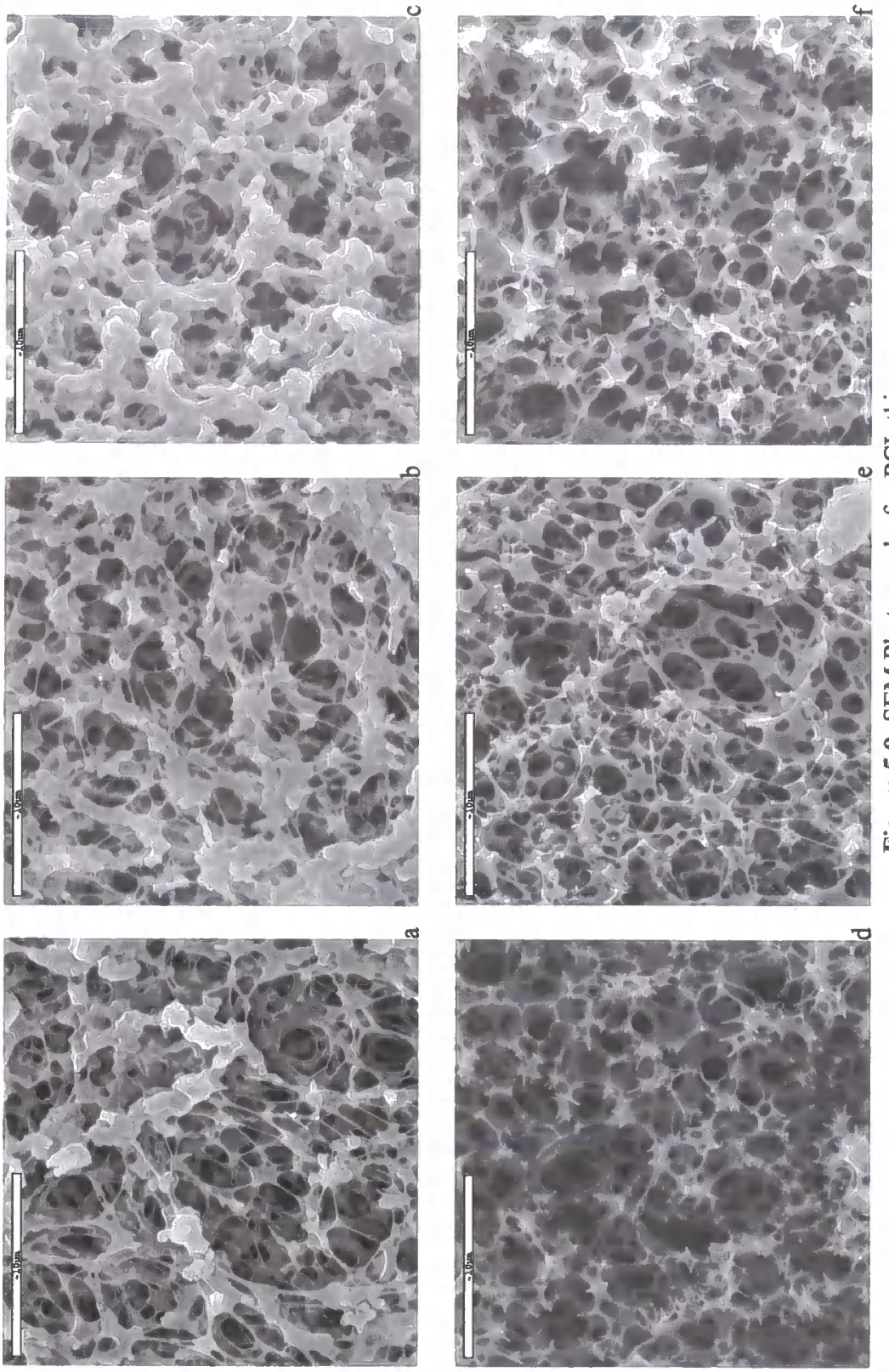

Figure 5.9 SEM Photographs for PCL thin
Outer (a) 5 days, (b) 30days, (c) 70 days Inner (d) 5 days, (e) 30 days, (f) 70 days (all 10 μm scale bars)

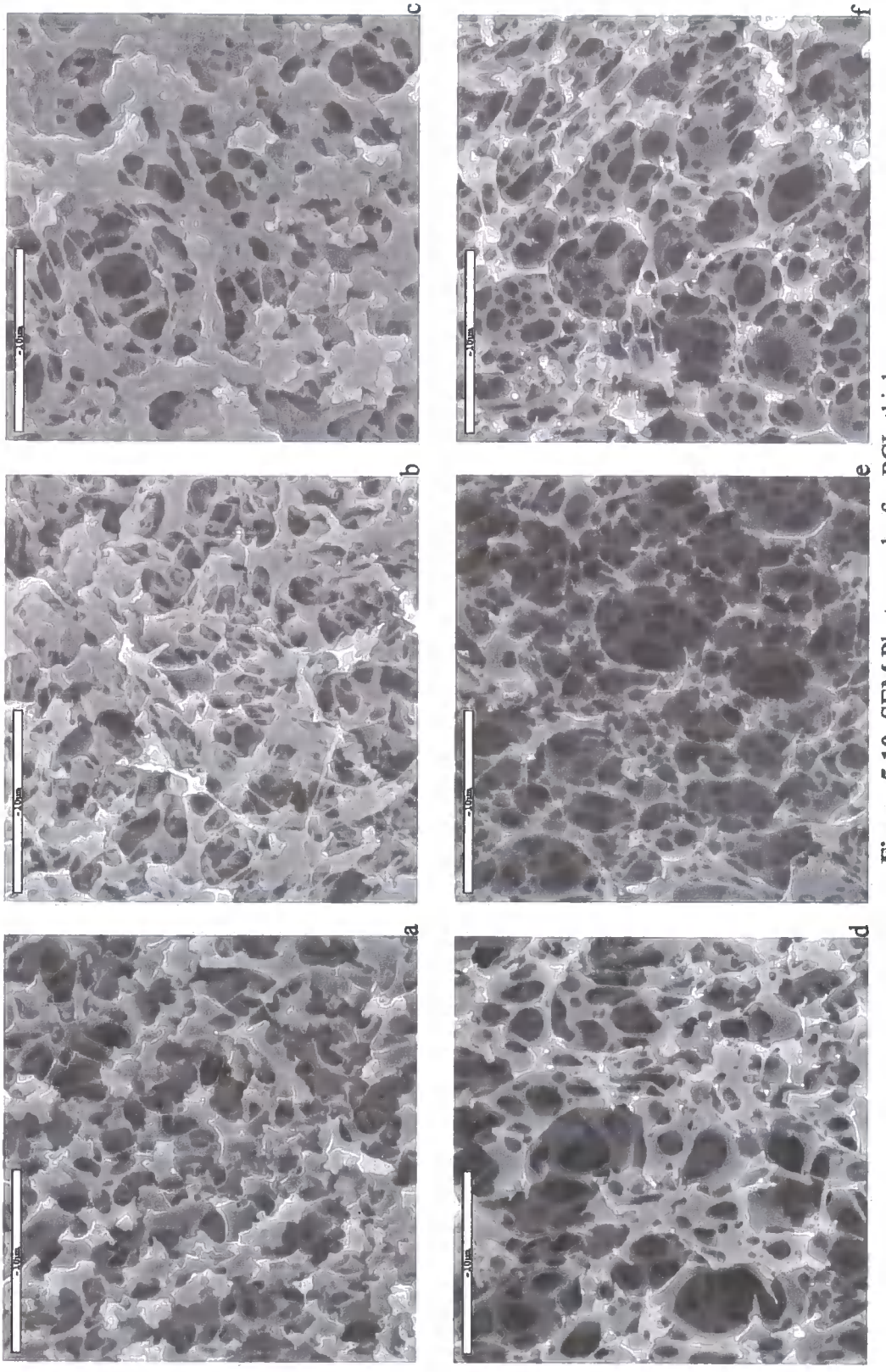

Figure 5.10 SEM Photographs for PCL thick
Outer (a) 8 days, (b) 20 days, (c) 70 days Inner (d) 5 days, (e) 20 days, (f) 70 days (all 10 μm scale bars)

5.3.5 Visual Assessment of Changes in Size and Appearance

Figures 5.11 – 5.17 reveal photographs of: (a) a control (0 days) plus one sample from each time interval, which have been placed against 2 rulers so that the reader can gain an indication of any change in size; (b) a series of 4 samples taken at 5, 15, 30 and 70 days have also been photographed. They show that, while there was little change in weight and not all of the SEM pictures showed degradation, some erosion had occurred at the surface of all 4 material types at some point. Whilst conducting the experiment, it also became apparent that the material was becoming more brittle towards the end of the 70 days period and also small but visible pieces of the foam were floating in the buffer solution, although evidently loss of these did not affect significantly the weight of the samples.

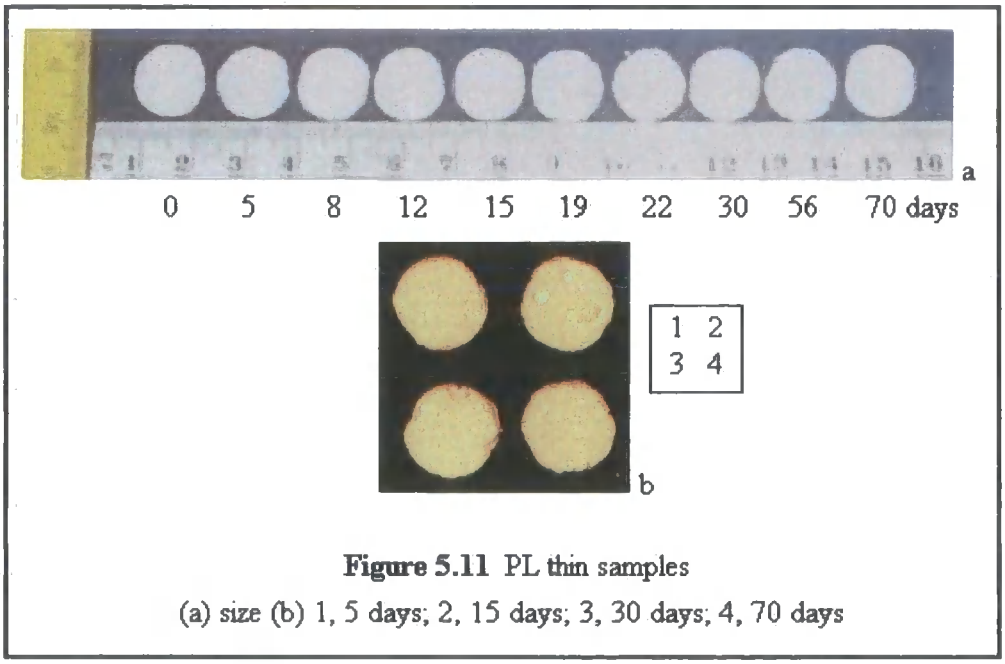

Figure 5.11 PL thin samples
(a) size (b) 1, 5 days; 2, 15 days; 3, 30 days; 4, 70 days

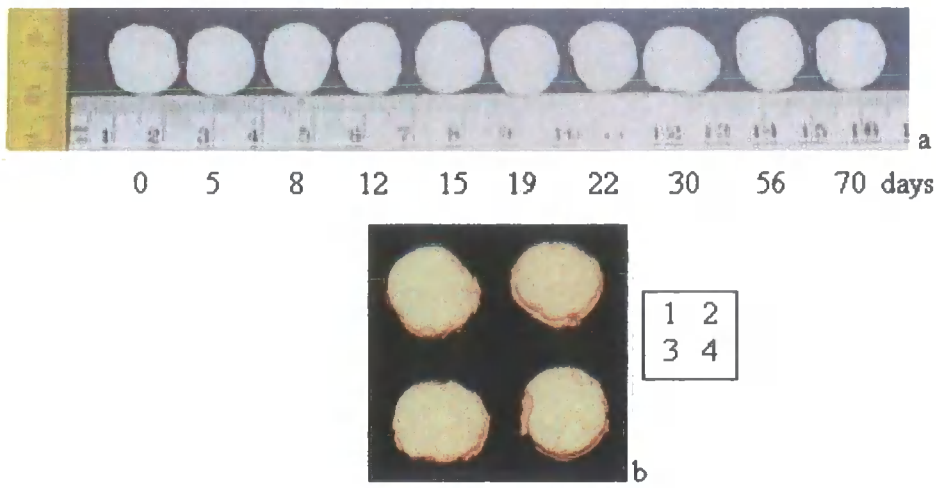

Figure 5.12 PL thick samples

(a) size (b) 1, 5 days; 2, 15 days; 3, 30 days; 4, 70 days

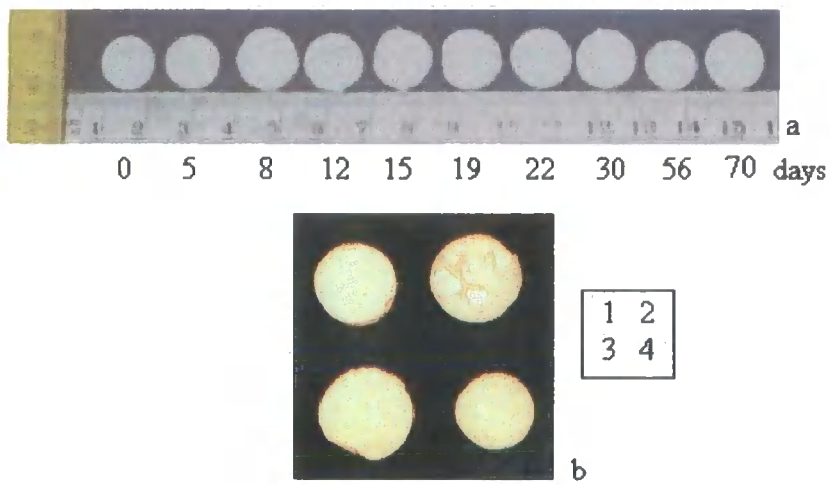

Figure 5.13 PCL thinsamples

(a) size (b) 1, 5 days; 2, 15 days; 3, 30 days; 4, 70 days

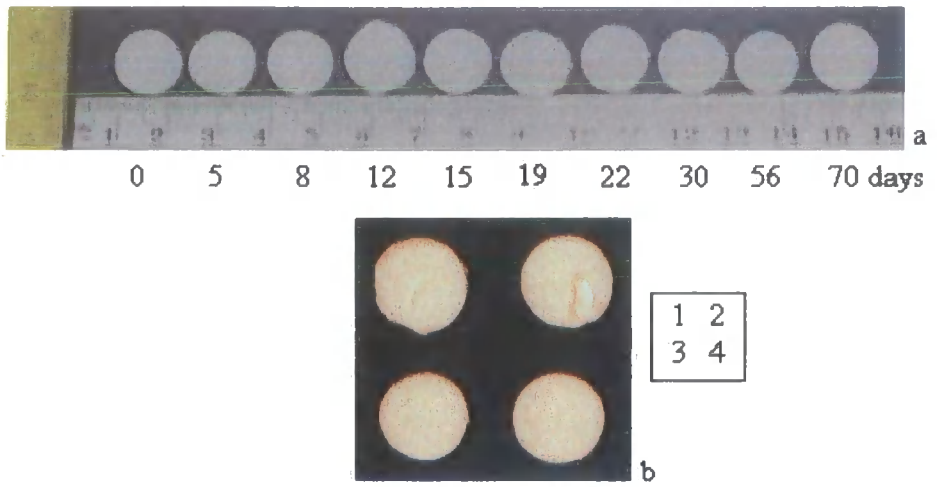

Figure 5.14 PCL thick samples
(a) size (b) 1, 5 days; 2, 15 days; 3, 30 days; 4, 70 days

5.4 Conclusions

The length of time over which the experiment was conducted was not long enough to demonstrate the full degradation of the polyester component of the foam samples. However, some valuable information was gained. From photographs, it was possible to see that degradation was starting to happen at the surface of the material. SEM pictures backed this up and indicated for the PL foams at least, that degradation was also happening within the material. The brittleness of the materials towards the end of the 70 day period would give an indication that the crosslinked network was being broken down. However, until the polymer chains are cleaved sufficiently to dissolve in the buffer, no consistent significant change in weight would be expected to be detected. As the polystyrene is not degradable, this would also remain suspended in the buffer solution. Statistical evidence also indicated that there was significant weight loss by some of the samples due to biodegradation.

Optimising Morphology

Chapter 6

6 OPTIMISING MORPHOLOGY

6.1 Introduction

Emulsion stability leading to formation of a PolyHIPE is affected by factors such as: temperature; concentration and nature of a surfactant; viscosity and electrolytes. The more stable the emulsion the smaller the droplet size and therefore, the smaller cell size of the PolyHIPE. This effect is brought about by a reduction in the surface energy per unit area - a lowering in the interfacial tension.

Work published by Williams et al. investigated the effect of monomer concentration, surfactant content and salt content on the formation of PolyHIPEs prepared using mixtures of DVB and styrene as the oil phase [189]. They found that while monomer concentration in the emulsion had little influence on the cell size of the PolyHIPE - the smaller the content of surfactant in the emulsion, the larger the cell size of the PolyHIPE. This result applied for both DVB- and styrene-based PolyHIPEs [189] and also 50 / 50 styrene-DVB PolyHIPEs [97]. Also that crosslinked PolyHIPEs produced an open cellular structure over a wider range of surfactant levels than foams polymerised from 100% styrene-based emulsions [189].

The same paper also described the effect of replacing the aqueous-based initiator, potassium persulphate, with AIBN, which is soluble only in the organic phase. Using AIBN allows the preparation of a PolyHIPE containing no salt. The results showed that the average size of cells for the PolyHIPEs made using AIBN as the initiator were an order of magnitude larger than those made with potassium persulphate as the initiator. They also discovered that while both sets of PolyHIPEs were identical in chemical composition, the foams made from AIBN were half as stiff as those made from potassium

persulphate. They, therefore, drew the conclusion that as the cells of a foam become smaller, the stiffness of the material increases.

Electrolytes have also been reported to change the PolyHIPE structure by effecting the size and number of pores within the cells, i.e. the interconnectedness of the material [190]. A high ionic strength* is indicative of an increased pore size. Williams et al. also explored the effect of increasing salt content when using AIBN as the initiator and 5% DVB / 95% styrene. They found that as the concentration of salt increased, the size of the cells decreased with a 10 times reduction in cell size as potassium sulphate was increased from 0 g / 100 mL to 10 g / 100 mL. The addition of salt reduces the electrostatic interference between the polar head groups of the surfactant molecules and this in turn lowers the interfacial tension. The above effect leads to a more compact, stronger film that stabilises the emulsion by preventing coalescence of the water droplets, therefore, the overall cell sizes will be smaller.

6.2 Experimental

6.2.1 Materials and Instrumentation

6.2.1.1 Materials

Styrene and MMA were freed of inhibitor by passing through a pad of basic Al_2O_3 and all other reagents were used as supplied. Poly (ε-caprolactone) diacrylate (Macromonomer **2**) synthesis was reported in Chapter 3, sections 3.3.2.1 and 3.4.1. Span 80 (sorbitan monooleate) was obtained from Aldrich.

* Ionic strength is defined as ½Σ molarity, (valence of electrolyte species)^2 where persulphate is used as an initiator, it must also be included in the calculation [190].

6.2.1.2 Instrumentation

FTIR spectra (KBr disks) were recorded on a Perkin Elmer 1600 Series FTIR spectrometer. NMR spectra were recorded on a Varian ASM-100 Unity-300 spectrometer at 300 MHz (^{1}H) and Bruker AM-250 spectrometer at 63 MHz (^{13}C) both using $CDCl_3$ as solvent. Solid state ^{13}C spectra were obtained with cross polarisation, high-power proton decoupling and magic angle spinning using a Varian unity-plus 300 spectrometer at 75.43MHz and ambient probe temperature (296K). A sapphire 7mm outer diameter rotor with Kel-F caps were used in a Doty probe. Elemental analysis (C, H and N) was performed using a Exeter Analytical E-440 elemental analyser. MALDI-tof spectra of samples immobilised in a mixture of 2,5-dihydroxybenzoic acid (gentisic acid or dithranol and were recorded using a Kratos Kompact MALDI 4. Scanning electron microscopy was carried out at the University of Newcastle using a Hitachi S2400 scanning electron microscope operating at 25kV. Fractured samples were prepared for SEM by mounting on aluminium stubs using adhesive carbon disks to increase the conductivity. All samples were sputter-coated with a thin layer of gold prior to viewing to enhance conductivity.

Mercury Intrusion Porosimetry measurements were carried out by using a Micrometrics Autopore III.

6.2.2 Methodology

The PolyHIPE's were synthesised according to the general method as described in section 3.3.2.3. The compositions that were used are shown in Table 6.1.

Table 6.1 Compositions Used for Optimisation of Morphology

Ref	Foam	PCL / g	Co-monomer / g	NaCl / g	Surfactant / g	Water / mls
1	NS	1	styrene 4	0	1	45
2	DS	1	styrene 4	1	1	45
3	HS	1	styrene 4	1.5	1	45
4	2gs	1	styrene 4	2	1	45
5	3gs	1	styrene 4	3	1	45
6	LS	1	styrene 4	0.5	0.5	45
7	LSNS	1	styrene 4	0	0.5	45
8	LSDS	1	styrene 4	1	0.5	45
9	LSHS	1	styrene 4	1.5	0.75	45
10	HSDS	1	styrene 4	1	1.5	45
11	AIBNns*	1	styrene 4	0	1	45
12	HW	1	styrene 4	0.5	1	47
13	LS1.5g	1.5	styrene 3.5	0.5	1	45
14	PMS	1	styrene 2 MMA 2	0.5	1	45

*Normal initiator potassium persulphate (0.1g), replaced with AIBN (0.1g)

6.3 Results and Discussion

This piece of work was originally started when it was realised that a minimum pore size of 5 – 8 μm was required for the nucleus of a cell to pass through the foams. However, the results have allowed us to look at the effect of varying the composition of the emulsions on PolyHIPE morphology. The results for the different compositions have been divided into 3 sections: salt content; surfactant and salt content; miscellaneous. A further section then addresses the results of an increase in pore size.

6.3.1 Effect of Salt Content

All of the PCL-styrene foams were made using the standard composition - see experimental section 3.3.2.3 for details, except the quantity of salt, NaCl, was varied. The standard method for making a PolyHIPE from a 50 ml emulsion uses 0.5 g NaCl. The following results present PolyHIPEs formed using a range of salt contents:

0 g, 1 g, 1.5 g, 2 g and 3 g. Only the PolyHIPE made with 0 g of NaCl (ref. 1 in Table 6.1) shrank visibly during the drying process. The SEM pictures indicate that the most stable composition was made with 1.5 g of NaCl (Figure 6.3). Lower and higher salt contents produced larger cells and bigger pores, although more so below 1.5 g of NaCl. The SEM pictures are shown in Figures 6.1 - 6.5. Figure 6.1 (a) and (b) show the SEM pictures for NS (Table 6.1, ref. 1) they reveal large cells of 20 μm and smaller cells of approximately 5 μm with a maximum pore size of 1 μm. This would indicate that the effect of lowering the salt content has destabilised the emulsion, with water droplets coalescing to form the larger cells, on polymerisation of the PolyHIPE.

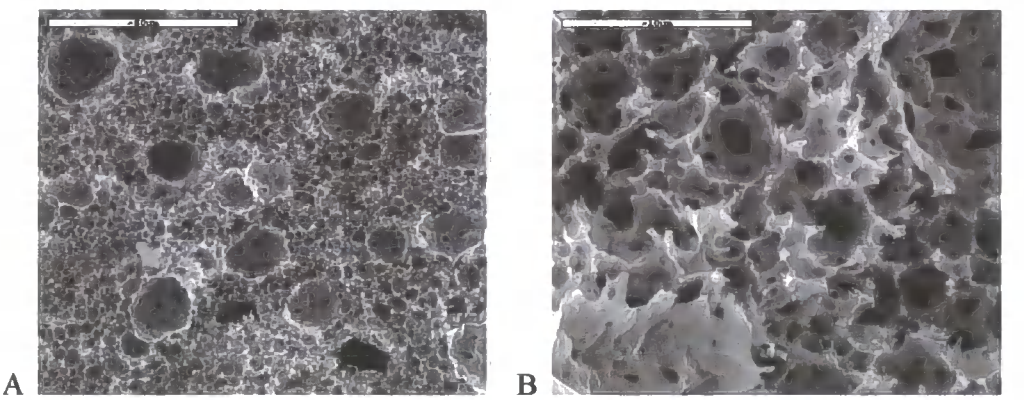

Figure 6.1 SEM Photographs (a) 0 g salt (NS) (50 μm scale bar); (b) 0 g salt (NS) (10 μm scale bar)

SEM pictures of PolyHIPEs made with 0.5 g of NaCl can be found in chapter 3, Figure 3.6 (a) and (b) they show a mixture of cell sizes increasing up to 25 μm and increased pore sizes over those in Figure 6.1 (b) up to 2 μm. SEM pictures for the PolyHIPEs prepared from 1 g NaCl, DS (Table 6.1, ref. 2) are shown in Figure 6.2.

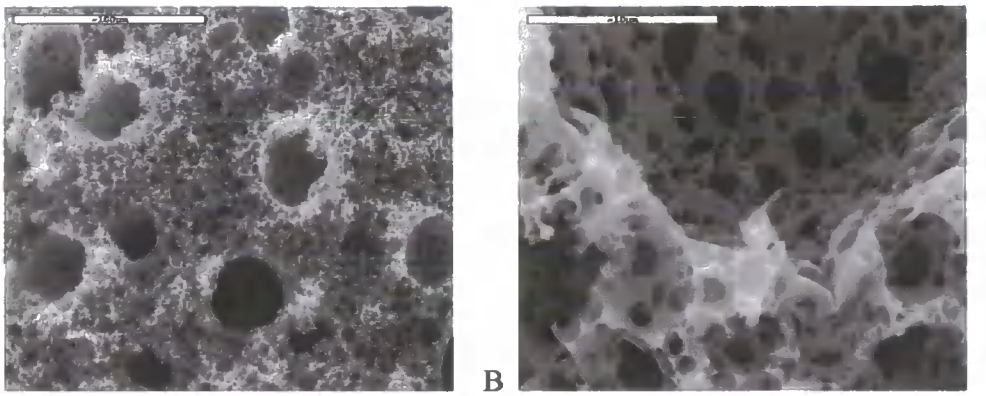

Figure 6.2 SEM Photographs (a) 1 g salt (DS) (100 μm scale bar); (b) 1 g salt (DS) (10 μm scale bar)

Upon doubling the salt content compared to the standard formulation, the size of some of the cells has increased to 50 μm (notice the lower magnification, scale bar = 100 μm), whereas the pore size has remained at ~ 2 μm, as for 0.5 g salt (NS). However, as the salt content was increased to 1.5 g, HS (Table 6.1, ref. 3) the stability of the emulsion appears to have increased with very few large cells - the large cells being 20 μm - leaving an interconnected network of pores around 1 μm. These can be seen in Figure 6.3.

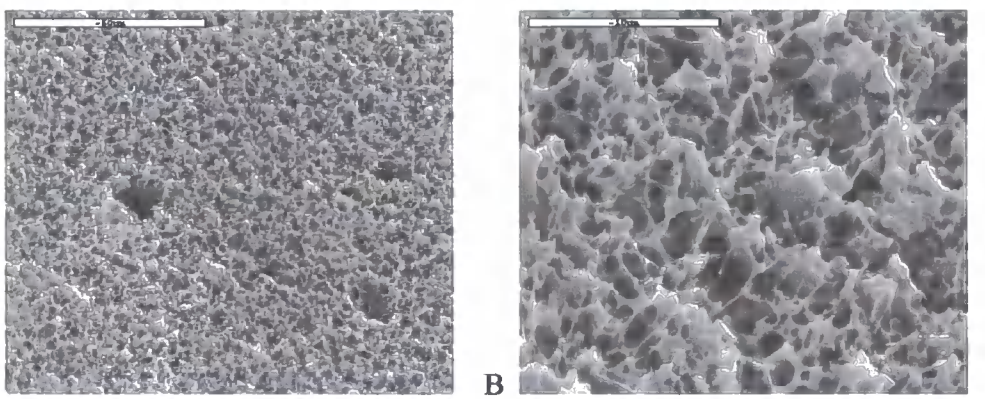

Figure 6.3 SEM Photographs (a) 1.5 g salt (HS) (50 μm scale bar); (b) 1.5 g salt (HS) (10 μm scale bar)

As the salt content was further increased to 2 g, 2gs (Table 6.1, ref. 4), the emulsion has again become noticeably unstable, Figure 6.4.

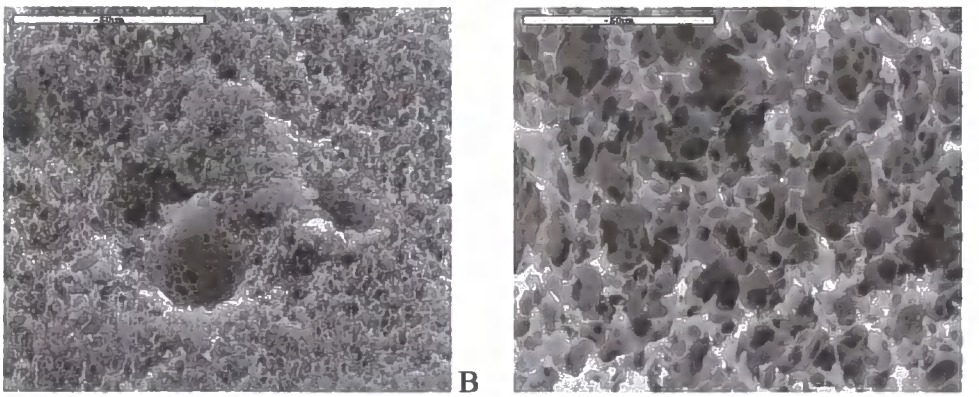

Figure 6.4 SEM Photographs (a) 2 g salt (2gs) (50 μm scale bar); (b) 2 g salt (2gs) (50 μm scale bar)

There are again a number of cells appearing at 20 μm that contain pores of approximately 5 μm, but generally the average pore size is again 1 μm with cells of 5 μm. Figure 6.5 shows the SEM pictures for the PolyHIPEs made using a salt content of 3 g, 3gs (Table 6.1, ref. 5).

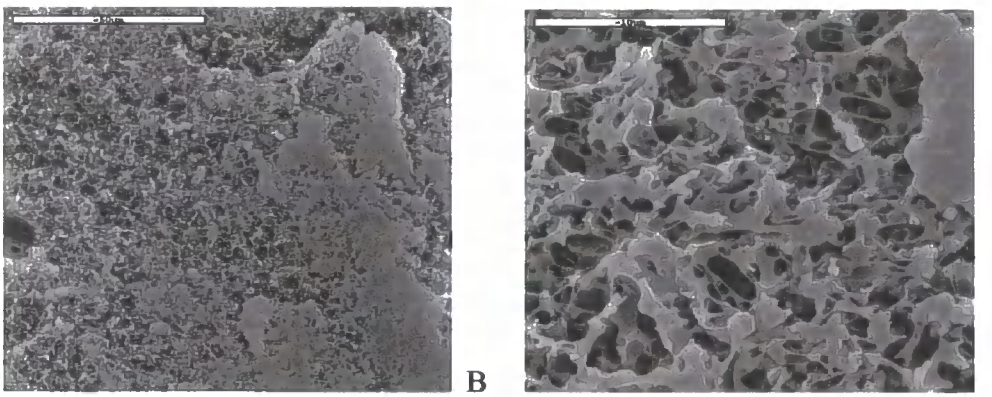

Figure 6.5 SEM Photographs (a) 3 g salt (3gs) (50 μm scale bar); (b) 3 g salt (3gs) (10 μm scale bar)

Figure 6.5 (b) would indicate that the foam has shrunk on drying, however, visual observation of the sample shows this was not the case. It is more likely that the mechanical strength of the foam is lower and it had become compressed during

preparation for taking the SEM photographs. However, it would appear that there are a few larger cells of about 10 μm but the average cell size is 5 μm with pores averaging 1 – 2 μm.

Work looking at the effect of electrolytes on PolyHIPE morphology previously discussed in the Introduction found that more salt led to formation of smaller cells. It would appear that this does not apply for the 1 g PCL / 4 g styrene system, using sodium chloride as the salt. Increasing salt content from 0 g to 1 g caused a decrease in emulsion stability shown by the increasing cell and pore sizes. As the other factors that would be expected to affect the PolyHIPE morphology, i.e. viscosity, temperature, surfactant concentration, were kept constant and the changes must be attributed to the salt concentration. It would be expected that as the salt concentration was increased, the interfacial tension of the film between the continuous phase and water droplets would be lowered and as a result coalescence reduced, therefore, smaller cells created upon polymerisation of the emulsion. It would appear that a salt content of between 1 g and 1.5 g was needed before the interfacial tension was sufficiently lowered to prevent emulsion instability.

6.3.2 Effect of Surfactant and Salt Concentration

A random combination of surfactant, Span 80 and salt concentrations was examined and the SEM results are presented below in Figures 6.6 – 6.10. The first PolyHIPE of the set looked at the effect of halving the amount of surfactant added from 1 g to 0.5 g, LS (Table 6.1, ref. 6). The SEM pictures are shown below in Figure 6.6. Lowering the surfactant has resulted in production of larger cells of 50 μm containing few pores - implying that coalescence has occurred and a set of smaller cells averaging

10 μm with small pores of a maximum 1 μm. Compared to a standard composition foam there are considerably less pores, suggesting that the film separating adjacent emulsion droplets are relatively thick.

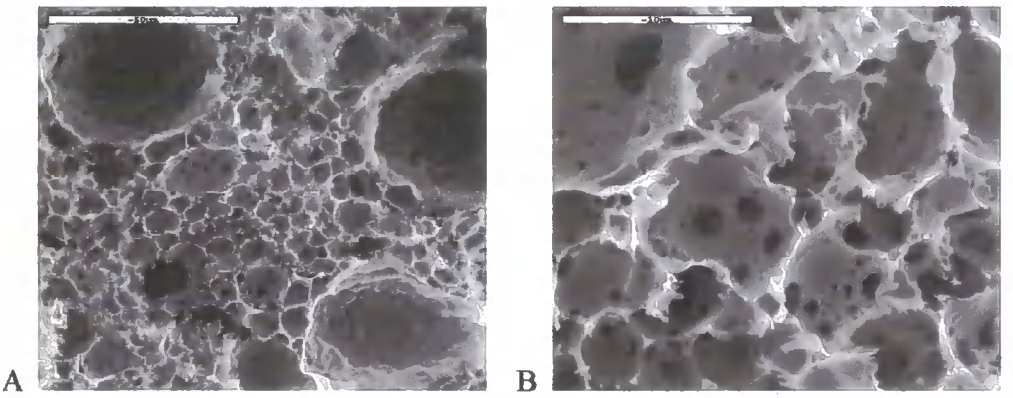

Figure 6.6 SEM Photographs (a) 0.5 g surfactant (LS) (50 μm scale bar); (b) 0.5 g surfactant (LS) (10 μm scale bar)

Following this it was, therefore, proposed to try a combination of low surfactant and no salt, LSNS (Table 6.1, ref 7) to try and create larger pores within large cells. The SEM results are presented in Figure 6.7.

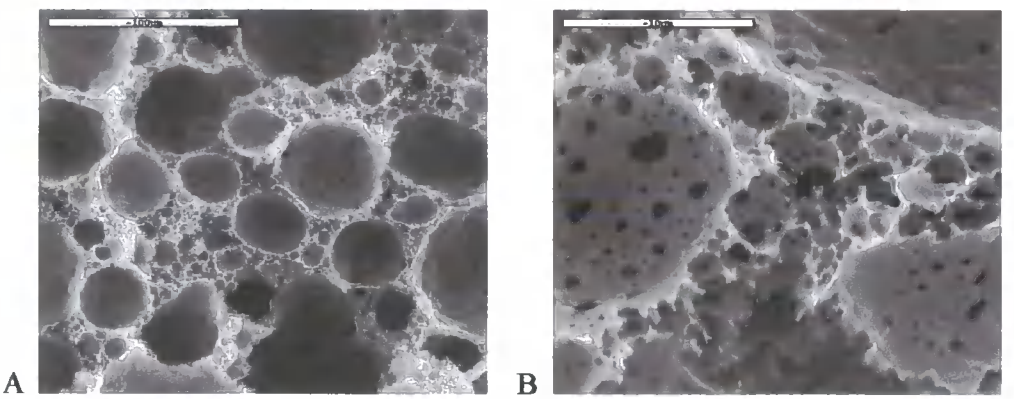

Figure 6.7 SEM Photographs (a) 0.5 g surfactant, 0 g salt (LSNS) (100 μm scale bar); (b) 0.5 g surfactant, 0 g salt (LSNS) (10 μm scale bar)

From Figure 6.7 it can be observed that fewer small cells were produced, showing this composition has further destabilised the emulsion. Although the number of pores in the large cells has increased, they are only 1 – 2 μm in diameter. We then decided to see

what impact using double the salt concentration with a low surfactant concentration, LSDS (Table 6.1, ref. 8), would have on the foam morphology. The results for this are shown in Figure 6.8.

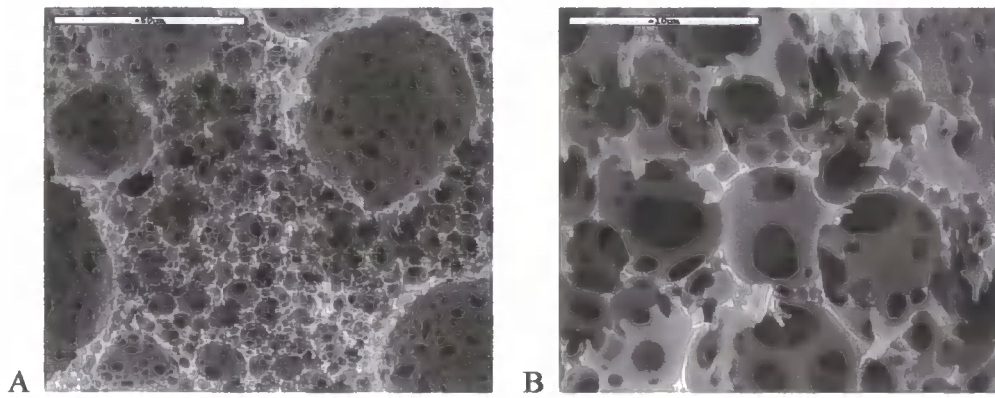

Figure 6.8 SEM Photographs (a) 0.5 g surfactant, 1 g salt (LSDS) (50 μm scale bar); (b) 0.5 g surfactant, 1 g salt (LSDS) (10 μm scale bar)

The results showed that as with using low surfactant there is a mixture of larger and smaller cells 5 μm, 10 μm up to 50 μm. However, when coupled with a higher salt content the interfacial tension has been lowered sufficiently to cause a thinning of the surfactant film and larger pores have resulted up to 4 μm. The next step was to see if using an even higher concentration of salt would further increase the pore size, LSHS (Table 6.1, ref. 9). The results are shown in Figure 6.9.

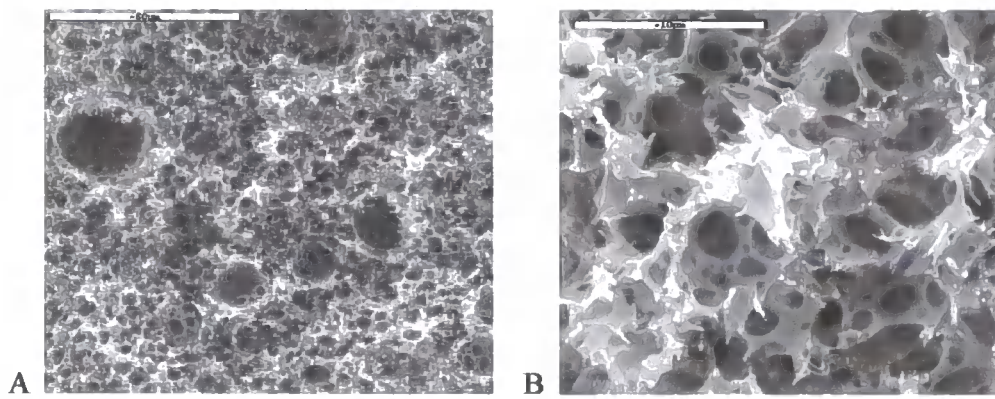

Figure 6.9 SEM Photographs (a) 0.75 g surfactant, 1.5 g salt (LSHS) (50 μm scale bar); (b) 0.75 g surfactant, 1.5 g salt (LSHS) (10 μm scale bar)

As was seen when increasing the salt content alone, the emulsion has become more stable - reducing the size of the cells, one or 2 cells are large at 10 and 20 μm but the majority of cells are 5 μm. The pores have increased in number but as a result are smaller up to 2 μm. The final combination tried was taking the 1 g salt that had so far yielded the biggest pores and increasing the surfactant content to 1.5 g, HSDS (Table 6.1, ref. 10). The SEM results are shown in Figure 6.10.

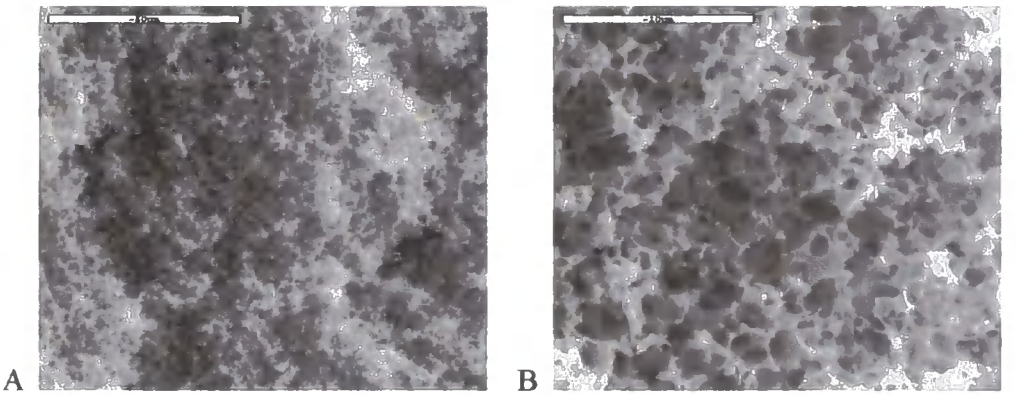

Figure 6.10 SEM Photographs (a) 1.5 g surfactant, 1 g salt (HSDS) (50 μm scale bar); (b) 1.5 g surfactant, 1 g salt (HSDS) (10 μm scale bar)

As can be seen in Figure 6.10 (a) the cells seen in the PolyHIPE are smaller than any of the previous results in this thesis, the average cell size would appear to be 3 μm. The pore sizes are an average 1 μm. The results for surfactant effect are in agreement with the work discussed in the introduction by Williams et al. [190] in which a lower surfactant concentration leads to bigger cells. This would be expected because a lower concentration of surfactant would result in a thinner film separating the droplets, therefore, coalescence would be more likely to occur from the film rupturing.

6.3.3 Miscellaneous

The final set of PolyHIPEs have no common compositional change, so the results for the foams are presented in alphabetical order. Work by Willams et al. [190] reported in the Introduction found that switching from an aqueous-based initiator to an initiator that is soluble in the organic phase, increased the cell size by an order of magnitude. This was, therefore, a logical composition to try, AIBNns (Table 6.1, ref. 11). The SEM results are shown in Figure 6.11. The first noticeable difference to other foams in this thesis is the presence of extremely large cells (scale bar = 1 mm).

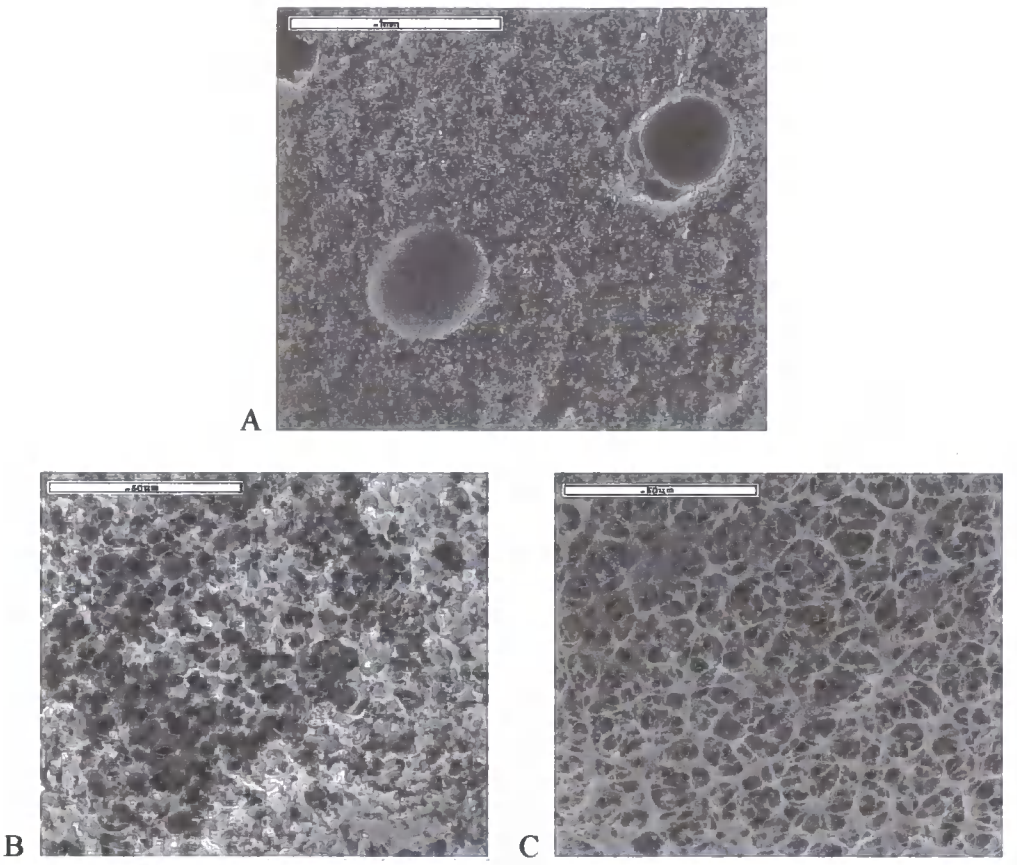

Figure 6.11 SEM Photographs (a) AIBN, 0 g salt (AIBNns)(1mm scale bar) (b) AIBN, 0 g salt (AIBNns) (50 μm scale bar), non pore morphology; (c) AIBN, 0 g salt (AIBNns) (50 μm scale bar), morphology in cell;

D 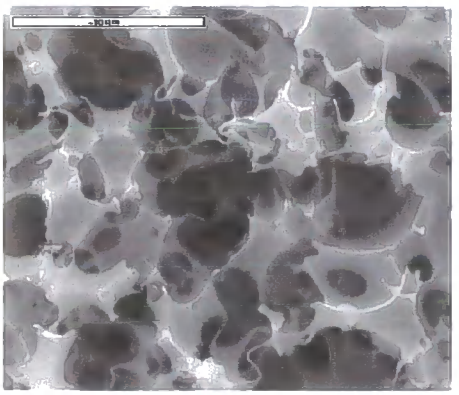 E 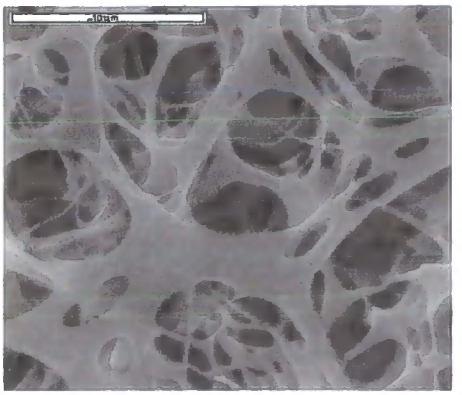

Figure 6.11 SEM Photographs
(d) AIBN, 0 g salt (AIBNns) (10 μm scale bar), non pore morphology;
(e) AIBN, 0 g salt (AIBNns) (10 μm scale bar), morphology in cell

Figure 6.11 (b) – (e) show that there are 2 distinct morphologies within the foam - (b) and (d) taken from the surface of the foam, which reflect the typical morphology for a PolyHIPE with large pores from 5 μm up to 8 μm. Figures 6.11 (c) and (e) are the surface within the large cells of the foam seen in Figure 6.11 (a) - where there would appear to be a network of pores of approximately 10 μm.

Using a increased water content but keeping the remaining components of the emulsion constant as described in 3.4.4, we hoped to produce a foam with increased pore size, HW (Table 6.1, ref. 12). This would be expected to occur because stretching the organic phase film over an increased volume of water, would increase thinning of the comonomer films separating adjacent water droplets. The SEM results are shown in Figure 6.12. Increasing the water content appears to have produced a high number of smaller pores up to 2 μm, however, the PolyHIPE shrank by approximately 50% during the drying process and these pictures are not necessarily representative of the emulsion and pre-dried PolyHIPE. Making the foam a second time and drying at a lower temperature or freeze-drying could prevent the shrinkage.

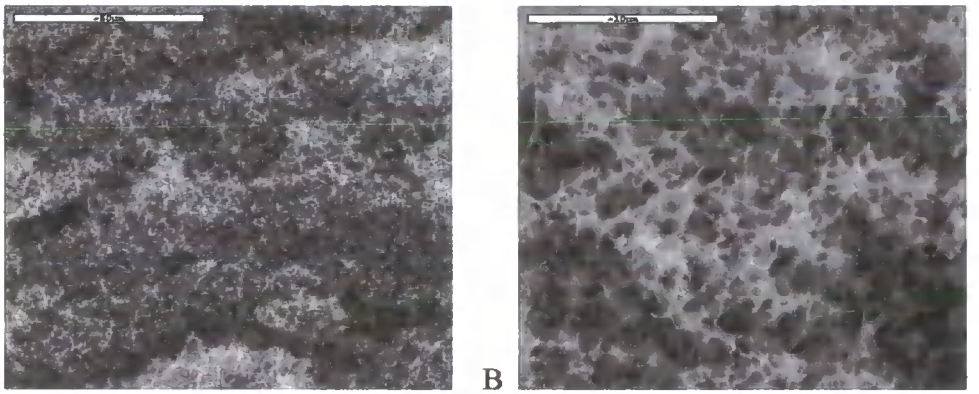

Figure 6.12 SEM Photographs (a) 47 ml water (50 μm scale bar); (b) 47 ml water (10 μm scale bar)

The final 2 foams had different polymer contents. From work reported earlier, we were already aware that increasing the polymer content increased the number of pores (Figure 3.6 (b) and Figure 3.8 (a), (b) and (c)) and also that using a low surfactant concentration increased the size of the cells, Figure 6.6. We, therefore, decided to look at the effect of low surfactant concentration (0.5 g) and increased PCL content (1.5 g) on the foam morphology, LS1.5g (Table 6.1, ref. 13), the SEM results are shown in Figure 6.13. The foam did not appear to have shrunk on visual inspection, however, the SEM pictures reveal large areas of non-porous material but also some porous parts.

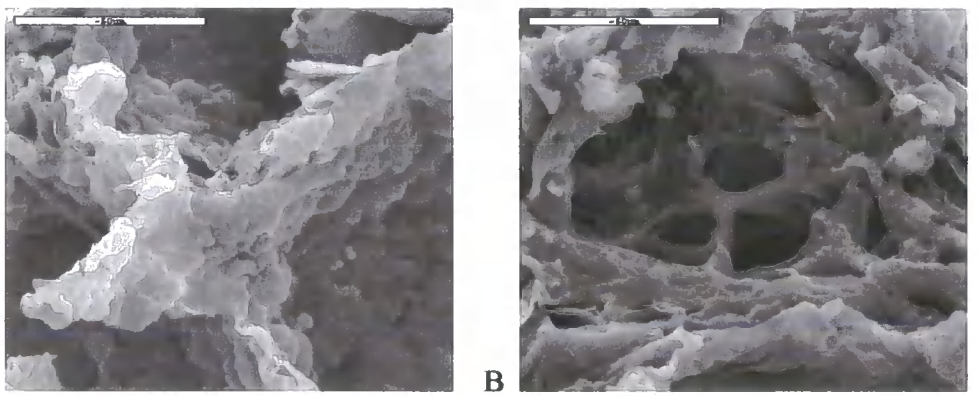

Figure 6.13 SEM Photographs
(a) 0.5 g surfactant, 1.5 g PCL (LS1.5g) (50 μm scale bar);
(b) 0.5 g surfactant, 1.5 g PCL (LS1.5g) (50 μm scale bar);

C 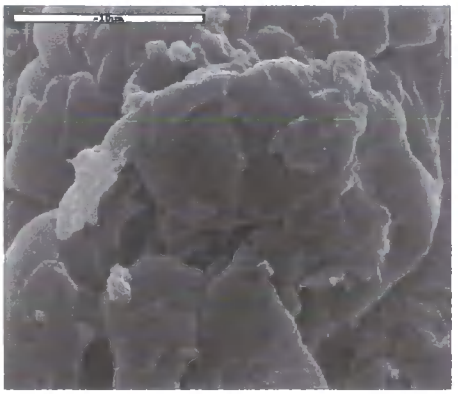

Figure 6.13 SEM Photographs
(c) 0.5 g surfactant, 1.5 g PCL (LS1.5g) (10 μm scale bar)

The final compositional change used 1 g PCL, 2 g styrene and 2 g MMA, PMS (Table 6.1, ref.14). SEM pictures are shown in Figure 6.14.

A 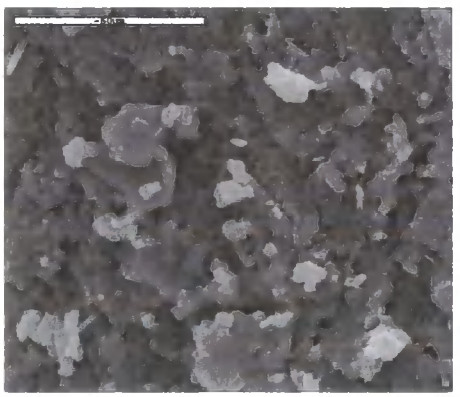 B 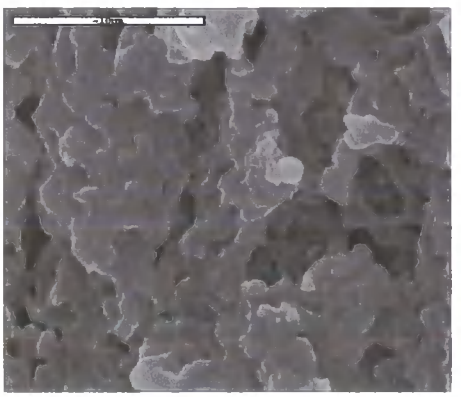

Figure 6.14 SEM Photographs (a) PSM (50 μm scale bar); (b) PSM (10 μm scale bar)

The resultant structure appears to be porous in places, however, the foam collapsed by approximately 75% during the drying process, therefore, again the SEM pictures may not be an accurate representation of the emulsion or the pre-dried PolyHIPE.

6.3.4 Mercury-IntrusionPorosimetry Results

Mercury-intrusion porosimetry is a technique by which mercury is forced into the spaces or openings of materials at high pressure under vacuum. The data obtained can be

used as a guide to pore opening size, the range of pore sizes, wall area and the volume of pores. All of the foams described in sections 6.3.1, 6.3.2 and 6.3.3 along with the following compositions: 0.2-H-S*; 0.2-H-M*; 0.2-L-S*; 0.2-L-M*; 0.2-S†; 0.2M†, i.e. PolyHIPEs prepared from 1 g of polymer and 4 g of co-monomer, were analysed using mercury porosimetry. The samples were measured in duplicate; the results cannot be taken as a true reflection of the porosity because the model that all the calculations are based on assuming a cylindrical pore shape. However, the data can be used for comparative purposes and to support the information seen in the SEMs. The actual data have been reported in Table 6.2.

Table 6.2 Average Pore Size as Measured by Mercury-intrusion Porosimetry

Foam	Median Pore Diameter (volume) µm	Median Pore Diameter (area) µm	Average Pore Diameter (4V/A) µm	Average of all 3 columns µm
2GS	1.71	1.24	1.73	
	1.84	1.44	1.73	1.62
3GS	1.58	1.38	1.55	
	1.75	1.42	1.70	1.56
AIBN	4.68	1.91	3.72	
	9.81	6.05	8.62	5.80*
DS	3.96	2.32	3.20	
	4.37	2.59	3.60	3.34
Hsalt1.5	2.15	1.39	1.95	
	3.87	2.73	3.34	2.57
HSDS	2.17	1.57	2.05	
	1.39	1.19	1.45	1.64
HW	3.20	1.77	2.	
	1.66	1.25	1.66	2.05
LS	1.28	1.25	1.30	
	1.28	1.26	1.29	1.27
LS1.5sty	2.14	1.39	2.27	1.60
LSDS	2.50	2.25	2.30	
	2.47	2.34	2.20	2.21
LSHS	1.33	1.30	1.38	
	1.35	1.32	1.35	1.67
LSNS	1.32	1.19	1.39	
	1.40	1.31	1.45	1.34

* See Chapter 3, Experimental for key
† See Chapter 4, Experimental for key

Foam	Median Pore Diameter (volume) µm	Median Pore Diameter (area) µm	Average Pore Diameter (4V/A) µm	Average of all 3 columns µm
NS	0.96	0.95	1.06	
	0.98	0.97	1.06	1.13
PCLmma2k	1.90	1.46	1.82	
	1.95	1.72	1.97	1.54
PCLmma53	9.09	7.85	9.95	
0	10.45	8.52	11.25	6.97*
PCLsty2k	5.32	2.50	3.99	
	4.58	2.11	3.47	5.80
PCLsty530	1.99	1.79	1.79	
	1.97	1.79	1.78	2.36
PLmma	1.53	1.47	1.53	
	1.75	1.64	1.73	1.69
PLsty	2.51	1.81	2.12	1.94
	2.20	1.71	2.02	
PMS	361.72	2.41	27.53	130.55)*

*Average pore size is greater than 5 µm, target pore size for cell studies

6.2.4.1 Comparison of PCL and PL foams

In general the porosimetry results displayed in Figure 6.15 reflect the results obtained from SEM. For example the PL-MMA foam, 0.2-M, (Figure 4.12 (a)) contains smaller cells and pores than its equivalent PCL-MMA, 0.2-L-M, (Figure 3.9 (a)) and 0.2-H-M, (Figure 3.9 (c)) and this pattern is repeated in the pore size distribution plots in Figure 6.15. In the case of the foams where styrene is the comonomer - the PL-styrene foam, 0.2-S and the PCL-styrene, 0.2-L-S have approximately the same pore size distribution, although 0.2-S seems to have the larger pore volume (Figure 4.10 (a) and (b)). However, the indication is that the pore and cell size distribution of the PCLmma530 is much larger, further examination of Figure 3.6 (c) and (d) reveal that this is an accurate conclusion with the pore size being small but the cell size much larger than that of the PL styrene foam and it is likely that this larger cell size is reflected in the pore size distribution.

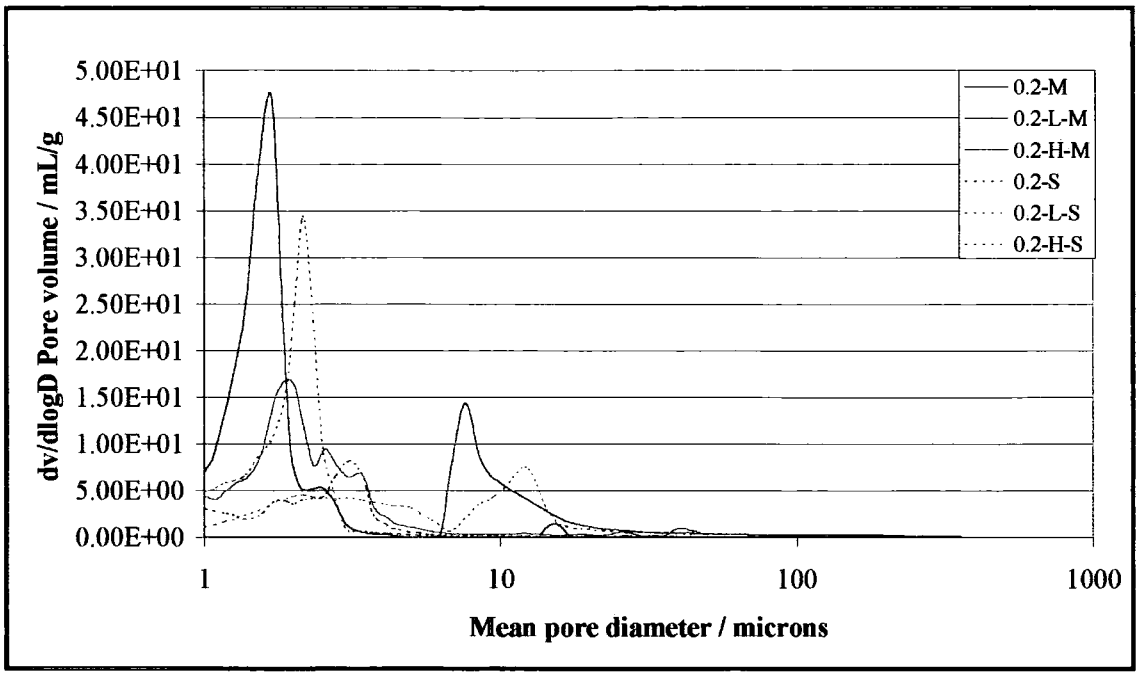

Figure 6.15 Chart Comparing PCL and PL Porosimetry Results

6.3.4.2 Salt Content

The porosimetry results for the foams made with increasing NaCl content are given in Figure 6.16, again, the results reflect those already seen in the SEMs, Figures 6.1 – 6.5. The smallest pores were obtained with 0 g salt, generally increasing with increasing salt content up to 1.5 g. Upon the addition of 2 g and 3 g of salt to the aqueous phase the pore size was discovered to decrease. With these foams there was also a broader pore and cell size distribution. Mercury-intrusion porosimetry looks at the overall distribution of both cell and pore size, where the cell size and the pore size were more uniform the distribution appears on the graphs, Figures 6.15 – 6.17 as a single distribution peak. Irregular cell sizes, also tend to have irregular pore sizes and these are reflected in the broad peak distribution of the mercury porosimetry results.

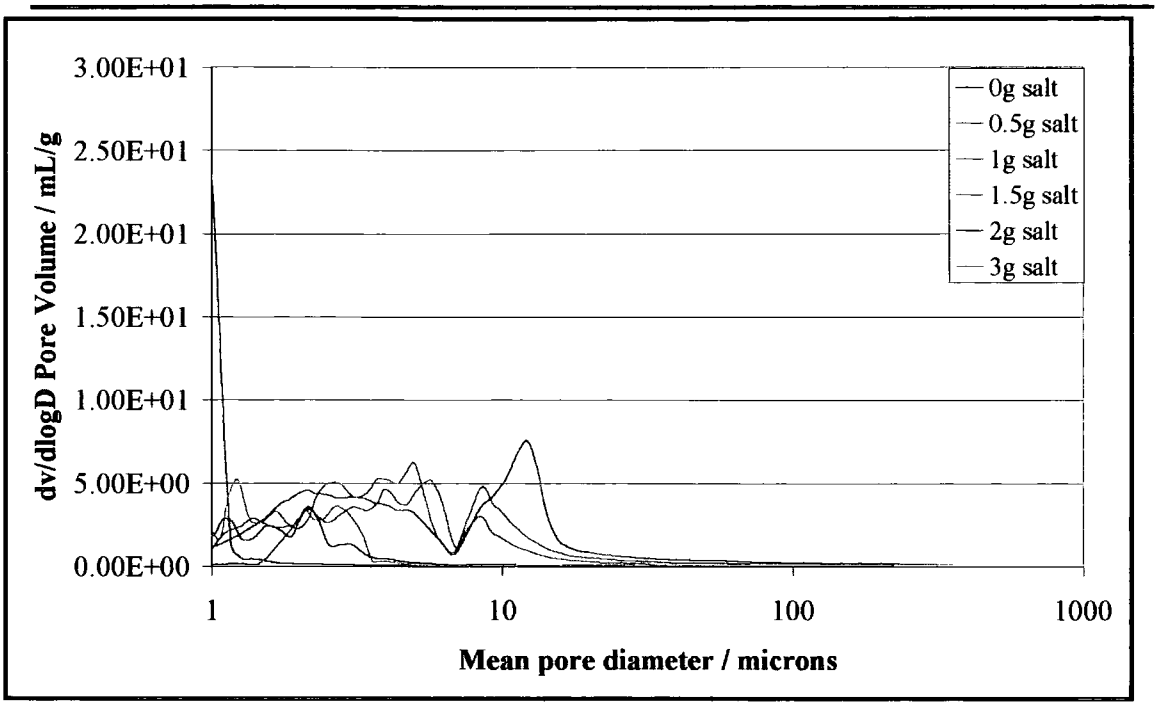

Figure 6.16 Chart Comparing Pore Size with Increasing Salt Content

6.3.4.3 Potassium Persulphate Versus AIBN

From Figure 6.17 it is evident that the foam synthesised with 1 g of polymer and 4 g of comonomer and AIBN as the initiator contains a number of pores that are larger than the foams made using the same composition but with potassium persulphate as the initiator, with maximum peaks at 2 μm, 8 μm and 10μm. The PCL-styrene foam, 0.2-H-S, has been previously discussed in section 6.3.4.1. The distribution given for the AIBN foam is likely to be characteristic of the pore size – with cells being much larger and not represented. The distribution for 0.2-H-S is likely to include both the smaller pores and the cells which can be as large as 20 μm (Figure 3.6 (a)).

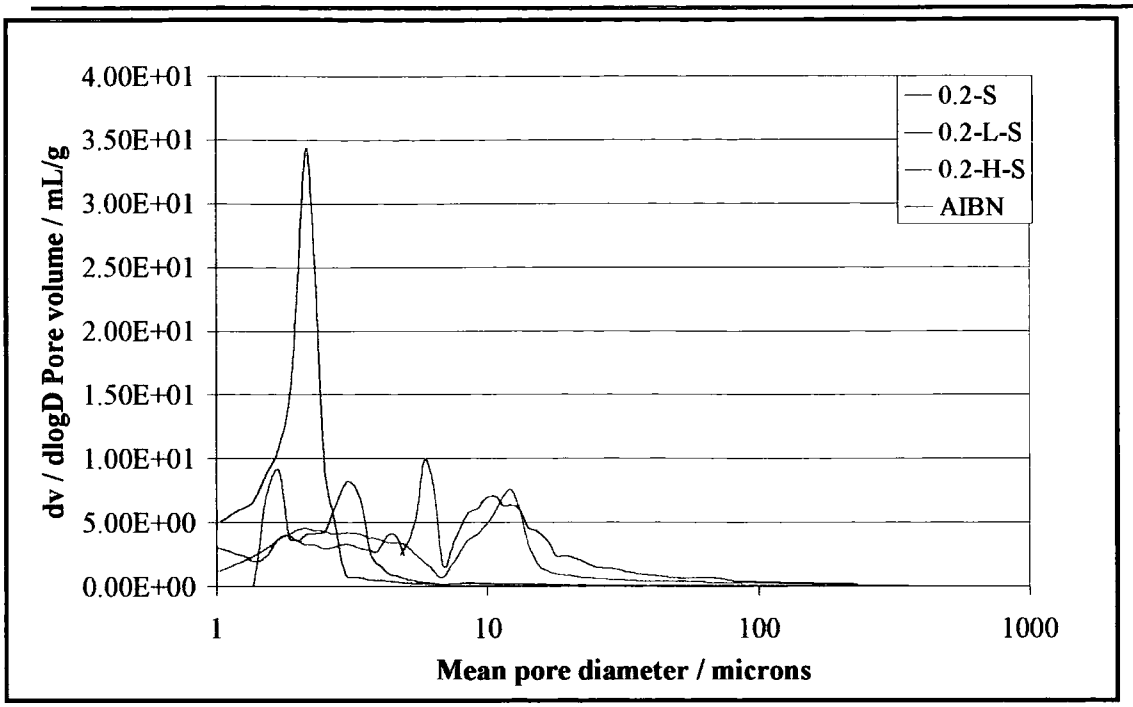

Figure 6.17 Chart Comparing Potassium Persulphate (PCL/PL-styrene) with AIBN

6.4 Conclusions

From this section of work it is apparent that there are a number of factors, such as: salt content, initiator and water content, which can influence the size and number of both cells and pores within a PolyHIPE. Although the pore size can be varied it would appear that using potassium persulphate as the initiator the maximum pore size for the compositions investigated was 5 μm. To obtain a larger pore size it was necessary to use an oil-soluble rather than a water-soluble initiator, which increased the pore size to between 5 μm and 10 μm. This increased pore size should be large enough to allow the passage of cells through and to grow within the foam scaffolds, but the foams with small pore and cell sizes will limit the applications in which these PolyHIPEs could be used.

Cell Studies

Chapter 7

7 CELL STUDIES

7.1 Introduction

7.1.1 Cells

The basic building blocks determining structure and function in living organisms are **cells**. A representative animal cell is shown in Figure 7.1.

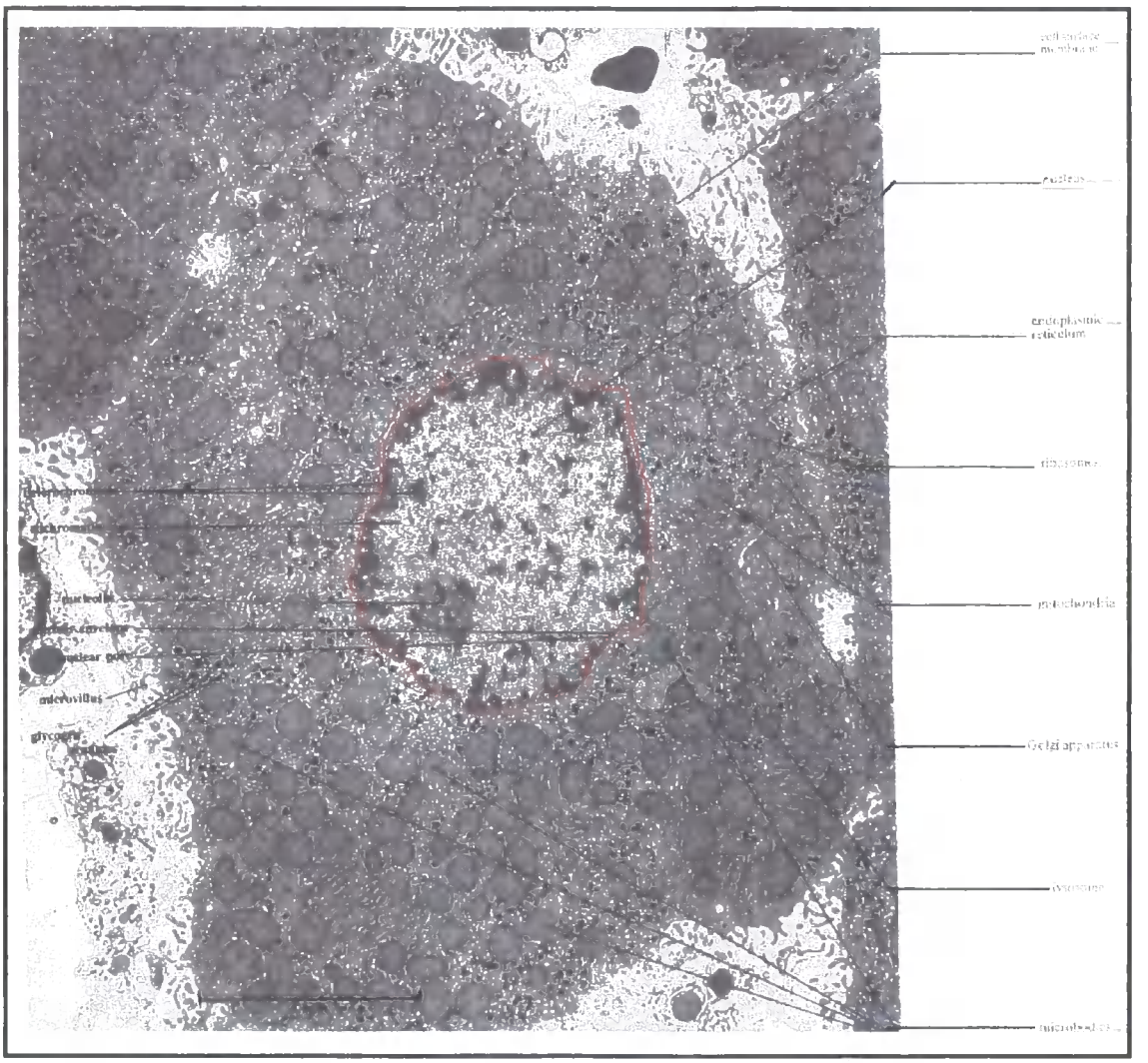

Figure 7.1 Electron Micrograph of a Rat Liver Cell [191]

In 1855 Virchow discovered that new cells are derived from existing cells by cell division [192]. Cells are separated from their environment and each other by a cell

membrane. The cell membrane is semi-permeable allowing the exchange of raw materials needed for growth, development and sustenance and the removal of waste products. When growing cells on external matrices, the feature that determines the minimum pore size required to allow cells to grow into the material is the nucleus. In Figure 7.1, the scale bar on the picture represents 5 μm and it is therefore apparent that the nucleus is approximately 5 – 6 μm in diameter. However, it should be stressed that the nucleus is not the only factor that determines the minimum pore size in tissue engineering, but it was the main consideration for the cells grown in this thesis.

7.1.2 Tissue

When a group of cells serving a similar function and/or having a similar structure are grouped together they are described as **tissue**. Animal tissue can be divided into 5 groups: epithelial (often secretory that line a cavity or are surface covering), connective, muscle, nervous, vascular (transport of fluid). The tissue is defined by cells that are physically linked and/or by any intercellular substances that are specific to a function or functions. Different tissues can be linked by similar functions and are then known as **organs** e.g. liver, heart.

7.1.3 Fibroblasts

Connective tissue can be formed from cells known as **fibroblasts**. Fibroblasts are responsible for the production of 3 fibres: reticular (connective tissue), collagen and elastin (providing the tissues with strength and resilience). The cells are generally flattened and spindle-like in configuration with an oval shaped nucleus [193].

7.1.4 Cells and Biomaterials

7.1.4.1 Cell Attachment to Biomaterials

In order for cells to be capable of proliferation on any scaffold the first stage following seeding must be their attachment and flattening [194]. Attachment can happen in one of three ways [195]:

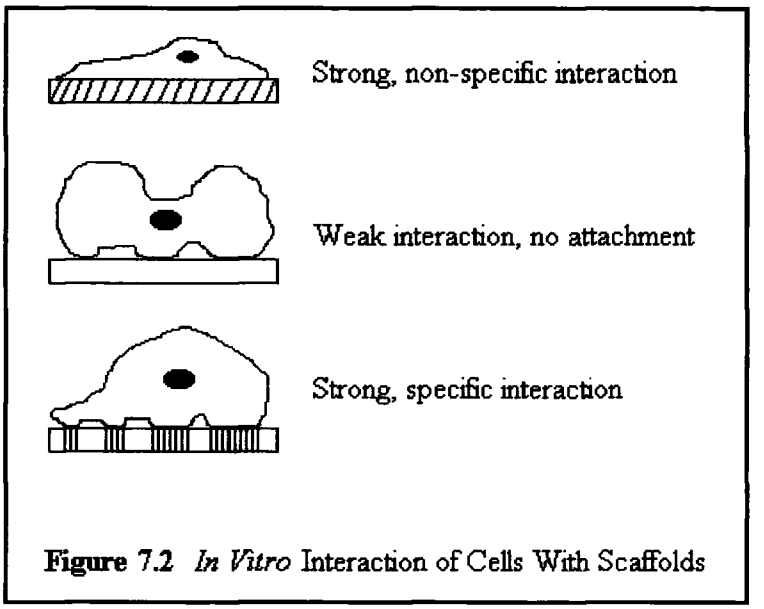

Figure 7.2 *In Vitro* Interaction of Cells With Scaffolds

The type of attachment has implications for the development of the cells. A strong but non–specific interaction results in attachment and proliferation of the cells. A weak interaction does not produce attachment, but as a result, response by the immune system and fibrosis - the formation of fibrous tissue leading to scarring - can be reduced. Where the cells interact strongly and specifically, specific cell responses can be induced. Features of the scaffold that can affect the interaction of cells include the rigidity / pliability of the material and whether it contains a macro-/microporous structure (pore size and distribution) [196]. Once attached the cells will begin to produce their own ECM.

In an *in vivo* application where the biomaterial is implanted for tissue induction (ingrowth of cells into the material), i.e. there is no seeding of cells, proteins, such as fibronectin, victronectin or laminin [197] from bodily fluids adsorb to the material's surface. The surface properties of the material, such as the functional groups present and the surface charge [197], affect the conformation and composition of the proteins that become adsorbed. Fibroblasts [198], endothelial cells [199] and kidney epithelial cells [200] adhere and proliferate more readily on more hydrophilic than hydrophobic materials.

In 3D scaffolds, rapid cell attachment is important [201] and inhibition is caused by gravity. Cultured cells that have been trypsinised (the enzyme trypsin is used to detach cells from the surface of culture flasks) often cannot adhere to new surfaces [194]. Typically, following seeding, the cells are subjected to a 2 – 24 h. time lag interval - a period of exponential growth followed by no or minimal growth [202].

7.1.4.2 Effect of Cell Concentration on Growth

Vacanti and coworkers looked at the effect of seeding various concentrations of cells into biodegradable PGA scaffolds. After seeding, the scaffolds were cultured *in vitro* for one week followed by 12 weeks of growth in nude mice [203]. The cells studied were chondrocytes (cartilage cells) isolated from the shoulders of calves. The concentrations used were 2, 10, 20 and 100 million cells per cc. Analysis of the weight of the wet scaffolds (24 per concentration) over 12 weeks showed an increase in weight with increased in seeding concentration:

Table 7.1 Effect of Cell Seeding Concentration on Average Wet Weights of Resorbable Polymer Implants after 12 Weeks

Cell Concentration Seeded / Million per cc	Average Weight after 12 weeks / mg
2	53.5
10	90
20	120
100	160

The thickness of the implants also showed a similar trend, increasing by 100% going from 2 to 20 to 100 x 10^6 / cc respectively. Histological examination of the implants revealed a decrease in cell number per area for the 20 and 100 x 10^6 / cc concentrations. The scaffolds loaded with 2 million cells / cc showed only 20% cartilage development, the remaining 80% comprised fibrous tissue and polymer. The 2 highest concentrations were similar and showed over 90% cartilage formation. A second paper by Ishaug-Riley and Mikos et al. looked at 2 different concentrations of neonatal rat calvarial osteoblasts – 11.1 x 10^5 and 22.1 x 10^5 per cm^2 of foam [204]. They found that, while initially lower with the lower seeding density, the cell number, activity and mineralisation results were comparable to those of the 22.1 x 10^5 per cm^2 of foam after 56 days in culture.

7.1.4.3 Characterisation of Cell Growth

There are a number of methods that can be used to characterise the growth of cells the most common being:

SEM, the cells are fixed using glutaraldehde then stained using osmium tetraoxide allowing cells on the surface of scaffolds to be observed.

DNA Assay, using fluorometric quantification. A fluorescent dye targeting cell DNA is measured on a fluoroescence spectrophotometer and the results compared with cell standard curves. This method was developed by West et al. [205]

Alkaline Phosphatase (ALPase) Assay, an enzyme often found in conjunction with antibodies. A dye, *p*-nitrophenyl phosphate, is deposited at the site of the bound-antibody following reaction with the enzyme [206]. The concentration of dye is monitored by light absorbance and the slope from a plot of absorbance versus time used to determine ALPase activity [204].

Confocal Microscopy / Fluorescent Dye, cells are dyed using a fluorescent dye, 2',7'-*bis*-(2-carboxyethyl)-5-(and-6-)carboxyfluorescein, acetoxymethyl ester (BCECF-AM)[3].

Histological Analysis, samples are dehydrated in increasing ethanol solutions, then saturation in xylene or Hemo-De (xylene was found to dissolve PLGA scaffolds [204]), paraffin saturated xylene / Hemo-De then molten paraffin. Sections of 5 μm thick blocks can be stained e.g. by hematoxylin and eosin for cells and tissue or von Kossa's silver nitrate for mineralisation.

MTT (3-[4,5-dimethylthiazol-2-yl]-2,5-diphenyltetrazolium bromide), the assay is based on the conversion of the tetrazolium salt by mitochondria, the organelle responsible for adenosine triphosphate (ATP) production. The assay measures absorbency using an ELISA(enzyme-linked immunosorbent assay) reader at 550 nm. Cell numbers are calculated from a standard curve based on their MTT absorbency [194].

7.2 Experimental

7.2.1 Materials and Instruments

7.2.1.1 Materials

Sodium phosphate, dibasic and sodium phosphate, monobasic were both obtained from Aldrich. Paraformaldehyde, glutaraldehyde and osmium tetraoxide, 2% solution were obtained from Agar Scientific Ltd. Eagle's MEM with Earle's salts, glutamax and $NaHCO_3$, fetal bovine serum, gentamycin sulphate and 10 x P.BS, pH 7.2 were kindly supplied by the Biologocal Sciences department, University of Durham, who purchased them from Gibco / BRL. Giemsa stain was obtained from Sigma Diagnostics. All materials were used as supplied unless otherwise stated in the text. Culture flasks and plates were obtained from Nunc.

7.2.1.2 Instruments

Cell suspensions were centrifuged using a Sigma / Philip Harris Scientific 3-15 centrifuge. Cells were counted using a haemocytometer. Cell numbers were monitored using a Nikon inverted transmission optical microscope. Pictures other than SEM were captured using a Zeiss Stemi SVII microscope with a Scott KL1500 electronic as the light source.

7.2.2 Experiments

7.2.2.1 General Information

Cell experiments used biopsies taken from human fibroblasts (from consenting adult patients). Explants used sections of tissue cut from newborn nude mice or

6½ / 8½ day old chicken embryos. The culture medium used throughout was comprised of 500 ml. of Eagle's MEM - containing Earle's salts, glutamax and $NaHCO_3$ - to which was added 50 ml of fetal bovine serum and 0.5 ml of gentamycin sulphate (an antibiotic). The presence of sodium carbonate in the medium regulated the pH at 7.2 when placed in a CO_2 atmosphere, such as an oven. Before any experimental work could begin, the fume-cupboard surfaces were sprayed with a 70 % ethanol solution and any materials placed into the fume-cupboard were also wiped, including hands. During the experiments it was important to ensure that no glassware made contact with any other glassware to avoid contamination.

7.2.2.2 Foam Disc Preparation

PolyHIPEs were made from 1 g PCL or PL and 4 g co-monomer / diluent using the foam preparation method described in sections 3.3.2.3 and 3.4.4. The emulsions were transferred to moulds of the style shown in Figure 7.3. These moulds were placed in the

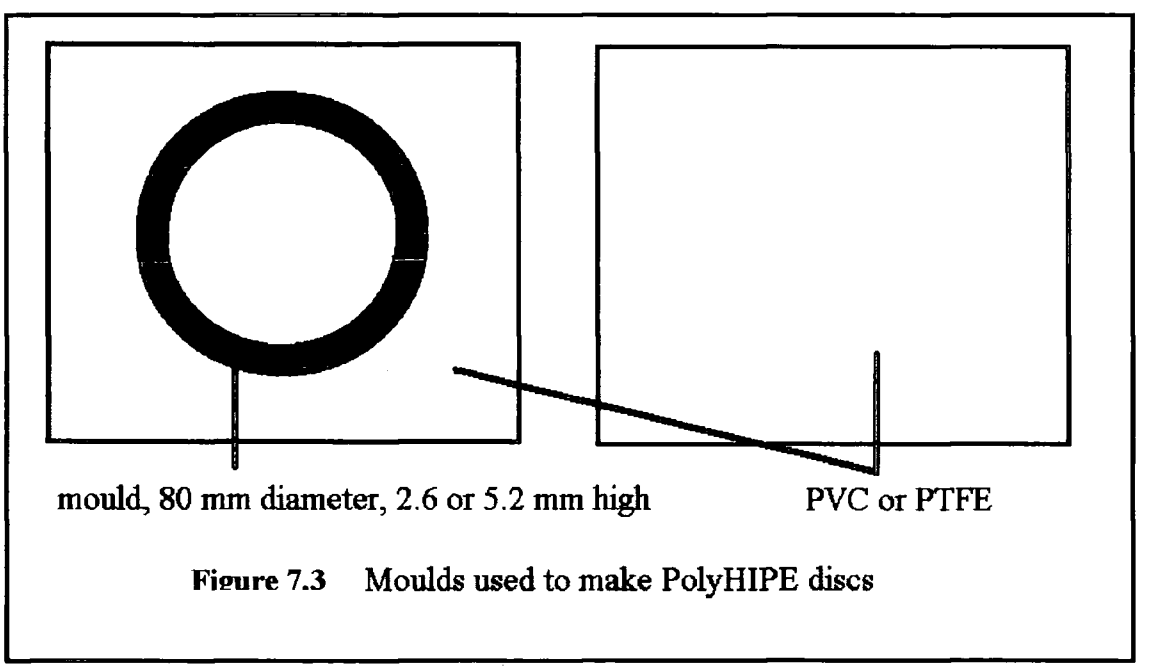

Figure 7.3 Moulds used to make PolyHIPE discs

oven at 60 °C for 48 h. after which they were washed in crystallising dishes for several days first in water then IPA. Discs of diameter 14 mm were punched using a cork borer then dried *in vacuo* for 48 h., or the foams were dried and then the discs punched – no difference was observed between these 2 methods. The foam discs were placed under UV light for 3 – 4 h. to sterilise them before being placed in culture dishes containing 4 wells - approximately 15 mm in diameter and 10 mm deep. Each disc then had a small glass ring placed on top of 13 mm diameter, sterilised first in 70 % ethanol then under UV light.

7.2.3.1 Cell Seeding and Tissue Growth

For both human and rat fibroblasts the same procedure was carried out. The cell numbers were expanded in a culture flask containing 8 – 9 ml of culture medium, which was changed every 2 - 3 days. The flasks were kept in an oven maintained at 37 °C and their cell numbers were monitored using an optical microscope. When the flask was 80 % full of cells, 95 % of the medium was discarded and the cells were washed briefly using 5 ml of phosphate buffer saline (P.BS) containing EDTA. This process was repeated twice more then a further 2 ml portion containing an enzyme, 0.25 % trypsin solution, was used to sever the contact between the cells and the flask surface. The cells were examined to see if they had rounded, indicating they had been severed, using the optical microscope and if necessary placed in an oven for 1 – 2 min. and then checked for a second time. 8 ml of fresh culture medium was added to quench the enzymatic reaction and then the medium containing the separated cells was transferred to a universal container. The cells were centrifuged at 1000 rpm for 5 minutes to form a "pellet". The

supernatant layer was poured off in one swift movement and the cells re-suspended in a specific quantity of medium, either 2 ml, 10 ml, or 12ml.

7.2.3.2 Rat Explant

A section of skin tissue approximately 1 cm^2 was removed from the mid-body area of a newborn female white Wistar rat. It was placed in a petri dish with a drop of culture media and spliced into very small pieces of approximately 1 mm^2. The tissue was then re-suspended in 2 ml of culture media and distributed evenly between 4 foam discs contained in culture dishes described in section 7.2.2.2. This method was used for both the PCL and PL foam discs.

7.2.3.3 Chicken Explant

A section of skin tissue approximately 1 cm^2 was removed from the body area of a 8½ day old chicken embryo for the PL foams and for the PCL foams an entire 6½ day old chicken embryo. The removed tissue / embryo was placed in a petri dish with a drop of culture medium and spliced into very small pieces of approximately 1 mm^2. The tissue was then treated as described in section 7.2.3.2.

7.2.3.4 Chicken Egg CAM (Chorioallantoic Membrane)

Chicken eggs were placed in an incubator at 37 °C for 8½ days and diagrams showing the change in the eggs after incubation are shown in Figure 7.4. The shell of each egg was scored using a small hacksaw blade to give the outline of a rectangle approximately 1.5 x 1cm^2. A pair of tweezers was used to carefully remove the outer shell and inner membrane. Then even more carefully a "square" of the chorioallantoic

membrane was also removed to reveal the developing chick. A small piece of the waste foam that had been discarded following the pressing of 1.5mm disks for experiments 1 and 2, was placed on top of the developing chick. Two pieces of cellotape were stuck perpendicular to each other across the "window" and the egg was placed back in the incubator. The experiment was repeated to give 2 eggs for the experiment. A third egg was discarded as the chick had not developed leaving an opaque yellow solid.

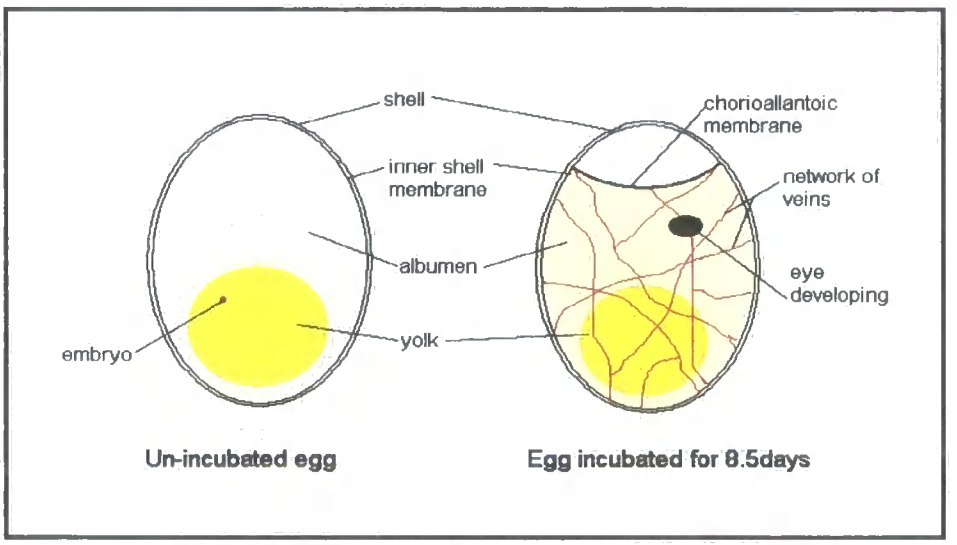

Figure 7.4 Diagram of Egg Before and After Incubation

7.2.3.5 Human Cells

The following experiment used the human skin cells described and prepared in section 7.2.3.1. The cells were re-suspended in 4 ml of culture medium using a pipette then distributed in 1 ml portions between 4 wells containing 0.2-H-S* foam discs. The wells were topped up with medium until they were ¾ full, then placed in an oven at 37 °C and left untouched for 2½ days.

* See Chapter 3, Experimental section for key

7.2.3.6 6 Day Experiment

Cells were allowed to grow on PCL and PL foam discs, 0.2-H-S* and 0.2-S† respectively for periods of 3 h, 3 days and 6 days. These experiments utilised the human skin cells as described and prepared in section 7.2.3.1. The cells were re-suspended in 2 ml of culture medium and their number estimated using a haemocytometer. Approximately 1 x 10^5 cells were added per well and 2 wells were set up for each foam type for a given time period. A set of 4 wells would therefore contain 2 PCL discs and 2 PL discs, all allocated for a specific length of time. Each set of wells was placed in an oven regulated at 37 °C and left untouched for the required length of time, before being prepared for either SEM or Giemsa staining, as described in the following 2 sections.

7.2.4 Preparation of Cells For SEM / Giemsa Stain

7.2.4.1 Preparation of Cells for SEM

The fixative was prepared as follows:

Paraformaldehyde (aq): 2 g. of paraformaldehyde was dissolved in 20 ml of distilled water by heating in a beaker with a magnetic stirrer to between 60 and 65 °C. After which 1 M sodium hydroxide solution was added dropwise until the solution became clear. **0.2M Buffer:** 19.5 ml of monobasic sodium phosphate solution was combined with 30.5 ml of dibasic sodium phosphate solution and made up to 100 ml with D.I. water. **Fixative:** 50 ml of sodium phosphate buffer, 10 ml of 25 % glutaraldehyde aqueous solution and the prepared paraformaldehyde were combined and D.I. water

* See Chapter 3, Experimental section for key
† See Chapter 4, Experimental section for key

added to give a 100 ml solution. The above quantities produced a fixative that would be 2 % paraformaldehyde and 2.5 % glutaraldehyde in 0.1 M buffer.

The culture medium was removed using a pipette and the samples were washed several times with P.BS. The fixative was poured over the foam and cells and left for 2 h. with occasional agitation. **Post Fixative:** The samples were washed several times with the remaining 0.2 M buffer solution to remove all the glutaraldehyde. The samples were then covered with 1 % buffered osmium tetraoxide (2 % osmium tetraoxide was diluted with an equal volume of 0.2 M buffer solution) for one h. **Sample dehydration:** The samples were placed in solutions of increasing alcohol content as follows, 15 % ethanol 3 x 5 minutes each, 35 % ethanol 3 x 5 minutes each, 60 % ethanol 3 x 5 minutes each, 80 % ethanol 3 x 5 minutes each, 100 % ethanol 3 x 10 minutes each. During each wash the samples were agitated to encourage the absorption of the liquid into the foams. **Critical point drying:** The samples were placed in a boat full of 100 % ethanol. The vessel was sealed and the chamber flooded with CO_2 until full. A valve at the base of the chamber was opened and the solvent expelled, until all was replaced by CO_2, at this point the chamber is pressurised to approximately 900 Psi. This is left for 2 h, after which there are 2 liquid levels, one near the boat, the other towards the top of the chamber. After 2 h. the level of the lower liquid is adjusted so that it is equal to the top of the boat and the vessel is heated under pressure to the critical point, 35 – 36 °C and 1100 Psi. This is achieved by circulating warm water around the chamber. At the critical point, the solvent meniscus vanishes. The water is switched off and the CO_2 expelled very slowly, i.e. no condensation should be visible at the exit valve.

7.2.4.2 Preparation of Cells for Giemsa Stain

In their wells with rings in place, the remainder of the foams and cells were washed several times with P.BS. Each well was filled with a 50/50 mix of P.BS and methanol, which was left for about 30 seconds then removed. This process was repeated then the wells were filled with 100 % methanol and left for 8 minutes. The foams were transferred to petri dishes and left to air dry for 30 minutes. The above process allowed the cells to be fixed in preparation for staining. After being replaced in their wells, sufficient Giemsa stain was added to cover the surface of the foam. The wells were then topped up with distilled water and again left for 8 minutes. A large container was filled with distilled water and the dishes and wells were completely submerged. This removed any oily residue from the surface. The foams were soaked in several changes of water for 1 – 2 h. periods to remove excess stain, following which they were transferred to a petri dish where they were left to air dry overnight. To capture images the stained foams and cells were covered in water then examined under an optical microscope fitted with a camera.

7.2.5 *In Vivo* Implants

The following procedure was carried out by Colin Jahoda, Department of Biological Sciences, University of Durham, UK.

The animals used were 2 littermate adult PVG rats. Each rat was anaesthetized with a combination of Hypnorm and Valium. The skin was wiped with alcohol and an incision of about 1.5 cm was made in the mid-flank region. Forceps were then inserted into the incision to separate the skin from the underlying muscle layer. While the incision

was held open with one pair of forceps, another pair then inserted a disc of material into the opening. The skin was then sutured. Two discs (either PL or PCL) were implanted into each animal, one on either side. At the end of the operation the animal was allowed to recover under observation in a warm environment. At the end of the experimental period animals were killed and the discs retrieved.

Once the discs were retrieved they were placed in culture medium and examined, images were captured.

7.3 Results and Discussion

The initial study to find out whether or not cells could survive on the PolyHIPE foams synthesised in Chapter 3, was carried out by the University of Durham's Biological Sciences Department. They were supplied with PolyHIPEs made from PCL and each of styrene, MMA and toluene, 0.2-H-S, 0.2-H-M and 0.2-H-T* respectively. Rat fibroblast cells were seeded onto the foams and left for one month during which time the culture medium was topped up every 2 – 3 days. Following fixing and staining, by the author, of the cells as outlined in section 7.2.4.1, SEM pictures were taken with little success. It is not known whether the cells had been left *in vitro* for too long, however 2 photographs, Figures 7.5 (a) and (b) have been included because they show cells that are 'happy' being on the PolyHIPE surface (a) and cells that are not (b). Specifically

* See Chapter 3 Experimental section for key

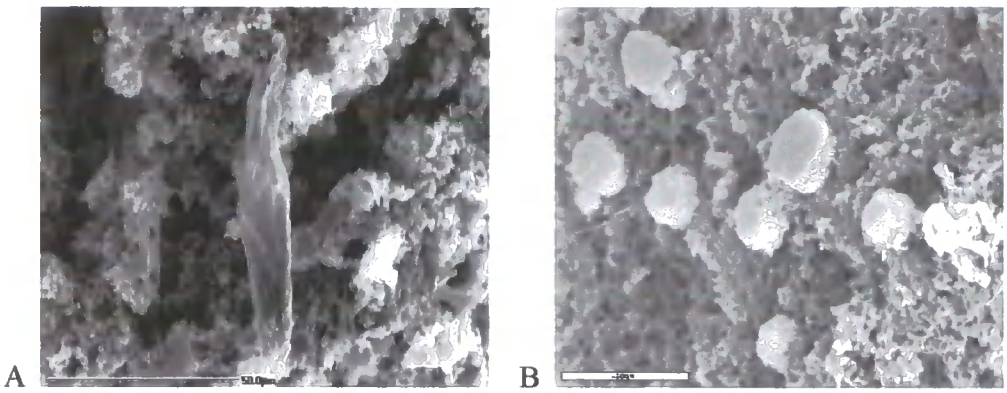

Figure 7.5 SEM Photographs (a) Cell on 0.2-H-S (50 μm scale bar), (b) cells on 0.2-H-M (50 μm scale bar)

with the MMA foams, where it was noted that the foam absorbed the medium very rapidly and this may have affected the growth and development of the cells. All subsequent work was carried out by the author and on foams made from 1 g polyester and 4 g styrene because the cells were seen to grow on the foams without the need for further work. The egg CAM work, reported in section 7.2.3.4 did not produce any photographs but the chick embryos carried on developing and there appeared to be no adverse immune response or any indication that the developing chicks had rejected the foam discs. Subsequent experiments used small foam discs stamped using a cork borer from a large disc of PolyHIPE - the method and moulds used were reported in section 7.2.2.2. The hydrophobic nature of the foams meant that when the wells were filled with the aqueous based culture medium the discs began to float to the surface. To prevent this they were weighed down by small glass rings cut from a 13 mm hollow glass tube (glass was chosen because it would be inert to the cells).

7.3.1 Cell and Explant Studies

7.3.1.1 Growth of Human Fibroblasts on 0.2-H-S

Human skin fibroblasts were transferred from a three quarter-full culture flask to the surface of four 0.2-H-S foams. They were left to grow in an oven at 37 °C for 2½ days and were then fixed. Two foams were then prepared for SEM and the other 2 were treated with Giemsa stain to be examined using an optical microscope. From the giemsa-stained images of the samples shown in Figure 7.6 (a) the pink areas are the foam surface and the cells are stained purple.

A 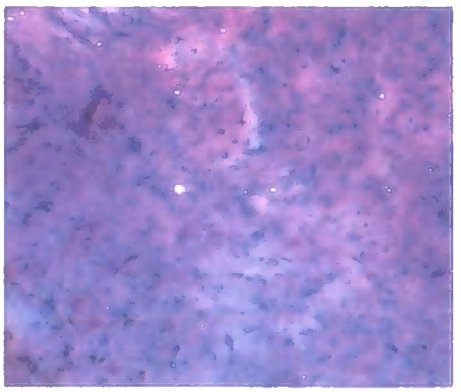 B 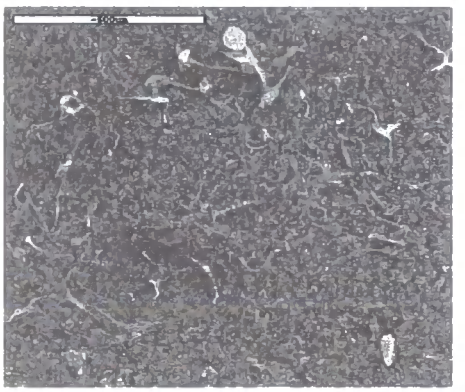

Figure 7.6 (a) Gimesa stained human fibroblasts on foam 0.2-H-S
(b) SEM Photograph equivalent to (a) (500 μm scale bar)

The photograph reveals there to be a good coverage of cells on the foam surface and that a proportion of these show a splayed and flattened morphology, demonstrating that the cells were proliferating and tissue growth was proceeding. Figure 7.6 (b) also shows surface coverage of the foam by skin fibroblats. Higher magnification SEM photographs show in more detail growth and interaction between the cells and matrix (Figure 7.7).

A 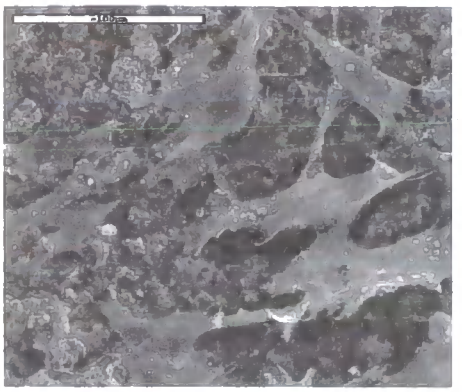 B 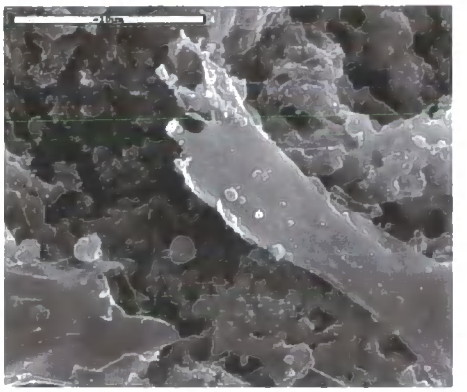

Figure 7.7 SEM Photographs of human fibroblasts, (a) (100 μm scale bar); (b) (10 μm scale bar)

The presence of ECM, proliferations, flattening out and contact between growing cells all indicate that the PCL-based PolyHIPE foams are capable of supporting the growth of human fibroblasts.

7.3.2 Chicken and Rat Explant Experiments

7.3.2.1 Chicken Explant

The chicken explant experiment involved placing 1 mm^2 pieces of tissue suspended in culture medium onto the foams and leaving them in an oven at 37 °C for 7 days. The explants took well to both types of material and this is shown in the photographs in Figure 7.8. For both the PL foam (Figure 7.8 (a)) and PCL foam (Figure 7.8 (d)) the giemsa staining shows outgrowth of many cells from the explants as blue / purple staining against the pink foam background, with the highest density of growth being closest to the explants. The SEM pictures also show the dense covering of cells over both of the foams, with slightly more of the PCL foam visible than the PL, Figures 7.8 (e) and (f) showing the PCL and Figures 7.8 (b) and (c) the PL.

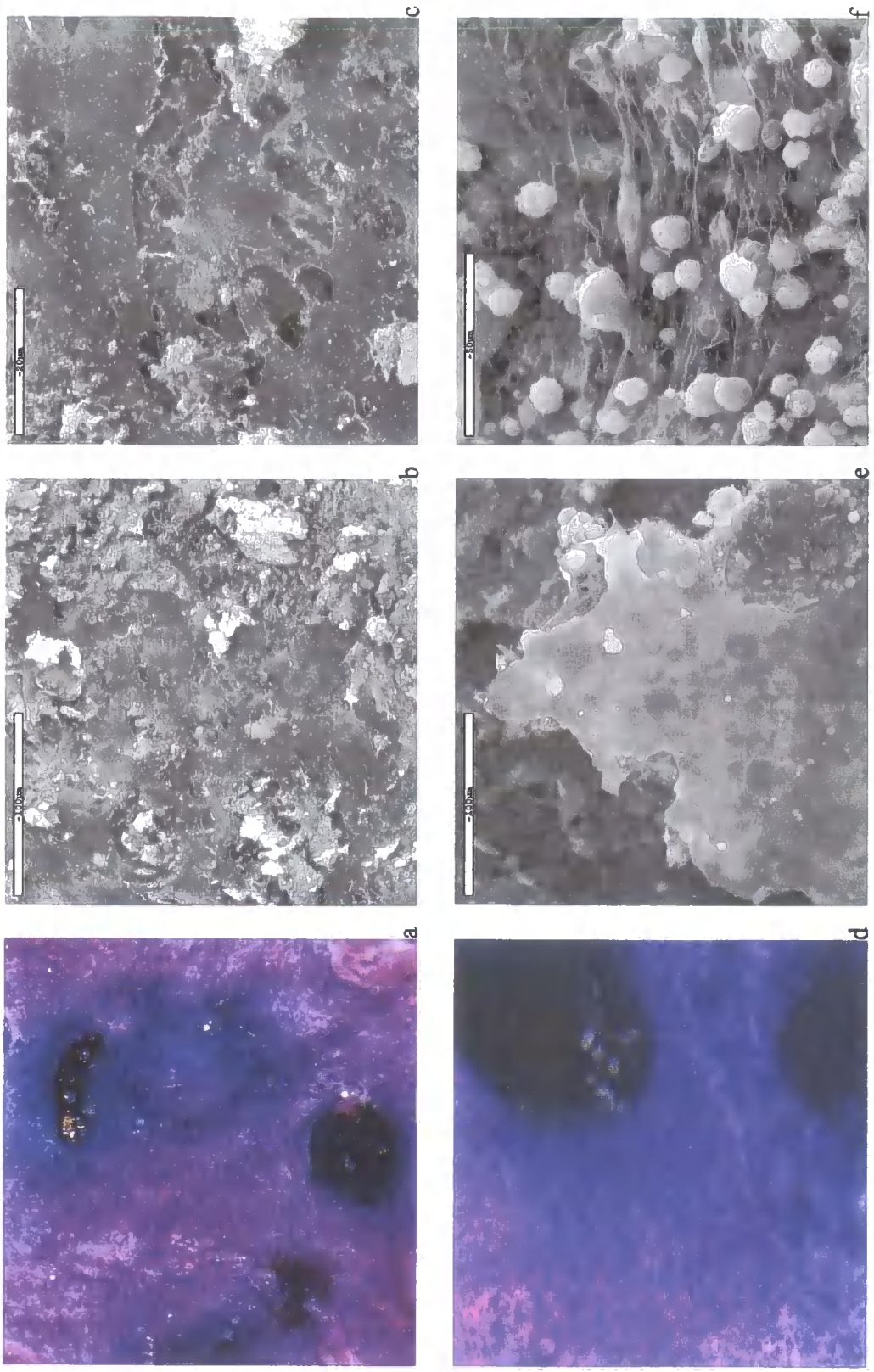

Figure 7.8 Chicken Explants
PL (a) giemsa x5 (b) SEM x500, (c) SEM x2000; PCL (d) giemsa x6, (e) SEM x500 (f) SEM x1000

Figure 7.8 (f) also displays the cells layering on top of one another, while most appear as balls there is one cell that is flattening out with proliferations at each end. Although not shown, it was observed that there were many different cell types including skin and nerve covering the foam surface.

7.3.2.2 Rat Explant

As for the chicken explants, the rat explant experiments involved placing 1 mm^2 pieces of tissue chopped from a 1 cm^2 piece of tissue from the body region of a newborn rat onto foam samples. The explant pieces were suspended in medium and dropped on to the foam surface then placed in an oven at 37 °C for 5 days. Photographs of the resulting foams are shown in Figure 7.9 (a) – (f). The giemsa-stained cells and PL foam, Figure 7.9 (a), show once again the the outgrowth of blue / purple stained cells against the pink stained foam. The SEM pictures, Figure 7.9 (b) and (c), show clumps of newly developing cells and in Figure 7.9 (b) in the bottom left corner - a group of a different cell type, probably muscle. With the PCL foams, the SEM pictures in Figure 7.9 (d), (e) and (f) show that there are no or very few visible cells; the growing explant is visible by the wave of extracellular material deposited by the developing tissue.

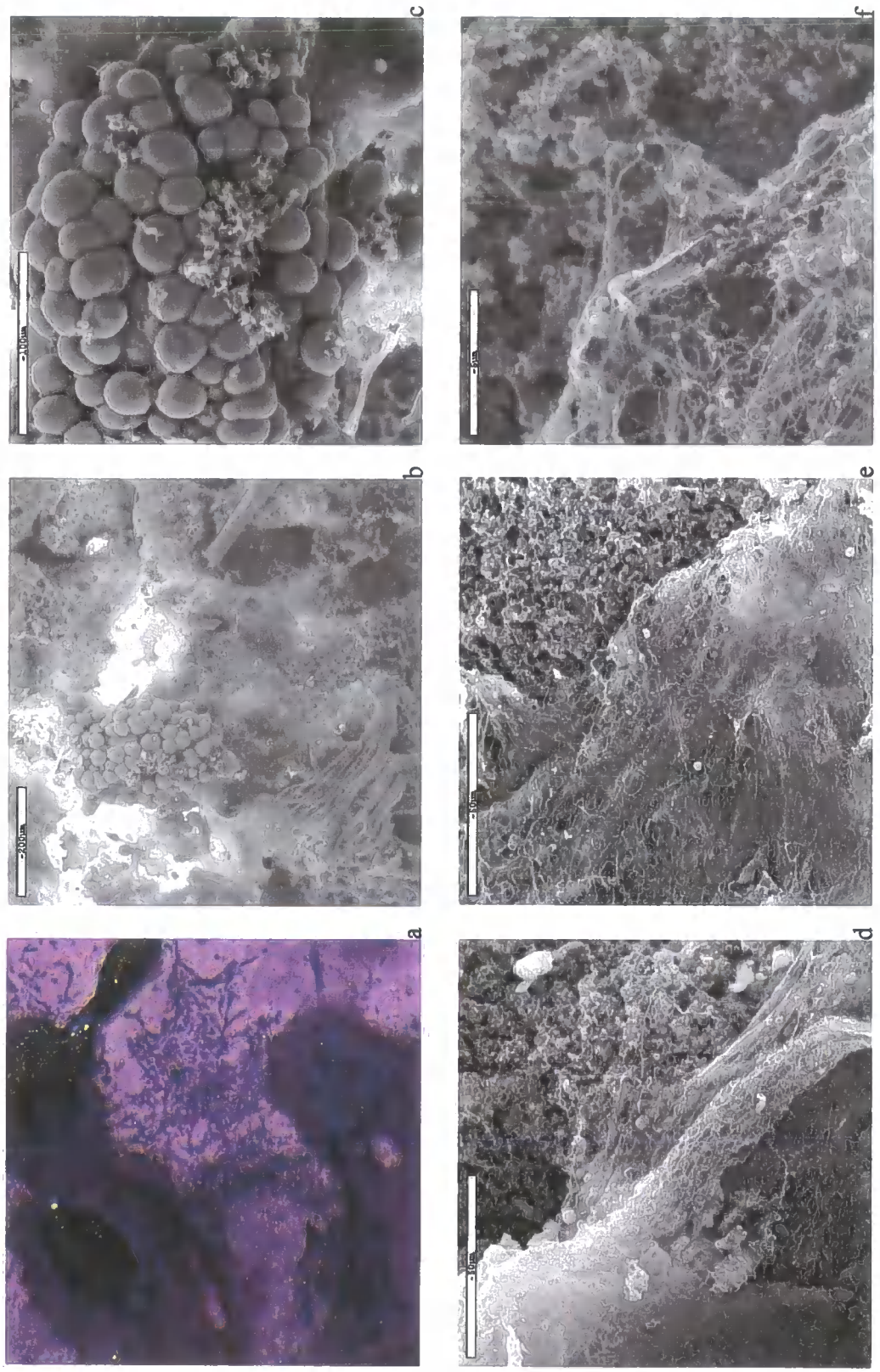

Figure 7.9 Rat Explants
PL (a) giemsa x5 (b) SEM x150, (c) SEM x500; PCL (d) SEM x1000, (e) SEM x1000 (f) SEM x8000

7.3.3 Study of Cell Attachment and Growth over 6 Days

Flask-cultivated human skin fibroblasts were seeded onto both PCL and PL foams in order to study the way in which the cells attached and changed over approximately a one-week interval. The time intervals chosen were 3 h. (this was deemed sufficient time for the majority of cells to have adhered to the surface of the foams), 3 days and 6 days. For each time interval there were 4 foams, 2 PCL and 2 PL, one of each was stained using giemsa and the remaining were fixed and stained for SEM.

The results of the PCL foams are shown in Figure 7.10. From the giemsa picture Figure 7.10 (a) it can be seen that there are a large number of dots on the foam's blue surface, showing that a large number of cells have adhered. In Figure 7.10 (b) the cells can be seen to be flattening out and by 6 days, Figure 7.10 (c), the cells are covering a good deal of the foam surface. In the SEM photographs at 3 h., Figure 7.10 (d) it was difficult to distinguish any cells, however, the top right hand corner of the photograph shows what would appear to be a flat sheet, inconsistent with the porous structure of a PolyHIPE. We believe this is likely to be cells that have flattened out. By 3 days, the evidence of cell growth on the foams surface is indisputable. Figure 7.10 (e) shows cells still curled up and a region of flattened cells with proliferations stretching to other groups of cells and to the foams surface. Figure 7.10 (f) shows that the growth of the cells continued to form a layer covering the scaffolds surface.

In comparison, with the PL foams, shown in Figure 7.11, the giemsa-stained sample after 3 h. (Figure 7.11 (a)) shows the attachment of fewer cells than the corresponding PCL sample (Figure 7.10 (a)). However, it was noted throughout the experiment that the PL foams, being of a less hydrophobic nature, rapidly absorbed

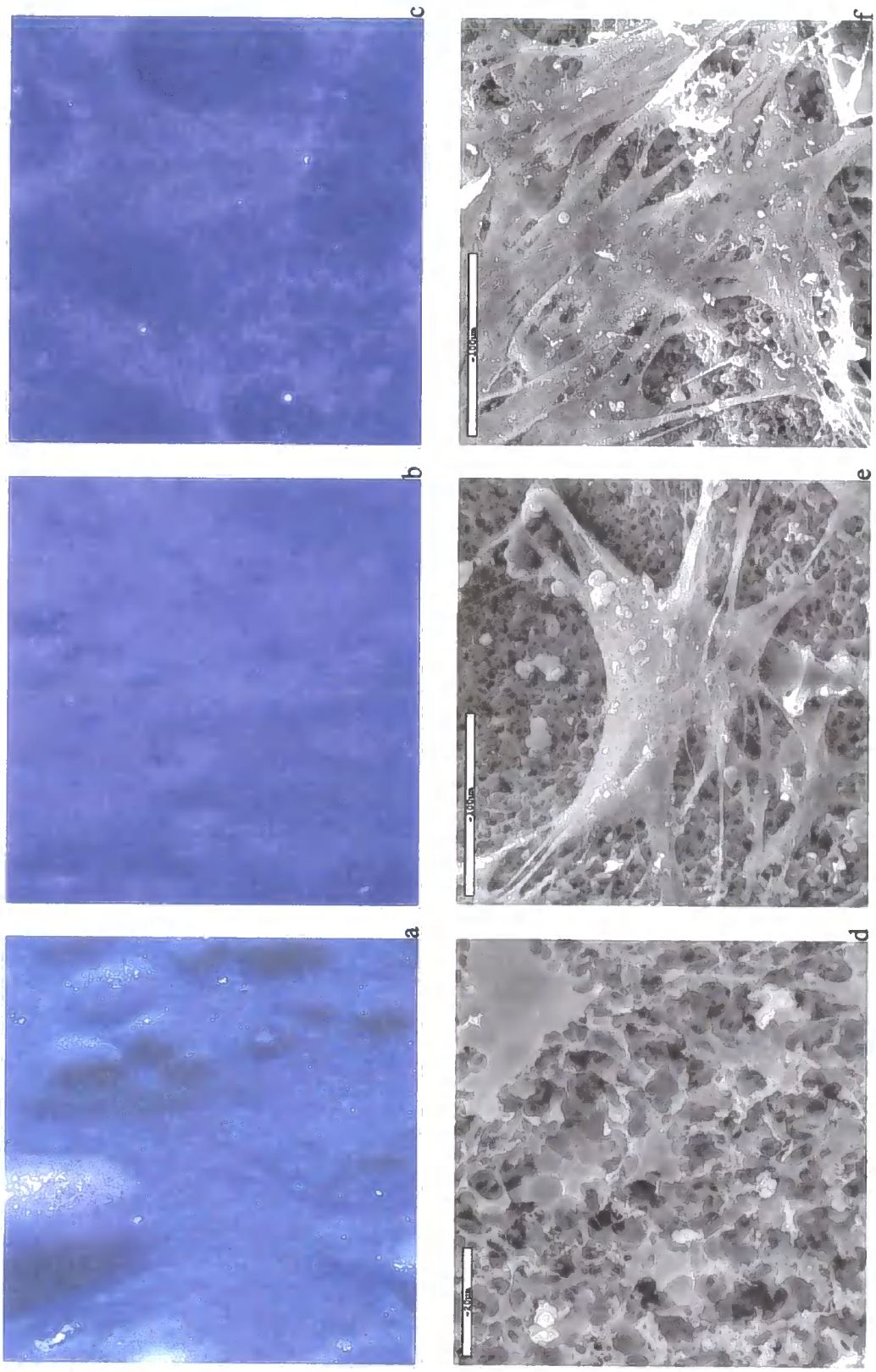

Figure 7.10 PCL cells after 3 h (a+d), 3 days (b+e), 6 days (c+f) giemsa (a) x5 (b) x6, (c) x6; SEM (d) x1500, (e) x500 (f) x500

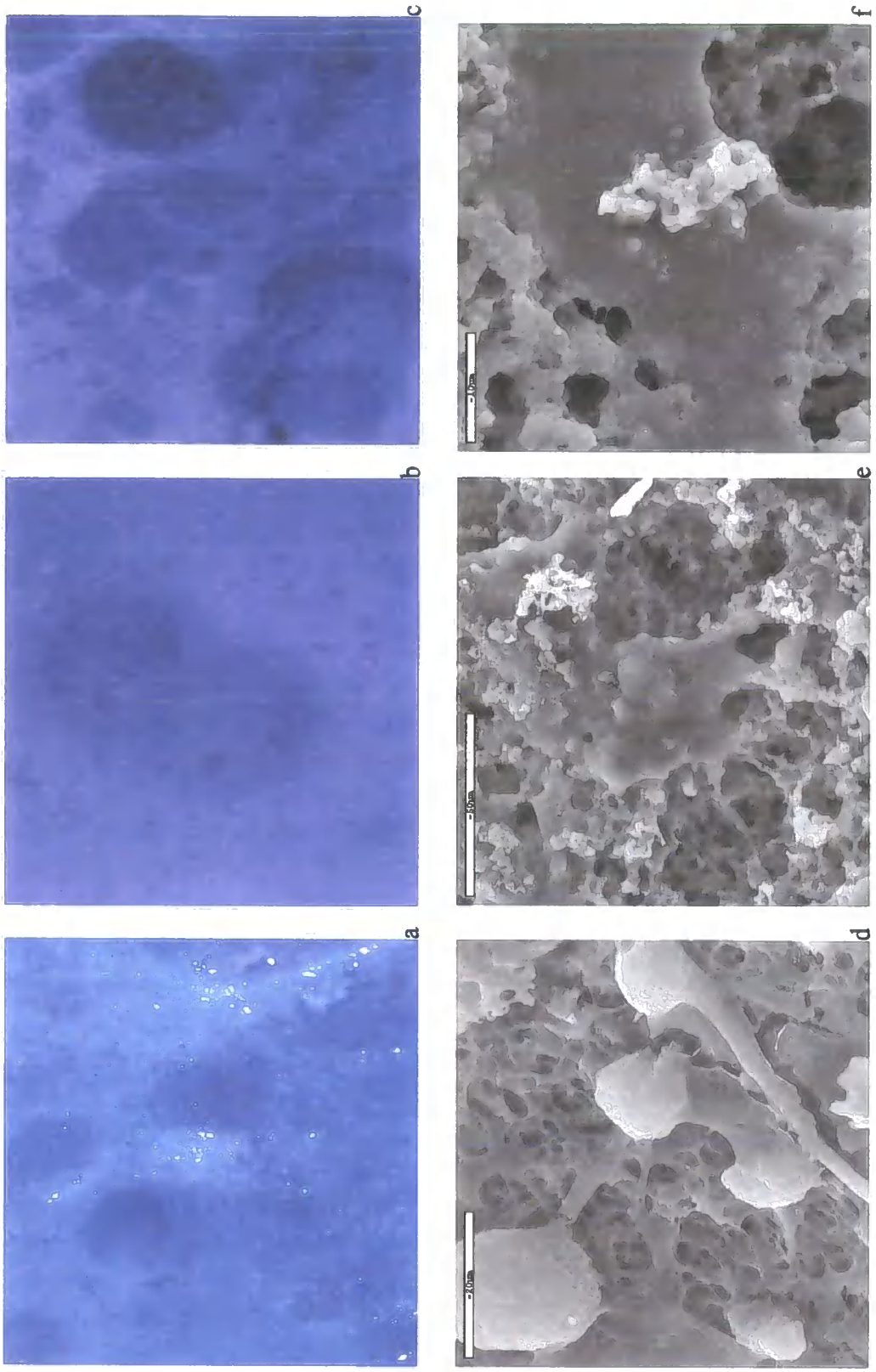

Figure 7.11 PL cells after 3 h (a+d), 3 days (b+e), 6 days (c+f) giemsa (a) x6 (b) x6, (c) x6; SEM (d) x2000, (e) x1000 (f) x3000

any medium into their pores, leaving the surface dryer and less favourable for cell growth.

The cells stained and photographed in Figure 7.11 (b) do not show the classic single cell flattened structure. Although by 6 days, Figure 7.11 (c), much of the surface had become covered by cells (blue stain). Figure 7.11 (d) shows cells in several stages of growth: curled up - top left; flattening out – towards the middle; elongated and stretched out – to the right of the previous; and along the left hand side a cell that has flattened. Figure 7.11 (e) reflects the results seen in Figure 7.11 (b), that the cells are not flattening out then forming tissues, as seen with the PCL material in Figures 7.10 (e) and (f), but are flattening out as a continuous sheet of cells. The middle left of picture 7.11 (f) shows two proliferations connecting different cells. Possible reasons for this unusual cell development could be the cells response to the polylactide used in the scaffold and/or as was described previously in this chapter that the PL-scaffolds absorbed medium more rapidly, leaving a dry surface and this could well have affected the way in which the cells developed.

7.3.4 *In Vivo* Chicken CAM and Rat Implants

7.3.4.1 Chicken CAM

A small fragment of PCL / styrene scaffold was placed against the chorioallantoic membrane in the egg of a developing chicken embryo, see Figure 7.4 (experimental section). Visual observation after one week revealed that the developing chicken had not rejected the implant and continued to develop. The surrounding of the implant by the developing chicken made it impossible to extract or photograph the results.

7.3.4.2 PCL Rat Implants

Having established that the PCL- and PL-scaffold materials were capable of supporting and sustaining cell growth, it seemed a logical step to find out how the material would behave and affect a living animal. With the cooperation of the staff of the Biological Sciences Department of the University of Durham, operations were carried out to place the implants in 2 rats, one rat having 2 PCL implants and with the other 2 PL implants. They also removed the discs, which were then examined by the author. The experiment was carried out over a period of 10 weeks to allow comparison of the discs with the *in vitro* biodegradation experiment (results are shown in section 7.3.4.4). The first important result obtained was that the rats remained alive and healthy for the duration of the experiment, so the scaffolds were not toxic to the rats.

Figure 7.12 show photographs, taken using a zoom camera, of the area in which the implant was made, Figure 7.12 (a). The implant is visible under the skin where the fur is only beginning to grow back and for the remainder of the region where the animal was shaved in preparation for the operation the fur has failed to grow back. This was the same for the implants on both sides of the rat. It is however unlikely that the bald area is in response to the material and more likely a result of the stage at which the hair follicle growth was in its cycle. There was also no evidence of inflammation such as swelling, which would show that the implants had been rejected. Figures 7.12 (b) and (c) reveal both implants. It is evident from the pictures that over the 10 weeks there has been no immunological response to the material - the engulfing of the material in a white "cloud" as the bodies immune system attempted to surround and destroy the foreign material would have indicated this.

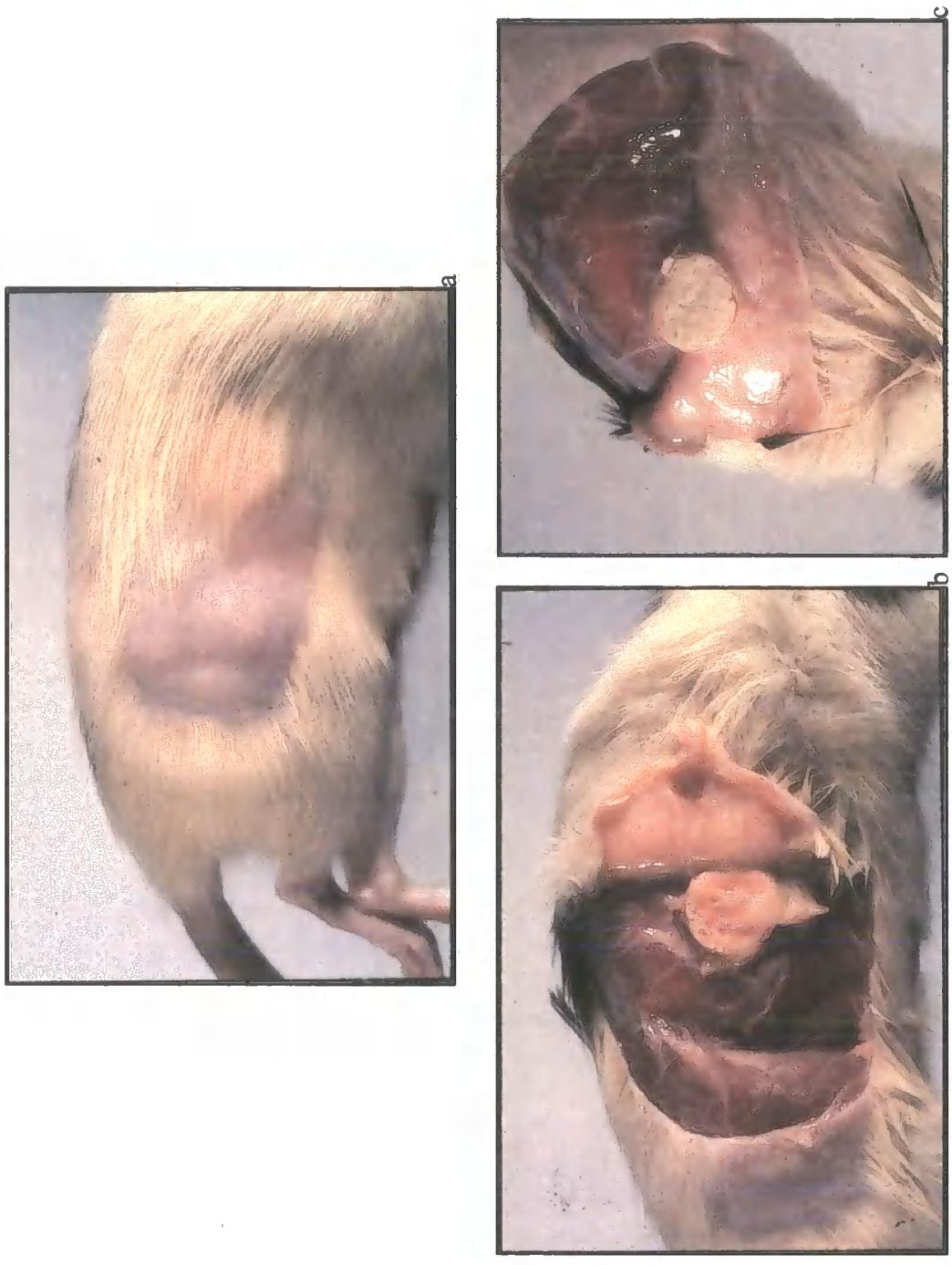

Figure 7.12 *In vivo* PCL rat implant photographs (a) Area of implant (b) left side implant (c) right side implant

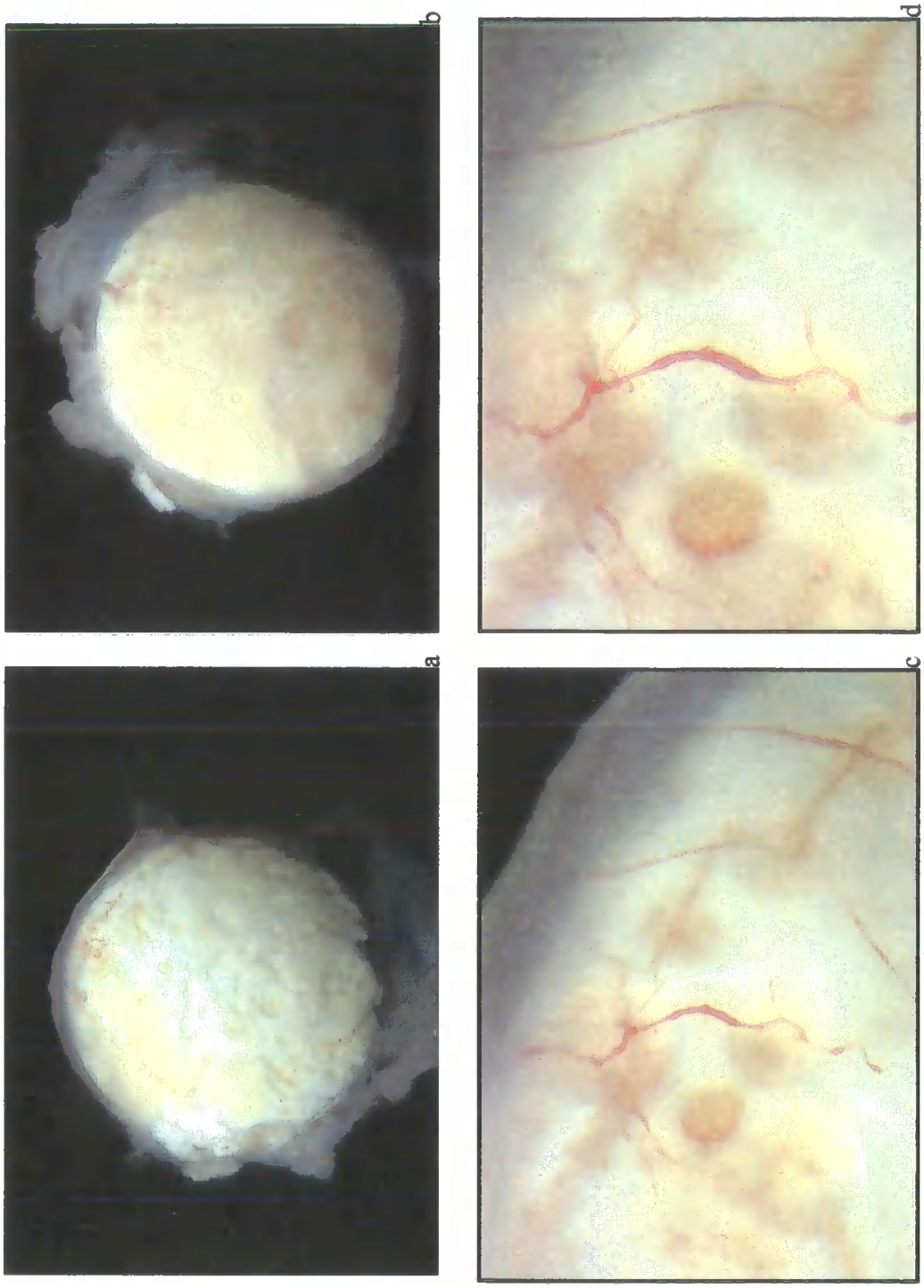

Figure 7.13 *In vivo* PCL rat implant (a) x0.6 (b) x0.6, (c) x4 (d) x6

The implants were then removed to allow closer examination. Figures 7.13 (a) and (b) show a complete view of both sides of one implant. The pictures show that the scaffold has been completely surrounded by cells and closer examination of the implants, Figures 7.13 (c) and (d) reveal the growth of blood vessels on the surface of the foams and in to the pores of the scaffold; this would indicate that cells have also penetrated into the scaffold.

7.3.4.3 PL Implants

In the case of the PL implants, the site at which the implant was placed has completely healed and the implant is not visible but could be detected physically, Figure 7.14 (a). As for the PCL material, there was no evidence of an inflammatory response - swelling about the wound site or infection. Photographs of the revealed implants, Figures 7.14 (b) and (c) also showed no immunological response.

Removal of the implants and closer examination, as with the PCL scaffolds, show even more clearly the growth of blood vessels into the pores of the scaffold, Figures 7.15 (c) and (d). Again this gives a good indication that cells are growing into as well as on the surface of the material.

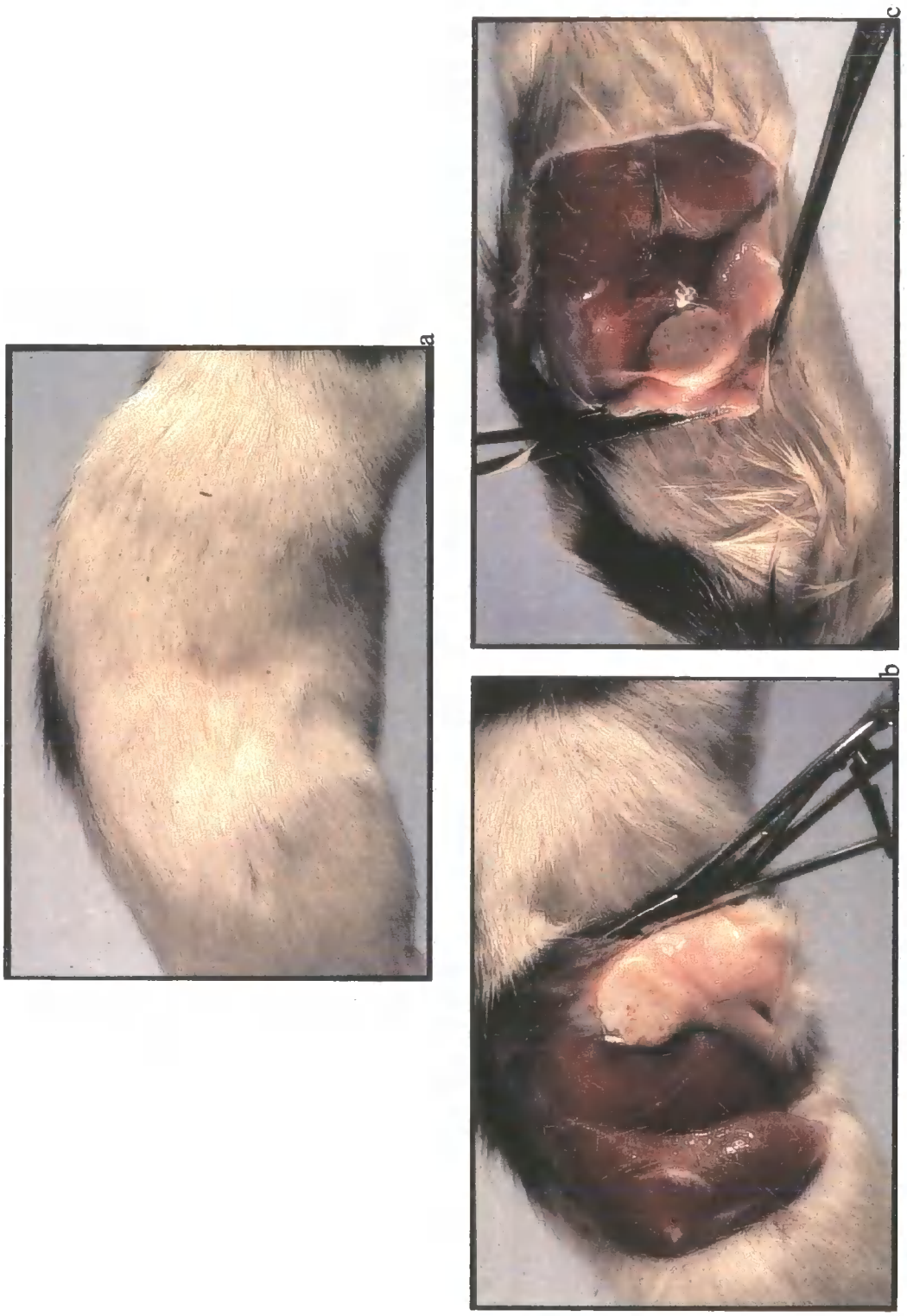

Figure 7.14 *In vivo* PL rat implant photographs (a) area of implant (b) left side implant (c) right side implant

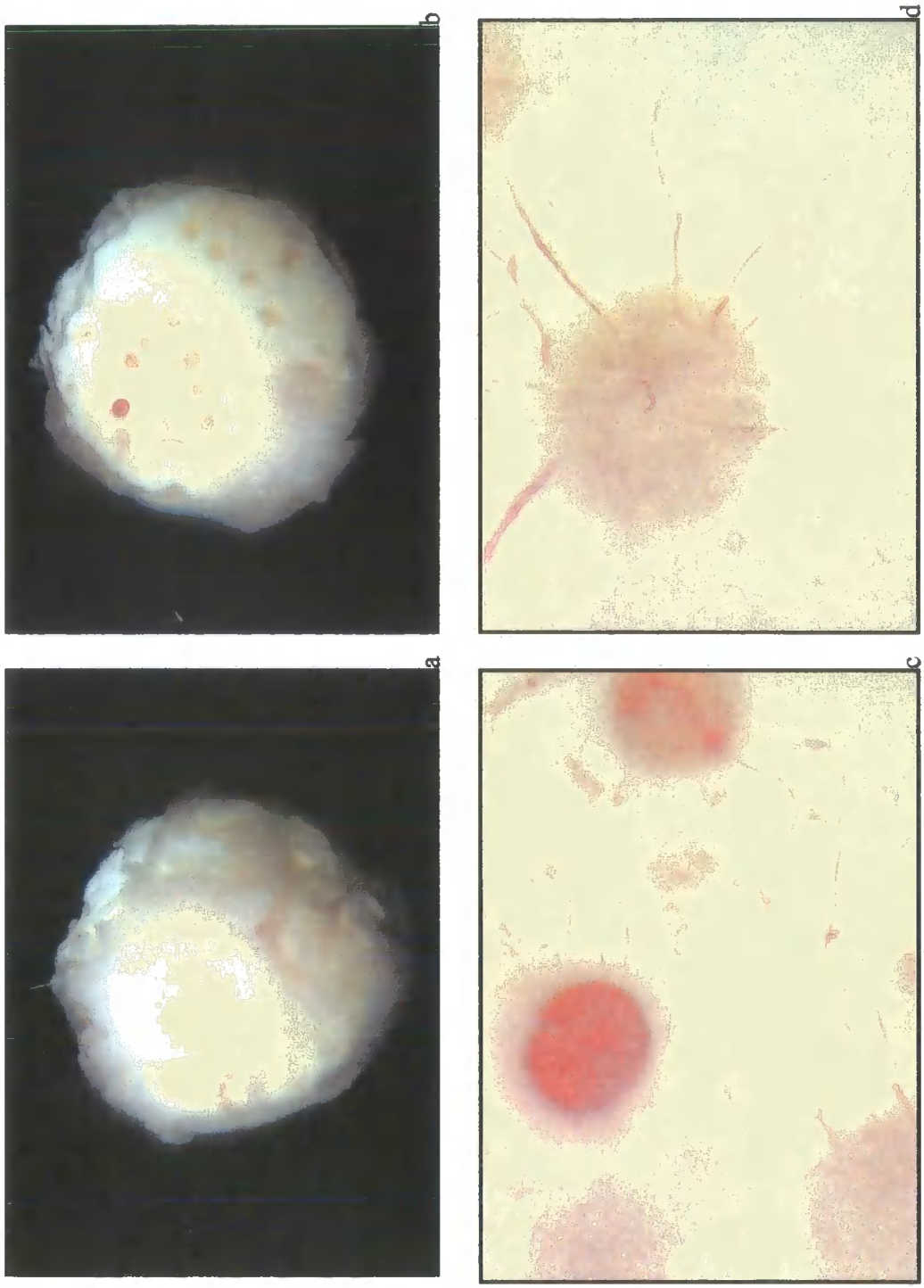

Figure 7.15 *In vivo* PL rat implant
(a) x0.6 (b) x0.6, (c) x4 (d) x6

7.3.4.4 *In Vivo* Degradation of the Implants

Placing the implants into the rats also allowed observation of whether and by how much the scaffolds degraded visibly over the 10 week duration of the experiment. Photographs of the removed implants are shown in Figure 7.16.

A 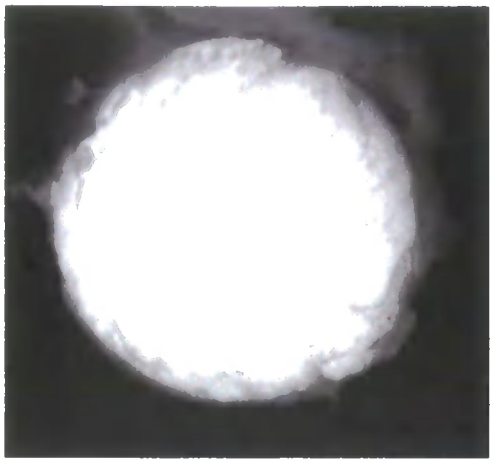 B 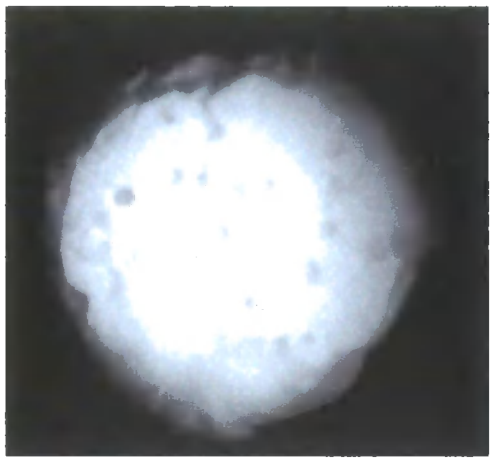

Figure 7.16 (a) PCL implant x0.6 (b) PL implant x0.6

When looking at the photographs it would appear that the PL foam, Figure 4.16 (b) has shown signs of degradation at the edges of the disc. This was more apparent on visual observation than in the photograph. As was seen in the *in vitro* study, chapter 5, the PCL foam showed very little evidence of degradation over the 10 weeks. It is difficult to say whether there has been an increase in degradation with enzymatic degradation as well as hydrolytic that the *in vivo* study adds. Figure 5.12 for the PL and Figure 5.14 for the PCL are the equivalent foams in the *in vitro* study and would indicate that the edges of the foams from the *in vivo* study appear to have shown greater degradation. However, the surfaces of the foams in the *in vitro* study showed signs of degradation while the 2 foams in the *in vivo* study have not changed.

7.4 Conclusions

The above study shows that both PCL-styrene and PL-styrene PolyHIPEs are capable of supporting the growth and proliferation of a number of different cell types. There would appear to be differences in the way cells respond to the 2 materials, this response, however, requires further investigation. The *in vivo* study revealed that the scaffolds do not provoke an immune response and that blood vessels and cells were able to penetrate the scaffolds pores. There appeared to be little degradation during the 10 week study so it is not known if the scaffold material would prove toxic or provoke an inflammatory response as the cross-linked network was broken down.

191 N. P. O. Green, G. W. Stout and D. J. Taylor, *Biological Sciences 1 & 2 2nd Edition,* R. Soper (ed), Cambridge University Press, 188 (1991)

192 N. P. O. Green, G. W. Stout and D. J. Taylor, *Biological Sciences 1 & 2 2nd Edition,* R. Soper (ed), Cambridge University Press, 185 (1991)

193 N. P. O. Green, G. W. Stout and D. J. Taylor, *Biological Sciences 1 & 2 2nd Edition,* R. Soper (ed), Cambridge University Press 237 (1991)

194 G. Zund, Q. Ye, S. P. Hoerstrup, A. Schoeberlein, A. C. Schmid, J. Grunenfelder, P. Vogt and M. Turina, *Eur. J. Cardio-thorac. Surg.* **15**, 524 (1999)

195 J. S. Roman, A. Gallardo, C. Elvira, B. Vazquez, A. Lopez-Bravo, J. A. de Pedro and D. Tomas, *Macromol. Symp.* **168**, 89 (2001)

196 Z. Gugala and S. Gogoewski, *J. Biomed. Mat. Res.* **49(2)**, 191 (2000)

197 T. Groth and G. Altankov, *PIMS 2000 9th International Conference on Polymers in Medicine and Surgery*, 213 (2000)

198 R. L. Julian and S. Haskill, J. Cell Biology 120, 585 (1993); K. Webb, V. Hlady, P. A. Tresco, *J. Biomed. Mat. Res.* **41**, 430 (1998)

199 P. B. van Wachem, T. Begling, J. Feijen, J. P. Detmers and W. G. van Aken, *Biomaterials* **6**, 408 (1985); T. G. Ruardy, H. E. Moorlag, J. M. Schakenraad, H. C. Van der Mei, H. J. Busscher, A. Underwood, H. Elwing and H. B. Lee, *Cells and Materials* **7**, 133 (1997)

200 F. Fey-Lamprecht, T. H. Groth, W. Albrecht, D. Paul, M. Fromm and A. H. Gitter, *J. Mat. Sci.- Mat. Med.* **9**, 715 (1998); F. Fey-Lamprecht, T. H. Groth, W. Albrecht, D. Paul and U. Gross, *Biomaterials* **21(2)**, 192 (2000)

201 M. Sittinger, J. Bujia, N. Rotter, D. Reitual, W. W. Minuth and G. R. Burmester, *Biomaterials* **17**, 242 (1996)

202 R. I. Freshney, *Animal Cell Culture: a practical approach, 2nd edt.* Oxford IRL Press 11 (1992)

203 W. C. Puelacher, S. W. Kim, J. P. Vacanti, B. Scloo, D. Mooney and C. A. Vacanti, *Int. J. Oral. Maxillofac. Surg.* **23**, 53 (1994)

204 S. L. Ishaug-Riley, G. M. Crane-Kruger, M. J. Yaszemski and A. G. Mikos, *Biomaterials* **19**, 1412 (1998)

205 D. C. West, A. Sattar and S. Kumar, *Anal. Biochem.* **147**, 295 (1985)

[206] P. M. B. Walker (ed), *Chambers Science and Technology Dictionary*, W & R Chambers Ltd and Cambridge University Press, p. 23 (1988)

Conclusions and Future Work

Chapter 8

8 CONCLUSIONS AND FUTURE WORK

8.1 Conclusions

In Chapter 2, section 2.4 a series of aims was set out as the ultimate goals of the project. This thesis has managed to meet most of those aims and therefore, set the project well on its way.

I Both polycaprolactone and polylactide have been utilised to produce PolyHIPE foams.

II The polymers were cross-linked with styrene and MMA producing a range of materials with different physical properties. Also toluene was used as a diluent to give PolyHIPEs containing mostly polyester.

III An initial study has shown that the PCL- and PL-styrene based PolyHIPEs are at least partially biodegradable; the process will take more than 3 months because of the cross-linked nature of the scaffolds. However, due to the high polystyrene content, these materials are unlikely to degrade completely.

IV The PCL- and PL-styrene PolyHIPEs have been shown to support the proliferation of a number of cell and tissue types: human skin fibroblasts; rat skin tissue; chicken tissue. The scaffolds were shown to be nontoxic and produced no inflammatory response during *in vivo* studies in rats over 10 weeks.

V From the work done to date there appears to be an upper pore size limit of around 10 μm, this may limit the applications for which the PolyHIPEs can be used as scaffolds.

8.2 Future Work

8.2.1 Future Work on the PolyHIPEs

From the work done to date it would appear that the pore size of the PolyHIPE materials made in this project is limited to a maximum of 5 μm when using potassium persulphate as the initiator and 10 μm if the initiator is AIBN. However, the work done in this project only looked at the PCL- and PL-styrene foam compositions 0.2-H-S and 0.2-S respectively. There was no work done on the PolyHIPEs were the comonomer was MMA or toluene was used as a diluent. It is also possible that the lower molecular weight PCL will produce foams with different void sizes.

It is also possible that, by applying different drying techniques e.g. freeze drying foams or drying under vacuum at lower temperatures, the collapse of the polyester only PolyHIPEs could be avoided. It would be expected that these scaffolds would be almost entirely degradable and therefore, more suitable for use in people.

A more flexible PolyHIPE can also be produced by replacing some or all of the cross-linker with 2-ethylhexyl acrylate.

8.2.2 Biodegradation

Work done in this thesis showed that the PolyHIPEs had not degraded to any degree within 10 weeks. A more extensive study would need to take in to account the possibility that the material may take many months to degrade.

8.2.3 Further Work on Cell Studies

There are numerous ways in which the PolyHIPEs can be improved to function more effectively as scaffolds; a few of these are,

- Pre-soaking of the foams in solutions of increasing alcohol content, followed by solutions of reduced alcohol and increased medium concentration. Providing a material saturated in culture medium would aid the supply of nutrients to the developing cells.
- Coating of the surface of the scaffolds with proteins to encourage adhesion of the cells.
- Attachment of growth factors to promote growth of specific cells.
- Use of a gentle vacuum or syringe and needle to place cells at the centre of the scaffold allowing cells to grow outwards rather than inwards.

There are also a number of techniques that can be used to study how far into the scaffold cells are penetrating, involving staining, embedding in PMMA then sectioning and techniques such as the MTT test to count the extent by which the cells have proliferated. These methods were discussed in the introduction section of chapter 7.

Last but not least this thesis has only looked at 1 human cell type, skin fibroblasts, the human body is composed of many different types of cells, in the most part trial and error would be needed to see if PolyHIPEs would be a suitable scaffold for a particular cell type.

References

REFERENCES

1 L. G. Cima, J. P. Vacanti, C. Vacanti, D. Ingber, D. Mooney and R. Langer, *J. Biochem. Eng.* **113**, 143 (1991)

2 D. J. Mooney and A. G. Mikos, *Scientific American.* **April**, 38 (1999)

3 D. Mooney et al, *Nature Biotechnology* **17**, 551 (1999)

4 V. Bisceglie, *Ztschr. Krebsforsch* **40**, 140 (1933)

5 J. P. Vacanti and C. A. Vacanti, *Principles of Tissue Engineering*, 2nd Edn. Academic press ISBN 0124366309, ch. 1

6 J. P. Vacanti, *Arch. Surg.* **123**, 545 (1988)

7 P. S. Russell, *Ann. Surg.* **201**, 262 (1985)

8 S. Gogolewski and A.J. Penning, *Makromol. Chem., Rapid Commun.* **4**, 680 (1983)

9 A. A. Demetriou, S. M. Levenson, P. M. Novikoff, A. B. Novikoff, R. Chowdhury, N. Whiting Jr, A. Reisner and R. Chowdhury Jr, *Proc. Nat. Acad. Sci. USA* **83**, 7479 (1986)

10 J. P. Vacanti, M. A. Morse, W. M. Saltzman, A. J. Domb, A. Perez-Atayde and R. Langer, *J. Pediatric Surg.* **23**, 3 (1988)

11 H. Elma, J. H. deGroot, A. J. Nijenhius, A. J. Penrings, R. P. H. Veth, *Colloid Polym. Sci.* **268 (12)**, 1088 (1990)

12 L. G. Cima, J. P. Vacanti, C. Vacanti, D. Ingber, D. Mooney and R. Langer, *J. Biochem. Eng.* **113**, 143 (1991)

13 R. S. Langer and J. P. Vacanti, *Scientific American* **April** 64 and 65 (1999)

14 C. A. Vacanti, R. Langer, B. Schloo and J. P. Vacanti, *Plast. Reconstr. Surg.* **88**, 753 (1991)

15 R. Langer and J. P. Vacanti, *Science* **260**, 920 (1993)

16 R. Madison, *Exp. Neurol.* **88**, 767 (1985); R. F. Valentini, T. G. Vargo, J. A. Gardella and P. Aebischer Jr., *Biomaterials* **13**, 183 (1992); A.S. Chang and I.V. Yannas in *Neuroscience Year*, B. Smith and G. Adelman (ed), Birkhauser: Boston, p. 126 (1992)

References

17 H. Kobayashi, Y. Ikada, T. Moritera, Y. Ogura and Y. Honda, *J. Appl. Biomater.* **2**, 261 (1991); V. Trinkaus-Randall et al., *Invest. Opthalmol. Vis. Sci.* **29**, 393 (1988); K. P. Thompson et al., *Refractive Corneal Surg.* **7**, 240 (1991); R. Sipehia, A. Garfinkle, W. B. Jackson and T. M. S. Chang, *Biomater. Artif. Cells Artif. Organs* **18**, 643 (1990)

18 J. F. Hansbrough et al., *Surgery* **111**, 438 (1992)

19 M. L. Yarmush, J. C. Y. Dunn and R.G. Tompkins, *Cell Transplant.* **1**, 323 (1992)

20 S. J. Sullivan et al., *Science* **252**, 718 (1991)

21 A. Atala et al., *ibid.* **148**, 658 (1992)

22 M. F. Grower, E. A. Russell Jr. and D. E. Cutright, *Biomater. Artif. Cells Artif. Organs* **17**, 291 (1989)

23 K. R. Stone, W. G. Rodkey, R. J. Webber, L. McKinney and J. R. Steadman, *Clin. Orthop. Relat. Res.* **252**, 129 (1990)

24 L. Freed et al., *J. Biomed. Mater. Res.* **27**, 11 (1993)

25 J. Goshima et al., *Clin. Orthop. Relat. Res.* **269**, 274 (1991); S.E. Haynesworth et al., *Bone* **13**, 81 (1992)

26 B. E. Jarrell and S. K. Williams, *J. Vasc. Surg.* **13**, 733 (1991); J. M. Wilson et al., *Science* **244**, 1344 (1989)

27 L. E. Freed, J. C. Marquis, A. Nohria, J. Emmanual, A. G. Mikos and R. Langer, *J. Biomed. Mat. Res.* **27**, 11 (1993)

28 A. G. Mikos, G. Sarakinos, S. M. Leite, J. P. Vacanti and R. Langer, *Biomaterials* **14 (5)**, 330 (1993)

29 A. G. Mikos, M. D. Lynman, L. E. Freed and R. Langer, *Biomaterials* **15 (1)**, 55 (1994)

30 S. J. Peter, M. J. Miller, A. W.Yasko, M. J. Yaszemzki and A. G. Mikos, *J. of Biomed. Mat. Res.* **43(4)**, 427 (1998)

31 S. L. Ishaug – Riley, G. M. Crane, A. Gurlek, M. J. Miller, A. W. Yasko, *J. Biomed. Mat. Res.* **36**, 8 (1997)

32 K. Whang, C. H. Thomas, K. E. Healy and G. Nuber, *Polymer* **36**, 842 (1995)

33 R.C. Thomson, M.C. Wake, M.J. Yaszemski and A.G. Mikos, *Adv. Polym. Sci.* **122**, 274 (1995)

[34] D.K. Han and J.A. Hubbell, *Macromolecules* **30**, 6083 (1997)

[35] S. L. Ishaug-Riley, G. M. Crane, M. J. Miller, A. W. Yasko, M. J. Yaszemski and A. J. Mikos, *J. Biomed. Mat. Res.* **36**, 28 (1997)

[36] R.H. Li, M. White, S. Williams and T. Hazlett, *J. Biomater. Sci. Polymer Edn* **9 (3)**, 258 (1998)

[37] D. J. Mooney and A. G. Mikos, *Scientific American* **April**, 38 (1999)

[38] D. J. Mooney and A. G. Mikos, *Scientific American* **April**, pg 40 and 41 (1999)

[39] G. Naughton, *Scientific American* **April**, 61 (1999)

[40] R. S. Langer and J. P. Vacanti, *Scientific American* **April**, 62 (1999)

[41] D. Ferber, *Science* **284**, 422 (1999)

[42] S. Terada, M. Sato, A. Sevy and J.P. Vacanti, *Yonsei Medical Journal* **41 (6)** 691 (2000)

[43] S. Kaihara, S. Kim, B.S. Kim, D.J. Mooney, K. Tanaka and J.P. Vacanti, *J. Pediatr. Surg.* **35**, 1290 (2000)

[44] S. S. Kim, H. Utsunomiya, J. A. Koski, B. M. Wu, M. J. Cima, J. Sohn, K. Mukai, L. G. Griffith and J. P. Vacanti, *Ann Surg* **28 (1)**, 13 (1998)

[45] S. Kaihara, J. Borenstein, R. Koka, S. Lalan, E.R. Ochoa et al., *Tissue Eng.* **6**, 117 (2000)

[46] S. S. Kim, S. Kaihara, M. S. Benvenuto, B. S. Kim, D. J. Mooney and J. P. Vacanti, *J. Pediatr. Surg.* **33**, 996 (1998)

[47] S. Kaihara, S. S. Kim, M. S. Benvenuto, R. Choi, B. S. Kim, D. J. Mooney et al. *Transplantation* **67**, 245 (1999); S. Kaihara, S. S. Kim, M. S. Benvenuto, B. S. Kim, D. J. Mooney et al. *Tissue Eng.* **5**, 346 (1999); S. Kaihara, S. S. Kim, B. S. Kim, D. J. Mooney, K. Tanaka and J. P. Vacanti, *Transplantation* **69**, 1932 (2000)

[48] T. Shinoka, P. X. Ma, T. D. Shum et al. *Circulation* **94** Suppl:II, 168 (1996); T. Shinoka, T. D. Shum, P. X. Ma, et al. *Circulation* **96** Suppl:II 107 1997); C. K. Breuer, T. Shinoka, R. E. Tanel, D. J. Mooney et al. *Biotech. Bioeng.* **50**, 567 (1999)

[49] N. Isogai, W. Landis, T. H. Kim, L. C. Gerstenfeld, J. Upton and J. P. Vacanti, *J. Bone Joint Surg.* **81-A**, 316 (1991)

[50] U. A. Stock and J. P. Vacanti, *Annual Rev. Med.* **52**, 451 (2001)

[51] D. K. Gilding and A. M. Reed, *Polymer* **20**, 1464 (1979)

[52] R. F. Storey and T. P. Hickey, *J. Polym. Sc.: PartA: Polym. Chem.* **31**, 1838 (1993)

[53] R. F. Storey, S. C. Warren, C. J. Allison, J. S. Wiggins and A. D. Puckett, *Polymer* **34**, 4365 (1993)

[54] M. C. Wake, P. K. Gupta and A. G. Mikos, *Cell Transplantation* **5 (4)** 473 (1996)

[55] J. H. deGroot, H. W. Kuijper and A. J. Pennings, *J. Mat. Sc. Mat. in Med.* **8**, 712 (1997)

[56] D. A. Barrera, E. Zylstra, P. T. Lansbury and R. J. Langer, *Am. Chem. Soc.* **115**, 110 (1993)

[57] D. A Barrera, E. Zylstra, P. T. Lansbury and R. J. Langer, *Macromolecules* **28**, 425 (1995)

[58] J. H. Aubert and R. L. Clough, *Polymer* **26,** 2054 (1985)

[59] N. Rotter, J. Aigner, A. Naumann, H. Plank, C. Hammer, G. Burmester and M. Sittinger, *J. Biomed. Mater. Res.* **42 (3)**, 356 (1998)

[60] W. Amass, A. Amass and B. Tighe, *Polym. Int.* **47**, 144 (1998)

[61] R. A. Stile, W. R. Burghardt and K. E. Healy, *Macromolecules* **32**, 7379 (1999)

[62] K. T. Paige, L. G. Cima, M. J. Yaremchuk, J. P. Vacanti and C. A. Vacanti, *Plast. Reconstr. Surg.* **96**, 1390 (1995)

[63] Y. Cao, A. Rodriguez, M. Vacanti, C. Ibarra, C. Arevalo and C. A. Vacanti, *J. Biomater. Sci., Polm. Ed.* **9**, 475 (1998)

[64] M. Heskins and J. E. Guillet, *J. Macromol. Sci., Chem. Ed.* **A2**, 1441 (1968)

[65] A. S. Goldsrein, G. Zhu, G. E. Morris, R. K. Meszlenyi and A. G. Mikos, *Tissue Eng.* **5 (5)**, 433 (1999)

[66] K. A. Athanassiou, J. P. Schmitz and C. M. Agrawal, *Tissue Eng.* **4**, 53 (1998)

[67] B. -S. Kim and D. J. Mooney, *J. Biomed. Mater. Res.* **41**, 332 (1998)

[68] S. J. Huang and L-H. Ho, *Macromol. Symp.* **144**, 32 (1999)

[69] H. R Allcock, *Macromol. Symp.*, **144**, 46 (1999)

[70] S. Brocchini, K. James, V. Tangspasuthadol and J. Kohn, *J Biomed. Mater. Res.* **42**, 75 (1998)

71 K. Whang, K. E. Healy and D. R. Elenz, *Tissue Eng.* **5 (1)**, 51 (1999)

72 B. D. Boyan, J. Lincks, C. H. Lohmann et al., *J Orthop. Res.* **17**, 457 (1999)

73 J. C. Hamble, Z. Schwartz, S. W. Windeler et al., *J Orthop. Res.* **12**, 542 (1994)

74 Z. Schwartz, C. H. Lohmann, G. G. Niederauer et al., *Trans. Orthop. Res. Soc.* **24**, 805 (1999)

75 B. D. Boyan, C. H. Lomann, J. Romero and Z. Schwartz, *Clin. In Plastic Surg.* **26 (4)** 645 (1999)

76 B. Chevallay, N. Abdul-Malak and D. Herbage, *J Biomed. Mater. Res.* **49**, 459 (2000)

77 E. Middlekoop, H. J. C. de Vries, L. Ruuls, V. Everts, C. H. R. Wildevuur and W. Westerhof, *Cell Tissue Res.* **280**, 453 (1995)

78 G. Vaissere, B. Chevally, D. Herbage and O. Damour, *Med. Biol. Eng. Comput.* **38**, 218 (2000)

79 Y. Ikada and H. Tsuji, *Macromol. Rapid Commun.* **21**, 132 (2000)

80 Y. Ikada, *ACS Symp. Ser.* **540**, 35 (1994)

81 G. Chen, T. Ushida and T. Tateishi, *Chem. Commun.* 1506 (2000)

82 E. Ruckenstein and J. S. Park, *Polymer* **33(2)**, 417 (1992)

83 P. Becher, *Emulsion, Theory and Practise.* Reinhold, New York (1965)

84 A. L. Smith, *Theory and Practise of emulsion Technology*, Academic Press, New York, Ch. 19 (1976)

85 M. P. Aronson and M. F. Petko, *J. Coll. Interf. Sci.*, **159**, 149 (1993)

86 N. R. Cameron and D. C. Sherrington, *Adv. Polym. Sci.* **126**, 164 (1995)

87 K. J. Lissant and K. G, Mayhan, *J. Coll. Interf. Sci.* **42**, 208 (1973)

88 W. C. Griffin, *J. Soc. Cosmet. Chem.* **5**, 249 (1954)

89 W. C. Griffin, *J. Soc. Cosmet. Chem.* **1**, 326 (1949

90 J. Boyd, C. Parkinson and P. Sherman, *J. Coll. Interf. Sci.* **41 (2)** 370 (1972)

91 K. Shinoda and S. Freiberg, *Emulsions and Solubilisation*; Wiley, New York (1986)

92 J. A. Kitchener and P. R. Musselwhite, "*The Theory of Stability of Emulsions*", in P. Sherman (ed.), "*Emulsion Science*"

93 J. Kizling and B. Kronberg, *Coll. Surf.* **50**, 131 (1990)

94 N. R. Cameron and A. Barbetta, *J. Mater. Chem.* **10**, 2466 (2000)

95 N. R. Cameron, D. C. Sherrington, L. Albiston and D. P. Gregory, *Coll. Polym. Sci.* **274**, 595 (1996)

96 D. Barby and Z. Haq, EU Pat. 0, 060, 138 (to Unilever) (1982)

97 J. M. Williams and D. A. Wrobleski, *Langmuir* **4**, 656 (1988)

98 J. M. Williams, A. J. Gray and M. H. Wilkerson, *Ibid.* **6**, 437 (1988)

99 M. P. Aronson and M. F. Petko, *J. Coll. Interf. Sci.* 159, 149 (1993)

100 F. O. Opawale and D. J. Burgess, *J. Coll. Interf. Sci.* **197**, 150 (1998)

101 E. Ruckenstein, *Adv. Polym. Sci.* **127**, 57 (1997)

102 D. C. Sherrington and P. W. Small, U.S. Pat. 4, 965, 289 (1990)

103 E. Ruckenstein and X-B. Wang, *Biotech. Bioeng.* **44**, 86 (1994)

104 J. R. Duke Jr, M. A. Hoisington, D. A. Langlois and B. C. Benicewicz, *Polymer* **39 (18)**, 4378 (1998)

105 A. Mercier, H. Deleuze and O. Mondain-Monval, *React. Funct. Polym.* **46**, 79 (2000)

106 E. C. Peters, F. Svec, J. M. M. Frèchet, *Chem. Mater.* **9**, 1898 (1997)

107 D. B. Hough, K. Hammond, C. Morris and R. C. Hammond, U.S. Pat. 5, 071, 747 (1991)

108 Brady et al., U.S. Pat. 4, 629, 742 (1986)

109 Metcalfe et al. U.S. Pat. 4, 539, 294 (1985)

110 N. Kitagawa, International Pat. PCT/US98/12797 (to Biopore Corporation) (1998)

111 G. Akay, S. Downes and V. J. Price PCT/GB99/04076 (1999)

References

112 J. M. Cowie, *Polymers: Chemistry and Physics of Modern Materials* 2nd Edn., Blackie Academic & professional (1997)

113 W. J. Bailey, *Polym. J.* **17(1)**, 95 (1985)

114 W. J. Bailey and P-Z. Feng, *Polym. Prep. ACS Division Polym. Chem.* **28 (1)**, 154 (1987)

115 W. J. Bailey, J. L. Chou, P-Z. Feng, B. Issan, V Kuniganh and L-L. Zhou, *Journal Macromolecular Science – Chem.* **A25 (5-7)**, 798 (1988)

116 W. J. Bailey, P. Ni and Z. Wu, *Macromolecules* **15**, 711 (1982)

117 W. J. Bailey, Z. Ni and S-R. Wu, *J. Polym. Sc., Polym. Chem. Edt.* **20**, 3030 (1982)

118 W. J. Bailey, S-R. Wu and Z. Ni, *Makromol. Chem.* **183**, 1920 (1982)

119 W. J. Bailey, S-R. Wu and Z. Ni, *J. Macromol. Sc. – Chem.* **A18(6)**, 986 (1982)

120 H. Kricheldorf, T. Mang and J. Jonte, *Macromolecules* **17**, 2173 (1984)

121 M. Yasin and B. J. Tighe, *Biomaterials* **13 (1)**, 16 (1992)

122 G. L. Brode and J. V. Koleske, *J. Macromol. Sci. – Chem* **A6 (6)**, 1114 (1972)

123 E. E. Schmitt and R. A. Polistina, U.S. Pat. 3,297,033 (1967); C.C. Chu and A. J. J. Browning, *J. Biomed. Mater. Res.* **22**, 699 (1988)

124 S. J. Huang, H. Yang-kyoo and P. G. Edelman, *J. Macromol. Sci. Chem. (A)* **25**, 847 (1988); A. J. Domb, E. Mathiowitz, E. Ron, S. Giannos and R. Langer, *J. Polym. Sci., Poly. Chem. Edn.* **29**, 571 (1991); R. F. Storey and J. S. Wiggins, *Soc. Plast. Eng. Tech. Papers* **38**, 734 (1992)

125 R. F. Storey, J. S. Wiggins, K. A. Mauritz and A. D. Puckett, *Am. Chem. Soc. Div. Polym. Chem. Polym. Prepr.* **31**, 492 (1990)

126 R. F. Storey and J. S. Wiggins, *Soc. Plast. Eng. Tech. Papers* **38**, 734 (1992)

127 W. J. Bailey, N. Zhende and W. J. Shang-Ren, *J. Polym. Sci.,Polym. Chem. Edn.* **20**, 3021 (1982)

128 P. Hainey, I.M. Huxham, B. Rowatt, D.C. Sherrington and L. Tetly, *Macromolecules* **24**, 117 (1991)

129 J. A. Greig and D. C. Sherrington, *Polymer* **19**, 163 (1979)

130 J. M. Williams, *Langmuir* 7, 1370 (1991)

131 E. Ruckenstein and F. Sun, *J. Appl. Polym. Sci.* **46**, 1271 (1992)

132 N. R. Cameron, D. C. Sherrington, L. Albiston and D. P. Gregory, *Colloid Polym. Sci.* **274**, 592 (1996)

133 G. B. Kharas, F. Sanchez-Riera, D. K. Severson, in: *Plastics from Microbe*, D. P. Mobely, (ed.), Hanser Publishers, New York, p. 37 (1994)

134 M. Asano, H. Fukuzaky and M. Yoshida, *J. Contr. Rel.* **9**, 111 (1989)

135 Ph. Dubois, R. Jerome and Ph. Teyssie, *Makromol. Chem., Macromol. Symp.* **42/43**, 116 (1991)

136 A. Schindler, Y. M. Hibionada and C. G. Pitt, *J. Polym. Sci., Polym. Chem.* **20**, 319 (1982)

137 Y. Okamoto, *Makromo/. Chem., Macromol. Symp.* **42/43**, 117 (1991)

138 H. Tsuji, S. -H. Hyon and Y. Ikada, *Macromolecules* **24**, 5651 (1991)

139 S. -H. Hyon, K. Jamishada and Y. Ikada, *Biomaterials* **18**, 1503 (1997)

140 H. Fukuzahy, M. Yoshida and M. Asano, *Eur. Polym. J.* **24**, 1029 (1988)

141 W. J. Boyle, Aliied-Signal, WO 89/05664 (1989)

142 E. Lilly and R. C. Schulz, *Makromolek. Chem.* **176**, 1901 (1975)

143 J. A. P. P van Dijk, J. A. M. Smit, F.E. Kohn and J. Feijen, *J. Polym. Sci., Polym. Chem. Ed.* **21**, 208 (1983)

144 F. E. Kohn, J. G. van Ommen and J. Feijen, *Eur. Polym. J.* **19 (12)**, 1088 (1983)

145 R. C. Schulz, *Proc. IUPAC Int. Symp. Makromolek. Chem.*, Budapest, 185 (1969)

146 T. Ouhadi, C. Stevens and Ph. Teyssie, *Makromol. Chem.* **Suppl. 1**, 191 (1975)

147 J. M. Vion, R. Jerome, Ph. Teyssie, M. Aubin and R. E. Prid'homme, *Macromolecules* **19**, 1828 (1986)

148 Ph. Dubois, Ch. Jacobs, R. Jerome and Ph. Teyssie, *Macromolecules* **24**, 2266 (1986)

149 I. Barakat, Ph. Dubois, R. Jerome, Ph. Teyssie and M. Mazurek, *Macromol. Symp.* **88**, 244 (1994)

[150] I. Barakat, Ph. Dubois, R. Jerome, Ph. Teyssie and E. Goethals, *J. Polym. Sci., Part A: Polym. Chem.* **32**, 2099 (1994)

[151] Ph. Dubois, R. Jerome and Ph. Teyssie, *Macromolecules* **24**, 977 (1991)

[152] Ph. Degee, Ph. Dubois and R. Jerome, *Macromol. Symp.* **123**, 84 (1997)

[153] Ph. Degee, Ph. Dubois and R. Jerome, Macromol. Chem. Phys. 198, 1984 (1997)

[154] Ph. Dubois, C. Jacobs, R. Jerome and Ph. Teyssie, *Macromolecules* **24(9)**, 2270 (1991)

[155] Ph. Dubois, R. Jerome and Ph. Teyssie, *Macromol. Chem., Macromol. Symp.* **42/43**, 116 (1991)

[156] I. Barakat, Ph. Dubois, R. Jerome, Ph. Teyssie and M. Mazurek, *Macromol. Symp.* **88**, 244 (1994)

[157] M. Bero, G. Adamus, J. Aperczyk and H. Jansczyk, *Polym. Bull.* **31**, 9 (1993)

[158] H. Kricheldorf and I. Kreiser-Saunders, *Macromol. Chem.* **191**, 1057 (1990)

[159] F. Chabot, M. Vert, S. Chapelle and P. Granger, *Polymer* **24**, 53 (1983)

[160] M. Hakkarainen, A. -C. Albertsson and S. Karlsson, *Polym. Degradation Stability* **52**, 291 (1996)

[161] K. Stridsberg and A.-C. Albertsson, *J. Polym. Sci., Part A, Polym. Chem.* **8**, 1784 (2000)

[162] R. F. Storey, S. C. Warren, C. J. Allison and J. S. Wiggins, *Polymer* **20 (34)**, 4372 (1993)

[163] R. W. Lenz, *Adv. Polym. Sci.* **107**, 40 (1993)

[164] L. G. Ljungdahl and K. -E Eriksson, *Adv. Microbiol Ecology*, **8**, K. C. Marshall (ed.), New York, p. 237 (1985)

[165] *Biochemistry and genetics of cellulose degradation.*, J. -P. Aubert, P. Beguin and J. Millet (ed.),Academic, New York (1988)

[166] M. S. Reeve, S. P. McCarthy and R. A. Gross, *Polym. Mat. Sci. Eng.* **67**, 84 (1992)

[167] C. G. Pitt, F. I. Chasalous, Y. M. Hibionada, D. M. Klimas and A. Sclinder, *J. Appl. Polym. Sci.* **26**, 3787 (1981)

[168] C.C. Chu, *J. Appl. Polym. Res.* **15**, 1727 (1981)

[169] S. C. Woodward, P. S. Brewer, F. Moatamed, A. Schindler and C. G. Pitt, *J. Biomed. Mat. Res.* **19**, 437 (1985)

[170] J. H. deGroot, F. M. Zijlstra, H. W. Kuipers, A. J. Penning, J. Klampmaker, R. P. H. Veth and H. W. B. Jansen, *Biomaterials* **18 (8)**, 622 (1997)

[171] J. -Z Bei, J. -M Li, Z. -F Wang, J. -C Le and S. -G Wang, *Polym. Adv.d Tech.* **8(11)**, 696 (1997)

[172] W. J. Bailey, V. K. Kuruganti and J. S. Angle, *ACS Symposium Ser.* **433**, 160 (1990)

[173] M. Hakkarainen, A. -C. Albertsson and S. Karlsson, *Polym. Degrad. Stab.* **52**, 291 (1996)

[174] S. Li, H. Garreau and M. Vert, *J. Mat. Sci., Mat. Med.* **1**, 130 (1990)

[175] S. Li, H. Garreau and M. Vert, *J. Mat. Sci., Mat. Med.* **1**, 139 (1990)

[176] S. Li and S. McCarthy *Biomaterials* **20**, 44 (1999)

[177] M. Vert, S. Li and H. Garreau, *J. Controlled Release* **16**, 26 (1991)

[178] E. A. Schmitt, D. R. Flanagan and R. J. Linhardt, *Macromolecules* **27**, 748 (1994)

[179] M. A. Tracy, K. L. Ward, L. Firouzabadian, Y. Wang, N. Dong, R. Qian and Y. Zhang *Biomaterials* 20, 1062 (1999)

[180] N. S. Mason, C. S. Miles and R. E. Sparks. *Hydrolytic degradation of poly (D,L-lactide), Biomedical and dental applications of polymers.* C. G. Gebelein and F. F. Koblitz (ed) New York: Plenum Press 279 – 291 (1981)

[181] P. Menei, V. Daniel, C. Montero-Menei, M. Brouillard, A. Pouplard-Barthelaix and J.P. Benoit *Biomaterials* **14**, 478 (1993).

[182] I. Grizzi, H. Garreau, S. Li and M. Vert *Biomaterials* **16**, 311 (1995)

[183] D. E. Cutright and E. E. Hunsuck *Oral Surg. Oral Med. Oral Pathol.* **31**, 134 (1971)

[184] L. Lu, S. J. Peter, M. D. Lyman, H. -L. Lai, S. M. Leite, J. A. Tamada, J. P. Vacanti, R. Langer and A. G. Mikos *Biomaterials* **21**, 1605 (2000)

[185] ISO 13781:1997 *Poly(L-lactide) resins and fabricated foams for surgical* implants – In vitro degradation testing.

186 A. M. Glauret, Fixation, *Dehydration and Embedding of Biological Specimens, Practical Methods in Electron Microscopy*, North-Holland, p. 5 (1980)

187 W. P. Ye, F. S. Du, W. H. Jin, J. Y. Yang and X. Yong, *Reactive and Functional Polym.* **32**, 168, 1997

188 ISO 15814:1999(E) *Implants for surgery – Copolymers and blends based on polylactide – In vitro degradation testing*

189 J. M. Williams, A. J. Gray and M. H. Wilkerson, *Langmuir* **6**, 444 (1990)

190 D. P. Gregory, M. Sharples and I. M. Tucker, EU Pat. 0, 299, 762 (to Unilever) (1988)

191 N. P. O. Green, G. W. Stout and D. J. Taylor, *Biological Sciences 1 & 2 2nd Edition,* R. Soper (ed), Cambridge University Press, p.188 (1991)

192 N. P. O. Green, G. W. Stout and D. J. Taylor, *Biological Sciences 1 & 2 2nd Edition,* R. Soper (ed), Cambridge University Press, p. 185 (1991)

193 N. P. O. Green, G. W. Stout and D. J. Taylor, *Biological Sciences 1 & 2 2nd Edition,* Ed. R. Soper (ed), Cambridge University Press, p. 237 (1991)

194 G. Zund, Q. Ye, S. P. Hoerstrup, A. Schoeberlein, A. C. Schmid, J. Grunenfelder, P. Vogt and M. Turina, *Eur. J. Cardio-thorac. Surg.* **15**, 524 (1999)

195 J. S. Roman, A. Gallardo, C. Elvira, B. Vazquez, A. Lopez-Bravo, J. A. de Pedro and D. Tomas, *Macromol. Symp.* **168**, 89 (2001)

196 Z. Gugala and S. Gogoewski, *J. Biomed. Mat. Res.* **49(2)**, 191 (2000)

197 T. Groth and G. Altankov, *PIMS 2000 9th International Conference on Polymers in Medicine and Surgery*, p. 213 (2000)

198 R. L. Julian and S. Haskill, J. Cell Biology 120, 585 (1993); K. Webb, V. Hlady, P. A. Tresco, *J. Biomed. Mat. Res.* **41**, 430 (1998)

199 P. B. van Wachem, T. Begling, J. Feijen, J. P. Detmers and W. G. van Aken, *Biomaterials* **6**, 408 (1985); T. G. Ruardy, H. E. Moorlag, J. M. Schakenraad, H. C. Van der Mei, H. J. Busscher, A. Underwood, H. Elwing and H. B. Lee, *Cells and Materials* **7**, 133 (1997)

200 F. Fey-Lamprecht, T. H. Groth, W. Albrecht, D. Paul, M. Fromm and A. H. Gitter, *J. Mat. Sci.- Mat. Med.* **9**, 715 (1998); F. Fey-Lamprecht, T. H. Groth, W. Albrecht, D. Paul and U. Gross, *Biomaterials* **21(2)**, 192 (2000)

201 M. Sittinger, J. Bujia, N. Rotter, D. Reitual, W. W. Minuth and G. R. Burmester, *Biomaterials* **17**, 242 (1996)

202 R. I. Freshney, *Animal Cell Culture: a practical approach, 2nd edt.* Oxford IRL Press, p.11 (1992)

203 W. C. Puelacher, S. W. Kim, J. P. Vacanti, B. Scloo, D. Mooney and C. A. Vacanti, *Int. J. Oral. Maxillofac. Surg.* **23**, 53 (1994)

204 S. L. Ishaug-Riley, G. M. Crane-Kruger, M. J. Yaszemski and A. G. Mikos, *Biomaterials* **19**, 1412 (1998)

205 D. C. West, A. Sattar and S. Kumar, *Anal. Biochem.* **147**, 295 (1985)

206 *Chambers Science and Technology Dictionary*, P. M. B. Walker (ed), W & R Chambers Ltd and Cambridge University Press, p. 23 (1988)

Appendix

Appendix A

Papers Published:

PolyHIPE Foams Containing Poly (ε-caprolactone) as Potential Matrices for Tissue Engineering, *Biomacromolecules* 2, 154 – 164 (2001)

Tissue Engineering Matrixes by Emulsion Templating, submitted 03/10/01 to *Polymer International*, following request after a presentation

Examined Courses Attended:

Lasers in Chemistry
Practical Spectroscopy: NMR and Mass Spectroscopy
Numerical Methods

Conferences Attended:

Macromolecules '99,
Polymers in the New Millenium
University of Bath, 5th – 9th September 1999

Conferences Attended with Poster Presentation:

RSC Young Researchers Meeting and Specialist Symposia
RSC Annual Conference
U.M.I.S.T., 16th – 18th and 19th – 20th April 2000

Tissue Engineering 2000,
Advances in Tissue Engineering, Biomaterials and Cell Signalling
University of York, 16th – 19th July 2000

Pacifichem 2000
Honolulu, Hawaii 14th – 19th December 2000

IRC Industrial Club Seminar
University of Durham, 19th – 21st September 2001

Conferences Attended with Oral and Poster Presentation:

Macrogroup UK
Young Researchers Meeting on Recent Advances in Polymer Science
University of Strathclyde, 17th – 19th April 2001

Appendix B

Seminars Attended:

Dr S. Rimmer, Polymer Centre, University of Lancaster
New Polymer Colloids
7th October 1998

Prof. M. F. Hawthorne, Dept of Chem. & Biochem., UCLA, USA,
RSC endowed lecture
9th October 1998

Prof. P. Unwin, Dept of Chem., University of Warwick
Dynamic Electrochemistry: small is beautiful
21st October 1998

Prof. A. Unsworth, University of Durham
What's A joint Like This Doing in a Nice Girl Like You
27th October 1998

Prof. J. P. S. Badyal, Dept of Chem. University of Durham
Tailoring Solid Surfaces, Inaugural Lecture
28th October 1998

Dr. C. J. Ludman, University of Durham
Bonfire Night Lecture
3rd November 1998

Dr Martin Wills, Dept of Chem., Warwick University
New Methodology for the Assymetric Transfer Hydrogenation of Ketones. Wednesday
11th Nov. 1998

Prof. Stephen Loeb, University of Windsor, Ontario, Canada
From Macrocycles to Metallo-Supramolecular Chemistry
12th November 1998

Dr Ruth Cameron, Dept of Materials Science& Metallurgy, Cambridge University,
Biodegradable Polymers
18th November 1998

Dr. B. G. Davis, University of Durham
Sugars and Enzymes
24th November 1998

Prof. N. Billingham, University of Sussex
Plastics in the Environment – Boon or Bane
1st December 1998

Dr. J. Mann, University of Reading
The Elusive Magic Bullet and Attempts to Find it?
19th January 1999

Dr Anita Jones, Dept. of Chem., Edinburgh University
Light-emitting Polymers
20th January 1999

Dr Christopher Schofield, Oxford University
Studies on the Stereoelectronics of Enzyme Catalysis
3rd February 1999

Dr. C. Viney, Heriot-Watt University
Spiders, Slugs and Mutant Bugs
23rd February 1999

Prof. G. Fleet, University of Oxford
Sugar Lactones and Amino Acids
13th October 1999

Prof. S. Collins, University of Waterloo, Canada
Methacrylate Polymerisation Using Zerconium Enolate Initiators: Polymersiation Mechanisms and Control of Polymer Tacticity
25th October 1999

Prof. A. Holmes, University of Cambridge
Conjugated Polymers for the Market Place
16th November 1999

Prof. D. Crout, University of Warwick
More than Simply Sweet: Carbohydrates in Medicine and Biology
8th December 1999

Prof. D. Haddleton, University of Warwick
Atom Transfer Polymerisation – What's All the Hype About?
12th January 2000

Dr. P. R. Fielden, U.M.I.S.T.
Miniatuarised Chemical Analysis (Lab-on-a-chip): Functional or merely Fashionable?
19th January 2000

Prof. S. Flisch, University of Edinburgh
The Challenges Involved in Protein Glcosylation – Synthesis of Glycan Chains and Selective Attachment to Proteins
26th January

Dr. S. Moratti, University of Cambridge
Shape and Stereoselectivity in Polymer
9th February 2000

Prof. E. Rizzardo, CSIRO Mol. Sci. Victoria, Australia
Designed Polymers by Free Radical and Addition-Fragmentation Processes
21 March 2000

Dr. S. F. Campbell, Former Sen. Vice President of Pfizer
Science, Art and Drug Delivery, A personal Perspective
25th October 2000

Prof. M. Thompson, University of Toronto
Scanning Kelvin Microprobe in the Characterisation of Material Surfaces
1st November 2000

J. P. L. Cox, University of Bath
Cosmic: A Universal DNA-based language for Communicating with Aliens and Other Intelligent Lifeforms
8th November 2000

Dr. W. Hayes, University of Reading
Synthesis of Novel Dendrimers and Hyperbranched Polymers
22nd November 2000

Prof. S. Armes, University of Sussex
10th January 2001

Dr. A. deMello, Imperial College, London
Chemical Integrated Circuits: Organic Synthesis and Analysis on a Small Scale
24th January 2001

Dr. S. T. Howard, University of Cardiff
Calculating the Distribution of Bonding Energy in Polyatomic Molecules
14th February 2001

Dr. A. W. G. Platt, University of Staffordshire
Transition Metal Complexes of Alkylsulphonated Phosphines and their Antitumor Properties
2nd May 2001